Chapter V

SPECTRUM IN A STRAINED CRYSTAL

§28. EFFECT OF STRAIN ON CRYSTAL SYMMETRY

A small homogeneous strain is defined by the symmetric strain tensor $\varepsilon_{\alpha\beta}$:

$$\varepsilon_{\alpha\beta} = \frac{1}{2}\left(\frac{\partial u_\alpha}{\partial x_\beta} + \frac{\partial u_\beta}{\partial x_\alpha}\right), \tag{28.1}$$

where $\boldsymbol{u}(\boldsymbol{x})$ is the displacement vector of a point due to strain. In elasticity theory, the connection between the strain tensor and the stress tensor $P_{\alpha\beta}$ is determined by the stiffness tensor $\boldsymbol{S}$:

$$\varepsilon_{\alpha\beta} = \sum_{\gamma\delta} S_{\alpha\beta,\,\gamma\delta} P_{\gamma\delta}. \tag{28.2}$$

The form of the tensor $S_{\alpha\beta,\,\gamma\delta}$ depends on the crystal class F.

Equations (28.1) and (28.2) define the macroscopic strain tensor of an anisotropic elastic medium not possessing internal structure.

In crystals which have more than one atom in the primitive cell, the strain tensor (28.1) determines only the deformation of the primitive cell as a whole, but the relative displacements of the atoms within the cell, being proportional to the stress (strain), differ for different atoms.

In the general case, application of a stress to a crystal reduces its symmetry.

The symmetry point group K' of the Bravais lattice of the strained crystal is a subgroup of the symmetry group K of the Bravais lattice of the unstrained crystal, containing those elements of K which are preserved under the strain.

The Bravais lattice basic vectors $\boldsymbol{a}_i'$ of the strained crystal are obtained by deforming the vectors $\boldsymbol{a}_i$ of the unstrained crystal:

$$\boldsymbol{a}_i' = (1 + \boldsymbol{\varepsilon})\boldsymbol{a}_i, \quad \text{or} \quad a_i'^{\alpha} = a_i^{\alpha} + \sum_{\beta} \varepsilon_{\alpha\beta} a_i^{\beta}. \tag{28.3}$$

The volume Ω_0' of the primitive cell based on the vectors $\boldsymbol{a}_i'$ is

$$\Omega_0' = \Omega_0(1 + \varepsilon_{xx} + \varepsilon_{yy} + \varepsilon_{zz}) = \Omega_0(1 + \mathrm{Tr}\,\varepsilon). \tag{28.4}$$

Note that the strain may alter the type of the Bravais lattice, in accordance with the possible lattice types for the new system K' (see Figure 16); the new Bravais lattice is then characterized by basic vectors which may be quite different from $\boldsymbol{a}_i'$ (28.3), but the volume of the new primitive cell always differs from Ω_0 by a factor proportional to the strain (see (28.4)). The Brillouin zone of the strained crystal, which is independent of the specific

choice of basic vectors, is obtained by a suitable deformation of the Brillouin zone of the unstrained crystal.

Let us consider the effect of a homogeneous strain on the symmetry of the Bravais lattice.

Application of a strain to a cubic lattice of class O_h along a fourfold axis gives $K' = D_{4h}$; according to Figure 16, the cubic lattices Γ_c, Γ_c^f and Γ_c^v become lattices Γ_q and Γ_q^v of the tetragonal system: $\Gamma_c \to \Gamma_q$; Γ_c^f, $\Gamma_c^v \to \Gamma_q^v$.

As shown in §5, lattices of the tetragonal system D_{4h} will yield orthorhombic lattices D_{2h} when deformed in either of two ways:

1. Application of a strain along a twofold axis parallel to an edge of the base of the Bravais parallelepiped ($\varepsilon_{xx} \neq 0$ or $\varepsilon_{yy} \neq 0$, if the z-axis lies along the fourfold axis, and the x- and y-axes along the edges of the base of the parallelepiped). In this case, $\Gamma_q \to \Gamma_0$, $\Gamma_q^v \to \Gamma_0^v$.

2. The strain is applied along another (inequivalent) twofold axis lying on the diagonal of the base: $\varepsilon_{xy} \neq 0$. Then $\Gamma_q \to \Gamma_0^b$, $\Gamma_q^v \to \Gamma_0^f$.

Lattices of the orthorhombic system will yield monoclinic lattices, $K' = C_{2h}$, when a shear strain is applied to the Bravais parallelepiped in a plane normal to one of the twofold axes, destroying the horizontal twofold axes (in other words, a nonzero component ε_{xy}, ε_{xz} or ε_{yz}, if the x-, y- and z-axes lie along the mutually perpendicular twofold axes). According to Figure 16, we have Γ_0^b, $\Gamma_0 \to \Gamma_m$ and $\Gamma_0^v, \Gamma_0^f \to \Gamma_m^b$.

The lattices Γ_m^b, Γ_m of the monoclinic system yield the lattice Γ_t of the triclinic system when strained at an angle (neither zero nor 90°) to the twofold axis, so that the strain tensor has nonzero shear components ε_{xz}, ε_{yz} (the z-axis lies along the twofold axis).

The Bravais lattices of the cubic system yield the lattice Γ_r of the rhombohedral system when strained along the diagonal of the Bravais cube. The Bravais lattices of the hexagonal system yield the lattice Γ_m when strained in a plane normal to the sixfold axis.

The crystal class F' of the strained crystal is a subgroup of the class F of the unstrained crystal, obtained from it by omitting the rotational elements destroyed by the strain. It may turn out that the class F' belongs not to the system K' obtained from K under the strain, but rather to a system K'' subordinate to K'. The Bravais lattice of the strained crystal will then have higher symmetry than implied by the crystal class. At first sight, this statement seems to contradict the discussion in §5, but it is approximate and valid only in the linear stress approximation. If we include quadratic terms in $\varepsilon_{\alpha\beta}$, the symmetry of the Bravais lattice of the strained crystal (28.3) corresponds to its crystal class F', in complete agreement with §5.

Let us consider the change in the crystal classes when the symmetry is reduced by a strain.

In transition from system O_h to system D_{4h}, when a fourfold axis is destroyed, the crystal classes of system O_h yield:

$$O_h \to D_{4h}, \quad O \to D_4, \quad T_d \to D_{2d}, \quad T_h \to D_{2h}, \quad T \to D_2.$$

Classes D_{4h}, D_4 and D_{2d} belong to system D_{4h}, but classes D_2 and D_{2h} possess the lower symmetry D_{2h}. Thus classes T and T_h exemplify the situation described above, in which the lattice of the strained crystal possesses higher symmetry D_{4h} than required by the crystal class.

However, if we include the quadratic stress terms in the strain tensor, describing the change in the elastic constants $S_{\alpha\beta,\gamma\delta}$ due to strain,

$$e_{\alpha\beta} = \sum_{\gamma\delta} S_{\alpha\beta,\gamma\delta} P_{\gamma\delta} + \sum_{\gamma\delta,\gamma'\delta'} B_{\alpha\beta\gamma\delta\gamma'\delta'} P_{\gamma\delta} P_{\gamma'\delta'},$$

where $B_{\alpha\beta\gamma\delta\gamma'\delta'}$ is a sixth rank tensor defined by the crystal class of the unstrained crystal, the Bravais lattice of the strained crystal, defined by the vectors $\mathbf{a}_i'$ (28.3), belongs precisely to system D_{2h} rather than D_{4h}, and corresponds to classes D_{2h} and D_2 of the strained crystal. Indeed, in classes T and T_h we have $B_{xxzzzz} \neq B_{yyzzzz}$ (the x-, y- and z-axes lie along the twofold axes of the group T); therefore, if a cubic crystal of class T or T_h is dilated along the z-axis we get a distortion of the Bravais parallelepiped along the x- or y-axis, which is quadratic in the strain. For crystals of class T_d, O or O_h, which have a fourfold axis (or a fourfold improper rotation axis), $B_{xxzzzz} = B_{yyzzzz}$, and the Bravais parallelepiped dilated along the z-axis remains a rectangular prism, in accordance with the classes D_{4h}, D_4 and D_{2d} characterizing the strained crystal.

In transition from the tetragonal to the orthorhombic system, when the fourfold axis becomes a twofold axis, the classes of the tetragonal system yield:

$$C_4 \to C_2, \quad S_4 \to S_2, \quad C_{4v} \to C_{2v}, \quad D_4 \to D_2, \quad D_{4h} \to D_{2h},$$
$$C_{4h} \to C_{2h}, \quad D_{2d} \to D_2.$$

As in the case of the cubic system considered above, the lowest symmetry classes of system D_{4h} (C_4, S_4, C_{4h}) become classes of the monoclinic system.

Application of a strain in the reflection plane of D_{2h} eliminates the twofold axes in the reflection plane, and the classes of the orthorhombic system become classes of the monoclinic system:

$$C_{2v} \to C_2, \quad D_2 \to C_2, \quad D_{2h} \to C_{2h}.$$

Upon further reduction of symmetry, from C_{2h} to S_2,

$$C_2 \to e, \quad C_s \to e, \quad C_{2h} \to S_2.$$

The transition from the cubic to the rhombohedral system is effected by applying a strain along the diagonal of the cube. The remaining symmetry elements are: one threefold axis, three reflection planes passing through the axis, and three twofold axes perpendicular to it. The classes of the cubic system become classes of the rhombohedral system:

$$T \to C_3, \quad T_h \to S_6, \quad T_d \to C_{3v}, \quad O \to D_3, \quad O_h \to D_{3d}.$$

Application of an arbitrary strain to lattices of the hexagonal system in a plane perpendicular to the sixfold axis transforms the classes of the hexagonal system as follows:

$$C_3 \to e, \quad C_{3v} \to e, \quad C_6 \to C_2, \quad S_6 \to S_2, \quad D_3 \to C_2, \quad D_{3d} \to C_2,$$
$$C_{3h} \to C_s, \quad D_{3h} \to C_s, \quad C_{6h} \to C_{2h}, \quad C_{6v} \to C_2, \quad D_6 \to D_2, \quad D_{6h} \to D_{2h}.$$

In a similar manner, we easily find the system, lattice type and crystal class of the strained crystal for an arbitrary small strain, since in the linear strain approximation any strain can be expressed through successive application of several simple strains.

Thus, in each case we can determine the space group G' of the strained crystal, since each of the rotational elements remaining in the new group F' has the same nonprimitive translations relative to the new lattice vectors (28.3) as it had in the space group G of the unstrained crystal.

The states of elementary excitations in the strained crystal must be classified according to the irreducible representations of the space group G'.

In the general case, application of a strain reduces the crystal symmetry, and so degeneracy of the excitation energy spectrum in a solid is partially or wholly lifted. However, we cannot directly apply the results of §15 concerning the splitting of terms due to reduction of symmetry, for the space groups G and G' are different insofar as they have different Bravais lattices, and G' is not a subgroup of G.* In order to avoid this difficulty, we "deform" the coordinates of the strained crystal by introducing x' coordinates

$$x' = (1+\varepsilon)^{-1}x = 1 - \varepsilon x \tag{28.5}$$

in such a way that the Bravais lattice of the strained crystal in the new coordinates coincides with that of the unstrained crystal in the old coordinate system. Of course, this does not mean that the crystal lattices are identical, since in crystals with more than one atom in the primitive cell the distribution of atoms in the strained crystal in the x' coordinates (28.5) does not coincide with their distribution in the unstrained crystal in the x coordinates.

In the new coordinates (28.5), G' is a subgroup of G, and in order to ascertain how terms split upon application of stress we have to expand an irreducible representation of G in terms of irreducible representations of its subgroup G'. As shown in §12, every irreducible representation $\mathscr{D}_\nu^{\{k\}}$ of the space group G is characterized by an irreducible star $\{k\}$, which is defined by any one of its points, and by an index ν designating an irreducible representation of the little group G_k or a projective representation $\mathscr{D}_\nu(r)$ of the point group. In the strained crystal, the representations are characterized by a star $\{k'\}$ and an index ν'. Under the strain, the point k goes into the point $k' = (1-\varepsilon)k$. In the x' coordinates (28.5), the Brillouin zones of the unstrained and strained crystals coincide, and the point k' "returns" to its original position k.

The total degeneracy of the state in the crystal is the product of the dimension of the projective representation $\mathscr{D}^k(r)$ and the number of points in the star $\{k\}$.

In the general case, the strain has a twofold effect: the star $\{k\}$, which is irreducible in the group G, becomes reducible in the group G', and the degeneracy at k is removed. Thus the expansion of the representation $\mathscr{D}_\nu^{\{k\}}$ may be carried out in two steps. We must first decompose the star $\{k\}$ into irreducible stars in the group G', and then express the projective representations $\mathscr{D}_\nu^k(r)$ of the group F_k in terms of irreducible projective representations $\mathscr{D}_\mu'^k(r)$ of the group F_k'.

The star $\{k\}$ is easily expressed in terms of irreducible stars in the group G',

$$\{k\} = \{k_1\} + \{k_2\} + \ldots, \tag{28.6}$$

by the method of §12. If the band is not degenerate at k, the expansion (28.6)

* A similar difficulty will be met in §29, in construction of the perturbation operator representing a strain which alters the spatial periodicity of the crystal.

determines the strain-induced splitting of the spectrum, since different irreducible stars $\{k_i\}$ determine states with different energies.

The expansion of the irreducible projective representation $\mathscr{D}^k_\nu(r)$ of F in terms of irreducible representations $\mathscr{D}'^k_\mu(r)$ of F'_k describes the band splitting at k.

Each representation $\mathscr{D}'^k_\mu(r)$ of F' participating in the expansion is a projective representation of F'_k, whose factor system coincides with that of $\mathscr{D}^k_\nu(r)$ on the elements of F'_k. This factor system belongs to one of the classes of factor systems of F'_k. In practice, therefore, we must first find the factor system $\omega(r_1, r_2)$ of F'_k resulting from the factor system of the representation $\mathscr{D}^k_\nu(r)$ of F_k, and then, using the characters of the irreducible projective representations of F_k corresponding to this factor system, decompose the representation $\mathscr{D}^k_\nu(r)$ into irreducible representations $\mathscr{D}'^k_\mu$ in accordance with (13.38).

Based on the results of §14, we can establish the general relation between the factor system classes of the point group F and its subgroup F'.

It is clear that any vector representation, i.e., representation of class K_0 of the group F, becomes a vector representation of the subgroup F'. For vector representations, this problem reduces to the corresponding problem for the ordinary point group representations. We may therefore confine ourselves to the relation between the other factor system classes of F and F' for point groups, conforming to the existing hierarchy of crystal systems.

In transition from the cubic to the tetragonal system, the crystal class O_h becomes D_{4h}. By (3.13), the generators $a = c_4$, $s = s_6$ of the group O_h satisfy the relations $a^4 = e$, $s^6 = e$, $as^3 = s^3a$, $sa^3s = a$. The generators of the group D_{4h} may be chosen as $a = c_4$, $b = u$, where u is a twofold axis ($u = s^4as^4$) and C is the reflection plane $\sigma_h(c = a^2s^3)$; these generators satisfy the defining relations (3.5)

$$a^4 = e, \quad b^2 = e, \quad c^2 = e, \quad ba = a^3b, \quad ac = ca, \quad bc = cb,$$

which follow directly from the defining relations (3.13) for O_h.

By (14.74), the matrices $\boldsymbol{A} = \mathscr{D}(a)$, $\boldsymbol{B} = \mathscr{D}(s)$ of the projective representations of the group O_h satisfy the relations

$$\boldsymbol{A}^4 = \alpha\boldsymbol{I}, \ \boldsymbol{B}^6 = \boldsymbol{I}, \ \boldsymbol{AB}^3 = \beta\boldsymbol{B}^3\boldsymbol{A}, \ \boldsymbol{BA}^3\boldsymbol{B} = \boldsymbol{A}, \quad \text{where} \quad \alpha, \beta = \pm 1. \tag{28.7}$$

It follows from (28.7) that the matrices $\boldsymbol{A} = \mathscr{D}(a), \boldsymbol{U} = \mathscr{D}(u), \boldsymbol{C} = \mathscr{D}(c)$ of the projective representations for the generators D_{4h} satisfy the relations

$$\boldsymbol{A}^4 = \alpha\boldsymbol{I}, \quad \boldsymbol{U}^2 = \alpha\beta\boldsymbol{I}, \quad \boldsymbol{C}^2 = \alpha\boldsymbol{I}, \quad \boldsymbol{UA} = \alpha\beta\boldsymbol{A}^3\boldsymbol{U}, \quad \boldsymbol{AC} = \beta\boldsymbol{CA}, \quad \boldsymbol{UC} = \alpha\beta\boldsymbol{CU}. \tag{28.8}$$

Comparing (28.8) with (14.37), we see that the classes K_1, K_2, K_3 of factor systems of O_h go into factor system classes of D_{4h} in the following manner:

$$K_1(O_h) \to K_7(D_{4h}), \quad K_2(O_h) \to K_4(D_{4h}), \quad K_3(O_h) \to K_6(D_{4h}).$$

A similar argument reveals the relation between the factor system classes of the groups $O \to D_4$, $T_d \to D_{2d}$, $T_h \to D_{2h}$, $T \to D_2$:

$$K_1(O) \to K_1(D_4), \quad K_1(T_d) \to K_1(D_{2d}), \quad K_1(T) \to K_1(D_2),$$
$$K_1(T_h) \to K_7(D_{2h}).$$

In transition from the cubic to the rhombohedral system D_{3d}, we need consider only factor system classes of the groups $O_h \to D_{3d}$, since the projective representations of the other subgroups of D_{3d} are all p-equivalent to vector representations and therefore all the factor system classes of O_h go into the class K_0 for these subgroups. This implies removal of essential band degeneracy.

Note that if a factor system goes into class K_0 due to reduction of symmetry, this does not yet mean that it becomes the identity factor system.

Reasoning in the same way as for the groups O_h and D_{4h}, we see that

$$K_1(O_h) \to K_0(D_{3d}), \quad K_2(O_h), \quad K_3(O_h) \to K_1(D_{3d}).$$

In transition from the tetragonal to the orthorhombic system, the relation between the classes is

$$K_1(C_{4v}) \to K_1(C_{2v}), \quad K_1(D_4) \to K_1(D_2), \quad K_1(C_{4h}) \to K_1(C_{2h}),$$
$$K_1(D_{2d}) \to K_1(D_2), \quad K_i(D_{4h}) \to K_i(D_{2h}) \quad (i = 1, \ldots, 7).$$

In transition from the orthorhombic to the monoclinic system, the correspondence of factor system classes for the groups D_{2h} and C_{2h} is

$$K_1(D_{2h}), \quad K_2(D_{2h}), \quad K_7(D_{2h}) \to K_0(C_{2h}),$$
$$K_3(D_{2h}), \quad K_4(D_{2h}), \quad K_5(D_{2h}), \quad K_6(D_{2h}) \to K_1(C_{2h}).$$

In transition from the monoclinic to the triclinic system, each factor system class goes into class K_0.

The relations between the classes show at a glance whether essential band degeneracy may be removed by reduction of symmetry. To include the effect of time reversal on the electron spectrum of the strained crystal, one proceeds as in the unstrained crystal. In certain cases additional degeneracies caused by time reversal may be removed by a strain.

§29. EFFECT OF STRAIN ON THE SPECTRUM

In order to construct a matrix $\mathcal{H}(k, \varepsilon)$ defining the various strain-induced effects, we must first find the operator representing the change in the spectrum due to a homogeneous strain. The Schrödinger operator for an electron in a strained crystal is

$$\mathcal{H}(\varepsilon) = \frac{p^2}{2m} + V_\varepsilon(x) + \frac{\hbar}{4m^2c^2}(\nabla V_\varepsilon [p\sigma]), \tag{29.1}$$

where $V_\varepsilon(x)$ is the potential in the strained crystal; this operator is the Hamiltonian of the unstrained crystal

$$\mathcal{H}_0 = \frac{p^2}{2m} + V_0(x) + \frac{\hbar}{4m^2c^2}(\nabla V_0 [p\sigma]) \tag{29.2}$$

with $V_0(x)$ replaced by $V_\varepsilon(x)$.

The effect of a small strain may be treated as a perturbation, and we may restrict ourselves to the terms linear in the strain, i.e., proportional to the components of the strain tensor ε. However, in the case of a homogeneous static strain, we cannot interpret the difference $V_\varepsilon - V_0$ directly as a perturbation operator $\mathcal{H}'$, since it is generally not small. Indeed, if we fix, say,

a Bravais lattice point a_0 at the origin ($m_1 = m_2 = m_3 = 0$), then the lattice point $m(m_1, m_2, m_3)$ whose position a_m^0 in the unstrained lattice is defined by equation (5.1) is displaced by the strain to the point

$$a_m = (1 + \varepsilon) a_m^0, \tag{29.3}$$

where εa is the vector with components

$$(\varepsilon a)_i = \sum_j \varepsilon_{ij} a_j. \tag{29.4}$$

Therefore, at a sufficient distance from the point a_0 the relative displacement $\Delta a_m = a_m - a_m^0 = \varepsilon a_m^0$ due to an infinitesimal strain is comparable with the lattice constant, and accordingly the difference $V_\varepsilon(x) - V_0(x)$ will be of the order of $V(x)$, irrespective of the magnitude of the strain.

Of course, we may always consider a sufficiently small volume near an undisplaced cell, but even then we cannot utilize ordinary perturbation theory directly.

The point is that in perturbation theory the wave function of the perturbed Hamiltonian is always expressed as a superposition of wave functions of the unperturbed operator $\mathcal{H}_0$ (29.2) satisfying the same boundary conditions. In a crystal, the boundary conditions are laid down by periodicity, but it is clear from (29.3) that the periods of the potentials $V_0(x)$ and $V_\varepsilon(x)$ are different, and consequently so are the periods of the Bloch modulating factors $u_{k_s}(x)$ for the equations (29.1) and (29.2). To avoid these difficulties, we subject (29.3) to a coordinate transformation similar to (28.5), making the positions of the Bravais lattice points in the new coordinate system a'_m coincide with their positions in the unstrained lattice in the old coordinate system. This is done by putting

$$x' = (1 + \varepsilon)^{-1} x \approx (1 - \varepsilon) x \quad \text{or} \quad x = (1 + \varepsilon) x'. \tag{29.5}$$

The transformation (29.5) takes the operator $p = -i\hbar\nabla$ into

$$p = (1 - \varepsilon) p', \quad \text{where} \quad p'_i = -i\hbar \frac{\partial}{\partial x'_i}, \tag{29.6}$$

p^2 into

$$p^2 \approx p'^2 - 2 \sum_{ij} p'_i \varepsilon_{ij} p'_j = p'^2 - 2(p' \varepsilon p'), \tag{29.7}$$

and $V_\varepsilon(x)$ into $V_\varepsilon[(1 + \varepsilon) x']$.

If we now return to the old notation ($x' \to x$), the potentials $V_\varepsilon[(1 + \varepsilon) x]$ and $V_0(x)$ will have the same periods, and their difference can be expanded in a series in terms of ε:

$$V_\varepsilon[(1 + \varepsilon) x] - V_0(x) = \sum_{ij} V_{ij}(x) \varepsilon_{ij} \equiv (V\varepsilon), \tag{29.8}$$

where

$$V_{ij}(x) = \frac{1}{2 - \delta_{ij}} \lim_{\varepsilon \to 0} \frac{V_\varepsilon[(1 + \varepsilon) x] - V_0(x)}{\varepsilon_{ij}}. \tag{29.9}$$

The factor before the limit in (29.9) is needed because for given ε_{ij} ($i \neq j$) formula (29.8) contains two identical terms $V_{ij}\varepsilon_{ij}$ and $V_{ji}\varepsilon_{ji}$. Consequently, the transformation (29.5) yields the Hamiltonian

$$\mathcal{H}'(\varepsilon) = \mathcal{H}_0 + \mathcal{H}_\varepsilon + \mathcal{H}_{\varepsilon\mathrm{so}}, \tag{29.10}$$

where

$$\mathcal{H}_\varepsilon = -\frac{(p\varepsilon p)}{m} + (V\varepsilon), \tag{29.11}$$

$$\mathcal{H}_{\varepsilon so} = \frac{\hbar}{4m^2c^2}\{((\varepsilon\nabla V_0)[\sigma p]) - (\nabla(\varepsilon V_0)\cdot[\sigma p]) - ([\sigma\nabla V_0](\varepsilon p))\}. \tag{29.12}$$

The first term in (29.12) appears because under the transformation (29.5) the operator ∇ must be replaced by $(1-\varepsilon)\nabla$. The Hamiltonian $\mathcal{H}'(\varepsilon)$ in the new coordinates has the same periodicity as $\mathcal{H}_0$.

Under the transformation (29.5), an eigenfunction $\psi_{\varepsilon k'} = u_{\varepsilon k'}(x)e^{ik'x}$ of $\mathcal{H}(\varepsilon)$ (29.1) corresponding to energy $E(\varepsilon, k')$ and wave vector k' in the strained crystal goes into

$$\psi'_k = u'_{\varepsilon k'}[(1+\varepsilon)x']e^{ik'(1+\varepsilon)x'} = u'_k[(1+\varepsilon)x']e^{ikx},$$

where

$$k = (1+\varepsilon)k'.$$

This function has the same periodicity as the functions ψ_{nk} or φ_{nk} with the same wave vector k and may be expanded in terms of these functions:

$$\psi'_k = \sum_n c_{nk}\varphi_{nk} = \frac{1}{\sqrt{\mathcal{V}}}\sum_n c_{nk}\psi_{nk_0}e^{ikx}, \tag{29.13}$$

where the ψ_{nk_0} are the eigenfunctions of $\mathcal{H}_0(x)$ at k_0, and k is measured from the point k_0.

Using perturbation theory, let us find the change in energy due to the strain:

$$\delta E(\varepsilon) = E(\varepsilon, (1-\varepsilon)k) - E_0(k), \tag{29.14}$$

where $E(\varepsilon, (1-\varepsilon)k)$ is the energy in the strained crystal at the point $k' = (1-\varepsilon)k$ to which k is displaced by the strain. For this purpose, we substitute (29.13) into (29.10), multiply on the left by $\varphi^*_{n'k'}$ and integrate over x. The result is a system of equations similar to (21.6):

$$\sum_n\left[\left(E_{nk_0} - E\right)\delta_{nn'} + \mathcal{H}'_{n'n}\right]c_n = 0, \tag{29.15}$$

where

$$\mathcal{H}' = \mathcal{H}_k + \mathcal{H}_\varepsilon + \mathcal{H}_{\varepsilon so} + \mathcal{H}_{\varepsilon k}. \tag{29.16}$$

Here $\mathcal{H}_\varepsilon$ and $\mathcal{H}_{\varepsilon so}$ are defined by (29.11) and (29.12), and it follows from (21.9) and (17.33) that

$$\mathcal{H}_k = \frac{\hbar^2k^2}{2m} + \frac{\hbar k\pi}{m}, \quad \text{where } \pi = p + \frac{\hbar}{4m^2c^2}[\sigma\nabla V_0]. \tag{29.17}$$

The perturbation $\mathcal{H}_{\varepsilon k}$ contains terms proportional to products of the components of ε and k. In the nonrelativistic approximation,

$$\mathcal{H}_{\varepsilon k} = -2\frac{(p\varepsilon k)}{m}. \tag{29.18}$$

In accordance with general degenerate perturbation theory (see §15), in order to determine the energy $E_m(\varepsilon, k)$ in the strained crystal in the vicinity of the point k_0 in a band m, we must transform away interband terms $\mathcal{H}'_{mn}$ in (29.15), using (15.33); this gives a system of equations

$$\sum_m (\mathcal{H}_{m'm} - E\delta_{m'm})\,\bar{c}_m = 0,$$

which includes only coefficients $\bar{c}_m$ belonging to one band. The energy $E(\varepsilon, \boldsymbol{k})$, measured here from $E_{m\boldsymbol{k}_0}$, is found by solving the secular equation

$$|\mathcal{H}_{m'm} - E\delta_{mm'}| = 0. \tag{29.19}$$

By (15.47), (29.17), (29.18), in the nonrelativistic approximation the matrix elements $\mathcal{H}_{m'm}$ will include the following terms:

$$\mathcal{H}^{\boldsymbol{k}}_{m'm} = \frac{\hbar^2 k^2}{2m}\delta_{mm'} + \frac{\hbar}{m}\boldsymbol{k}\boldsymbol{p}_{m'm} + \frac{\hbar^2}{m^2}\sum_s \frac{(\boldsymbol{k}\boldsymbol{p}_{m's})(\boldsymbol{k}\boldsymbol{p}_{sm})}{E_m - E_s}, \tag{29.20}$$

$$\mathcal{H}^{\varepsilon}_{m'm} = \sum_{ij}\left(-\frac{(p_i p_j)_{m'm}}{m} + V^{ij}_{m'm}\right)\varepsilon_{ij} = \sum_{ij} D^{ij}_{m'm}\varepsilon_{ij}, \tag{29.21}$$

$$\mathcal{H}^{\varepsilon\boldsymbol{k}}_{m'm} = -2\frac{(\boldsymbol{p}_{m'm}\varepsilon\boldsymbol{k})}{m} + \frac{\hbar}{m}\sum_s \frac{(\boldsymbol{k}\boldsymbol{p}_{m's})\mathcal{H}^{\varepsilon}_{sm} + \mathcal{H}^{\varepsilon}_{m's}(\boldsymbol{k}\boldsymbol{p}_{sm})}{E_m - E_s}, \tag{29.22}$$

where

$$D^{ij}_{m'm} = -\frac{(p_i p_j)_{m'm}}{m} + V^{ij}_{m'm}.$$

The first term in (29.22) is due to the perturbation $\mathcal{H}_{\boldsymbol{k}\varepsilon}$ (29.18); the second, which is usually more important, arises in second order perturbation theory from $\mathcal{H}_\varepsilon$ and $\mathcal{H}_{\boldsymbol{k}}$. At an extremum, the first term always vanishes, but the second may differ from zero. If the little group contains inversion and the element $(i|\boldsymbol{\tau})$ commutes with all the elements of the group, these terms vanish, since for functions of like parity $P_{ms} = 0$, and for functions of unlike parity $\mathcal{H}^{\varepsilon}_{ms} = 0$.

As in §21, the relativistic term $\mathcal{H}_{so}$, which describes spin-orbit coupling at $\boldsymbol{k}_0$, may either be included in $\mathcal{H}_0$ or treated as a perturbation. In the latter case, when calculating the relativistic corrections proportional to ε we must take into account not only the contribution from $\mathcal{H}_{\varepsilon so}$ in first order perturbation theory but also the relativistic terms due to $\mathcal{H}_\varepsilon$ and $\mathcal{H}_{so}$ in second order perturbation theory; the latter terms are usually larger than the former.

We shall not write out all the terms explicitly, especially as it is far simpler to introduce them by the theory of invariants.

Note that all the matrix elements in (29.20)–(29.22) are calculated between wave functions $\psi_{n\boldsymbol{k}_0}$ of the unstrained crystal, and the selection rules depend on the little group $G_{\boldsymbol{k}_0}$ in the unstrained crystal. Equation (29.14) shows that in so doing one determines the spectrum at the point $\boldsymbol{k}'_0$ of the strained crystal corresponding to the point $\boldsymbol{k}_0$ of the unstrained reciprocal cell, where $\boldsymbol{k}'_0 = (1-\varepsilon)\boldsymbol{k}_0$. By (29.14) and (29.16), the energy change at the same point $\boldsymbol{k}$, $\Delta E(\varepsilon) = E(\varepsilon, \boldsymbol{k}) - E_0(\boldsymbol{k})$, is determined by the operator

$$\mathcal{H}''(\varepsilon, \boldsymbol{k}) = \mathcal{H}'(\varepsilon, (1+\varepsilon)\boldsymbol{k}). \tag{29.16a}$$

When actually calculating the matrix $\mathcal{H}(\boldsymbol{k}, \varepsilon)$ at a given point $\boldsymbol{k}_0$, one must calculate the matrix elements of the operator $\mathcal{H}_\varepsilon$ between the eigenfunctions of the operator $\mathcal{H}_0$ which transform according to a given representation of the little group $G_{\boldsymbol{k}_0}$. These matrix elements have dimensions of energy and are called the deformation potential constants.

In accordance with the selection rules presented in §19, in order to determine the nonzero elements $\mathscr{H}^{\varepsilon}_{m'm}$ we must know how the components V_{ij} transform.

Invariance of the Hamiltonian $\mathscr{H}_\varepsilon$ under the coordinate transformation implies that

$$\sum_{ij} V'_{ij}\varepsilon'_{ij} = \sum_{ij} V_{ij}\varepsilon_{ij}. \tag{29.23}$$

where $V'_{ij}(\boldsymbol{x}) = V_{ij}(g^{-1}\boldsymbol{x})$ and ε'_{ij} are the values of the components V_{ij} and ε_{ij} in the new coordinate system. Using (29.23), we easily show that the components $V'_{ij}(\boldsymbol{x})$ transform under all the operations g of the space group G according to the same representation $\mathscr{D}_\varepsilon$ as the components ε_{ij}, i.e., like the products p_ip_j or x_ix_j, and therefore the presence or absence of these terms in (29.11) in no way affects the selection rules. We stress that this transformation rule for the components V_{ij} is valid only when $g \in G_{\boldsymbol{k}_0}$, whereas the analogous transformation for the components ε_{ij}, p_ip_j is valid for arbitrary coordinate transformations. It is clear that the coefficients of ε_{ij} in $\mathscr{H}_{\varepsilon so}$ transform like V_{ij}.

The explicit form of $V_{ij}(\boldsymbol{x})$ is much more difficult to determine than the unperturbed potential $V_0(\boldsymbol{x})$, since this requires exact solution of the self-consistent problem in the strained crystal, making it possible to find the deviation of $V_\varepsilon(\boldsymbol{x})$ from $V_0(\boldsymbol{x})$ for small strains.

In the earlier versions of scattering theory, in which, as we shall see below, the same quantities V_{ij} appear, various assumptions were adopted concerning the relation between $V_0(\boldsymbol{x})$ and $V_\varepsilon(\boldsymbol{x})$. Although, as shown above, the explicit form of $V_{ij}(\boldsymbol{x})$ has no effect on the selection rules, so that it may be important only in numerical evaluation of the integrals, we shall devote a brief discussion to these models.

In the first of these models, proposed by Bloch and known as the deformable ion approximation, it was assumed that if a point $\boldsymbol{x}$ goes into $\boldsymbol{x}'$ when the lattice is deformed, the potential $V_\varepsilon(\boldsymbol{x}')$ is equal to the potential $V_0(\boldsymbol{x})$ in the unstrained lattice, in other words, under a homogeneous strain, $\boldsymbol{x}' = (1+\varepsilon)\boldsymbol{x}$,

$$V_\varepsilon[(1+\varepsilon)\boldsymbol{x}] = V_0(\boldsymbol{x}).$$

By (29.9), this implies that in the deformable ion approximation $V_{ij}(\boldsymbol{x}) = 0$, and

$$\mathscr{H}^{\varepsilon}_{m'm} = -\sum_{ij} \frac{\varepsilon_{ij}(p_ip_j)_{m'm}}{m}. \tag{29.24}$$

In a second model, proposed by Nordheim and known as the rigid ion approximation, it was assumed that the potential $V(\boldsymbol{x})$ is the sum of the potentials of the individual ions, and deformation of the lattice causes only a displacement $\boldsymbol{R}_n$ of the centers of the ions, without distorting their potentials. In this model, for an electron-hole pair in atomic semiconductors, one must assume that $V(\boldsymbol{x})$ is the sum of potentials of the individual atoms V_a.

If the primitive cell contains one atom, then

$$V_0(\boldsymbol{x}) = \sum_n V_a(\boldsymbol{x} - \boldsymbol{R}_n), \quad V_\varepsilon(\boldsymbol{x}) = \sum_n V_a(\boldsymbol{x} - (1+\varepsilon)\boldsymbol{R}_n),$$

since the ion displacement is $\delta\boldsymbol{R}_n = \varepsilon\boldsymbol{R}_n$. Hence

$$V_\varepsilon[(1+\varepsilon)\boldsymbol{x}] - V_0(\boldsymbol{x}) = \sum_n V_a[(1+\varepsilon)(\boldsymbol{x} - \boldsymbol{R}_n)] - V_a(\boldsymbol{x} - \boldsymbol{R}_n) = \sum_n \sum_{ij} \frac{\partial V_a(\boldsymbol{x} - \boldsymbol{R}_n)}{\partial x_i} \varepsilon_{ij}(\boldsymbol{x} - \boldsymbol{R}_n)_j$$

and consequently, by (29.9),

$$V_{ij}(\boldsymbol{x}) = \frac{1}{2}\sum_n \left\{ \frac{\partial V_a(\boldsymbol{x}-\boldsymbol{R}_n)}{\partial x_i}(\boldsymbol{x}-\boldsymbol{R}_n)_j + \frac{\partial V_a(\boldsymbol{x}-\boldsymbol{R}_n)}{\partial x_j}(\boldsymbol{x}-\boldsymbol{R}_n)_i \right\}. \qquad (29.25)$$

If the primitive cell contains more than one atom, deformation of the crystal may bring about displacement of one sublattice relative to another. This displacement $\boldsymbol{u}^{lm} = \boldsymbol{u}_l - \boldsymbol{u}_m$ is determined by a third rank tensor Γ, which is symmetric in the last two indices:

$$u_k^{lm} = \sum_{ij} \Gamma_{kij}^{lm} e_{ij}. \qquad (29.26)$$

The nonzero components of this tensor may be determined by the rules of §20. The representations according to which the components u_k^{lm} transform coincide with the representation corresponding to optical modes at $\boldsymbol{q} = 0$ and can be determined by the general rules of §15. An alternative method is based on the observation that, under all group operations which do not change the positions of the sublattice, the components u_k^{lm} transform like the components of an ordinary vector. If the group contains operations under which the sublattices change position, these operations change the sign of the $\boldsymbol{u}^{lm}$. For example, in a Ge-type lattice, where these components transform according to the representation F_2^+, i.e., like xy, xz and yz, the tensor Γ has one nonzero independent component $\Gamma_{xyz} = \Gamma_{xyz} = \Gamma_{zxy}$.

If the primitive cell contains two like atoms at points $\boldsymbol{R}_n$ and $\boldsymbol{R}'_n$, then, in the rigid ion model,

$$V_0(\boldsymbol{x}) = \sum_n [V_a(\boldsymbol{x}-\boldsymbol{R}_n) + V_a(\boldsymbol{x}-\boldsymbol{R}'_n)],$$

$$V_\varepsilon(\boldsymbol{x}) = \sum_n [V_a(\boldsymbol{x}-(1+\varepsilon)\boldsymbol{R}_n) + V_a(\boldsymbol{x}-(1+\varepsilon)\boldsymbol{R}'_n - \Gamma\varepsilon)].$$

Hence,

$$V_{ij}(\boldsymbol{x}) = \frac{1}{2}\sum_n \left\{ \frac{\partial}{\partial x_i}[V_a(\boldsymbol{x}-\boldsymbol{R}_n) + V_a(\boldsymbol{x}-\boldsymbol{R}'_n)](\boldsymbol{x}-\boldsymbol{R}_n)_j + \right.$$

$$\left. + \frac{\partial}{\partial x_j}[V_a(\boldsymbol{x}-\boldsymbol{R}_n) + V_a(\boldsymbol{x}-\boldsymbol{R}'_n)](\boldsymbol{x}-\boldsymbol{R}_n)_i \right\} + \sum_{kn} \Gamma_{kij} \frac{\partial V_a(\boldsymbol{x}-\boldsymbol{R}'_n)}{\partial x_k}. \qquad (29.27)$$

Quantitative results for silicon /24.1/ have shown that the deformable ion and rigid ion models both yield deformation potential constants which differ markedly from the experimental values. For numerical calculations, therefore, more sophisticated models are needed. We reiterate, though, that the number of nonzero linearly independent components $D_{m'm}^{ij}$ does not depend in any way on the model chosen, but is determined only by the little group and the representations according to which the wave functions transform at an extremum point.

In nondegenerate bands, i.e., one-dimensional representations, the only nonzero matrix elements are those of the components $D_{ij} = -p_i p_j/m + V_{ij}$ which transform according to the identity representation; in other words, by (21.14) and (21.15), only the components ε_{ij} or combinations of them which are invariant under transformations of the little group may appear in $E(\boldsymbol{\varepsilon}, \boldsymbol{k})$. At an arbitrary point of the Brillouin zone where the little group $G_{\boldsymbol{k}_0}$ does not contain any elements besides the identity and possibly inversion, all the components of the tensor of deformation potential constants are in

principle nonzero. Like the effective mass tensor m^{*-1}, this tensor can be transformed to principal axes, and in the appropriate coordinate system

$$E(\varepsilon) = D_{xx}\varepsilon_{xx} + D_{yy}\varepsilon_{yy} + D_{zz}\varepsilon_{zz}. \tag{29.28}$$

The principal axes of the tensors m^{*-1} and D do not coincide in general, but when the directions of the principal axes are determined by the symmetry axes they are naturally the same for both tensors. Thus, if the little group contains threefold or higher-order axes, then $D_{xx} = D_{yy} = D_\perp$, $D_{zz} = D_\parallel$, and

$$E(\varepsilon) = D_\perp(\varepsilon_{xx} + \varepsilon_{yy}) + D_\parallel\varepsilon_{zz}. \tag{29.29}$$

Instead of the components $D_\perp$ and $D_\parallel$, one frequently defines $\Xi_d = D_\perp$ and $\Xi_u = D_\parallel - D_\perp$. If the band extrema lie at different points k_α of the star $\{k_0\}$ (this is the case, for example, in the conduction band of Ge and Si), then equation (29.28) or (29.29) is valid for each extremum in its system of principal axes. These axes are, of course, different for different extrema, leading to the shift of inequivalent extrema derived in the preceding section from general group-theoretic considerations.

A strain is usually referred to the principal crystal axes, whereas the symmetry of the tensor D is determined by the positions of the symmetry axes for the extremum in question. To determine this shift, then, we must find the components of the strain tensor in the system of symmetry axes at the extremum. These components ε^α_{ij} are related to the corresponding components $\varepsilon_{i'j'}$ in the crystal system of principal axes:

$$\varepsilon^\alpha_{ij} = \sum_{i'j'} \cos(i'i)\cos(j'j)\varepsilon_{i'j'}, \tag{29.30}$$

where $\cos(i'i)$ is the cosine of the angle between the i and i' axes. If the directions of these axes are designated by the crystallographic indices i, k, l and i', k', l' respectively, then for cubic systems

$$\cos(i, k, l; i', k', l') = \frac{ii' + kk' + ll'}{[(i^2 + k^2 + l^2)(i'^2 + k'^2 + l'^2)]^{1/2}}. \tag{29.31}$$

Using the symmetry of the tensor ε, it is convenient to replace the two-component notation ε_{ij} by a one-component notation ε_j, as in /15.4/, denoting $\varepsilon_{xx} = \varepsilon_1$, $\varepsilon_{yy} = \varepsilon_2$, $\varepsilon_{zz} = \varepsilon_3$, $2\varepsilon_{xy} = \varepsilon_6$, $2\varepsilon_{xz} = \varepsilon_5$, $2\varepsilon_{yz} = \varepsilon_4$. Then the last equation may be rewritten

$$\varepsilon^\alpha_l = \sum_{l'} \Theta^\alpha_{ll'}\varepsilon_{l'}, \tag{29.32}$$

where

$$\Theta_{11} = \cos^2(xx'), \quad \Theta_{16} = \cos(xx')\cos(xy'), \quad \Theta_{61} = 2\Theta_{16},$$
$$\Theta_{66} = \cos(xx')\cos(yy') + \cos^2(xy') \text{ etc.}$$

Since the components ε'_l of the strain tensor will differ for different extrema, the shift of these extrema may also differ.

In cubic little groups, all three tensor components coincide, $D_{ii} = C$, and accordingly

$$E(\varepsilon) = C\varepsilon = C\sum_i \varepsilon_{ii}. \tag{29.33}$$

By (29.11), the deformation potential constant appearing here is

$$C=\frac{1}{3\mathcal{V}}\left\{\frac{\hbar^2}{m}\int\psi^*_{k_0}\nabla^2\psi_{k_0}\,dx+\int\psi^*_{k_0}\mathrm{Tr}V\psi_{k_0}\,dx\right\}, \tag{29.34}$$

where $\mathrm{Tr}V=\sum_i V_{ii}(x)$.

In the deformable ion approximation, it follows from (29.24) that the second term in (29.34) vanishes, and the deformation potential constant at $k=0$ is

$$C=-\frac{1}{3\Omega}\frac{\hbar^2}{m}\int_\Omega|\nabla u_0|^2\,dx. \tag{29.35}$$

We have used Green's formula according to which, for arbitrary functions φ and ψ,

$$\int\psi\nabla^2\varphi\,dx+\int\nabla\psi\nabla\varphi\,dx=\oint\psi\frac{\partial\varphi}{\partial n}\,ds=\oint\psi(\nabla\varphi\,ds). \tag{29.36}$$

The integral over the surface s of the primitive cell vanishes thanks to the periodicity of the Bloch factor $u_0(x)$.

In the rigid ion approximation, by (29.25), we have at $k=0$

$$C=-\frac{1}{3\Omega}\left[\frac{\hbar^2}{m}\int_\Omega|\nabla u_0|^2\,dx-\int_\Omega(x\nabla V_0)|u_0|^2\,dx\right]. \tag{29.37}$$

Here the field of all atoms other than that at the center of the primitive cell is neglected, i.e., we are assuming that $V_0(x)=V_a(x)$. Although this assumption is apparently not really justifiable, it is usually adopted in this model. Through simple but rather cumbersome manipulations, expression (29.37) may be rewritten /28.7/

$$C=-\frac{1}{3\Omega}\oint x_n(E-V_0)|u_0|^2\,ds, \tag{29.37a}$$

where x_n is the component of the radius vector normal to the surface.

In the case of degenerate bands, the strain not only shifts the band as a whole, but may also split bands as a result of partial or complete removal of degeneracy upon the reduction of symmetry. Therefore, the effect of the strain on the spectrum is more complicated. As an example, we shall discuss in the next section the effect of strain on the valence band spectrum in germanium, silicon and A_3B_5 compounds.

Along with terms proportional to ε, k^2 and εk, the Hamiltonian $\mathcal{H}(\varepsilon, k)$ may contain terms proportional to εk^2. These terms, which describe the change in the effective masses due to the strain, belong to third order perturbation theory.

In accordance with the general equation (15.48) and equation (29.16a), we have for a nondegenerate band

$$\begin{aligned}\Delta E_m^{\varepsilon k^2}=&-\mathcal{H}^\varepsilon_{mm}\sum_s\frac{\mathcal{H}^k_{ms}\mathcal{H}^k_{sm}}{(E_s-E_m)^2}+\\&+\sum_{ss'}\frac{\mathcal{H}^k_{ms}\mathcal{H}^k_{ss'}\mathcal{H}^\varepsilon_{s'm}+\mathcal{H}^k_{ms}\mathcal{H}^\varepsilon_{ss'}\mathcal{H}^k_{s'm}+\mathcal{H}^\varepsilon_{ms}\mathcal{H}^k_{ss'}\mathcal{H}^k_{s'm}}{(E_s-E_m)(E_{s'}-E_m)}-\\&-\sum_s\frac{\mathcal{H}^{\varepsilon k}_{ms}\mathcal{H}^k_{sm}+\mathcal{H}^k_{ms}\mathcal{H}^{\varepsilon k}_{sm}}{E_s-E_m}+2\,\mathrm{Re}\frac{\hbar^2}{m^2}\sum_s\frac{(kp_{ms})(k\varepsilon p_{sm})}{E_m-E_s}.\end{aligned} \tag{29.38}$$

As a rule, effects due to a change in effective mass are significant only if the relative change is considerably greater than the magnitude of the relative strain ε. The last terms in (29.38) do not cause such effects, but the first ones may, if the energy denominator $E_s - E_m$ for one or more bands is small compared with the corresponding deformation potential constant, i.e., if the nearest bands are closely spaced and the momentum matrix element or matrix element of the operator $\mathscr{H}_\varepsilon$ (or both) between the corresponding states s and m does not vanish; this may happen when the functions ψ_{sk_0} and ψ_{mk_0} do not possess a definite parity. If only the momentum matrix element between the nearest bands is nonzero, then

$$\Delta E_m^{\varepsilon k^2} = \sum_s \left(\mathscr{H}^\varepsilon_{ss} - \mathscr{H}^\varepsilon_{mm}\right) \frac{\mathscr{H}^k_{ms}\mathscr{H}^k_{sm}}{(E_s - E_m)^2} + \sum_{s' \neq s} \frac{\mathscr{H}^k_{ms}\mathscr{H}^k_{s'm}\mathscr{H}^\varepsilon_{ss'}}{(E_s - E_m)(E_{s'} - E_m)}. \tag{29.39}$$

In case only the interaction of the two nearest bands is significant, and these bands are not degenerate, the change in effective mass is proportional to the change ΔE_g in the band gap:

$$\Delta E_g = \mathscr{H}^\varepsilon_{ss} - \mathscr{H}^\varepsilon_{mm} = \sum_{ij} \left(D^s_{ij} - D^m_{ij}\right) \varepsilon_{ij}; \tag{29.40}$$

in this case

$$\Delta E_m = \frac{\delta E_g(\varepsilon)}{E_g^2} \frac{\hbar^2}{m^2} (\boldsymbol{kp})_{ms} (\boldsymbol{kp})_{sm},$$

i.e.,

$$\Delta \frac{1}{m^*_{ij}} = \frac{\delta E_g(\varepsilon)}{E_g} \frac{1}{m^{sm}_{ij}}, \tag{29.41}$$

where

$$\frac{1}{m^{sm}_{ij}} = \frac{1}{m^2 E_g} p^i_{ms} p^j_{sm}$$

is the contribution to the effective mass due to the interaction of the m and s bands. In this case, therefore, only those masses to which the major contribution is the interaction of the nearest bands experience a significant change. The strain does not alter the symmetry of the constant energy surface, i.e., equal masses vary in the same way under strain.

If a state s in (29.39) is degenerate, then, as we show in the next section, the symmetry of the spectrum may change. A similar effect may also occur when the matrix element of $\mathscr{H}_\varepsilon$ between the nearest bands does not vanish. By (29.38), if these bands are not degenerate, then

$$\Delta E_m^{\varepsilon k^2} = \frac{\hbar^2}{m^2} \frac{1}{E_s - E_m} 2\mathrm{Re}\left\{\mathscr{H}^\varepsilon_{sm} \sum_{s'} \frac{(\boldsymbol{kp})_{ms'} (\boldsymbol{kp})_{s's}}{E_{s'} - E_m}\right\}. \tag{29.42}$$

Equation (29.41) is directly applicable to crystals of PbS, PbSe, PbTe, in which the band extrema are located at the point L on the edge of the Brillouin zone. In the nonrelativistic approximation, the interaction of these bands determines only the transverse mass $m^*_\perp$. If we include the relativistic effects, which are significant in these crystals (since the spin-orbit splitting is comparable with the crystal splitting and with the band gap), the interaction of the nearest bands determines both masses.

Si is an example of a crystal in which the second effect determined by equation (29.42) is significant. The conduction band extrema of Si lie on the [100] axes at a point $\boldsymbol{k}_0$ distant $0.15\,(2\pi/a_0)$ from the band edge, i.e., from the point X, and correspond to the representation Δ_1. At X the two branches Δ_1 and Δ_2' of the spectrum merge and form the representation X_1 or X_3; hence their splitting at $\boldsymbol{k}_0$ is comparatively small, amounting to about 0.5 ev.

In accordance with the selection rules, the matrix element of the operator $\mathcal{H}^{\varepsilon}_{yz}, \mathcal{H}^{\varepsilon}_{yz}=\mathcal{H}^{\varepsilon}_{zy}=C'$, between the states Δ_1 and Δ_2' does not vanish, since, as we see from Table 11.1 (p. 73), the components y, z transform according to the representation $B_2=\Delta_1^*\times\Delta_2'$ of C_{4v}, which is the point group for the points Δ.

The only representation Δ_s for which the matrix elements p_{s1} and $p_{s2'}$ vanish simultaneously is Δ_5, according to which the functions Y_l and Z_l transform. The nonzero matrix elements are $\langle 1|p_y|Y_l\rangle=\langle 1|p_z|Z_l\rangle$ and $\langle X|p_z|Y_l\rangle=\langle X|p_y|Z_l\rangle$.

Since all these representations are real and $\boldsymbol{k}_0\neq-\boldsymbol{k}_0$, it follows from (19.7) that

$$p^{\boldsymbol{k}_s}_{\alpha\beta}=-p^{-\boldsymbol{k}_s}_{\beta\alpha} \quad \text{and} \quad \mathcal{H}^{\varepsilon\boldsymbol{k}_s}_{\alpha\beta}=\mathcal{H}^{\varepsilon,-\boldsymbol{k}_s}_{\beta\alpha}.$$

Thus, by (29.42), $\Delta E_{\varepsilon k^2}$ for the point $\boldsymbol{k}_0$ is

$$\Delta E_{\varepsilon k^2}=\frac{2\hbar^2C'\varepsilon_{yz}k_yk_z}{m'\Delta}, \tag{29.43}$$

where

$$C'=\langle X|\mathcal{H}^{\varepsilon}_{yz}|1\rangle, \quad \Delta=E_{\Delta_2'\boldsymbol{k}_0}-E_{\Delta_1\boldsymbol{k}_0},$$
$$\frac{1}{m'}=\frac{2}{m^2}\sum_l\frac{\langle 1|p_y|Y_l\rangle\langle Y_l|p_z|X\rangle}{E_{\Delta_1\boldsymbol{k}_0}-E_{\Delta_l\boldsymbol{k}_0}}. \tag{29.44}$$

If we now go over to the system of axes $x'[100]$, $y'[011]$, $z'[01\bar{1}]$, then, in view of (29.43), we can write the spectrum $E(\varepsilon,\boldsymbol{k})$ as

$$E(\varepsilon,\boldsymbol{k})=\frac{\hbar^2k_x^2}{2m_\parallel}+\frac{\hbar^2k_y^2}{2m_\perp}\left(1+\frac{2m_\perp C'\varepsilon_{yz}}{m'\Delta}\right)+\frac{\hbar^2k_z^2}{2m_\perp}\left(1-\frac{2m_\perp C'\varepsilon_{yz}}{m'\Delta}\right). \tag{29.45}$$

Note that if the εk^2 corrections to the spectrum had been evaluated by the theory of invariants, other invariants of the group C_{4v} would have appeared together with the term $\varepsilon_{yz}k_yk_z$ in $\Delta E_{\varepsilon k^2}$, namely (see Tables 11.1 and 26.1), the terms $(\varepsilon_{yy}-\varepsilon_{zz})(k_y^2-k_z^2)$, εk^2, $\varepsilon_{xx}k^2$, εk_x^2, $\varepsilon_{xx}k_x^2$. As we shall show in the following section, the predominant contribution of the term $\varepsilon_{yz}k_yk_z$ is due to the singularities of the spectrum at the point X, which is near the extremum $\boldsymbol{k}_0$.

§30. EFFECT OF STRAIN ON DEGENERATE BANDS IN CUBIC CRYSTALS

Let us consider how the spectrum changes at points of zero slope in degenerate bands. In any cubic crystal, if spin is neglected, this is the case, for example, at the point Γ, where there are six (for T_d, three) representations which are degenerate when spin is neglected: Γ_{12}, Γ_{12}', Γ_{15}, Γ_{15}', Γ_{25}, Γ_{25}'. Because of spin-orbit coupling, the three-dimensional representations Γ_{15}, Γ_{15}'

and Γ_{25}, Γ'_{25} split off a two-dimensional (counting spin) representation Γ_6^+, Γ_6^- or Γ_7^+, Γ_7^- and a fourfold degenerate representation Γ_8^+, Γ_8^-. The representations Γ_{12}, Γ'_{12} also become Γ_8^+, Γ_8^- counting spin.

In Ge, Si and most of the A_3B_5 compounds, the top of the valence band corresponds precisely to the representation Γ_8^+ or Γ_8, formed by splitting of the representations Γ'_{25} or Γ_{25}. In crystals of class T_d, for example, in ZnS lattices, the operator $\mathcal{H}(\boldsymbol{k})$ for the representation Γ_8 includes relativistic terms linear in $\boldsymbol{k}$, whose role will be examined below. In crystals of O_h whose group contains inversion there are no such terms. In diamond-type crystals (O_h^7), X and L are also points of zero slope for degenerate representations.

We first consider the point Γ. The basis functions of the representations Γ_{15} and Γ'_{15} transform under all group transformations like x, y, z or J_x, J_y, J_z, respectively, while the basis functions of the representations Γ'_{25} and Γ_{25} transform like yz, zx, xy or xz^2y^2, yz^2x^2, zx^2y^2. For brevity, we shall denote both sets of functions by X, Y, Z, since the selection rules for the intraband matrix elements of the operators $\mathcal{H}_{\boldsymbol{k}}$ and $\mathcal{H}_{\varepsilon}$ are the same for all these representations.

Since the operator D in (29.1) is even and by Table 26.2 (p. 250) its components D_{ij}, like the components ε_{ij}, transform according to the representations Γ_1, Γ_{12}, Γ'_{25}, it follows from (19.45) that in the present case, case (a_1), the operator has three nonzero linearly independent matrix elements:

$$l = D_{xx}^{xx}, \quad m = D_{yy}^{xx}, \quad n = D_{xy}^{xy}, \tag{30.1}$$

and so the form of the matrix $\mathcal{H}(\varepsilon)$ relative to the basis X, Y, Z is similar to (24.5):

$$\mathcal{H}(\varepsilon) = \begin{vmatrix} l\varepsilon_{xx} + m(\varepsilon_{yy} + \varepsilon_{zz}) & n\varepsilon_{xy} & n\varepsilon_{xz} \\ n\varepsilon_{xy} & l\varepsilon_{yy} + m(\varepsilon_{xx} + \varepsilon_{zz}) & n\varepsilon_{yz} \\ n\varepsilon_{xz} & n\varepsilon_{yz} & l\varepsilon_{zz} + m(\varepsilon_{xx} + \varepsilon_{yy}) \end{vmatrix}. \tag{30.2}$$

As noted above, spin-orbit coupling splits the sixfold degenerate (counting spin) representations Γ_{15}, Γ'_{15}, Γ_{25}, Γ'_{25} into Γ_6^+, Γ_6^- or Γ_7^+, Γ_7^- and Γ_8^+, Γ_8^-. We already have basis functions for these representations (see equation (23.2)). Using (30.2), we easily verify that relative to this basis for the representations Γ_8 the matrix $\mathcal{H}(\varepsilon)$ has a form similar to (24.13):

$$\mathcal{H}(\varepsilon) = \begin{vmatrix} f & h & j & 0 \\ h^* & g & 0 & j \\ j^* & 0 & g & -h \\ 0 & j^* & -h^* & f \end{vmatrix}, \tag{30.3}$$

where

$$\begin{gathered} f = \frac{l+m}{2}(\varepsilon_{xx} + \varepsilon_{yy}) + m\varepsilon_{zz}, \quad g = \frac{1}{3}\{f + 2[m(\varepsilon_{xx} + \varepsilon_{yy}) + l\varepsilon_{zz}]\}, \\ h = -\frac{1}{\sqrt{3}} n(i\varepsilon_{xz} + \varepsilon_{yz}), \quad j = \frac{1}{\sqrt{3}}\left[\frac{1}{2}(l-m)(\varepsilon_{xx} - \varepsilon_{yy}) - in\varepsilon_{xy}\right]. \end{gathered} \tag{30.4}$$

Thus the determinant $|\mathcal{H}(\boldsymbol{k}) + \mathcal{H}(\varepsilon) - IE|$ has the same form as the determinant of (24.13) for the unstrained crystal, the only difference being that F is replaced by $F = F + f$, etc. As shown in §24, the general solution of the secular equation has the form (24.14).

Substituting the values of the elements from (24.13) and (30.4) into (24.14), we find the electron spectrum in the strained crystal:

$$E_{1,2} = Ak^2 + a\varepsilon \pm [\mathscr{E}_k + \mathscr{E}_{\varepsilon k} + \mathscr{E}_\varepsilon]^{1/2}, \tag{30.5}$$

where

$$\mathscr{E}_k = B^2k^4 + C^2(k_x^2k_y^2 + k_x^2k_z^2 + k_y^2k_z^2), \tag{30.6}$$

$$\mathscr{E}_{\varepsilon k} = Bb[3(k_x^2\varepsilon_{xx} + k_y^2\varepsilon_{yy} + k_z^2\varepsilon_{zz}) - k^2\varepsilon] + 2Dd(k_xk_y\varepsilon_{xy} + k_xk_z\varepsilon_{xz} + k_yk_z\varepsilon_{yz}), \tag{30.7}$$

$$\mathscr{E}_\varepsilon = \frac{b^2}{2}[(\varepsilon_{xx} - \varepsilon_{yy})^2 + (\varepsilon_{yy} - \varepsilon_{zz})^2 + (\varepsilon_{zz} - \varepsilon_{xx})^2] + d^2(\varepsilon_{xy}^2 + \varepsilon_{xz}^2 + \varepsilon_{yz}^2). \tag{30.8}$$

Here

$$a = \frac{l + 2m}{3}, \quad b = \frac{l - m}{3}, \quad d = \frac{n}{\sqrt{3}}, \quad C^2 = D^2 - 3B^2.$$

The operator $\mathscr{H}(\varepsilon)$ may also be obtained by the theory of invariants, like the operator $\mathscr{H}(k)$ in §26. For the representation $\Gamma_8^\pm$, operator $\mathscr{H}(\varepsilon)$ includes components $\varepsilon_{\alpha\beta}$ which transform according to the representations $[\Gamma_8^{\pm 2}] = \Gamma_1 + \Gamma_{12} + \Gamma_{25}'$, and since these components also transform like the product $k_\alpha k_\beta$ the result is similar to (26.12) and (24.13):

$$\mathscr{H}(\varepsilon) = \left(a + \frac{5}{4}b\right)\varepsilon - b\sum_i J_i^2\varepsilon_{ii} - \frac{1}{\sqrt{3}}d\sum_{ij}[J_iJ_j]\varepsilon_{ij}. \tag{30.9}$$

If the representation Γ_8^+, Γ_8^- arises from the representation Γ_{12}, Γ_{12}', the operator $\mathscr{H}(\varepsilon)$ in the nonrelativistic approximation will contain only components ε_{ij} that transform according to the representations $[\Gamma_{12}^2] = \Gamma_1 + \Gamma_2 + \Gamma_{12}$; in other words, it will not contain components ε_{ij} with $i \neq j$ and, as in (26.16), $d = 0$.

It is evident from equation (30.5) that, in accordance with group-theoretic considerations, when a strain is applied, the light and heavy hole bands remain twofold degenerate owing to time reversal. Here an isotropic strain shifts the bands as a whole:

$$\Delta E = a\varepsilon, \tag{30.10}$$

while an anisotropic strain splits the bands at $k = 0$:

$$\delta E_{1,2} = E_1 - E_2 = 2\mathscr{E}_\varepsilon^{1/2}. \tag{30.11}$$

A dilation along the [001] axis results in a splitting of

$$\delta E_{1,2} = 2|b\varepsilon_{zz}'|, \tag{30.12}$$

where $\varepsilon_{zz}' = \varepsilon_{zz} - \varepsilon_{xx} = \varepsilon_{zz} - \varepsilon_{yy}$ is the relative strain along the [001] axis. Under a dilation of the crystal along the [111] axis, when (see (29.30)) $\varepsilon_{xy} = \varepsilon_{xz} = \varepsilon_{yz} = \varepsilon_{111}'/3$, where ε_{111}' is the relative elongation along the axis, $\varepsilon_{111}' = \varepsilon_{111} - \varepsilon_{1\bar{1}0} = \varepsilon_{111} - \varepsilon_{11\bar{2}}$, then

$$\delta E_{1,2} = \frac{2}{\sqrt{3}}|d\varepsilon_{111}'|. \tag{30.13}$$

Hence it is clear that the constant b determines the splitting due to dilation along the [100], [010], [001] axes, the constant d fills this role for the [111], [$\bar{1}$11], etc. axes.

We shall consider the spectrum for low kinetic energies $E_k \ll \delta E_{1,2}$ and high energies $E_k \gg \delta E_{1,2}$ separately, since the behavior of the spectrum in these regions is significantly different.

Low energies. To determine the spectrum near an extremum under an anisotropic strain, we must expand (30.5) in powers of $\mathscr{E}_{ek}/\mathscr{E}_e$, omitting the term $\mathscr{E}_k$. To a first approximation,

$$E_{1,2}(\varepsilon, \boldsymbol{k}) = a\varepsilon \pm \mathscr{E}_e^{1/2} + \left(A \mp \frac{Bb\varepsilon}{2\mathscr{E}_e^{1/2}}\right) k^2 \pm$$
$$\pm \left\{ \frac{3Bb}{2\mathscr{E}_e^{1/2}} (k_x^2 \varepsilon_{xx} + k_y^2 \varepsilon_{yy} + k_z^2 \varepsilon_{zz}) + \right.$$
$$\left. + \frac{Dd}{\mathscr{E}_e^{1/2}} (k_x k_y \varepsilon_{xy} + k_x k_z \varepsilon_{xz} + k_y k_z \varepsilon_{yz}) \right\}. \qquad (30.14)$$

We see that the constant energy surfaces near an extremum in the strained crystal are ellipsoids, whose principal axes are the principal axes of the reduced strain tensor:

$$\varepsilon'_{ij} = \begin{cases} \varepsilon_{ij} & \text{if} \quad i = j, \\ (Dd/3Bb)\,\varepsilon_{ij} & \text{if} \quad i \neq j. \end{cases} \qquad (30.15)$$

The directions of these axes and the tensor components ε'_{ij} relative to the principal axes may be determined by solving the secular equation

$$|\varepsilon'_{ij} - \varepsilon'' \delta_{ij}| = 0. \qquad (30.16)$$

The three roots of this cubic equation determine the three components ε''_{ii} referred to the principal axes. By (30.14), in this coordinate system

$$E_{1,2}(\boldsymbol{k}) = a\varepsilon \pm \mathscr{E}_e^{1/2} + \frac{\hbar^2}{2} \sum_i \frac{k^2}{m^*_{ii}}, \qquad (30.17)$$

where

$$\frac{\hbar^2}{2m^*_{ii}} = A \pm \frac{Bb}{2\mathscr{E}_e^{1/2}} (3\varepsilon''_{ii} - \varepsilon). \qquad (30.18)$$

For example, under a dilation along the [100], [010], or [001] axes (Figure 30), for the upper of the split-off bands,

$$\frac{\hbar^2}{2m^*_{\parallel}} = A \pm B, \quad \frac{\hbar^2}{2m^*_{\perp}} = A \mp \frac{B}{2}. \qquad (30.19)$$

The upper sign corresponds to $b\varepsilon'_{zz} > 0$, the lower sign to $b\varepsilon'_{zz} < 0$. For the lower of the bands, the signs are reversed.

Under a dilation along the [111] axis, for the upper of the bands

$$\frac{\hbar^2}{2m^*_{\parallel}} = A \pm \frac{D}{\sqrt{3}}, \quad \frac{\hbar^2}{2m^*_{\perp}} = A \mp \frac{D}{2\sqrt{3}}, \qquad (30.20)$$

where the upper sign corresponds to $d\varepsilon'_{111} > 0$, the lower sign to $d\varepsilon'_{111} < 0$. The z'-axis lies along the [111] direction, the x'- and y'-axes perpendicular to it, say along $[1\bar{1}0]$ and $[11\bar{2}]$:

$$k_{z'} = \frac{1}{\sqrt{3}}(k_x + k_y + k_z), \; k_{x'} = \frac{1}{\sqrt{2}}(-k_x + k_y), \quad k_{y'} = \frac{1}{\sqrt{6}}(k_x + k_y - 2k_z), \qquad (30.20a)$$

so that

$$2(k_x k_y + k_x k_z + k_y k_z) = 3k_{z'}^2 - k^2 = 2k_{z'}^2 - k_{x'}^2 - k_{y'}^2.$$

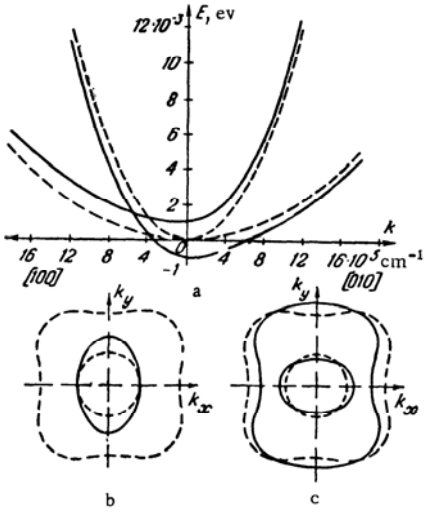

FIGURE 30. The spectrum $E(\boldsymbol{k})$ (a) and the shape of the constant energy surfaces in p-Ge, for a [100] strain; (b) low energy region, (c) high energy region. The dashed lines show the shape of $E(\boldsymbol{k})$ and the constant energy surface in the unstrained crystal.

Formulas (30.14), (30.17)–(30.20) are valid for the upper of the split-off electron bands, provided its kinetic energy $E(\boldsymbol{k})$ is small compared with the separation $\delta E_{1,2}$ to the other split-off band, as determined by (30.11)–(30.13). The effective masses themselves, as remarked in §28, do not depend on the magnitude of the strain but only on its direction. Only the energy of electrons satisfying (30.14) depends on the magnitude of the strain.

Expanding expression (30.5) up to k^4 terms, we can allow for the nonparabolic nature of the band in the strained crystal near the extremum. In this approximation,

$$E_{1,2} = Ak^2 + a\varepsilon \pm \left\{ \mathscr{E}_\varepsilon^{1/2} + \frac{1}{2}\frac{\mathscr{E}_{\varepsilon k}}{\mathscr{E}_\varepsilon^{1/2}} - \frac{1}{8}\frac{\mathscr{E}_{\varepsilon k}^2}{\mathscr{E}_\varepsilon^{3/2}} + \frac{1}{2}\frac{\mathscr{E}_k}{\mathscr{E}_\varepsilon^{1/2}} \right\}. \tag{30.21}$$

For large strains in crystals with small spin-orbit splitting, we must also introduce corrections due to the other split-off band, since the splitting caused by the strain may amount to a significant fraction of the spin-orbit splitting. The matrix $\mathscr{H}(\boldsymbol{k})$ for the two bands in the $(Y_m^{3/2}, Y_m^{1/2})$ representation is given in Table 24.1. The matrix $\mathscr{H}(\varepsilon)$ in this representation is readily derived from (30.2). It is similar in form to Table 24.1, except that F is replaced by f, I by j, H by h, and G by g.

To obtain the corrections to $E(\varepsilon, \boldsymbol{k})$ due to the other split-off band, we must partially diagonalize the matrix $\mathscr{H}(\boldsymbol{k}, \varepsilon)$, eliminating the interband terms. As shown in §15 (equation (15.49a)), this transforms the matrix $\mathscr{H}_{11}$ with components $\mathscr{H}_{m'm}$ $(m, m' = 1, 2, 3, 4)$ into

$$\tilde{\mathscr{H}}_{11} = \mathscr{H}_{11} + \frac{1}{\Delta}\mathscr{H}_{1\,11}\mathscr{H}_{11\,1}, \tag{30.22}$$

where $\mathcal{H}_{I\,II}$ is the off-diagonal matrix with components $\mathcal{H}_{ms}(m = 1, 2, 3, 4,\ s = 5,6)$ and Δ is the spin-orbit splitting, $\Delta = E_I - E_{II}$. As in (24.20), under the transformation (30.22) the matrix elements $\tilde{F} = F + f$, $\tilde{G} = G + g$, $\tilde{H} = H + h$, $\tilde{I} = I + j$ become, respectively,

$$\overline{F} = \tilde{F} + \frac{1}{2\Delta}(|\tilde{H}|^2 + 4|\tilde{I}|^2), \quad \overline{G} = \tilde{G} + \frac{1}{2\Delta}[(\tilde{F} - \tilde{G})^2 + 3|\tilde{H}|^2],$$
$$\overline{H} = \tilde{H} - \frac{1}{2\Delta}[\tilde{H}(\tilde{F} - \tilde{G}) + 2\sqrt{3}\tilde{I}\tilde{H}^*], \tag{30.23}$$
$$\overline{I} = \tilde{I} + \frac{1}{2\Delta}[2\tilde{I}(\tilde{F} - \tilde{G}) - \sqrt{3}\tilde{H}^2].$$

Substituting $\overline{F}$, $\overline{G}$, $\overline{H}$, $\overline{I}$ into (24.14) and retaining additional terms of order ε^2/Δ and $\varepsilon k^2/\Delta$, we obtain

$$E(\varepsilon, \boldsymbol{k}) = E_0(\varepsilon, \boldsymbol{k}) + \frac{1}{\Delta}\left(\mathscr{E}_\varepsilon \pm \frac{1}{2}\frac{\mathscr{E}_{\varepsilon^3}}{\mathscr{E}_\varepsilon^{1/2}}\right) + \frac{1}{\Delta}\left[\mathscr{E}_{\varepsilon k} \pm \frac{1}{2\mathscr{E}_\varepsilon^{1/2}}\left(\mathscr{E}_{\varepsilon^2 k^2} - \frac{1}{2}\frac{\mathscr{E}_{\varepsilon^3}\mathscr{E}_{\varepsilon k}}{\mathscr{E}_\varepsilon}\right)\right], \tag{30.24}$$

where $E_0(\varepsilon, \boldsymbol{k})$ is defined by (30.14), $\mathscr{E}_{\varepsilon k}$ and $\mathscr{E}_\varepsilon$ by (30.7) and (30.8), and

$$\mathscr{E}_{\varepsilon^3} = -b^3[(\varepsilon - 3\varepsilon_{xx})(\varepsilon - 3\varepsilon_{yy})(\varepsilon - 3\varepsilon_{zz})] + 6\sqrt{3}\,d^3\varepsilon_{xy}\varepsilon_{xz}\varepsilon_{yz} +$$
$$+ 3bd^2[(\varepsilon - 3\varepsilon_{xx})\varepsilon_{yz}^2 + (\varepsilon - 3\varepsilon_{yy})\varepsilon_{xz}^2 + (\varepsilon - 3\varepsilon_{zz})\varepsilon_{xy}^2], \tag{30.25}$$

$$\mathscr{E}_{\varepsilon^2 k^2} = -Bb^2[(k^2 - 3k_x^2)(\varepsilon - 3\varepsilon_{yy})(\varepsilon - 3\varepsilon_{zz}) +$$
$$+ (k^2 - 3k_y^2)(\varepsilon - 3\varepsilon_{xx})(\varepsilon - 3\varepsilon_{zz}) + (k^2 - 3k_z^2)(\varepsilon - 3\varepsilon_{xx})(\varepsilon - 3\varepsilon_{yy})] +$$
$$+ 6\sqrt{3}\,Dd^2[k_x k_y \varepsilon_{xz}\varepsilon_{yz} + k_x k_z \varepsilon_{xy}\varepsilon_{yz} + k_y k_z \varepsilon_{xy}\varepsilon_{xz}] +$$
$$+ 3Bd^2[(k^2 - 3k_x^2)\varepsilon_{yz}^2 + (k^2 - 3k_y^2)\varepsilon_{xz}^2 + (k^2 - 3k_z^2)\varepsilon_{xy}^2] +$$
$$+ 6Dbd[k_y k_z \varepsilon_{yz}(\varepsilon - 3\varepsilon_{xx}) + k_x k_z \varepsilon_{xz}(\varepsilon - 3\varepsilon_{yy}) + k_x k_y \varepsilon_{xy}(\varepsilon - 3\varepsilon_{zz})]. \tag{30.26}$$

We see from equation (30.24) that inclusion of the split-off band leads to two effects: first, a nonlinear dependence of the degenerate band splitting under strain. Counting the split-off band,

$$\delta E_{1,2} = E_1 - E_2 = 2\mathscr{E}_\varepsilon^{1/2} + \frac{\mathscr{E}_{\varepsilon^3}}{\Delta\mathscr{E}_\varepsilon^{1/2}}. \tag{30.27}$$

Thus, for a [001] strain

$$\delta E_{1,2} = 2|b\varepsilon'_{zz}|\left(1 + \frac{b\varepsilon'_{zz}}{\Delta}\right), \tag{30.28}$$

and for a [111] strain

$$\delta E_{1,2} = \frac{2}{\sqrt{3}}|d\varepsilon'_{111}|\left(1 + \frac{d\varepsilon'_{111}}{\sqrt{3}\,\Delta}\right). \tag{30.29}$$

It is clear that the sign of the correction quadratic in ε depends on that of $b\varepsilon'$ or $d\varepsilon'$, respectively. This effect thus makes it possible to determine the sign of the constants b and d.

The second effect, which also enables us to determine the sign and the magnitude of these constants, is a change in effective masses in a strongly strained crystal, described by the last term in (30.24).

According to this equation, for a [100] strain the upper of the split-off bands gives*

* E is the electron energy, and so the highest value of E corresponds to the lower hole level.

$$\frac{\hbar^2}{2m_\parallel^*} = A \pm B\left(1 + 2\frac{|b\varepsilon'_{zz}| + b\varepsilon'_{zz}}{\Delta}\right),$$
$$\frac{\hbar^2}{2m_\perp^*} = A \mp \frac{B}{2}\left(1 + 2\frac{|b\varepsilon'_{zz}| + b\varepsilon'_{zz}}{\Delta}\right). \tag{30.30}$$

Clearly, if $b\varepsilon'_{zz} < 0$ the effect is absent, while if $b\varepsilon'_{zz} > 0$ the change in inverse mass is

$$\delta\left(\frac{\hbar^2}{2m_\parallel^*}\right) = 4B\frac{b\varepsilon'_{zz}}{\Delta}, \quad \delta\left(\frac{\hbar^2}{2m_\perp^*}\right) = -2B\frac{b\varepsilon'_{zz}}{\Delta}. \tag{30.30a}$$

Similarly, for a [111] strain the effect does not appear for the upper of the split-off bands if $d\varepsilon'_{111} < 0$; it is also absent for the lower band if $d\varepsilon'_{111} > 0$. If $d\varepsilon'_{111} > 0$, then for the upper band

$$\delta\left(\frac{\hbar^2}{2m_\parallel^*}\right) = \frac{4}{3}D\frac{d\varepsilon'_{111}}{\Delta}, \quad \delta\left(\frac{\hbar^2}{2m_\perp^*}\right) = -\frac{2}{3}D\frac{d\varepsilon'_{111}}{\Delta}. \tag{30.31}$$

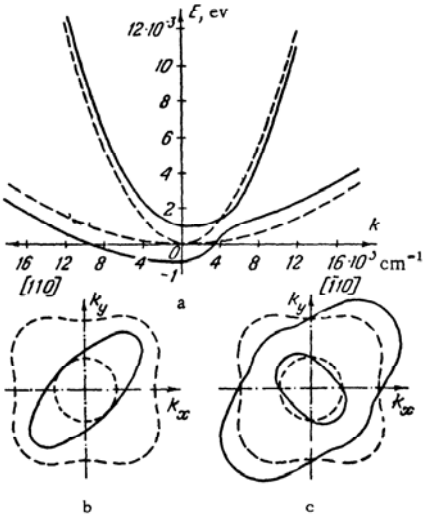

FIGURE 31. The spectrum $E(\boldsymbol{k})$ (a) and the shape of the constant energy surfaces in Ge for a [110] strain; (b) low energy region, (c) high energy region.

The nonappearance of the effect for one of the bands, depending on the sign of the strain, is not a general feature of equation (30.27) but occurs only for the [100] and [111] directions. In other cases the effect appears irrespective of the sign. For example, for a dilation along the [110] axis (Figure 31), if $\varepsilon_{110} = -\varepsilon_{1\bar{1}0} = \varepsilon_{xy} \neq 0$, then, for the upper band

$$\frac{\hbar^2}{2m^*_{z'z'}} = A, \quad \frac{\hbar^2}{2m^*_{x'x'}} = A \pm \frac{D}{2}, \quad \frac{\hbar^2}{2m^*_{y'y'}} = A \mp \frac{D}{2}. \tag{30.32}$$

The upper sign corresponds to $d\varepsilon_{110} > 0$, the lower sign to $d\varepsilon_{110} < 0$. The effective mass corrections proportional to the strain are determined by the

expressions:

$$\delta\left(\frac{\hbar^2}{2m_{x'x'}}\right)=\mp 3B\frac{|de_{110}|}{\Delta},$$
$$\delta\left(\frac{\hbar^2}{2m_{x'x'}}\right)=\frac{1}{\Delta}\left(De_{110}\pm\frac{3}{2}B|de_{110}|\right), \qquad (30.32a)$$
$$\delta\left(\frac{\hbar^2}{2m_{y'y'}}\right)=\frac{1}{\Delta}\left(-De_{110}\pm\frac{3}{2}B|de_{110}|\right)$$

(the upper sign corresponds to the upper band, the lower sign to the lower band). The x'-axis is directed along [110], y' along [1$\bar{1}$0], and z' along [001].* From (30.31), (30.32), (30.32a), we see that in all cases

$$\delta\left(\frac{1}{m_{xx}}+\frac{1}{m_{yy}}+\frac{1}{m_{zz}}\right)=0.$$

In the above derivation we assumed that the spin-orbit splitting Δ is independent of the strain. The exact Hamiltonian $\mathcal{H}(\varepsilon)$ for the two valence bands Γ_7 and Γ_9, incorporating the change in spin-orbit splitting and the mixture of states Γ_7 and Γ_9 due to the strain, is similar to (26.15) ($j=1$):

$$\mathcal{H}(\varepsilon)=(a+2b)\varepsilon-3b\sum_i J_i^2\varepsilon_{ii}-2\sqrt{3}\,d\sum_{i>j}[J_iJ_j]\varepsilon_{ij}+$$
$$+\frac{1}{3}\Delta(J\sigma)+\left(\alpha+\frac{1}{2}\beta\right)(J\sigma)\varepsilon-\frac{3}{2}\beta\sum_i J_i\sigma_i\varepsilon_{ii}-\sqrt{3}\,\delta\sum_{i>j}[J_i\sigma_j]\varepsilon_{ij}. \qquad (30.33)$$

The constants β and δ are of the same order of magnitude as the spin-orbit splitting Δ, and therefore the relative contribution of the last three terms in (30.33) is small. When they are taken into account, the corrections to a, b, d in (30.3)–(30.8), are α, β, δ, respectively.

High energies. For high energies, $\mathcal{E}_k\gg\mathcal{E}_{\varepsilon k}\gg\mathcal{E}_\varepsilon$, the effect of strain may be treated as a perturbation. We can thus omit the term $\mathcal{E}_\varepsilon$ in the general equation (30.5) and expand the term under the radical sign in powers of $\mathcal{E}_{\varepsilon k}/\mathcal{E}_k$; the result is

$$E_{1,2}(k)=E_{01,2}(k)+\Delta E_{1,2}=$$
$$=E_{01,2}(k)+a\varepsilon\pm\frac{1}{2\mathcal{E}_k^{1/2}}\{Bb[3(k_x^2e_{xx}+k_y^2e_{yy}+k_z^2e_{zz})-k^2\varepsilon]+$$
$$+2Dd[k_xk_ye_{xy}+k_xk_ze_{xz}+k_yk_ze_{yz}]\}, \qquad (30.34)$$

where $E_{01,2}=Ak^2\pm\mathcal{E}_k^{1/2}$ is the energy in the unstrained crystal (24.14a). The behavior of $E(k)$ and the shape of the constant energy surfaces at high energies were shown in Figures 30 and 31.

* In analysis of experimental data in this case, it should be remembered that when the stress P is applied along the [110] direction the compression along the [110] and [001] axes is not the same; in other words, apart from the relative dilation along the [110] direction,

$$e'_{110}=e_{110}-\frac{1}{2}(e_{1\bar{1}0}+e_{001})=\frac{P}{4}(S_{11}-S_{12}+\frac{3}{2}S_{44}),$$

a dilation occurs along the [001] direction:

$$e_{001}-e_{1\bar{1}0}=\frac{P}{2}(S_{12}-S_{11}+\frac{1}{2}S_{44}).$$

Corresponding expressions for the effective masses are readily derived from the general equations (30.14) and (30.27).

We see from (30.34) that the energy correction $\Delta E_{1,2}$ due to strain satisfies the condition

$$\frac{1}{4\pi}\int \Delta E_{1,2}(\boldsymbol{k})\, d\Omega = a\varepsilon. \tag{30.35}$$

The integral is evaluated over the solid angle Ω for fixed $|\boldsymbol{k}|$. Indeed, because of the cubic symmetry of $\mathscr{E}_{\boldsymbol{k}}$,

$$\int \frac{k_x^2}{\mathscr{E}_{\boldsymbol{k}}^{1/2}}\, d\Omega = \int \frac{k_y^2}{\mathscr{E}_{\boldsymbol{k}}^{1/2}}\, d\Omega = \int \frac{k_z^2}{\mathscr{E}_{\boldsymbol{k}}^{1/2}}\, d\Omega;$$

hence

$$\int \frac{k^2 - 3k_i^2}{\mathscr{E}_{\boldsymbol{k}}^{1/2}}\, d\Omega = 0.$$

Similarly, for $i \neq k$

$$\int \frac{k_i k_k}{\mathscr{E}_{\boldsymbol{k}}^{1/2}}\, d\Omega = 0.$$

Condition (30.35) means that the ratio of the concentrations of light and heavy holes,

$$\frac{n_1}{n_2} = \frac{\int \exp\left\{-\left(E_1^0 + \Delta E_1\right)/kT\right\} k^2\, dk\, d\Omega}{\int \exp\left\{-\left(E_2^0 + \Delta E_2\right)/kT\right\} k^2\, dk\, d\Omega},$$

is invariant under strain in the linear ε approximation.

It is characteristic that the energy correction $\Delta E_{1,2}$ due to strain does not depend on the magnitude of $\boldsymbol{k}$ but only on its direction. Thus, for a [001] strain

$$\Delta E_{1,2}(\boldsymbol{k}) = a\varepsilon \pm \frac{Bb}{2\mathscr{E}_{\boldsymbol{k}}^{1/2}}\left(3k_z^2 - k^2\right)\varepsilon'_{zz}, \tag{30.36}$$

where ε'_{zz} is the relative elongation along the [001] axis. For a [111] strain

$$\Delta E_{1,2}(\boldsymbol{k}) = a\varepsilon \pm \frac{Dd}{6\mathscr{E}_{\boldsymbol{k}}^{1/2}}\left(3k_{z'}^2 - k^2\right)\varepsilon'_{111}, \tag{30.37}$$

where, as in (30.20a), the z'-axis lies along [111] and ε'_{111} is the relative elongation along this axis.

As we shall show in §34, it is precisely this effect of strain on the spectrum that causes relatively large changes in conductivity and other kinetic coefficients under strain. Equations (30.34)–(30.37) are also valid for semiconductors with a zinc blende lattice, such as InSb, CaAs, since the linear $\boldsymbol{k}$ terms that appear in this lattice owing to the absence of an inversion center are usually insignificant at the fairly high temperatures for which these equations are applicable. In the low energy range, however, these terms may be significant.

Spectrum in strained InSb-type crystals at low energies As shown in §26, the Hamiltonian $\mathscr{H}(\boldsymbol{k})$ for InSb-type crystals includes a matrix $\mathscr{H}'$ (26.17),

$$\mathscr{H}' = \frac{4}{\sqrt{3}}\,\boldsymbol{\mathcal{k}}(\boldsymbol{V}\,\boldsymbol{k}), \tag{30.38}$$

which contains linear k terms is given by (26.17a). In the unstrained crystal, these linear terms remove degeneracy and shift the extremum from $k = 0$ to equivalent points on the [111] axis. In the strained crystal, the linear terms split each of the two bands formed as a result of the strain and shift the extremum. If the energy change due to the linear k terms, i.e., the difference between the energy at $k = 0$ and the energy at the extremum k_0, is much smaller than the separation of the bands split by the strain, we may regard the matrix $\mathcal{H}'$ as a perturbation and find the appropriate energy corrections by calculating the matrix elements of $\mathcal{H}'$ between eigenfunctions F_l^l which diagonalize the Hamiltonian $\mathcal{H}(\varepsilon, k)$ defined by (30.3) and (24.13) and correspond to one of the split-off bands. These functions are defined by an equation similar to (24.19), with E, F, G, I, H replaced by E_l, F, G, H, I, which involve both quadratic k terms and terms linear in the strain (see (24.11), (30.4), (30.5)). Here first order perturbation theory can account for only the lower of the split-off bands. When we include the linear k terms, the spectrum $E(\varepsilon, k)$ is determined by the secular equation

$$|IE_l + \mathcal{H}_l' - IE| = 0, \tag{30.39}$$

where $\mathcal{H}_l'$ is the matrix of the operator (30.38) in the representation (24.19). When calculating δE_l in a strongly strained crystal, we need include only terms proportional to the strain tensor components, i.e., one set $F = f$, etc., where f, g, h, j are defined by (30.4). Inclusion of k^2 terms would result in corrections proportional to k^3. To this approximation, the energy correction due to the linear k terms is

$$\delta E = \pm \frac{|\mathcal{k}|}{\mathcal{E}_\varepsilon^{1/2}} \left\{ \sum_{l>j} \alpha_{lj} k_l k_j \right\}^{1/2}, \tag{30.40}$$

where

$$\begin{aligned} \alpha_{xx} &= 3b^2(\varepsilon_{yy} - \varepsilon_{zz})^2 + 4d(\varepsilon_{xy}^2 + \varepsilon_{xz}^2), \\ \alpha_{xy} &= \mp 4\sqrt{3}\, d\mathcal{E}_\varepsilon^{1/2}\varepsilon_{xy} + 4d^2\varepsilon_{xz}\varepsilon_{yz}, \end{aligned} \tag{30.41}$$

and so on. The upper sign in the expression for α_{xy} corresponds to the upper band, the lower sign to the lower band.

It follows from (30.19) and (30.40) that when a strain is applied along the [100] axis the spectrum for the upper band near the extremum is given by

$$E^{\pm}(k) = (A \pm B)k_z^2 + \left(A \mp \frac{B}{2}\right)(k_\perp - k_\perp^0)^2, \tag{30.42}$$

where

$$k_\perp^2 = k_x^2 + k_y^2, \quad k_\perp^0 = \frac{\sqrt{3}}{2} \frac{|\mathcal{k}|}{A \mp \frac{B}{2}}.$$

Here, as in (30.19), the upper sign for B corresponds to $b\varepsilon_{zz} > 0$, the lower to $b\varepsilon_{zz} < 0$.

The linear k terms cause complete removal of degeneracy and shift the extremum from $k = 0$ to the annulus $k_\perp = k_\perp^0$. Near the extremum the constant energy surfaces are toroidal.

The spectrum has the same form for a [111] strain, provided $d\varepsilon_{111}' > 0$, for then, by (30.20) and (30.40),

$$E^{\pm} = \left(A + \frac{D}{\sqrt{3}}\right) k_{z'}^2 + \left(A - \frac{D}{2\sqrt{3}}\right)(k_\perp - k_\perp^0)^2, \tag{30.43}$$

where

$$k_\perp^0 = \frac{\sqrt{2}\, k}{A - (D/2\sqrt{3})}.$$

If $de'_{111} < 0$, the extrema are shifted along the z'-axis to a distance $\pm k_{z'}^0$ from $k = 0$, and the constant energy surfaces are two displaced ellipsoids:

$$E^{\pm} = \left(A - \frac{D}{\sqrt{3}}\right)(k_{z'} \pm k_{z'}^0)^2 + \left(A + \frac{D}{2\sqrt{3}}\right) k_\perp^2, \tag{30.44}$$

where

$$k_{z'}^0 = \frac{\sqrt{2}\,|k|}{A - (D/\sqrt{3})}.$$

In equations (30.42)–(30.44) the energy is measured from the new extremum point. As noted above, these expressions are valid for strains such that the band splitting $\delta E_{1,2}$ (i.e., $2\,|b e'_{zz}|$ or $(2/\sqrt{3})|d e'_{111}|$, respectively) considerably exceeds the difference between the energies at $k = 0$ and at the new extremum point k_0, which is $\frac{3}{4}k^2 \Big/ \left(A \mp \frac{B}{2}\right)$ for a [001] strain and $2k^2 \Big/ \left(A - \frac{D}{2\sqrt{3}}\right)$ ($d e_{111} > 0$) or $2k^2 \Big/ \left(A - \frac{D}{\sqrt{3}}\right)$ ($d e_{111} < 0$) for a [111] strain. Of course, the energy $E(k)$ must also be small compared to $\delta E_{1,2}$.

Corrections to effective mass due to interaction with a degenerate band. As mentioned in the preceding section, interaction with a degenerate band may change the symmetry of the spectrum in a nondegenerate band when the crystal is strained. For example, the change in the spectrum for the representation $\Gamma_1^{\pm}$ or $\Gamma_2^{\pm}$, due to interaction with the representation $\Gamma_{15}^{\mp}$ or $\Gamma_{25}^{\mp}$, respectively, is (see (29.39))

$$\Delta E(\mathbf{e}, k) = \frac{1}{3}\frac{\hbar^2}{m^2}|p|^2 k^2 (C - a)\left(\frac{1}{(E_g + \Delta)^2} + \frac{2}{E_g^2}\right)\mathbf{e} + \\ + \frac{1}{3}\frac{\hbar^2}{m^2}|p|^2 \mathscr{E}'_{\mathbf{e}k}\left(\frac{2}{E_g(E_g + \Delta)} + \frac{1}{E_g^2}\right) + C\mathbf{e}, \tag{30.45}$$

where $\mathscr{E}'_{\mathbf{e}k}$ is defined by the formula obtained from (30.7) when 1 is substituted for B and $D/\sqrt{3}$. The first term, which arises from the first term in (29.39), describes an isotropic change in effective mass, as in (29.41) and (29.42), while the second slightly distorts the spherical shape of the constant energy surface when the strain is anisotropic.

The derivation of this equation uses the fact that the matrix elements of the operator $\mathscr{H}(\mathbf{e})$ defined by equation (30.33) (which is similar to Table 24.1) have both nonzero "intraband" elements between the functions of the representation $\Gamma_8^{\pm}$ and nonzero "interband" elements between the functions of the representations $\Gamma_8^{\pm}$ and $\Gamma_6^{\pm}$ or $\Gamma_7^{\pm}$. By (24.34), the operator $\mathscr{H}_k$ has nonzero matrix elements $\langle S|p_x|X\rangle = \langle S|p_y|Y\rangle = \langle S|p_z|Z\rangle = p$ (or $\langle XYZ|p_z|XY\rangle$, ...), and the spectrum in the unstrained crystal is

$$E^0(k) = \frac{1}{3}\frac{\hbar^2|p|^2}{m^2}k^2\left(\frac{1}{E_g + \Delta} + \frac{2}{E_g}\right). \tag{30.46}$$

Effect of strain on spectrum in Sn and HgTe crystals. It has recently been established that in gray tin crystals, which have a diamond

lattice structure, and also in HgTe crystals with a zinc blende structure, the bands Γ_8 and $\Gamma_6(\Gamma_7)$ at $k = 0$ are reversed in comparison with Ge or InSb; to be precise: Γ_6 (or Γ_7^-), which is the conduction band in InSb and Ge, lies below Γ_8 (or Γ_8^+), between the latter and the band Γ_7 (Γ_7^+) which splits off from Γ_8 (Γ_8^+) owing to spin-orbit coupling.* Since the curvature of one of the branches of Γ_8 (the band forming the light hole band in Ge) and Γ_6 is determined mainly by their kp-interaction, the curvature of these bands in Sn and HgTe is the reverse of that in Ge and InSb (Figure 32). Thus the band Γ_6 (Γ_7^-) is completely filled, i.e., it is the lowest valence band, and the branch corresponding to heavy holes in the band Γ_8 (Γ_8^+) is also completely filled, while the light hole branch in Ge is empty, i.e., it is the conduction band in Sn and HgTe. Since the two branches of Γ_8 converge at $k = 0$, these crystals are semimetals, i.e., they display no band gap.

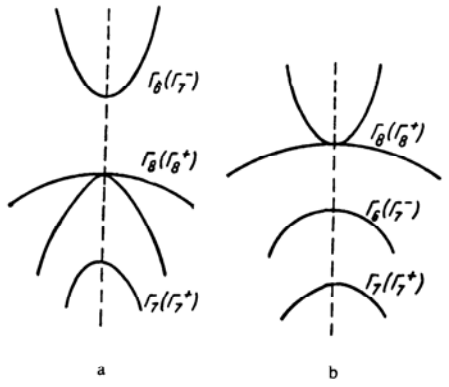

FIGURE 32. Positions of bands in Ge and InSb crystals (a), HgTe and gray tin (b).

The spectrum in the three bands Γ_8 (Γ_8^+), Γ_7 (Γ_7^+) and Γ_6 (Γ_7^-) in these crystals is described as before by the system of levels in Table 24.2, but with E_g replaced by $-E_g$. Moreover, $E_g < \Delta_{so}$. The spectrum of the bands converging near the extremum is described by equations (24.13), (24.14). It should be noted that now, as opposed to Ge and Si, the constant A is positive, and $|B| > A$ since the heavy hole band, as in Ge, points downward. The most interesting feature of strain-induced effects in such crystals is that a uniaxial strain which splits the Γ_8 (Γ_8^+) band converts them from semimetals into semiconductors. The width of the band gap is then proportional to the strain and is given by equations (30.11)–(30.13). The nature of the spectrum in the two bands is determined by equations 30.5)–(30.8), in the limiting low energy case by equations (30.14)–(30.21), and in the high energy case by (30.34) (note that for these crystals $A > 0$, $|B| > A$ and $|D|/\sqrt{3} > A$). Since the nearest band to Γ_8 (Γ_8^+) is Γ_6 (or Γ_7^-), the nonparabolic nature of the Γ_8 band and the behavior of the band gap and the effective masses under large strains are also determined, as in InSb, by the interaction of the bands Γ_8 (Γ_8^+) and Γ_6 (Γ_7^-), while the effect of the band Γ_7 (Γ_7^+), which plays the major role in Ge and Si, is less important here.

* See, e.g., /27.10–27.12/ for references to earlier publications.

Change in spectrum at X in an O_h lattice. As shown in §24, in the diamond lattice X is a point of zero slope for the representations X_1 and X_3. The spectrum at this point is most conveniently determined by the theory of invariants. By (25.36), in this case the operator $\mathscr{H}(k, \varepsilon)$ must involve even functions of k and ε which transform according to the representations $A_1^+ + B_1^- + B_2^+$, and odd functions of k which transform according to the representation A_2^-. These functions are given in Table 26.1. Taking matrices which transform according to these representations in the same form as in equation (26.6), we write $\mathscr{H}(k, \varepsilon)$ (without relativistically small terms) as

$$\mathscr{H}(k, \varepsilon) = \lambda I + \sigma_z (A_3 k_y k_z + D_3 \varepsilon_{yz}), \tag{30.47}$$

where

$$\lambda = A_1 k_x^2 + A_2 (k_y^2 + k_z^2) + D_1 \varepsilon_{zz} + D_2 (\varepsilon_{yy} + \varepsilon_{zz}). \tag{30.48}$$

Hence

$$E(k, \varepsilon) = \lambda \pm (A_3 k_y k_z + D_3 \varepsilon_{yz}). \tag{30.49}$$

It is evident that here band splitting at the extremum point may arise only from a shear ε_{yz}, and when this happens the constant energy surfaces near the extremum are ellipsoids:

$$E(k) = A_1 k_{x'}^2 + \left(A_2 \pm \frac{A_3}{2}\right) k_{y'}^2 + \left(A_2 \mp \frac{A_3}{2}\right) k_z^2, \tag{30.50}$$

where the y'- and z'-axes lie along the [011] and [01$\bar{1}$] axes, respectively.

A strain along the principal crystal axes [100], [010], or [001] does not cause splitting, but it does shift the different extrema relative to each other

The point X_2 is not a point of zero slope for the representations X_2 and X_4 In this case the operator $\mathscr{H}(\varepsilon, k)$ involves odd functions which transform according to the representation B_2^-, and even functions which transform according to $A_1^+ + A_1^- + B_2^+$. Functions of k and ε transforming according to these representations are given in Table 26.1; a suitable choice of matrices is σ_z, I, σ_x, σ_y. By (26.3)

$$\mathscr{H}(\varepsilon, k) = \lambda I + \sigma_x (A_3 k_y k_z + D_3 \varepsilon_{yz}) + A_4 \sigma_z k_x. \tag{30.51}$$

Hence

$$E(\varepsilon, k) = \lambda \pm [A_4^2 k_x^2 + (D_3 \varepsilon_{yz} + A_3 k_y k_z)^2]^{1/2}, \tag{30.52}$$

where λ is defined by equation (30.48).

As mentioned above, the conduction band extremum in Si corresponds to the representation Δ_1 and is located near the point X, where this representation, together with Δ_2', becomes X_2 or X_4.

If we assume that the expansion (30.52) is valid up to an extremum point k_0, a knowledge of the position of this point enables us to determine the constant A_4:

$$|A_4| = 2A_1 k_0.$$

Expanding the root in (30.52), we obtain the spectrum near this point:

$$E(\varepsilon, k) = A_1 (k_x - k_0)^2 + A_2 (k_y^2 + k_z^2) - \frac{D_3 A_3 \varepsilon_{yz}}{|A_4| k_0} k_y k_z + D_1 \varepsilon_{xx} + D_2 (\varepsilon_{yy} + \varepsilon_{zz}). \tag{30.53}$$

The last term in (30.53) coincides with (29.43). In this approximation, the splitting at $k_x = k_0$ is $\Delta = 2|A_4|k_0$, and the matrix element of the operator $\mathcal{H}^e_{yz}$ between the functions 1 and X is the same at both points k_0 and X, i.e., $C_1 = D_3$. Consequently, $\hbar^2/m' = A_3$. Hence it is clear that the strain ε_{yz} induces a comparatively large change in the mass at k_0 precisely because it is the only strain that splits the band X_2 or X_4 at the nearby point X.

§31. EFFECT OF STRAIN ON SPECTRUM IN WURTZITE-TYPE CRYSTALS

As mentioned in §23, the wurtzite lattice (space group C^4_{6v}) is typical of many semiconductors of the A_2B_6 group: BeO, MgTe, ZnO, ZnS, ZnSe, ZnTe, CdS, CdSe.* The little groups for this structure have highest symmetry at points on the axis (points Δ) and on the edge (points P) of the Brillouin zone. As shown in §23, the representations of these groups are projectively equivalent to vector or spinor representations, differing from the corresponding representations of the point groups C_{6v} (for points Δ) and C_{3v} (for points P) as given in §§11 and 16 only by the factor $e^{-ik_0\tau}$, where k_0 is the position of the point and τ the translation corresponding to the rotational element in question.

Tables 31.1 and 31.2 list the characters of the usual and spinor representations for these points. The lower table lists the spinor representations which split off from the vector representations when spin-orbit coupling is introduced.

TABLE 31.1. Representations for Δ

Number of elements	Element of class	Characters								
		Δ_1	Δ_2	Δ_3	Δ_4	Δ_5	Δ_6	Δ_7	Δ_8	Δ_9
1	$(e\,\|\,0)$	1	1	1	1	2	2	2	2	2
1	$(c_6\,\|\,t_0/2)$	η_k	η_k	$-\eta_k$	$-\eta_k$	η_k	$-\eta_k$	$\sqrt{3}\,\eta_k$	$-\sqrt{3}\,\eta_k$	0
1	$(c_6^5\,\|\,t_0/2)$							$-\sqrt{3}\,\eta_k$	$\sqrt{3}\,\eta_k$	0
1	$(c_3\,\|\,0)$	1	1	1	1	−1	−1	1	1	−2
1	$(c_3^2\,\|\,0)$							−1	−1	2
1	$(c_2\,\|\,t_0/2)$	η_k	η_k	$-\eta_k$	$-\eta_k$	$-2\eta_k$	$2\eta_k$	0	0	0
3	$(\sigma\,\|\,0)$	1	−1	−1	1	0	0	0	0	0
3	$(\sigma'\,\|\,t_0/2)$	η_k	$-\eta_k$	η_k	$-\eta_k$	0	0	0	0	0

$\eta_k = e^{-ik_0t_0/2}$. For points Γ and K $\eta_k = 1$, for points A and H $\eta_k = -i$.

The classification of the representations according to their behavior under time reversal and the representations which are combined owing to

* Some of these compounds also crystallize in zinc blende and NaCl-type lattices.

TABLE 31.2. Representations for P

Number of elements	Element of class	Characters					
		P_1	P_2	P_3	P_4	P_5	P_6
1	$(e \mid 0)$	1	1	2	1	1	2
1	$(c_3 \mid 0)$	1	1	−1	−1	−1	1
1	$(c_3^2 \mid 0)$				1	1	−1
3	$(\sigma' \mid t_0/2)$	η_k	$-\eta_k$	0	$i\eta_k$	$-i\eta_k$	0

$\mathscr{D}_l$	Δ_1	Δ_2	Δ_3	Δ_4	Δ_5	Δ_6	P_1	P_2	P_3
$\mathscr{D}_l \times \mathscr{D}_{1/2}$	Δ_7	Δ_7	Δ_8	Δ_8	$\Delta_7 + \Delta_9$	$\Delta_8 + \Delta_9$	P_6	P_6	$P_4 + P_5 + P_6$

invariance under time reversal were discussed in §23; they are summarized in Table 31.3.

TABLE 31.3. Time reversal properties of representations

Case	Representations
a_1	Γ_1, Γ_2, Γ_3, Γ_4, Γ_5, Γ_6, Γ_7, Γ_8, Γ_9
a_2	K_1, K_2, K_3, K_4, K_5, K_6, H_3, H_6
b_1	$A_1 - A_4$, $A_2 - A_3$, $A_5 - A_6$, $A_7 - A_8$
b_2	$H_1 - H_2$, $H_4 - H_5$
b_3	Δ_1, Δ_2, Δ_3, Δ_4, Δ_5, Δ_6, Δ_7, Δ_8, Δ_9, P_1, P_2, P_3, P_4, P_5, P_6
c_1	$A_9 - A_9$

To construct the spectrum at points on the Δ and P axes by the theory of invariants, we need the representations of the point groups C_{6v} and C_{3v} according to which the functions of the components k_i, ε_{ij}, σ_i, J_i transform. Using the basis functions of Table 11.1 (p. 72), we readily establish the distribution of these components among the representations, as given in Table 31.4.*

Knowing the characters of the representations of the little groups and the representations according to which the components k_i transform, we can use the equations of §21 to determine for which representations the points under

* When constructing the invariants, it is convenient to have all the functions of one representation transform according to identical representations. Therefore, in contrast to §26, the operators σ_+, σ_- and J_+, J_- in Table 31.4 are taken to be

$$\sigma_\pm = \pm\frac{i}{2}(\sigma_x \pm i\sigma_y),\ J_\pm = \pm\frac{i}{\sqrt{2}}(J_x \pm iJ_y),$$

which transform under all C_{6v} operations like $k_+ = k_x + ik_y$ and $k_- = k_x - ik_y$, respectively. A unitary transformation of the basis functions can transform these matrices $\sigma_\pm$ into the usual form (26.3). In this case the components H_+ and H_- are also conveniently chosen in the same form when the magnetic field is included in $\mathscr{H}$.

TABLE 31.4. Distribution of functions of k, ε, σ, J according to representations of point groups C_{6v} and C_{3v}

Representations		Functions		Basis matrices
C_{3v}	C_{6v}	odd (relative to time reversal)	even (relative to time reversal)	
A_1K_1	Γ_1A_1	k_z	k_z^2; $k_\perp^2$; ε_{zz}; $\varepsilon_\perp$; $\sigma_+k_- + \sigma_-k_+$	J_z^2, I
	Γ_3B_2	—	—	—
A_2K_2	Γ_2A_2	σ_z	σ_zk_z; $\sigma_+k_- - \sigma_-k_+$	J_z
	Γ_4B_1	—	—	—
EK_3	Γ_5E_1	σ_+, σ_-; k_+, k_-	k_+k_z, k_-k_z, ε_{+z}, ε_{-z}; σ_+k_z, σ_-k_z; σ_zk_+, σ_zk_-	J_+, J_- $[J_+J_z]$, $[J_-J_z]$
	Γ_6E_2		k_+^2, k_-^2; ε_+, ε_-, σ_+k_+, σ_-k_-	J_+^2, J_-^2

$k_\pm = k_x \pm ik_y$, $\sigma_\pm = \frac{1}{2}(\pm i\sigma_x - \sigma_y)$, $J_\pm = \frac{1}{\sqrt{2}}(\pm iJ_x - J_y)$, $k_\perp^2 = k_x^2 + k_y^2$; $\varepsilon_{\pm z} = \varepsilon_{xz} \pm i\varepsilon_{yz}$, $\varepsilon_\pm = \varepsilon_{xx} - \varepsilon_{yy} \pm 2i\varepsilon_{xy}$, $\varepsilon_\perp = \varepsilon_{xx} + \varepsilon_{yy}$.

discussion are points of zero slope and which of the components k_i may appear in the Hamiltonian $\mathscr{H}(k)$ for the various representations. These data are given in Table 31.5. The components enclosed in parentheses do not appear in the vector representations, but only in the spinor representations which split off from them. As a rule, the coefficients of these components are small. The Hamiltonian $\mathscr{H}(k, \varepsilon)$ for all the representations is readily constructed by the methods of §26, since all these representations are one- or two-dimensional.

TABLE 31.5. Nonzero components k_i occurring in $E(k)$ for different representations

$\underline{\Delta_1, \Delta_2, \Delta_3, \Delta_4}$	$\underline{\Delta_5, \Delta_6}$	$\underline{\Delta_7, \Delta_8}$	$\underline{\Delta_9}$	$\underline{P_1, P_2}$	P_3	$\underline{P_4, P_5}$	$\underline{P_6}$
k_z	k_z	$k_z(k_\perp)$	k_z	k_z	k_z, $k_\perp$	k_z	$k_z(k_\perp)$
$\underline{\Gamma_1, \Gamma_2, \Gamma_3, \Gamma_4}$	$\underline{\Gamma_5, \Gamma_6}$	$\underline{\Gamma_7, \Gamma_8}$	$\underline{\Gamma_9}$	K_1, K_2	K_3	$\underline{K_4, K_5}$	$\underline{K_6}$
—	—	$(k_\perp)$	—	—	$k_\perp$	—	$(k_\perp)$
$A_1 - A_4, A_2 - A_3$	$A_5 - A_6$	$A_7 - A_8$	$A_9 - A_9$	$H_1 - H_2$	$\underline{H_3}$	$\underline{H_4 - H_5}$	H_6
k_z	k_z	$k_z(k_\perp)$	k_z	k_z	—	(k_z)	—

Possible points of zero slope are underlined. Components k_i whose coefficients are relativistically small are enclosed in parenthesis.

Point Δ. It follows from (25.14) that for the one-dimensional representations $\Delta_1, \ldots, \Delta_4$ the operator $\mathcal{H}(\varepsilon, k)$ will contain all the functions of k, ε and σ which transform according to the identity representations of the point group Γ_1. Hence, if the relativistic terms are neglected, each of these terms is twofold degenerate counting spin and the constant energy surfaces are ellipsoids of revolution. If the linear k relativistic terms are taken into account, the operator $\mathcal{H}(\varepsilon, k)$ for the representations $\Delta_1, \ldots, \Delta_4$ becomes

$$\mathcal{H}(\varepsilon, k) = A_0 k_z + \lambda + \alpha_1(\sigma_+ k_- + \sigma_- k_+), \tag{31.1}$$

where

$$\lambda = A_1 k_z^2 + A_2 k_\perp^2 + D_1 \varepsilon_{zz} + D_2 \varepsilon_\perp,$$
$$k_\perp^2 = k_x^2 + k_y^2, \quad \varepsilon_\perp = \varepsilon_{xx} + \varepsilon_{yy}.$$

Here k_z is measured from the value k_{z0} at Δ. The constants A_l and D_l in (31.1) must be real for the Hamiltonian to be hermitian (recall that the hermitian conjugates of k_+, σ_+, J_+ are k_-, σ_-, J_-).

We determine the spectrum from (31.1). At a point of zero slope, where $A_0 = 0$,

$$E_{1,2}(k, \varepsilon) = A_1 k_z^2 + A_2(k_\perp \pm k_\perp^0)^2 + D_1 \varepsilon_{zz} + D_2 \varepsilon_\perp, \tag{31.2}$$

where $k_\perp^0 = \alpha_1 / 2A_2$. The energy is measured from the minimum. It is clear that if the relativistic terms are included the minimum is on the circumference: $k_z = 0$, $k_\perp = k_\perp^0$, and the constant energy surfaces near the extremum are toroidal. The degeneracy is completely removed except at points on the Δ axis.

For large k values, the linear terms become negligible, and the constant energy surfaces are two slightly warped ellipsoids.

Equation (31.1) may also be derived by constructing $\mathcal{H}(\varepsilon, k)$ for the representations Δ_7 or Δ_8, noting that in this case $\mathcal{H}(k, \varepsilon)$ should include all the functions of k and ε which transform according to the representations occurring in

$$\Delta_7 \times \Delta_7^* = \Delta_8 \times \Delta_8^* = A_1 + A_2 + E_1.$$

By (26.3), (26.31), a suitable choice of the matrices X_i which transform according to these representations is

$$I(A_1), \quad \rho_z = \sigma_z(A_2), \quad \rho_+ = \sigma_+ \quad \text{and} \quad \rho_- = \sigma_-(E_1).$$

This construction automatically accounts for relativistic terms quadratic in k and linear in ε, and the result is

$$\mathcal{H}(k, \varepsilon) = A_0 k_z + \lambda + \alpha_1(\rho_+ k_- + \rho_- k_+) + \\ + \alpha_2 k_z(\rho_+ k_- + \rho_- k_+) + d(\rho_+ \varepsilon_{-z} + \rho_- \varepsilon_{+z}). \tag{31.1a}$$

The last term in (31.1a) shows that application of strains ε_{xz} and ε_{yz} completely removes the degeneracy, and the band splitting is $2d(\varepsilon_{xz}^2 + \varepsilon_{yz}^2)^{1/2}$.

For the representation Δ_9, $\mathcal{H}(\varepsilon, k)$ will include functions of ε and k which transform according to representations occurring in $\Delta_9 \times \Delta_9^* = A_1 + A_2 + B_2 + B_1$, and

$$\mathcal{H}(k, \varepsilon) = A_0 k_z + \lambda; \tag{31.3}$$

consequently, $E(\varepsilon, k)$ differs from (31.2) in the absence of a linear k_z term;

the band Δ_9 remains degenerate at all points, up to higher order terms in k and ε, and the constant energy surfaces are ellipsoids.

The representation Δ_9 arises from splitting of representations Δ_5 or Δ_6. According to (25.14), in order to construct the operator $\mathcal{H}(\varepsilon, k)$ simultaneously for the representations $\Delta_7 + \Delta_9$ or $\Delta_8 + \Delta_9$ which arise from Δ_5 or Δ_6, respectively, we must include in $\mathcal{H}(k, \varepsilon)$ all functions of k, ε and σ which transform according to the representations occurring in

$$\Delta_5 \times \Delta_5^* = \Delta_6 \times \Delta_6^* = A_1 + A_2 + E_2.$$

By (26.3) and (26.31), we may choose the matrices X_l which transform according to these representations as $I(A_1)$, $\rho_z(A_2)$, $\rho_+, \rho_-(E_2)$. Then the operator $\mathcal{H}(k, \varepsilon)$ is

$$\begin{aligned}\mathcal{H}(\varepsilon, k) = A_0 k_z + \lambda + \Delta_2 \rho_z \sigma_z + A_5(\rho_+ k_-^2 + \rho_- k_+^2) + \\ + D_5(\rho_+ \varepsilon_- + \rho_- \varepsilon_+) + \alpha_1(\sigma_+ k_- + \sigma_- k_+) + \alpha_2(\rho_+ \sigma_- k_- + \rho_- \sigma_+ k_+) + \\ + \alpha_6 \rho_z \sigma_z k_z + i\alpha_7 \rho_z(\sigma_+ k_- - \sigma_- k_+).\end{aligned} \tag{31.4}$$

The constants are indexed here in the same way as in (31.8).

In matrix form, the Hamiltonian (31.4) is written

$$\mathcal{H}(\varepsilon, k) = \begin{Vmatrix} F & j^* & \not{k}^* & 0 \\ j & G & l^* & \not{k}^* \\ \not{k} & l & G & h^* \\ 0 & \not{k} & h & F \end{Vmatrix}, \tag{31.5}$$

where

$$\begin{aligned} F &= \lambda + A_0 k_z + \Delta_2 + \alpha_6 k_z, & l &= \alpha_2 k_+, \\ G &= \lambda + A_0 k_z - \Delta_2 - \alpha_6 k_z, & j &= (\alpha_1 - i\alpha_7) k_+, \\ \not{k} &= A_5 k_+^2 + D_5 \varepsilon_+, & h &= (\alpha_1 + i\alpha_7) k_+. \end{aligned}$$

In the general case the secular equation $|\mathcal{H} - IE| = 0$ is a quartic. If we neglect the relativistic linear k terms in (31.5), the roots become twofold degenerate, since these are the terms which determine the splitting of each band. To this approximation, at a point of zero slope,

$$\begin{aligned}E_{1,2}(k, \varepsilon) = \lambda \pm \{\Delta_2^2 + A_5^2 k_\perp^4 + D_5^2[(\varepsilon_{xx} - \varepsilon_{yy})^2 + 4\varepsilon_{xy}^2] + \\ + 2A_5 D_5[(k_x^2 - k_y^2)(\varepsilon_{xx} - \varepsilon_{yy}) + 4\varepsilon_{xy} k_x k_y]\}^{1/2}.\end{aligned} \tag{31.6}$$

At energies $E(k) \gg \Delta_2$, when spin-orbit splitting may be neglected, the constant energy surfaces are two ellipsoids

$$E(k) = A_1 k_z^2 + (A_2 \pm A_5) k_\perp^2, \tag{31.7a}$$

which are displaced and warped by the strain.

If the kinetic energy and the strain-induced splitting are small compared to the spin-orbit splitting, the spectrum $E(\varepsilon, k)$ near the extrema $E_1^0 = \Delta_2$ and $E_2^0 = -\Delta_2$ is given by

$$\begin{aligned}E_{1,2}(\varepsilon, k) = \pm \Delta_2 + \lambda \pm \frac{1}{2\Delta_2}\{A_5^2 k_\perp^4 + D_5^2[(\varepsilon_{xx} - \varepsilon_{yy})^2 + 4\varepsilon_{xy}^2] + \\ + 2A_5 D_5[(k_x^2 - k_y^2)(\varepsilon_{xx} - \varepsilon_{yy}) + 4\varepsilon_{xy} k_x k_y]\}.\end{aligned} \tag{31.7b}$$

It is clear that the effective masses $m_\parallel^*$ and $m_\perp^*$ are the same for both extrema

in the unstrained crystal; we have $\hbar^2/2m_{\parallel}^* = A_1$, $\hbar^2/2m_{\perp}^* = A_2$, but strains $\varepsilon_{xx} \neq \varepsilon_{yy}$ and ε_{xy} lead to a comparatively large anisotropy of the transverse effective masses, of the order of $D_5\varepsilon/\Delta_2$.

Point Γ. The point Γ differs from the point Δ in that here $k_0 = -k_0$, and all representations at this point belong to case (a_1). Therefore, it follows from (25.36) that, as opposed to the point Δ, the operator $\mathcal{H}$ for the representations $\Gamma_1, \ldots, \Gamma_4$ will include only functions of k, ε and σ which are even with respect to time reversal and transform according to the representation A_1; in other words, at the point Γ the constant A_0 in (31.1) vanishes. For Γ_7 and Γ_8, $\mathcal{H}(k, \varepsilon)$ will include even functions transforming according to $\{\Gamma_7^2\} = \{\Gamma_8^2\} = A_1$ and odd functions transforming according to $[\Gamma_7^2] = [\Gamma_8^2] = A_2 + E_1$. Consequently, at the point Γ we must set $A_0 = 0$ and $\alpha_2 = d = 0$ in (31.2). For Γ_9, $\mathcal{H}(\varepsilon, k)$ will include even functions transforming according to $\{\Gamma_9^2\} = A_1$ and odd functions transforming according to $[\Gamma_9^2] = A_2 + B_2 + B_1$; thus $\mathcal{H}(\varepsilon, k)$ will be the same as for Δ_9 (31.3). For Γ_5 or Γ_6, $\mathcal{H}(\varepsilon, k)$ will include even functions which transform according to $[\Gamma_5^2] = [\Gamma_6^2] = A_1 + E_2$ and odd functions which transform according to $\{\Gamma_5^2\} = \{\Gamma_6^2\} = A_2$, so that $A_0 = 0$ and $\alpha_6 = \alpha_7 = 0$ in (31.4).

Experimental data and numerical band structure calculations show that in compounds of the A_2B_6 group, such as CdS, CdSe, ZnS, ZnO, the valence and conduction band extrema are at the point Γ; the representation Γ_7 arising from Γ_1 corresponds to the conduction band, while the valence band is made up of three close-lying bands which correspond to representations Γ_9, Γ_7 and Γ_7 and are separated from the other bands by a comparatively large interval (Figure 33). The reason for this pattern is that the arrangement of the atoms of the first coordination sphere in all these crystals is similar to their arrangement in a cubic lattice, where they are at the vertices of a tetrahedron. Indeed, in the crystals in question the ratio of the basis vector t_0 on the z-axis to the perpendicular basis vector t_1 is 1.60–1.64, while for a tetrahedral arrangement this ratio must be $2\sqrt{2}/3 = 1.632$. The direction of t_0 corresponds to the [111] direction of a cubic crystal.*

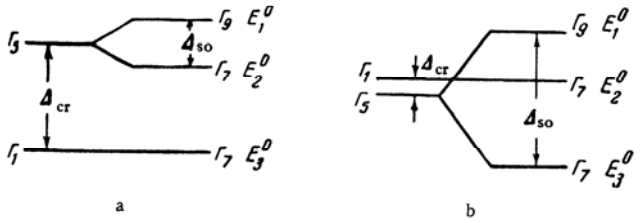

FIGURE 33. Origin of valence bands at Γ in crystals with wurtzite lattice. a) $\Delta_{cr} > \Delta_{so}$; b) $\Delta_{cr} < \Delta_{so}$.

Because of the relatively small deviation from cubic symmetry in these crystals, the distance between the terms Γ_1 and Γ_2, which are combined into one term Γ_{15} in the cubic lattice, is comparable with the spin-orbit splitting

* It should be borne in mind, though, that the positions of the atoms in the next coordination spheres in wurtzite and zinc blende lattices are quite different; consequently, in accordance with the hierarchy of systems developed in §5, no strain can convert one lattice into the other.

of the term Γ_5. In many situations, therefore, it is necessary to consider all three valence bands Γ_9, Γ_7, Γ_7 together. The Hamiltonian $\mathcal{H}(\varepsilon, k)$ for these three bands, which correspond to the representations Γ_1 and Γ_5, may be constructed following the rules outlined in §26.

According to (25.36), in case (a_1) $\mathcal{H}(\varepsilon, k)$ must contain functions which are even with respect to time reversal and transform according to $[(\Gamma_1+\Gamma_5)^2] = 2A_1+E_1+E_2$, and odd functions which transform according to $\{(\Gamma_1+\Gamma_5)^2\} = A_2+E_1$. In this case we may take the matrices J_i and their products in the representations Y_1^1, Y_0^1, and Y_{-1}^1 as the matrices $X_i^\varkappa$, since the representations Γ_1 and Γ_5 may be built up from basis functions of the representation $\mathcal{D}_1$. The distribution of these matrices according to the representations of C_{6v} was presented above in Table 31.4, and the matrices themselves are given in Table 31.7 below.

If we include in $\mathcal{H}(\varepsilon, k)$ only relativistic terms linear in k, as in (31.4), then the operator $\mathcal{H}(k, \varepsilon)$ is*

$$\begin{aligned}\mathcal{H}(k,\varepsilon) = {}& \Delta_1 J_z^2 + \Delta_2 J_z\sigma_z + \sqrt{2}\,\Delta_3(J_+\sigma_- + J_-\sigma_+) + (A_1 + A_3 J_z^2)k_z^2 + \\ & + (A_2 + A_4 J_z^2)k_\perp^2 - A_5(J_+^2 k_-^2 + J_-^2 k_+^2) - 2iA_6 k_z([J_z J_+]k_- - [J_z J_-]k_+) + \\ & + A_7(k_- J_+ + k_+ J_-) + (\alpha_1 + \alpha_3 J_z^2)(\sigma_+ k_- + \sigma_- k_+) + \\ & + \alpha_2(J_+^2 k_-\sigma_- + J_-^2 k_+\sigma_+) + 2\alpha_4\sigma_z([J_z J_+]k_- + [J_z J_-]k_+) + \\ & + 2i\alpha_5 k_z([J_z J_+]\sigma_- - [J_z J_-]\sigma_+) + (D_1 + D_3 J_z^2)\varepsilon_{zz} + (D_2 + D_4 J_z^2)\varepsilon_\perp - \\ & - D_5(J_+^2\varepsilon_- + J_-^2\varepsilon_+) - 2iD_6([J_z J_+]\varepsilon_{-z} - [J_z J_-]\varepsilon_{+z}).\end{aligned} \tag{31.8}$$

We emphasize that this operator, which has been derived from symmetry considerations alone, is valid regardless of the mechanism producing the levels Γ_9, Γ_7 and Γ_7. However, if the splitting between these levels is comparable with the separation E_g to the other bands, we must also include in (31.8) quadratic k and linear ε relativistic terms, since their coefficients may be of the order of $\Delta_{2,3}/E_g$, in which case they become comparable with the coefficients of the nonrelativistic terms.

There is an interesting relation between the coefficients in the Hamiltonian (31.8) in the "cubic" approximation. Let us transform the Hamiltonian $\mathcal{H}_{T_d}(k, \varepsilon)$, constructed for the representation $\Gamma_{15}(\Gamma_{25})$ of the group T_d, to a coordinate system in which the z'-axis is along [111] direction and the x'- and y'-axes along the $[11\bar{2}]$ and $[\bar{1}10]$ directions, respectively. In the cubic axes the form of this Hamiltonian is similar to (26.15), (30.33)**:

$$\begin{aligned}\mathcal{H}_{T_d}(k,\varepsilon) = {}& A_1' k^2 + \tfrac{1}{3}\Delta(\sigma J) + A_2'(Jk)^2 + (A_3' - A_2')\sum_{ij}[J_i J_j]k_i k_j + \\ & + D_1'\varepsilon + D_2'\sum_i J_i^2\varepsilon_{ii} + D_3'\sum_{ij}[J_i J_j]\varepsilon_{ij}.\end{aligned} \tag{31.9}$$

* We have denoted the deformation potential constants by D_i instead of C_i and put $2A_6$ for B_6, $2D_6$ for C_6, and $2\alpha_4$ and $2\alpha_5$ for β_4 and β_5 in the original paper /26.1/, in order to simplify the coefficients in the matrix (31.14). In addition, the numbering of the representations Γ_5 and Γ_6 conforms to the notation in most papers (unlike /14.2/, /14.3/ and /26.1/ where the symbols Γ_5 and Γ_6 are interchanged). The factor $\sqrt{2}$ in the third term has been introduced to enable us to simplify the form of the matrix by setting $\sigma_\pm = \pm(i/2)\times$ $\times(\sigma_x \pm i\sigma_y)$ throughout, while $J_\pm = \pm(i/\sqrt{2})(J_x \pm iJ_y)$.

** We have not included in (31.9) the linear k relativistic terms, which, for the representations Γ_{15} and Γ_{25} of T_d, have the form

$$\mathcal{H}_{T_d,\,so} = \alpha_1'\sum_i J_i^2(\sigma_{i+1}k_{i+1} - \sigma_{i+2}k_{i+2}) + 2\alpha_2'\sum_{i>j}[J_i J_j](\sigma_i k_j - \sigma_j k_i), \tag{31.9a}$$

and the quadratic k relativistic terms appearing in (26.15).

The constants A_i' and D_i' are defined in terms of the constants in (24.5), (24.12) and (30.2), (30.33) by

$$A_1' = L = A + 2B, \quad A_2' = M - L = -3B, \quad A_3' = -N = -\sqrt{3}\,D,$$
$$D_1' = l = a + 2b, \quad D_2' = m - l = -3b, \quad D_3' = -n = -\sqrt{3}\,d. \tag{31.10}$$

To transform (31.9) to the new coordinate system, we must replace x, y, z by

$$x = \frac{x'}{\sqrt{6}} - \frac{y'}{\sqrt{2}} + \frac{z'}{\sqrt{3}}, \quad y = \frac{x'}{\sqrt{6}} + \frac{y'}{\sqrt{2}} + \frac{z'}{\sqrt{3}}, \tag{31.10a}$$
$$z = -\frac{\sqrt{2}}{\sqrt{3}}x' + \frac{z'}{\sqrt{3}}.$$

The operator (31.9) is then written

$$\begin{aligned}
\mathcal{H}_{T_d}(\boldsymbol{k}, \boldsymbol{\varepsilon}) = {} & \tfrac{1}{3}\Delta(\sigma J) + \left(A_1' + \tfrac{2}{3}(A_2' - A_3')\right)k_z^2 + \left(A_1' + \tfrac{1}{3}(2A_2' + A_3')\right)k_\perp^2 + \\
& + A_3' J_z^2 k_z^2 - \tfrac{1}{2}A_3' J_z^2 k_\perp^2 - \tfrac{1}{6}(A_2' + 2A_3')(J_+^2 k_-^2 + J_-^2 k_+^2) - \\
& - i\frac{\sqrt{2}}{3}(2A_2' + A_3')([J_z J_+]\,k_z k_- - [J_z J_-]\,k_z k_+) + \\
& + \frac{\sqrt{2}}{3}(A_2' - A_3')(J_+^2 k_+ k_z + J_-^2 k_- k_z) + \\
& + \frac{i}{3}(A_2' - A_3')([J_z J_+]\,k_+^2 - [J_z J_-]\,k_-^2) + \left(D_1' + \tfrac{2}{3}(D_2' - D_3')\right)\varepsilon_{zz} + \\
& + \left(D_1' + \tfrac{1}{3}(2D_2' + D_3')\right)\varepsilon_\perp + D_3' J_z^2 \varepsilon_{zz} - \tfrac{1}{2}D_3' J_z^2 \varepsilon_\perp^2 - \\
& - \tfrac{1}{6}(D_2' + 2D_3')(J_+^2 \varepsilon_- + J_-^2 \varepsilon_+) - \\
& - i\frac{\sqrt{2}}{3}(2D_2' + D_3')([J_z J_+]\,\varepsilon_{z-} - [J_z J_-]\,\varepsilon_{z+}) + \\
& + \frac{\sqrt{2}}{3}(D_2' - D_3')(J_+^2 \varepsilon_{z+} + J_-^2 \varepsilon_{z-}) + \frac{i}{3}(D_2' - D_3')([J_z J_+]\,\varepsilon_+ - [J_z J_-]\,\varepsilon_-).
\end{aligned} \tag{31.11}$$

It is at once evident that this operator contains terms not appearing in (31.8). This is because C_{6v} is not a subgroup of the cubic groups T_d or O_h, and therefore certain invariants of the latter are not invariants of C_{6v}. The operator $\mathcal{H}(\boldsymbol{k}, \boldsymbol{\varepsilon})$ for C_{3v}, which is a subgroup of T_d, contains all these invariants. In case (a_1) it must include all functions which are even with respect to time reversal and transform according to $[(K_1 + K_3)^2] = 2A_1 + 2E$ and odd functions which transform according to $\{(K_1 + K_3)^2\} = A_2 + E$. For the group C_{3v}, therefore, $\mathcal{H}(\boldsymbol{k}, \boldsymbol{\varepsilon})$ will contain additional terms, not appearing in (31.8):

$$\begin{aligned}
\mathcal{H}_{C_{3v}} = {} & \mathcal{H}_{C_{6v}} + A_8(J_+^2 k_+ + J_-^2 k_-)k_z + 2iA_9([J_+ J_z]\,k_+^2 - \\
& - [J_- J_z]\,k_-^2) + D_8(J_+^2 \varepsilon_{+z} + J_-^2 \varepsilon_{-z}) + 2iD_9([J_+ J_z]\,\varepsilon_+ - [J_- J_z]\,\varepsilon_-) + \\
& + \alpha_6(J_+^2 \sigma_+ + J_-^2 \sigma_-)k_z + i\alpha_7(J_+^2 k_+ - J_-^2 k_-)\sigma_z + \\
& + 2i\alpha_8([J_+ J_z]\,\sigma_+ k_+ - [J_- J_z]\,\sigma_- k_-).
\end{aligned} \tag{31.12}$$

Comparing (31.8) and (31.12) with (31.11), we can establish relationships for the constants which must hold in the cubic approximation*:

$$\Delta_2 = \Delta_3 = \tfrac{1}{3}\Delta, \qquad A_6 = \frac{1}{3\sqrt{2}}(2A_2' + A_3'), \quad D_3 = D_3',$$
$$A_1 = A_1' + \tfrac{2}{3}(A_2' - A_3'), \quad A_7 = 0, \qquad D_4 = -\tfrac{1}{2}D_3',$$

* Similarly, in the cubic approximation all the relativistic constants $\alpha_1, \ldots, \alpha_8$ must be expressed in terms of α_1' and α_2' in (31.9a).

$$A_2 = A_1' + \tfrac{1}{3}(2A_2' + A_3'),\ A_8 = \frac{\sqrt{2}}{3}(A_2' - A_3'),\quad D_5 = \tfrac{1}{6}(D_2' + 2D_3'),$$
$$A_3 = A_3',\qquad A_9 = \tfrac{1}{6}(A_2' - A_3'),\qquad D_6 = \frac{1}{3\sqrt{2}}(2D_2' + D_3'),$$
$$A_4 = -\tfrac{1}{2}A_3',\qquad D_1 = D_1' + \tfrac{2}{3}(D_2' - D_3'),\ D_8 = \frac{\sqrt{2}}{3}(D_2' - D_3'),$$
$$A_5 = \tfrac{1}{6}(A_2' + 2A_3'),\qquad D_2 = D_1' + \tfrac{1}{3}(2D_2' + D_3'),\ D_9 = \tfrac{1}{6}(D_2' - D_3').$$

Hence, in the cubic approximation the constants Δ_i, A_i, D_i satisfy the relations

$$\Delta_2 = \Delta_3,\quad 4A_5 - \sqrt{2}\,A_6 = -A_3,\quad 2D_4 = -D_3 = D_1 - D_2,$$
$$2A_4 = -A_3 = A_1 - A_2,\quad A_7 = 0,\quad 4D_5 - \sqrt{2}\,D_6 = -D_3. \tag{31.13}$$

The relation $\Delta_2 = \Delta_3$ seems to be in excellent agreement with the situation in most of the above-mentioned crystals. According to the theoretical calculations in /25.11/ the quotient $(\Delta_2 - \Delta_3)/\Delta_2$ for CdS, CdSe, ZnS, ZnSe is at most $2\cdot 10^{-2}$. According to the latest experimental data, this ratio is $1\cdot 10^{-2}$ for CdS and $9\cdot 10^{-2}$ for CdSe. The constant A_7 is also very small, since judging from the data in /25.9/ the corresponding coefficient of the linear k term in (31.23) (see below) is also at most 10^{-9} ev/cm.

We now write the Hamiltonian in matrix form and find the shape of the spectrum near the extrema of each of the three bands. In order to avoid cumbersome expressions, we shall consider only the nonrelativistic terms, including the linear k term with coefficient A_7. Inclusion of the remaining linear terms would only affect the expressions for the coefficients of the linear term in (31.23).

In this approximation the matrix $\mathcal{H}(k, \varepsilon)$ has the form

$$\mathcal{H} = \begin{Vmatrix} F & 0 & -H^* & 0 & k^* & 0 \\ 0 & G & \Delta & -H^* & 0 & k^* \\ -H & \Delta & \lambda & 0 & l^* & 0 \\ 0 & -H & 0 & \lambda & \Delta & l^* \\ k & 0 & l & \Delta & G & 0 \\ 0 & k & 0 & l & 0 & F \end{Vmatrix}, \tag{31.14}$$

where

$$\Delta = \sqrt{2}\,\Delta_3,\qquad H = i(A_6 k_z k_+ + D_6 \varepsilon_{z+} + A_7 k_+),$$
$$F = \Delta_1 + \Delta_2 + \lambda + \theta,\qquad l = i(A_6 k_z k_+ + D_6 \varepsilon_{z+} - A_7 k_+),$$
$$G = \Delta_1 - \Delta_2 + \lambda + \theta,\qquad \lambda = A_1 k_z^2 + A_2 k_\perp^2 + D_1 \varepsilon_{zz} + D_2 \varepsilon_\perp,$$
$$k = A_5 k_+^2 + D_5 \varepsilon_+,\qquad \theta = A_3 k_z^2 + A_4 k_\perp^2 + D_3 \varepsilon_{zz} + D_4 \varepsilon_\perp.$$

If we retain in $\mathcal{H}$ only the matrix elements F, G, λ, and Δ that contain terms independent of k and ε, the roots of the resulting determinant $|\mathcal{H}_1 - IE| = 0$ are

$$E_1^1 = F,\qquad E_{2,3}^1 = \frac{G+\lambda}{2} \pm \left[\left(\frac{G-\lambda}{2}\right)^2 + \Delta^2\right]^{1/2}. \tag{31.15}$$

Equation (31.15) determines $E(k, \varepsilon)$ with accuracy up to first order terms in ε and k^2 (when $A_7 = 0$).

By (31.15), the position of the terms at the point $k = 0$ in the unstrained crystal is

$$E_1^0 = \Delta_1 + \Delta_2,\qquad E_{2,3}^0 = \frac{\Delta_1 - \Delta_2}{2} \pm \left[\left(\frac{\Delta_1 - \Delta_2}{2}\right)^2 + 2\Delta_3^2\right]^{1/2} \tag{31.16}$$

and the distance between the first level and levels E_2^0 and E_3^0 is

$$E_1^0 - E_{2,3}^0 = \frac{1}{2}\left[(\Delta_1 + 3\Delta_2) \mp \left[(\Delta_1 - \Delta_2)^2 + 8\Delta_3^2\right]^{1/2}\right]. \tag{31.16a}$$

In the absence of spin-orbit splitting, i.e., $\Delta_2 = \Delta_3 = 0$, we have $E_1^0 = E_2^0$, and $E_{1,2}^0 - E_3^0 = \Delta_1$. If $\Delta_1 = 0$ and $\Delta_2 = \Delta_3$, then $E_1^0 = E_2^0$ and $E_{1,2}^0 - E_3^0 = 3\Delta_2$. Therefore, the quantity Δ_1 is called the crystal splitting Δ_{cr}, and the quantity $3\Delta_2$ is usually put equal to $3\Delta_3$ and called the spin-orbit splitting Δ_{so}:

$$\Delta_1 = \Delta_{cr}, \quad \Delta_2 = \Delta_3 = \frac{1}{3}\Delta_{so}. \tag{31.17}$$

In the notation of (31.17) equation (31.16a) has the form

$$E_1^0 - E_{2,3}^0 = \frac{1}{2}\left\{(\Delta_{cr} + \Delta_{so}) \mp \left[(\Delta_{cr} + \Delta_{so})^2 - \frac{8}{3}\Delta_{cr}\Delta_{so}\right]^{1/2}\right\}. \tag{31.16b}$$

If the separation of the terms is known, we can determine Δ_{cr} and Δ_{so} (on the assumption that $\Delta_2 = \Delta_3$). However, since these quantities play entirely symmetric roles in (31.16b), we cannot decide which value must be ascribed to Δ_{cr} and which to Δ_{so} without appealing to additional considerations. For example, it will follow from equations (31.24) below that this can be established on the basis of the relative shift of the bands under a strain. Values of Δ_{cr} and Δ_{so} for a few crystals are given in Table 31.9 at the end of the section.

To determine the spectrum in each of the bands, the matrix (31.14) is conveniently expanded in the eigenfunctions of the Hamiltonian $\mathcal{H}_1$, whose eigenvalues are given by (31.15). A suitable set of eigenfunctions is

$$F_1 = \begin{Vmatrix} 1 \\ 0 \\ 0 \\ 0 \\ 0 \\ 0 \end{Vmatrix}; \quad F_2 = \begin{Vmatrix} 0 \\ 0 \\ 0 \\ 0 \\ 0 \\ 1 \end{Vmatrix};$$

$$F_{3,5} = B_{2,3}\begin{Vmatrix} 0 \\ -\Delta \\ G - E_{2,3}^1 \\ 0 \\ 0 \\ 0 \end{Vmatrix}; \quad F_{4,6} = B_{2,3}\begin{Vmatrix} 0 \\ 0 \\ 0 \\ G - E_{2,3}^1 \\ -\Delta \\ 0 \end{Vmatrix}, \tag{31.18}$$

where

$$B_{2,3} = \left[(G - E_{2,3}^1)^2 + \Delta^2\right]^{-1/2}.$$

Expressing the Hamiltonian $\mathcal{H}(\boldsymbol{k}, \boldsymbol{\varepsilon})$ in terms of (31.18), we obtain

$$\mathcal{H} = \begin{Vmatrix} E_1^1 & 0 & \gamma^* & \delta^* & \sigma^* & \rho^* \\ 0 & E_1^1 & \delta & \varkappa & \rho & \xi \\ \gamma & \delta^* & E_2^1 & \alpha^* & 0 & \eta^* \\ \delta & \varkappa^* & \alpha & E_2^1 & \vartheta & 0 \\ \sigma & \rho^* & 0 & \vartheta^* & E_3^1 & \beta^* \\ \rho & \xi^* & \eta & 0 & \beta & E_3^1 \end{Vmatrix}, \tag{31.19}$$

where

$$\begin{aligned}
&\delta = -B_2\Delta\mathcal{k}, && \xi = B_3(G-E_3^1)I,\\
&\rho = -B_3\Delta\mathcal{k}, && \eta = B_2B_3[(G-E_3^1)H-(G-E_2^1)I]\Delta,\\
&\gamma = -B_2(G-E_2^1)H, && \vartheta = B_1B_3[(G-E_2^1)H-(G-E_3^1)I]\Delta,\\
&\sigma = -B_3(G-E_3^1)H, && \alpha = B_2^2\Delta(G-E_2^1)(H-I),\\
&\varkappa = B_2(G-E_2^1)I, && \beta = B_3^2\Delta(G-E_3^1)(H-I),
\end{aligned}$$

and we can then introduce the interband terms using the perturbation theory of §15. By (15.47), in the second order theory, the matrix elements $\mathscr{H}'_{ik}$ for $E_i = E_k$ are

$$\mathscr{H}'_{ik} = \mathscr{H}_{ik} + \sum_l \frac{\mathscr{H}_{il}\mathscr{H}_{lk}}{E_i - E_l}. \tag{31.20}$$

Limiting ourselves to second order terms, we include the terms of order k^4, εk^2 and ε^2. It is therefore sufficient to retain only terms independent of k and ε in the coefficients of the off-diagonal terms in (31.19), after replacing E_l^1, E_l^0 and G by $\Delta_1 - \Delta_2$. In this approximation,

$$E_2^0 + E_3^0 = \Delta_1 - \Delta_2, \quad E_2^0E_3^0 = -\Delta^2 = -2\Delta_3^2 \tag{31.21}$$

and so

$$\begin{gathered}
G - E_2^0 = E_3^0, \quad G - E_3^0 = E_2^0, \quad B_2^{-2} = E_3^0(E_3^0 - E_2^0),\\
B_3^{-2} = E_2^0(E_2^0 - E_3^0).
\end{gathered} \tag{31.21a}$$

We shall also disregard the small contribution to the quadratic k terms from terms proportional to A_7. In this approximation

$$I = H, \quad \gamma = -\varkappa, \quad \sigma = -\xi, \quad \eta = -\vartheta; \tag{31.22}$$

the terms containing A_7 need be included only in the matrix elements α and which are proportional to $H - I = 2iA_7k_+$.

In this approximation, the energy in each band is determined by the expressions

$$\begin{aligned}
E_{1\pm}^{(2)} &= E_1^1 + \frac{(E_1^0 - E_2^0 - E_3^0)|H|^2 + E_1^0|\mathcal{k}|^2}{(E_1^0 - E_3^0)(E_1^0 - E_2^0)},\\
E_{2\pm}^{(2)} &= E_2^1 + \frac{(E_1^0 - E_2^0 + E_3^0)|H|^2 - E_2^0|\mathcal{k}|^2}{(E_1^0 - E_2^0)(E_2^0 - E_3^0)} \pm \frac{2\Delta A_7}{E_2^0 - E_3^0}k_\perp,\\
E_{3\pm}^{(2)} &= E_3^1 + \frac{(E_1^0 + E_2^0 - E_3^0)|H|^2 - E_3^0|\mathcal{k}|^2}{(E_1^0 - E_3^0)(E_3^0 - E_2^0)} \pm \frac{2\Delta A_7}{E_2^0 - E_3^0}k_\perp.
\end{aligned} \tag{31.23}$$

Equations (31.23) determine the strain-induced shift of the terms. They are valid for an arbitrary strain due to isotropic compression and dilation along the z-axis (of course, only up to terms of order $D_l\varepsilon/E'_g$, where E'_g is the separation to other bands) and for strains $\varepsilon_{xx} - \varepsilon_{yy}$, ε_{xy}, ε_{xz} and ε_{yz} such that the shift of each of the terms is small compared to their separations. If the formulas for E_l^1 are also limited to terms of order ε^2, equations (31.23) yield the following equations, which determine the shift of each term when $k = 0$:

$$E_1 - E_1^0 = (D_1 + D_3)\varepsilon_{zz} + (D_2 + D_4)\varepsilon_\perp + \\ + \frac{D_6^2(E_1^0 - E_2^0 - E_3^0)(\varepsilon_{xz}^2 + \varepsilon_{yz}^2) + D_5^2 E_1^0[(\varepsilon_{xx} - \varepsilon_{yy})^2 + 4\varepsilon_{xy}^2]}{(E_1^0 - E_2^0)(E_1^0 - E_3^0)}, \tag{31.24a}$$

$$E_2 - E_2^0 = \left(D_1 + D_3\frac{E_2^0}{E_2^0 - E_3^0}\right)\varepsilon_{zz} + \\ + \left(D_2 + D_4\frac{E_2^0}{E_2^0 - E_3^0}\right)\varepsilon_\perp - \frac{E_2^0 E_3^0}{(E_2^0 - E_3^0)^3}(D_3\varepsilon_{zz} + D_4\varepsilon_\perp)^2 + \\ + \frac{D_6^2(E_1^0 - E_2^0 + E_3^0)(\varepsilon_{xz}^2 + \varepsilon_{yz}^2) - D_5^2 E_2^0[(\varepsilon_{xx} - \varepsilon_{yy})^2 + 4\varepsilon_{xy}^2]}{(E_1^0 - E_2^0)(E_2^0 - E_3^0)}, \tag{31.24b}$$

$$E_3 - E_3^0 = \left(D_1 - D_3\frac{E_3^0}{E_2^0 - E_3^0}\right)\varepsilon_{zz} + \\ + \left(D_2 - D_4\frac{E_3^0}{E_2^0 - E_3^0}\right)\varepsilon_\perp + \frac{E_2^0 E_3^0}{(E_2^0 - E_3^0)^3}(D_3\varepsilon_{zz} + D_4\varepsilon_\perp)^2 - \\ - \frac{D_6^2(E_1^0 + E_2^0 - E_3^0)(\varepsilon_{xz}^2 + \varepsilon_{yz}^2) - D_5^2 E_3^0[(\varepsilon_{xx} - \varepsilon_{yy})^2 + 4\varepsilon_{xy}^2]}{(E_2^0 - E_3^0)(E_1^0 - E_3^0)}. \tag{31.24c}$$

The spectrum in each subband in the unstrained crystal is determined by expressions which differ from (31.24) by the substitution of $k_i k_j$ and A_i for ε_{ij} and D_i, respectively. In addition, $E(\boldsymbol{k})$ will of course contain the linear k terms from (31.23).

Hence we see that the effective masses in each subband are expressed in terms of the constants $A_1, \ldots, A_4$:

	Band 1	Band 2	Band 3
$\hbar^2/2m_\parallel$	$A_1 + A_3$	$A_1 + A_3\frac{E_2^0}{E_2^0 - E_3^0}$	$A_1 - A_3\frac{E_3^0}{E_2^0 - E_3^0}$
$\hbar^2/2m_\perp$	$A_2 + A_4$	$A_2 + A_4\frac{E_2^0}{E_2^0 - E_3^0}$	$A_2 - A_4\frac{E_3^0}{E_2^0 - E_3^0}$

(31.25)

In our model, therefore, the components $m_\parallel$ and $m_\perp$ for the three subbands must satisfy

$$\frac{1}{m_{i1}} - \frac{E_2^0}{E_2^0 + E_3^0}\frac{1}{m_{i2}} - \frac{E_3^0}{E_2^0 + E_3^0}\frac{1}{m_{i3}} = 0 \qquad (i = \parallel, \perp). \tag{31.26}$$

This relation can be used to verify to what extent these three bands may be considered in isolation from the other bands. It is clear from (31.24) that a similar relation must hold for the deformation potential constants of the three bands.

The cross terms $E_{\varepsilon k^2}$, which are proportional to εk^2, determine the strain-induced change in the effective masses. According to (31.23),

$$E_{\varepsilon k^2,1} = [(E_1^0 - E_3^0)(E_1^0 - E_2^0)]^{-1}\{2(E_1^0 - E_2^0 - E_3^0)D_6 A_6 k_z(\varepsilon_{xz}k_x + \varepsilon_{yz}k_y) + \\ + 2E_1^0 D_5 A_5[(\varepsilon_{xx} - \varepsilon_{yy})(k_x^2 - k_y^2) + 4\varepsilon_{xy}k_x k_y]\}, \tag{31.27a}$$

$$E_{\varepsilon k^2,2} = -(E_2^0 - E_3^0)^{-3}\{2E_2^0E_3^0(A_3k_z^2 + A_4k_\perp^2)(D_3\varepsilon_{zz} + D_4\varepsilon_\perp)\} +$$
$$+ [(E_1^0 - E_2^0)(E_2^0 - E_3^0)]^{-1}\{2(E_1^0 - E_2^0 + E_3^0)D_6A_6k_z(\varepsilon_{xz}k_x + \varepsilon_{yz}k_y) -$$
$$- 2E_2^0D_5A_5[(\varepsilon_{xx} - \varepsilon_{yy})^2(k_x^2 - k_y^2) + 4\varepsilon_{xy}k_xk_y]\}, \qquad (31.27b)$$

$$E_{\varepsilon k^2,3} = 2(E_2^0 - E_3^0)^{-3}\{E_2^0E_3^0(A_3k_z^2 + A_4k_\perp^2)(D_3\varepsilon_{zz} + D_4\varepsilon_\perp)\} -$$
$$- [(E_2^0 - E_3^0)(E_1^0 - E_3^0)]^{-1}\{2(E_1^0 + E_2^0 - E_3^0)D_6A_6k_z(\varepsilon_{xz}k_x + \varepsilon_{yz}k_y) -$$
$$- 2E_3^0D_5A_5[(\varepsilon_{xx} - \varepsilon_{yy})(k_x^2 - k_y^2) + 4\varepsilon_{xy}k_xk_y]\}. \qquad (31.27c)$$

In the limiting case, when the crystal splitting Δ_1 far exceeds the spin-orbit splittings Δ_2 and Δ_3, we have $E_{1,2}^0 = \Delta_1 \pm \Delta_2$, $E_3^0 = 0$, and expressions (31.23)–(31.27) for levels E_1 and E_2 reduce to (31.7).

Table 40.3 at the end of the book presents the currently known effective masses and deformation potential constants D_i for some crystals of the A_2B_6 group.

The eigenfunctions (31.18) may also be used to determine the relative probabilities of transition of an electron from one of the three valence bands to the conduction band upon absorption of light. The matrix elements for the three transitions, for a given direction of the electric field, are proportional to the coefficients of the corresponding components k_i in the interband operator $\mathcal{H}_{vc}$. This operator may be based on the matrices of the components of the polar vector $\boldsymbol{R}$, which transform according to the representations $\Gamma_1 \times (\Gamma_1 + \Gamma_5) = A_1 + E_1$. The operator $\mathcal{H}_{vc}$ must include invariant products of these components by functions of $\boldsymbol{k}$ and σ which transform according to the representations A_1 and E_1:

$$\mathcal{H}_{vc} = P_1R_zk_z + \frac{1}{\sqrt{2}}P_2(R_+k_- + R_-k_+) + \pi_1R_z(\sigma_+k_- + \sigma_-k_+) +$$
$$+ \sqrt{2}\pi_2k_z(R_+\sigma_- + R_-\sigma_+) - \frac{i}{\sqrt{2}}\pi_3\sigma_z(R_+k_- - R_-k_+). \qquad (31.28)$$

The matrices $\boldsymbol{R}_i$, in the same representation as the matrices in Table 31.7, are given in Table 31.8. The five constants P_i, π_i appearing in (31.28) determine the intensity of the transitions (the transition $\Gamma_9 - \Gamma_7$ is forbidden when $\mathcal{E} \| C$). If the three valence bands are sufficiently far away from the other bands, the relativistic constants π_1, π_2 and π_3 must be small. If we omit the corresponding terms, the matrix $\mathcal{H}_{vc}$ in the presentation (31.18) will have the form

$$\begin{Vmatrix} -\frac{P_2k_+}{\sqrt{2}} & 0 & B_2(G - E_2')P_1k_z & -\frac{B_1}{\sqrt{2}}\Delta P_2k_- & B_3(G - E_3')P_1k_z & -\frac{B_1}{\sqrt{2}}\Delta P_2k_- \\ 0 & \frac{P_2k_-}{\sqrt{2}} & -\frac{B_1}{\sqrt{2}}\Delta P_2k_+ & B_2(G - E_2')P_1k_z & \frac{B_1}{\sqrt{2}}\Delta P_2k_+ & B_3(G - E_3')P_1k_z \end{Vmatrix}. \qquad (31.29)$$

Hence, using (31.21a), we obtain the expressions given in Table 31.6 for the relative intensities of the transitions.

In the cubic approximation, when

$$\mathcal{H}_{vc} = P(\boldsymbol{R}\boldsymbol{k}) + \pi(\sigma[\boldsymbol{R}\boldsymbol{k}]), \qquad (31.30)$$

the constants P_i and π_i in (31.28) must satisfy the relations

$$P_1 = P_2 = P, \quad \pi_1 = \pi_2 = \pi_3 = \pi. \qquad (31.31)$$

Fulfillment of these relations for the oscillator forces in Table 31.6 may

serve as an indication of the validity of the three-band model and also of the cubic approximation.

TABLE 31.6. Relative intensities of transitions between valence bands and conduction band

Valence band	Polarization of light	
	$\gamma \parallel c$	$\gamma \perp c$
1 (Γ_9)	0	$\lvert P_2 \rvert^2$
2 (Γ_7)	$\frac{2E_3}{E_3 - E_2} \lvert P_1 \rvert^2$	$\frac{E_2}{E_2 - E_3} \lvert P_2 \rvert^2$
3 (Γ_7)	$\frac{2E_2}{E_2 - E_3} \lvert P_1 \rvert^2$	$\frac{E_3}{E_3 - E_2} \lvert P_2 \rvert^2$

$$E_{2,3} = \frac{\Delta_1 - \Delta_2}{2} \pm \left[\left(\frac{\Delta_1 - \Delta_2}{2}\right)^2 + 2\Delta_3^2\right]^{1/2}.$$

In the cubic approximation $\Delta_1 = \Delta_{cr}$, $\Delta_2 = \Delta_3 = \frac{1}{3}\Delta_{so}$, $P_1 = P_2$.

Point A. At the point A all representations belong to case (b_1) or (c_1) and are combined in pairs. It is not a point of zero slope for any representation.

Point P. The points P may be points of zero slope for the representations P_1 and P_2. In these representations, $\mathcal{H}(\boldsymbol{k}, \boldsymbol{\varepsilon})$ will include all the functions of $\boldsymbol{k}, \boldsymbol{\varepsilon}$ and σ which transform according to the identity representation of the point group C_{3v} (i.e., according to K_1), and

$$\mathcal{H}(\boldsymbol{k}, \boldsymbol{\varepsilon}) = \lambda \boldsymbol{I} + \boldsymbol{I} A_0 k_z + \alpha_1 (\sigma_+ k_- + \sigma_- k_+), \tag{31.32}$$

where, as before, $\lambda = A_1 k_z^2 + A_2 k_\perp^2 + D_1 \varepsilon_{zz} + D_2 \varepsilon_\perp$. Hence, if $A_0 = 0$,

$$E(\boldsymbol{k}, \boldsymbol{\varepsilon}) = \lambda \pm \alpha_1 k_\perp, \tag{31.33}$$

i.e., the spectrum $E(\boldsymbol{k}, \boldsymbol{\varepsilon})$ for these representations, like that for the representations $\Delta_1, \ldots, \Delta_4$, is determined by an equation similar to (31.2).

In the representations P_3, the points P cannot be points of zero slope, but in the representations P_4, P_5 and P_6, which result from spin-orbit splitting of P_3, the coefficients of all the linear k relativistic terms may vanish at these points.

Point K. At the point K there is an operation R, for example, $(c_2|t_0/2)$, which takes $\boldsymbol{k}_0$ into $-\boldsymbol{k}_0$, and the representations K_1, K_2, K_3 at this point belong to case (a_2).

In accordance with equation (25.36), in the representations K_1 and K_2 the operator $\mathcal{H}(\boldsymbol{k}, \boldsymbol{\varepsilon})$ will include functions which are even with respect to time reversal and transform according to the A_1 representations of the group C_{6v} and odd functions which transform according to B_1. Therefore, the constant A_0 in (31.32), (31.33) vanishes at the point K.

In the absence of spin-orbit splitting, K is not a point of zero slope in the representation K_3. However, in the representations K_4 and K_5, which split off from K_3, K is a point of zero slope, and in the representations K_6, $E(\boldsymbol{k})$ may contain only relativistic terms linear in $k_\perp$.

Point H. At the point H, the representations H_1 and H_2 belong to case (b_2) and are combined.

According to the rules in §26, the diagonal blocks contain functions of k, σ and ε which transform according to the representation $H \times H^* = A_1$ of the group C_{3v}. Functions which are even with respect to the operation $RK = c_2K$ then appear with the identity matrix, and even functions with the matrix ρ_z. By (25.16), the off-diagonal blocks contain functions which are even with respect to time reversal and transform according to the representation B_2 of the group $C_{3v} \times C_2 = C_{6v}$, and odd functions which transform according to A_2. A suitable set of matrices which transform according to these representations is ρ_x, ρ_y. Then

$$\mathcal{H}(\varepsilon, k) = \lambda I + A_3 I(\sigma_+ k_- + \sigma_- k_+) + A_0 \rho_z k_z + \Delta \rho_y \sigma_z. \tag{31.34}$$

Accordingly, the spectrum is

$$E_{1-4}(k, \varepsilon) = \lambda \pm \{\Delta^2 + A_0^2 k_z^2 + A_3^2 k_\perp^2 \pm 2A_0 A_3 k_\perp k_z\}^{1/2} \approx$$
$$\approx \lambda \pm \Delta^2 + \frac{1}{2\Delta}(A_0^2 k_z^2 + A_3^2 k_\perp^2 \pm 2A_0 A_3 k_\perp k_z). \tag{31.35}$$

In this case, then, the levels are twofold degenerate when $k = 0$. These levels correspond to representations H_6, which belong to case (a_2). As opposed to the representations $H_1 - H_2$, in these representations H is a point of zero slope.

TABLE 31.7. Matrices of the axial vector components J_z, J_+, J_- and their products in representations Γ_1^1, Γ_0^1, Γ_{-1}^1

$$J_z = \begin{Vmatrix} 1 & 0 & 0 \\ 0 & 0 & 0 \\ 0 & 0 & -1 \end{Vmatrix} \qquad J_+ = \begin{Vmatrix} 0 & 1 & 0 \\ 0 & 0 & 1 \\ 0 & 0 & 0 \end{Vmatrix} \qquad J_- = \begin{Vmatrix} 0 & 0 & 0 \\ 1 & 0 & 0 \\ 0 & 1 & 0 \end{Vmatrix}$$

$$J_z^2 = \begin{Vmatrix} 1 & 0 & 0 \\ 0 & 0 & 0 \\ 0 & 0 & 1 \end{Vmatrix} \qquad J_+^2 = \begin{Vmatrix} 0 & 0 & 1 \\ 0 & 0 & 0 \\ 0 & 0 & 0 \end{Vmatrix} \qquad J_-^2 = \begin{Vmatrix} 0 & 0 & 0 \\ 0 & 0 & 0 \\ 1 & 0 & 0 \end{Vmatrix}$$

$$2[J_+J_-] = \begin{Vmatrix} 1 & 0 & 0 \\ 0 & 2 & 0 \\ 0 & 0 & 1 \end{Vmatrix} \qquad 2[J_zJ_+] = \begin{Vmatrix} 0 & 1 & 0 \\ 0 & 0 & -1 \\ 0 & 0 & 0 \end{Vmatrix} \qquad 2[J_zJ_-] = \begin{Vmatrix} 0 & 0 & 0 \\ 1 & 0 & 0 \\ 0 & -1 & 0 \end{Vmatrix}$$

$$2[J_iJ_k] = J_iJ_k + J_kJ_i.$$

TABLE 31.8. Matrices of the components of the polar vector R in representations Γ_0^{0+}, Γ_1^{1-}, Γ_0^{1-}, Γ_{-1}^{1-}

$$R_z = \begin{Vmatrix} 0 & 0 & 1 & 0 \\ 0 & 0 & 0 & 0 \\ 1 & 0 & 0 & 0 \\ 0 & 0 & 0 & 0 \end{Vmatrix} \qquad R_+ = \begin{Vmatrix} 0 & 0 & 0 & -i \\ i & 0 & 0 & 0 \\ 0 & 0 & 0 & 0 \\ 0 & 0 & 0 & 0 \end{Vmatrix} \qquad R_- = \begin{Vmatrix} 0 & -i & 0 & 0 \\ 0 & 0 & 0 & 0 \\ 0 & 0 & 0 & 0 \\ i & 0 & 0 & 0 \end{Vmatrix}$$

$$R_z' = \begin{Vmatrix} 0 & 0 & i & 0 \\ 0 & 0 & 0 & 0 \\ -i & 0 & 0 & 0 \\ 0 & 0 & 0 & 0 \end{Vmatrix} \qquad R_+' = \begin{Vmatrix} 0 & 0 & 0 & 1 \\ 1 & 0 & 0 & 0 \\ 0 & 0 & 0 & 0 \\ 0 & 0 & 0 & 0 \end{Vmatrix} \qquad R_-' = \begin{Vmatrix} 0 & 1 & 0 & 0 \\ 0 & 0 & 0 & 0 \\ 0 & 0 & 0 & 0 \\ 1 & 0 & 0 & 0 \end{Vmatrix}$$

In the representation H_3, which belongs to case (a_2), it follows from (25.17) that $\mathcal{H}(k, \varepsilon)$ will contain functions which are even with respect to time reversal and transform according to A_1, B_2, E_2, and odd functions which transform according to A_2, B_1, E_1. Thus, the matrix $\mathcal{H}(k, \varepsilon)$ has the form

$$\mathcal{H}(k, \varepsilon) = \Delta_1 \rho_z \sigma_z + \alpha_1 (\sigma_+ k_- + \sigma_- k_+) + \rho_+ H^* + \rho_- H, \tag{31.36}$$

where $H = A_3 k_+ k_z + i\alpha_2 \sigma_z k_+ + \alpha_3 \sigma_+ k_z + D_3 \varepsilon_{+z}$.

Each of the terms at $k = 0$ is twofold degenerate, since the representations H_4 and H_5 belong to case (b_2) and are combined. Accordingly, if we neglect linear k relativistic terms,

$$E(\varepsilon, k) = \lambda \pm \left\{\Delta_1^2 + A_3 k_1^2 k_z^2 + 2A_3 D_3 (\varepsilon_{xz} k_x k_z + \varepsilon_{yz} k_y k_z) + D_3^2 (\varepsilon_{xz}^2 + \varepsilon_{yz}^2)\right\}^{1/2}. \tag{31.37}$$

In this case, we can evidently expect a comparatively large change in effective mass under strains ε_{xz} and ε_{yz}.

§32. INTERACTION OF ELECTRONS WITH LATTICE VIBRATIONS AND THE DEFORMATION POTENTIAL

The theory of electron-phonon interactions in semiconductors is directly connected with the theory of strain-induced effects.

Since the electron mass is much smaller than the atomic mass, the electron's potential energy essentially depends only on the instantaneous positions of the lattice atoms, and not on their velocity. In this approximation, known as the adiabatic approximation, the field acting on the electrons at a point x may be represented as the periodic potential $V_0(x)$ of an ideal lattice plus a perturbation $\delta V(x) = V(x) - V_0(x)$ determined by the displacement of the atoms from their equilibrium positions. For small displacements, $\delta V(x)$ can be expanded in terms of the atomic displacements:

$$\delta V(x) = \sum_{f\varkappa} \boldsymbol{V}_{f\varkappa}(x)\, u_{f\varkappa}.$$

Here $\boldsymbol{V}_{f\varkappa}(x) u_{f\varkappa}$ is the perturbation induced at the point x by a displacement $u_{f\varkappa}$ of the atom $f\varkappa$ located at the point $\varkappa$ of the primitive cell f, whose position is defined by the corresponding Bravais lattice point X_f. Because of the periodicity of the crystal, the field set up at x when the atom $f\varkappa$ is displaced will equal the field at the point $x - X_f$ for an equal displacement of an atom $\varkappa$ in the Bravais lattice whose point X_0 is at the origin. Consequently, $\boldsymbol{V}_{f\varkappa}(x) = \boldsymbol{V}_{0\varkappa}(x - X_f)$, so that $\boldsymbol{V}_{f\varkappa}(x)$ depends only on the difference $x - X_f$. Therefore, we can write the expression for $\delta V(x)$ as

$$\delta V(x) = \sum_{f\varkappa} \boldsymbol{V}_{\varkappa}(x - X_f)\, u_{f\varkappa}. \tag{32.1}$$

If the entire lattice undergoes a displacement u,

$$\delta V(x) = V_0(x - u) - V_0(x) = -u \nabla V_0,$$

and so

$$\sum_{f\varkappa} \boldsymbol{V}_{\varkappa}(x - X_f) = -\nabla V_0(x). \tag{32.2}$$

To deal with long wavelength modes, when the wavelength $\lambda = 2\pi/q$ greatly exceeds the lattice constant, it is convenient to introduce a quantity

$$\bar{u}_f = \sum_{\varkappa} M_{\varkappa} u_{f\varkappa} \Big/ \sum_{\varkappa} M_{\varkappa},$$

which defines the motion of the center of gravity of the cell X_f, and quantities $u_{f\varkappa\varkappa'} = u_{f\varkappa} - u_{f\varkappa'}$, which define the relative motion of the atoms $\varkappa$ and $\varkappa'$ in the primitive cell f. Then (32.1) may be rewritten

$$\delta V(x) = \sum_f \bar{u}_f \bar{V}(x - X_f) + \frac{1}{2} \sum_f \sum_{\varkappa\varkappa'} u_{f\varkappa\varkappa'} V_{\varkappa\varkappa'}(x - X_f). \tag{32.3}$$

Here

$$\bar{V}(x - X_f) = \sum_{\varkappa} V_{\varkappa}(x - X_f),$$

$$V_{\varkappa\varkappa'}(x - X_f) = \frac{1}{M_0}\left(V_{\varkappa}(x - X_f) M_{\varkappa'} - V_{\varkappa'}(x - X_f) M_{\varkappa}\right),$$

and $M_0 = \sum_{\varkappa} M_{\varkappa}$ is the mass of the primitive cell.

For long wavelength modes ($\lambda \gg a$, where a is the lattice constant), the potential $\delta V(x)$ is separable into two parts: $\delta V_s(x)$, due to the short-range component of the potential $V_{\varkappa}(x - X_f)$, which is determined by the motion of the atoms nearest the point x, and $\delta V_1(x) = -e\varphi(x)$, due to the long-range component of $V_{\varkappa}(x - X_f)$. The major contribution to the latter comes from the motion of atoms remote from the point x, at distances substantially exceeding the lattice constant and comparable with the phonon wavelength λ. Since the main contribution to the short-range part of $V(x)$ at x is made by atoms at distances $|x - X_f| \ll \lambda$, the displacements $\bar{u}_f$ in the sum differ only slightly from the average displacement $u(x)$ at x, and they can be expanded in series in $|x - X_f|$, taking only the first two terms:

$$\bar{u}_{fi} = u_i(x) + \sum_l \frac{\partial u_i(x)}{\partial x_l}(x - X_f)_l. \tag{32.4}$$

The relative displacements of the atoms $u_{\varkappa\varkappa'}$ in long wavelength acoustical modes are proportional to the wave vector q, i.e., to the derivative of the displacement at the point, since in the limit $q \to 0$, i.e., as $\lambda \to \infty$, the cells move as a whole and $u_{\varkappa\varkappa'} \to 0$. Consequently,

$$u_{\varkappa\varkappa', l} = \sum_{ik} \Gamma^{\varkappa\varkappa'}_{lij} e_{ij}. \tag{32.5}$$

The tensor $\Gamma^{\varkappa\varkappa'}_{lij}$ is defined by the space group of the crystal. Under all transformations of the space group which do not change the positions of the atoms in the primitive cell (i.e., do not contain nonprimitive translations), the tensor $\Gamma^{\varkappa\varkappa'}_{lij}$ does not change its upper indices, but transforms in its lower indices like an ordinary tensor. Under transformations which exchange the positions of atoms $\varkappa$ and $\varkappa'$, the tensor also changes sign. The other transformations correlate components $\Gamma^{\varkappa\varkappa'}_{lij}$ with different parameters $\varkappa, \varkappa'$ (if there are more than two like atoms). The number of linearly independent components of the tensor may be determined by the equations of §15, once the representations according to which the components e_{ij} and the displacements $u_{\varkappa\varkappa'}$ transform have been found. If the number $N_{\varkappa}$ of atoms in the primitive cell is > 2, not all the components $u_{\varkappa\varkappa'}$ are linearly independent; it is then

convenient to introduce $3(N_\varkappa-1)$ linearly independent components u^0_{ls} corresponding to the branch of optical modes l as $q\to 0$. By (15.27), the character of the representation according to which these components (or the values of $u_{\varkappa\varkappa',s}$ when $N_\varkappa=2$) transform is

$$\chi(c_\varphi)=(N_c-1)(1+2\cos\varphi),\qquad \chi(s_\varphi)=(N_c-1)(-1+2\cos\varphi),$$

where N_c is the number of atoms which are fixed (or displaced by a Bravais lattice vector) under the transformation in question. (For example, for cubic crystals O_h^7, the displacements $u_{1,2}$ transform according to the representation Γ_{15}^+ and the tensor Γ, as noted in §29, has one linearly independent component Γ_{xyz}.) Thus, by (32.2)—(32.5), the contribution of the short-range forces due to acoustical modes is*

$$V_{ac}(x)=-\bar{u}\nabla V_0(x)+\sum_{ij}V_{ij}(x)e_{ij}, \tag{32.6}$$

where

$$V_{ij}(x)=\frac{1}{2}\sum_f[(x-X_f)_iV_j(x-X_f)+(x-X_f)_jV_i(x-X_f)]+$$
$$+\frac{1}{2}\sum_{f\varkappa\varkappa'l}\Gamma^{\varkappa\varkappa'}_{lij}V_{\varkappa\varkappa',l}(x-X_f). \tag{32.6a}$$

For optical modes, in the limit as $q\to 0$, the center of gravity of the cells is fixed, i.e., $\bar{u}=0$, and the sublattice displacements are identical at all lattice points. Therefore, the potential V_{opt} which describes the contribution from short-range forces due to long wavelength optical modes may be limited to terms independent of q:

$$V_{opt}=\frac{1}{2}\sum_{\varkappa\varkappa'}u_{\varkappa\varkappa'}V^{\varkappa\varkappa'}_{opt}(x), \tag{32.7}$$

where, by (32.3),

$$V^{\varkappa\varkappa'}_{opt}(x)=\sum_f V_{\varkappa\varkappa'}(x-X_f). \tag{32.7a}$$

Long-range forces

Let us now consider the contribution to the potential $-e\varphi$ due to long-range forces. Since the major contribution to $\varphi(x)$ in (32.1) comes from terms with $|x-X_f|\gg a$, it follows that $\varphi(x)$, in contrast to the short-range forces, is practically constant within the bounds of a single primitive cell. From the phenomenological standpoint, therefore, this potential is conveniently regarded as a potential set up by the polarization P, i.e., by electric dipoles formed when the lattice vibrates. As independent variables, then, we take the atomic displacements $u_{f\varkappa}$ and the components of the macroscopic field $\mathcal{E}=-\nabla\varphi$, which determine the long-range forces. Then the internal

* Since a uniform rotation about the point x does not change the potential at the point, the antisymmetric components of the tensor V_{ij} vanish. It is also clear that this tensor coincides with that introduced in §29. Indeed, if the strain is homogeneous, we can transform out the first term in (32.6) by applying the coordinate transformation (29.5), and so the second term remaining in (32.6) will coincide with the second term in (29.11).

energy U may be expressed as the sum of three terms: U_u quadratic in the displacement, $U_{\mathscr{E}}$ quadratic in the field, and a cross term $U_{u\mathscr{E}}$.

By (15.17), (15.6b) and (15.13), (15.16b), the first term is

$$U_u = \frac{1}{2}\sum_{ii'll'} \Phi_{ii'}(ll')\, u_i(l)\, u_{i'}(l') = \frac{1}{2} M_0 N \sum_{q\varkappa\varkappa' ii'} D_{ii'\varkappa\varkappa'}(q)\, u_{i\varkappa}(-q)\, u_{i'\varkappa'}(q), \qquad (32.8a)$$

where the matrix $\boldsymbol{D}$ is defined by (15.13), (15.6b) and the components $u_{i\varkappa}(q)$ by (15.16b).

The second term is

$$U_{\mathscr{E}} = -\frac{1}{2}\sum_{ij}\int \alpha^{\infty}_{ij}\mathscr{E}_i(x)\,\mathscr{E}^{*}_j(x)\,dx = -\frac{\nu'}{2}\sum_{ijq}\alpha^{\infty}_{ij}\mathscr{E}_i(q)\,\mathscr{E}_j(-q). \qquad (32.8b)$$

Here

$$\mathscr{E}(q) = \frac{1}{\nu'}\int \mathscr{E}(x)\, e^{-iqx}\,dx,$$

where $\mathscr{E}(-q) = \mathscr{E}^{*}(q)$, and $\alpha^{\infty}_{ij} = \frac{1}{4\pi}(\varkappa^{\infty}_{ij} - 1)$ are the components of the polarizability tensor when the positions of the atoms are fixed.

The third term can be written

$$U_{u\mathscr{E}} = -\frac{\nu'}{\Omega_0}\sum_{qij\varkappa} Q^{\varkappa}_{ij}(q)\, u_{i\varkappa}(q)\,\mathscr{E}_j(-q). \qquad (32.8c)$$

Here $Q^{\varkappa}_{ij}$ are phenomenological constants with dimensions of charge and Ω_0 the volume of the primitive cell.

If we now go over to the representation in which the matrix U_u is diagonal, introducing the normal coordinates $a_{q\nu}$ by (15.16a), the internal energy U is written in the new representation as

$$U = 2M_0 N\sum_{q\nu}\omega^{02}_{q\nu}a_{q\nu}a_{-q\nu} - 2N\sum_{q\nu j} Q_{\nu j}(q)\, a_{q\nu}\mathscr{E}_j(-q) - \frac{\nu'}{2}\sum_{qij}\alpha^{\infty}_{ij}\mathscr{E}_i(q)\,\mathscr{E}_j(-q). \qquad (32.9)$$

Here $\omega^0_{q\nu}$ are the normal frequencies of the lattice vibrations when long-range effects are neglected,

$$\omega^{02}_{q\nu}\delta_{\nu\nu'} = \sum_{ii'\varkappa\varkappa'} e^{\nu}_{\varkappa i}(-q)\, D_{ii'\varkappa\varkappa'}(q)\, e^{\nu'}_{\varkappa' i'}(q), \qquad (32.9a)$$

and

$$Q_{\nu j}(q) = \sum_{i\varkappa} Q^{\varkappa}_{ij}(q)\, e^{\nu}_{\varkappa i}(q); \qquad (32.9b)$$

the components $e^{\nu}_{i\varkappa}(q)$ are defined by the system of equations (15.15).

If we expand the components $Q_{\nu j}(q)$ in q,

$$Q_{\nu j}(q) = Q^0_{\nu j} + \sum_l Q_{\nu jl}q_l + \sum_{ll'} Q_{\nu jll'}q_l q_{l'}, \qquad (32.9c)$$

then, using the aforementioned rules to determine the number of linearly independent tensor components and the representations according to which the normal coordinates $a_{q\nu}$ (or displacements $u_{i\varkappa}(q)$) and components $\mathscr{E}_j$ transform, we can find the number of nonzero components $Q_{\nu j}(q)$ (or $Q^{\varkappa}_{ij}(q)$) and the relation between the linearly dependent components, and the theory of invariants readily yields the Hamiltonian U (32.9).

It follows from equation (32.9) that the polarization $\boldsymbol{P}$ per unit volume is

$$P_l(\boldsymbol{q}) = -\frac{1}{\mathcal{V}}\frac{\partial U}{\partial \mathscr{E}_l(-\boldsymbol{q})} = \frac{2}{\Omega_0}\sum_{\nu} Q_{\nu l}(\boldsymbol{q})\, a_{\boldsymbol{q}\nu} + \sum_i \alpha_{il}^{\infty}\mathscr{E}_i(\boldsymbol{q}). \tag{32.10}$$

Transforming the equations of motion (15.6)

$$-M_{\varkappa}\omega^2 u_{l\varkappa i} = \frac{\partial U}{\partial u_{l\varkappa i}}$$

to the new variables according to (15.10) and (32.9), we obtain

$$\omega^2 a_{\boldsymbol{q}\nu} = \frac{1}{4M_0 N}\frac{\partial U}{\partial a_{-\boldsymbol{q}\nu}} = \omega_{\boldsymbol{q}\nu}^2 a_{\boldsymbol{q}\nu} - \frac{1}{2M_0}\sum Q_{\nu l}(-\boldsymbol{q})\mathscr{E}_l(\boldsymbol{q}). \tag{32.11}$$

In order to determine the lattice vibration spectrum allowing for long-range forces, we must supplement the system of equations (32.10) and (32.11) by Maxwell's equations; for plane waves, these are

$$(\boldsymbol{q}\mathscr{D}_{\boldsymbol{q}}) = 0, \quad (\boldsymbol{q}\boldsymbol{H}_{\boldsymbol{q}}) = 0, \quad [\boldsymbol{q}\mathscr{E}_{\boldsymbol{q}}] = \frac{\omega}{c}\boldsymbol{H}_{\boldsymbol{q}}, \quad [\boldsymbol{q}\boldsymbol{H}_{\boldsymbol{q}}] = -\frac{\omega}{c}\mathscr{D}_{\boldsymbol{q}}, \tag{32.12}$$

and they reduce to the single equation

$$\mathscr{D}_{\boldsymbol{q}} = \mathscr{E}_{\boldsymbol{q}} + 4\pi\boldsymbol{P}_{\boldsymbol{q}} = -\frac{c^2}{\omega^2}[\boldsymbol{q}(\boldsymbol{q}\mathscr{E}_{\boldsymbol{q}}) - \mathscr{E}_{\boldsymbol{q}}q^2]. \tag{32.13}$$

Expressing $a_{\boldsymbol{q}\nu}$ in (32.11) in terms of $\mathscr{E}_j$ and substituting into (32.10), we find that

$$\mathscr{D}_i(\boldsymbol{q}) = \sum \varkappa_{il}(\omega, \boldsymbol{q})\mathscr{E}_l(\boldsymbol{q}), \tag{32.14}$$

where

$$\varkappa_{il}(\omega, \boldsymbol{q}) = \frac{4\pi}{M_0\Omega_0}\sum_{\nu}\frac{Q_{\nu l}(\boldsymbol{q})\, Q_{\nu i}(-\boldsymbol{q})}{\omega_{\boldsymbol{q}\nu}^2 - \omega^2} + \varkappa_{il}^{\infty}. \tag{32.14a}$$

Substituting (32.14) into (32.13), we obtain a system of equations for the components $\mathscr{E}_i(\boldsymbol{q})$, whose determinant

$$\left|\varkappa_{il}^{\infty} - \frac{q^2c^2}{\omega^2}\delta_{il} + \frac{c^2}{\omega^2}q_i q_l\right| = 0 \tag{32.15}$$

determines the spectrum $\omega(\boldsymbol{q})$, both for photons and for those lattice vibrations which set up a nonzero electric field.

In consideration of electron-phonon interactions, we can usually disregard time lag, since for phonons with a wave vector close to the wave vector of the electrons, $q^2c^2/\omega^2 \gg 1$. In this approximation, the field $\mathscr{E}$, as is evident from (32.12) or (32.13), is longitudinal; it is easily determined by setting $\mathscr{E}_{\boldsymbol{q}} = -i\boldsymbol{q}\varphi_{\boldsymbol{q}}$ in the equation $(\boldsymbol{q}\mathscr{D}_{\boldsymbol{q}}) = q\mathscr{E}_{\boldsymbol{q}} + 4\pi(\boldsymbol{P}_{\boldsymbol{q}}\boldsymbol{q}) = 0$ and substituting $\boldsymbol{P}_{\boldsymbol{q}}$ from (32.10). The result is

$$\varphi_{\boldsymbol{q}} = -4\pi i(\boldsymbol{q}\boldsymbol{P}^{a}(\boldsymbol{q}))\Big/\sum_{il}\varkappa_{il}^{\infty}q_i q_l \tag{32.16}$$

and thus

$$\mathscr{E}(\boldsymbol{q}) = -4\pi\boldsymbol{q}(\boldsymbol{q}\boldsymbol{P}^{a}(\boldsymbol{q}))\Big/\sum_{il}\varkappa_{il}^{\infty}q_i q_l, \tag{32.16a}$$

where $\boldsymbol{P}^{a}(\boldsymbol{q})$ is the polarization induced by the lattice vibrations, which is, by

(32.10) and (32.8c),

$$P_l^{\mu}(q)=\frac{1}{\Omega_0}\sum_{l\varkappa}Q_{ll}^{\varkappa}(q)\,u_{l\varkappa}(q)=\frac{2}{\Omega_0}\sum_{l}Q_{\nu l}(q)\,a_{q\nu}. \tag{32.17}$$

Substituting (32.16a) and (32.17) into (32.11), we obtain the system of equations

$$\left(\omega_{q\nu}^{0\,2}-\omega^2\right)a_{q\nu}+\sum_{\nu'}\Theta_{\nu}(-q)\,\Theta_{\nu'}(q)\,a_{q\nu'}=0, \tag{32.18}$$

where

$$\Theta_{\nu}(q)=\left(\frac{4\pi}{M_0\Omega_0\sum_{ll}\varkappa_{ll}^{\infty}q_lq_l}\right)^{1/2}\sum_{l}Q_{\nu l}(q)\,q_l. \tag{32.18a}$$

Equating the determinant of this system to zero,

$$\left|\left(\omega_{q\nu}^{0\,2}-\omega^2\right)\delta_{\nu\nu'}+\Theta_{\nu}(-q)\,\Theta_{\nu'}(q)\right|=\prod_{\nu}\left(\omega_{q\nu}^{0\,2}-\omega^2\right)\left[1+\sum_{\nu'}\frac{\Theta_{\nu'}(q)\,\Theta_{\nu'}(-q)}{\omega_{q\nu'}^{0\,2}-\omega^2}\right]=0, \tag{32.18b}$$

we find the normal frequencies $\omega_{q\nu}$ allowing for long-range forces.

Equation (32.18b) shows that one term splits off from each n_ν-fold degenerate terms ω_ν^0 when the long-range effect is included and $\Theta_\nu\neq 0$. The frequency of these shifted terms is determined by the equation

$$\sum_{ll}\varkappa_{ll}^{\infty}q_lq_l+\frac{4\pi}{M_0\Omega_0}\sum_{\nu ll}\frac{Q_{\nu l}(q)\,Q_{\nu l}(-q)\,q_lq_l}{\omega_{q\nu}^{0\,2}-\omega^2}=0. \tag{32.18c}$$

This equation can be derived at once from the condition

$$(q\mathcal{D}_q)=-i\sum_{ll}\varkappa_{ll}q_lq_l\varphi_q=0,$$

whence it follows that if $\varphi_q\neq 0$

$$\sum_{ll}\varkappa_{ll}q_lq_l=0. \tag{32.18d}$$

Substituting $\varkappa_{ll}$ from (32.14a) into (32.18d), we obtain (32.18c).*

Determining the normal frequencies $\omega_{q\nu}$ from equations (32.18b, c, d), using equation (32.18), we find the displacements $a_{q\nu}^{\mu}$ corresponding to the frequency $\omega_{q\nu}$:

$$a_{q\nu}^{\mu}=A\frac{Q_{\nu}(-q)}{\omega_{q\mu}^2-\omega_{q\nu}^{0\,2}}. \tag{32.19}$$

* At first sight, the additional splitting of the terms in long wavelength modes, due to long-range effects, would seem to contradict the conclusions of group theory. However, this splitting actually occurs not for $q=0$ but for $q\sim 1/L$, where L is the dimension of the crystal. Because of the finite contribution of the surface to the vibration energy of a polar crystal, the arrangement of terms at $q=0$ is determined not only by the symmetry of the crystal lattice, but also by the symmetry of the specimen. Therefore, when $q\sim 1/L$, the spectrum suddenly changes: when $q\gg 1/L$ it no longer depends on the shape of the specimen, but then it depends in principle on q. The splitting of terms due to long-range effects is then usually less than permitted by the symmetry of the little group G_q.
The additional splitting due to short-range forces is proportional to qa, where a is the lattice constant, so it becomes significant at considerably larger q values. These terms must be taken into account when calculating the phonon dispersion.

The constant $A = \sum_{\nu} \Theta_{\nu}(q) a_{q\nu}$ is determined by the normalization condition

$$\sum_{\nu} |a^{\mu}_{q\mu}|^2 = |\bar{a}_{q\mu}|^2 = \text{const},$$

where $|\bar{a}_{q\mu}|^2$ is defined by (15.24). Substituting these values of $a^{\mu}_{q\nu}$ into (32.17), we find the polarization $\boldsymbol{P}^{\mu}(q)$, and then use (32.16a) and (32.16) to determine the field $\boldsymbol{\mathcal{E}}^{\mu}(q)$ and the potential φ^{μ}_{q} set up by the mode $q\mu$ with frequency $\omega_{q\mu}$.

Polarization proportional to the displacement (not vanishing at $q = 0$) is possible only for optical modes in polar crystals, i.e., crystals made up of atoms of different elements, or in crystals whose primitive cell contains more than two like atoms.

In cubic crystals whose primitive cell contains two atoms with masses M_1 and M_2, we can choose the polarization vectors $e^{l\,\text{opt}}_{\varkappa i}$ for the three branches of the optical modes as

$$e^{l\,\text{opt}}_{1i} = \sqrt{M_2/M_1}\,\delta_{il}, \quad e^{l\,\text{opt}}_{2i} = -\sqrt{M_1/M_2}\,\delta_{il}; \tag{32.20a}$$

correspondingly, the normal coordinates a^{opt}_{l} are

$$a^{\text{opt}}_{l} = \frac{\sqrt{M_1 M_2}}{2(M_1 + M_2)}(u_{1l} - u_{2l}) \tag{32.20b}$$

and transform like the i-th component of the coordinate. Only the diagonal components of the effective charge are nonzero:

$$Q^{\text{opt}}_{l,\,il}(0) = Q\delta_{il} \tag{32.20c}$$

and consequently, by (32.16),

$$\varphi^{\text{opt}}_{q} = -\frac{8\pi i Q(q a^{\text{opt}})}{\Omega_0 q^2}, \tag{32.21}$$

i.e., in the zeroth q-approximation the field φ^{opt} arises only in longitudinal optical modes, when the vector $\boldsymbol{a}^{\text{opt}}$ with components a^{opt}_{l} is parallel to q. By (32.18c), the frequency of these modes is

$$\omega_l^2 = \omega_t^2 + \frac{4\pi Q^2}{M_0 \Omega_0 \varkappa^{\infty}}, \tag{32.21a}$$

where $\omega_t = \omega^0$ is the frequency of the transverse modes.

In this case, according to (32.14a),

$$\varkappa(\omega) = \varkappa^{\infty} + \frac{4\pi Q^2}{M_0 \Omega_0 (\omega_t^2 - \omega^2)}, \tag{32.21b}$$

and so the effective charge Q may be expressed in terms of the difference of dielectric constants between the higher frequency $\varkappa^{\infty}$ ($\omega \gg \omega^0$) and the lower $\varkappa^0$ ($\omega \ll \omega^0$):

$$Q^2 = \frac{\varkappa^0 - \varkappa^{\infty}}{4\pi} M_0 \Omega_0 \omega_t^2. \tag{32.21c}$$

Equations (32.21a) and (32.21c) imply the well-known relation

$$\frac{\omega_l^2}{\omega_t^2} = \frac{\varkappa^0}{\varkappa^{\infty}}. \tag{32.21d}$$

For nonpolar crystals, the expansion (32.9c) begins with linear q terms. These are the terms that determine the dipole moment due to transverse optical modes in cubic polar crystals with two atoms per cell.

In the diamond lattice, the tensor Q, like the tensor Γ in (32.5), has one linearly independent component $Q^0_{xyz} = Q^0_{xzy} = Q$, and thus

$$\varphi_q^{\text{opt}} = -\frac{8\pi i}{\varkappa q^2} Q\left(q_x q_y a_z^{\text{opt}} + q_x q_z a_y^{\text{opt}} + q_y q_z a_x^{\text{opt}}\right), \tag{32.22}$$

where, by (32.20b), $a_l^{\text{opt}} = \frac{1}{4}(u_{1l} - u_{2l})$.

For acoustical modes, the expansion (32.9c) again begins with linear q terms, since motion of the crystal as a whole does not create an electric field. Rotation of the crystal does not induce an electric field either, and so the dipole moment due to acoustical modes may only be proportional to the strain:

$$P_l^u(q) = -i \sum_{lj} \beta_{llj} e_{lj}(q), \tag{32.23}$$

where

$$e_{lj}(q) = \frac{1}{\mathcal{V}} \int e_{lj}(x) e^{-iqx}\, dx = \frac{i}{2}(q_l u_{qj} + q_j u_{ql}). \tag{32.23a}$$

Crystals for which the tensor β does not vanish are known as piezoelectric crystals.

In cubic crystals of classes T and T_d, the tensor β has one linearly independent component $\beta_{xyz} = \beta_{xzy} = \beta$, and thus

$$\varphi_q^{\text{ac}} = -\frac{8\pi i \beta}{\varkappa^0 q^2}\left(q_x e_{yz}(q) + q_y e_{xz}(q) + q_z e_{xy}(q)\right). \tag{32.23b}$$

In cubic crystals of class O and crystals having an inversion center, $\beta = 0$, and the acoustical modes produce a dipole moment proportional to the second derivatives of the average displacements; these are precisely the normal coordinates for acoustical modes at $q = 0$, i.e., the expansion (32.9c) begins with second order terms in q:

$$P_l^u(q) = -\sum_{ikl} \gamma_{likl} u_{qi} q_k q_l. \tag{32.24}$$

The tensor γ is symmetric under permutation of the last pair of indices. It is easily seen from equation (20.10) that in a cubic crystal this tensor has three nonzero linearly independent components:

$$\gamma_{11} = \gamma_{xxxx},\quad \gamma_{12} = \gamma_{xxyy},\quad \gamma_{44} = \gamma_{yzyz}.$$

However, the quantity

$$\varphi_q^{\text{ac}} = -\frac{4\pi i}{\varkappa^0 q^2}(q P_q^u) = \frac{4\pi i}{\varkappa^0 q^2} \sum_{ijkl} \gamma_{likl} q_l q_k q_i u_{qj} \tag{32.25}$$

depends in a cubic crystal on only two independent constants, γ_{11} and $\gamma_{12} + 2\gamma_{44}$, since

$$\sum_{i \neq j} e_{lj}(q) q_i q_j = i \sum_{i \neq j} u_{qi} q_j q_i q_j = \sum_{i \neq j} e_{ii}(q) q_j^2 = e_q \cdot q^2 - \sum_i e_{ii}(q) q_i^2.$$

Therefore,

$$\varphi_q^{\text{ac}} = \frac{4\pi i}{q^2 \varkappa^0}\left[(\gamma_{12} + 2\gamma_{44}) e_q q^2 + (\gamma_{11} - \gamma_{12} - 2\gamma_{44}) \sum_i e_{ii}(q) q_i^2\right], \tag{32.25a}$$

where $e_q = \sum_i e_{ii}(q)$. In an isotropic medium $\gamma_{11} - \gamma_{12} = 2\gamma_{44}$, and

$$\varphi_q^{ac} = \frac{4\pi i}{\varkappa^0 q^2}(\gamma_{12} + 2\gamma_{44}) e_q q^2. \tag{32.25b}$$

For acoustical modes, the derivatives of the relative displacements $u^{\varkappa\varkappa'}$ need not be included separately in (32.23) and (32.24), since by (32.5) these displacements may be expressed in terms of $\partial u_i/\partial x_j$. However, they must be kept in mind in direct calculation of the constants β or γ. For example, by (32.8), (32.5) and (32.23), in piezoelectric crystals their contribution to β is

$$\beta'_{ilj} = \frac{1}{2\Omega_0} \sum_{k\varkappa\varkappa'} \Theta_{ik}^{\varkappa\varkappa'} \Gamma_{klj}^{\varkappa\varkappa'}.$$

and by (32.22), (32.5) and (32.24) their contribution to γ in nonpiezoelectric crystals may be written

$$\gamma'_{ijkl} = \frac{1}{2} \sum_{m\varkappa\varkappa'} \Phi_{imj}^{\varkappa\varkappa'} \Gamma_{mkl}^{\varkappa\varkappa'}.$$

For example, in the T_d^2 lattice this contribution to β_{xyz} is $\beta'_{xyz} = \Theta_{xx}\Gamma_{xyz}$, and in the diamond O_h^7 lattice the displacements $u_{1,2}$ yield a contribution to γ_{44}:

$$\gamma'_{xyxy} = \Phi_{xzy}\Gamma_{zxy}.$$

As noted in §22, the motion of an electron in sufficiently "gentle" external fields may be described in the effective mass approximation; in other words, instead of the exact Schrödinger equation for the Bloch functions one uses the equations for the smooth envelope functions $\mathcal{F}(x, t)$. The scattering of current carriers in semiconductors can be treated in this approximation. The potential $\varphi(x)$ due to long-range forces is smooth, and so it can be introduced directly in the potential $U(x)$ appearing in the operator $\mathcal{H}$ of (22.15), (22.16).

Short-range forces

The potential $\delta V_s(x)$ due to short-range forces, unlike $\varphi(x)$, varies rapidly within the bounds of one primitive cell. However, it is clear from (32.6) and (32.7) that if q is small this potential is almost periodic, since $\nabla V_0(x)$, $V_{ij}(x)$ and $V_0^{\varkappa\varkappa'}(x)$ are periodic functions with the same period as $V_0(x)$, so that we can describe the interaction of the electrons with the lattice using only the envelope functions $\mathcal{F}(x, t)$. In order to obtain the operator $\mathcal{H}_{\text{eff}}$ acting on these functions and determining the electron-phonon interaction, we first write the operator $\delta V(x)$ in the (k, n)-presentation. To this end we proceed as in §22, expressing the function Ψ as a linear combination (22.2) and then expanding $\mathcal{F}_n(x, t)$ in Fourier series (22.3). To derive the equation for the coefficients c_{nk} in (22.3) and (22.4), we must calculate the matrix elements of the operator $\delta V(x)$ between the functions $\varphi_{nk} = \frac{1}{\sqrt{\mathcal{V}}} \psi_{nk_0} e^{ikx}$. To do this, we expand the periodic function $\psi^*_{n'k_0} \nabla V_0 \psi_{nk_0}$ in Fourier series:

$$\psi^*_{n'k_0} \nabla V_0 \psi_{nk_0} = \mathcal{V}^{-1} \sum_M e^{-ib_M x} R_M,$$

where

$$\mathcal{V}^{\circ}\boldsymbol{R}_M = \frac{1}{\mathcal{V}^{\circ}}\int \psi^{*}_{n'k_0}\nabla V_0 \psi_{nk_0} e^{i\boldsymbol{b}_M \boldsymbol{x}}\, d\boldsymbol{x},$$

and $\boldsymbol{b}_M$ are reciprocal lattice vectors. Then the matrix elements of the operator $\mathcal{H}'' = -\boldsymbol{u}\nabla V_0$ may be written

$$\mathcal{H}''_{n'k',\,nk} = -\langle \varphi_{n'k'} \boldsymbol{u}\nabla V_0 \varphi_{nk}\rangle = -\sum_M \boldsymbol{R}_M \int \boldsymbol{u}(\boldsymbol{x})\, e^{i(\boldsymbol{k}-\boldsymbol{k}'-\boldsymbol{b}_M)\boldsymbol{x}}\, d\boldsymbol{x}.$$

If $\boldsymbol{k}$ and $\boldsymbol{k}'$ are sufficiently small, so that $\boldsymbol{q} = \boldsymbol{k}' - \boldsymbol{k}$ is within the Brillouin zone, only terms with $\boldsymbol{b}_M = 0$ remain, and then

$$\mathcal{H}''_{n'k',\,nk} = -\langle \varphi_{n'k'} \boldsymbol{u}\nabla V_0 \varphi_{nk}\rangle = -\boldsymbol{u}_{k'-k}\,(1/\mathcal{V}^{\circ})\langle \psi_{n'k'_0}\nabla V_0 \psi_{nk_0}\rangle. \tag{32.26}$$

Similarly, we can expand the periodic functions $\psi^{*}_{n'k'_0} V_{ij}\psi_{nk_0}$ and $\psi^{*}_{n'k'_0} V_0^{\varkappa\varkappa'}\psi_{nk_0}$ in Fourier series, and similar transformations then yield the matrix elements of the operators $\mathcal{H}' = (\varepsilon \boldsymbol{V})$ and $\mathcal{H}''' = \frac{1}{2}\sum_{\varkappa\varkappa'} \boldsymbol{V}_0^{\varkappa\varkappa'} u_{\varkappa\varkappa'}$:

$$\mathcal{H}'_{n'k',\,nk} = \langle \varphi_{n'k'}(\varepsilon \boldsymbol{V})\varphi_{nk}\rangle = (1/\mathcal{V}^{\circ})\sum_{ij} e_{q,\,ij}\langle \psi_{n'k_0} V_{ij}\psi_{nk_0}\rangle \delta_{q,\,k'-k}, \tag{32.27}$$

$$\mathcal{H}'''_{n'k',\,nk} = \frac{1}{2}\sum_{\varkappa\varkappa'}\langle \varphi_{n'k'} \boldsymbol{V}_0^{\varkappa\varkappa'} u_{\varkappa\varkappa'}\varphi_{nk}\rangle = \frac{1}{2\mathcal{V}^{\circ}}\sum_{\varkappa\varkappa'} u_q^{\varkappa\varkappa'}\langle \psi_{n'k_0}\boldsymbol{V}_0^{\varkappa\varkappa'}\psi_{nk_0}\rangle \delta_{q,\,k'-k}. \tag{32.28}$$

As a result we obtain a system of equations for the coefficients c_{nk}, similar to (22.11):

$$\sum_{nk}\{[\mathcal{H}_1 + \mathcal{H}' + \mathcal{H}''' + \mathcal{H}_2 + \mathcal{H}'']_{n'k',\,nk} + E_n\delta_{n'n}\delta_{k'k}\}\, c_{nk} = i\hbar\frac{\partial}{\partial t}\, c_{n'k'}, \tag{32.29}$$

where $\mathcal{H}_1$ and $\mathcal{H}_2$ are the operators defined in (22.10) in our treatment of the spectrum by kp-theory:

$$\mathcal{H}_{2\,n'k',\,nk} = \frac{1}{m}\hbar\boldsymbol{k}\boldsymbol{p}_{n'n}\delta_{k'k}, \qquad \mathcal{H}_{1\,n'k',\,nk} = \frac{\hbar^2 k^2}{2m}\,\delta_{n'n}\delta_{k'k}. \tag{32.30}$$

In order to go over from the exact system of equations (32.29) to a system containing coefficients c_{nk} for only one band, we must proceed as in §§21 and 22 to eliminate the interband matrix elements of $\mathcal{H}_2$ and $\mathcal{H}''$. At a point of zero slope, the operator $\mathcal{H}_2$ does not contain intraband matrix elements. Using the relation

$$(\nabla V_0)\psi = \nabla(\mathcal{H}_0\psi) - \mathcal{H}_0\nabla\psi = \{\nabla\mathcal{H}_0\}\psi = \frac{i}{\hbar}\{\boldsymbol{p}\mathcal{H}_0\}\psi,$$

we can express the matrix elements of the operator $\nabla V_0 = (i/\hbar)\{\boldsymbol{p}\mathcal{H}_0\}$ in the form (21.35):

$$(1/\mathcal{V}^{\circ})\langle \psi_{n'k'}\nabla V_0 \psi_{nk_0}\rangle = \frac{i}{\hbar}\sum_m (\boldsymbol{p}_{n'm}\mathcal{H}_{0mn} - \mathcal{H}_{0n'm}\boldsymbol{p}_{mn}) = -i\omega_{n'n}\boldsymbol{p}_{n'n}, \tag{32.31}$$

where $\omega_{n'n} = (E_{n'} - E_n)/\hbar$.

Thus, the operator $\mathcal{H}''$ also has only interband matrix elements. The operators $\mathcal{H}'$ and $\mathcal{H}'''$ have interband matrix elements too, but the operator $\mathcal{H}$ obtained by eliminating them would have terms which either are quadratic in the displacement or contain the second derivatives of the displacement $\boldsymbol{u}$

and the first derivatives of $u^{\varkappa\varkappa'}$. Since terms of this order are omitted in (32.6) and (32.7), they need not be considered here, and only the intraband elements of these operators need be retained.

Now the displacements u are time-dependent; thus, when the interband elements of $\mathcal{H}_2$ are eliminated, additional terms appear in $\mathcal{H}$ owing to the explicit dependence of the transformation matrix S (15.33) on t. However, as shown in §22, these terms are smaller than the principal terms by a factor $\omega/\omega_{n'n}$. Since $\omega \ll E_g/\hbar$, these additional terms may be omitted. As a result we obtain a system of equations similar to (22.12):

$$\sum_{mk} \mathcal{H}_{m'k',\,mk} \overset{=}{c}_{mk} = i\hbar \frac{\partial}{\partial t} \overset{=}{c}_{m'k'}, \tag{32.32}$$

where, by (15.47), $\mathcal{H}_{m'k',\,mk}$ contains the terms

$$\mathcal{H}_{m'k',\,mk} = \mathcal{H}'_{m'k',\,mk} + \mathcal{H}'''_{m'k',\,mk} + \sum_{sk} \frac{\mathcal{H}_{2m'k',\,sk''}\mathcal{H}''_{sk'',\,mk} + \mathcal{H}''_{m'k',\,sk''}\mathcal{H}_{2sk'',\,mk}}{E_m - E_s}. \tag{32.33}$$

apart from the terms determined by equation (21.19). Terms of second order in $\mathcal{H}''$, i.e., quadratic in the displacement, may be ignored. Using the equations (32.26), (32.30) and (32.31) for the matrix elements of the operators $\mathcal{H}_2$ and $\mathcal{H}''$, we can rewrite the last term in (32.33) as

$$\frac{i}{m} \sum_{s \neq m,\,m'} \sum_{i,\,l} (u_{k'-k,\,i} k_l - u_{k'-k,\,l} k'_i)\, p^i_{m's} p^l_{sm}.$$

We can then sum over s, using the fact that the functions φ_{nk} form a complete system and the matrix element $p_{mm'}$ vanishes at an extremum point, so that the summation may be extended to all s values, including $m, m', \ldots$ The result is

$$-\frac{1}{\mathcal{V}} \frac{i\hbar^2}{m} \sum_{il} (u_{k'-k,\,i} k_l - u_{k'-k,\,l} k'_i) \left\langle \psi_{m'k_0} \frac{\partial^2}{\partial x_i\, \partial x_l} \psi_{mk_0} \right\rangle =$$

$$= \frac{i\hbar^2}{m} \sum_{il} u_{qi} q_l \left\langle m' \left| \frac{\partial^2}{\partial x_i\, \partial x_l} \right| m \right\rangle = \frac{\hbar^2}{m} \sum_{il} e_{q,\,il} \left\langle m' \left| \frac{\partial^2}{\partial x_i\, \partial x_l} \right| m \right\rangle.$$

Here we have put $q = k' - k$. We have also utilized the invariance of the matrix element

$$\left\langle m' \left| \frac{\partial^2}{\partial x_i\, \partial x_l} \right| m \right\rangle$$

under permutation of the indices i and j. Combining this term with the first term in (32.33), we obtain an expression for the operator $\mathcal{H}^{ac}$ which describes the interaction with acoustical modes:

$$\mathcal{H}^{ac}_{q,\,m'm} = \sum_{il} e_{q,\,il} D^{il}_{m'm} = \sum_{il} e_{q,\,il} \left(\frac{\hbar^2}{m} \left\langle m' \left| \frac{\partial^2}{\partial x_i\, \partial x_l} \right| m \right\rangle + \langle m' | V_{il} | m \rangle \right). \tag{32.34}$$

The second term in (32.33) yields the operator $\mathcal{H}^{opt}$, which describes the interaction with optical modes:

438

$$\mathcal{H}^{opt}_{q,\,m'm} = \frac{1}{2} \sum_{\varkappa,\,\varkappa'} u^{\varkappa\varkappa'}_q V^{opt}_{m'm} = \frac{1}{2} \sum_{\varkappa,\,\varkappa'} u^{\varkappa\varkappa'}_q \langle m' | V^{\varkappa\varkappa'}_{opt} | m \rangle. \tag{32.35}$$

We now transform (32.32) to the x-representation, multiplying its right and left sides by $e^{ik'x}$ and summing over k', k as in §22 (equation (22.14a)); we obtain a system of equations for the functions $\mathcal{F}_m$:

$$\sum_m \left(\mathcal{H}_{m'm}(k) + \mathcal{H}^{ac}_{m'm} + \mathcal{H}^{opt}_{m'm} - E_m\right)\mathcal{F}_m = i\hbar \frac{\partial \mathcal{F}_{m'}}{\partial t}, \tag{32.36}$$

where

$$\mathcal{H}^{ac}_{m'm}(\varepsilon) = \sum_{il} \varepsilon_{il} D^{il}_{m'm}, \tag{32.36a}$$

$$\mathcal{H}^{opt}_{m'm}(u^{opt}) = \frac{1}{2}\sum_{xx'} u^{xx'} V^{xx'}_{m'm\,opt}. \tag{32.36b}$$

It is evident from equations (32.36a) and (29.21) that $\mathcal{H}^{ac}$ is precisely the operator $\mathcal{H}^{\varepsilon}$ defining the change in the spectrum under a homogeneous strain. The effective potential produced by the lattice vibrations, defined by equation (32.36), is called the deformation potential; the constants D appearing in $\mathcal{H}^{ac}$ are the deformation potential constants introduced above. The matrix $\mathcal{H}^{ac}$, and the matrix $\mathcal{H}^{opt}$ describing the interaction with optical modes associated with short-range forces, may be constructed by the theory of invariants. For this purpose, we write $\mathcal{H}^{opt}$ as a sum of products of matrices X, which transform according to irreducible representations, and the combinations of displacements $u_i^{xx'}$, which transform according to the conjugate representations. These combinations of $u^{xx'}$ are the normal modes corresponding to the limiting optical frequency.

When necessary, it is easy to find the relativistic corrections to the deformation potential constants by the theory of invariants. However, it is usually enough to allow for spin-orbit coupling only in the zeroth approximation with respect to k and ε, the eigenfunctions of the operator $\mathcal{H}_0$, which includes $\mathcal{H}_{so}$, being taken as the basis functions of the matrix $\mathcal{H}$.

To introduce the effect of long-range forces in (32.36), we must include the matrix $\mathcal{H}_{l.\,m'm} = -e\varphi\delta_{m'm}$, where φ is the potential set up by the corresponding vibrations, defined by equations (32.16), (32.21), (32.22), (32.23b) and (32.25). Comparing (32.36b) and (32.22), we see that in nonpolar crystals the contribution of both short- and long-range forces associated with optical modes to $\mathcal{H}$ is of the same order, namely, zeroth order, with respect to q, while, as we see from (32.21), in polar crystals the long-range forces contribute to a lower order: $\delta V_l \sim q^{-1}$. Similarly, piezoelectric acoustical modes produce a potential (32.23b) which is zero order in q, while according to (32.36a) and (32.25) both short- and long-range forces in nonpiezoelectric crystals are first order in q.

As to the relations between these forces in nonpiezoelectric crystals, at present there is no experimental evidence that long-range forces play a significant role in scattering by acoustical modes or in scattering by optical modes in nonpolar crystals. Henceforth, then, we shall disregard their contribution to scattering. On the other hand, neither is there any theoretical basis for the assumption that the potential $\varphi(x)$ in such crystals must be small compared to the deformation potential.

Transition probabilities

In order to calculate the probability of the transition of an electron between states due to the perturbations $\mathcal{H}^{ac}$ and $\mathcal{H}^{opt}$ in (32.36), we must first find the eigenfunctions of the operator $\mathcal{H}(\boldsymbol{k})$. In the case of degenerate bands, different values of $E_l(\boldsymbol{k})$ $(l = 1, 2, \ldots)$ correspond to the same value of $\boldsymbol{k}$. In crystals with an inversion center each of the states $\boldsymbol{k}l$ is twofold degenerate counting spin, i.e., for each energy $E_l(\boldsymbol{k})$ there are two functions $\mathcal{F}_{tl\boldsymbol{k}}$ $(t = 1, 2)$. Each of these functions may be written as a column matrix with elements $\mathcal{F}^s_{tl\boldsymbol{k}}$. The number of rows in this matrix is determined by the dimension of the representation. For example, for the Γ_8 representation in the Ge and Si lattice, the functions are given by equations (24.19). Let us expand the displacement of each of the atoms in Fourier series, as in (15.25). Thus, the expansion for a strain $\varepsilon_{ij}(\boldsymbol{x}) = \frac{1}{2}\left(\frac{\partial \bar{u}_i}{\partial x_j} + \frac{\partial \bar{u}_j}{\partial x_i}\right)$ due to long wavelength acoustical modes is

$$\varepsilon_{ij} = \sum_{q,\ \nu=1,2,3} a_{q\nu}\varepsilon'_{q\nu,\ ij}e^{iqx} + a^+_{q\nu}\varepsilon'^*_{q\nu,\ ij}e^{-iqx}, \tag{32.37}$$

where

$$\varepsilon'_{q\nu,\ ij} = \frac{i}{2}\left(e^\nu_i(\boldsymbol{q})\,q_j + e^\nu_j(\boldsymbol{q})\,q_i\right). \tag{32.38}$$

In this case, by (15.14),

$$e^\nu e^{\nu'*} = \delta_{\nu\nu'}, \qquad e^\nu e^{\nu'} = 0 \text{ for } \nu \neq \nu'. \tag{32.39}$$

The total wave function of the system is a product of electronic functions $\mathcal{F}$ and phonon functions. The selection rules for the operators a and a^+ acting on the phonon functions are determined by (15.26). The final expression for the probability of a transition from state $\boldsymbol{k}lt$ to state $\boldsymbol{k}'l't'$ with absorption of an acoustical phonon ν is

$$P_{\substack{l't',\ \boldsymbol{k}+\boldsymbol{q}\\ lt,\ \boldsymbol{k}}} = \frac{2\pi}{\hbar}\left(\frac{\hbar n_{q\nu}}{2\rho\omega_{q\nu}\mathcal{V}}\right)\left|\langle l't',\ \boldsymbol{k}+\boldsymbol{q}\,|\,\mathcal{H}(\varepsilon_{q\nu})\,|\,lt\boldsymbol{k}\rangle\right|^2 \times \\ \times\,\delta(E_l(\boldsymbol{k}) - E_{l'}(\boldsymbol{k}+\boldsymbol{q}) + \hbar\omega_{q\nu}), \tag{32.40}$$

where

$$\langle l't'\boldsymbol{k}'\,|\,\mathcal{H}\,|\,lt\boldsymbol{k}\rangle = \sum_{sr}\mathcal{F}^{s*}_{l't'\boldsymbol{k}'}\mathcal{H}_{sr}\mathcal{F}^r_{lt\boldsymbol{k}},$$

and the matrix $\mathcal{H}(\varepsilon_{q\nu})$ is defined by (32.36a). In order to obtain the total probability of transition of an electron from a state with energy $E_l(\boldsymbol{k})$ to a state $E_{l'}(\boldsymbol{k}')$, we must sum (32.40) over the final states t' and average over the initial states t and also over the initial states of the phonons. This reduces to replacing the occupation numbers $n_{q\nu}$ by their averages $\bar{n}_{q\nu}$, defined by equation (15.24). The transition probability is

$$P^{ac}_{\substack{l',\ \boldsymbol{k}+\boldsymbol{q}\\ l,\ \boldsymbol{k}}} = \frac{2\pi}{\hbar}\left(\frac{\hbar\bar{n}_{q\nu}}{2\rho\omega_{q\nu}\mathcal{V}}\right)W^{ac}_{\substack{l',\ \boldsymbol{k}+\boldsymbol{q}\\ l,\ \boldsymbol{k}}}(\varepsilon'_{q\nu})\,\delta(E_l(\boldsymbol{k}) - E_{l'}(\boldsymbol{k}+\boldsymbol{q}) + \hbar\omega_{q\nu}), \tag{32.41a}$$

where

$$W^{ac}_{\substack{l'\boldsymbol{k}'\\ l\ \boldsymbol{k}}}(\varepsilon'_{\boldsymbol{k}'-\boldsymbol{k},\,\nu}) = \frac{1}{2}\sum_{tt'}\left|\mathcal{H}(\varepsilon_{\boldsymbol{k}'-\boldsymbol{k},\,\nu})_{\substack{l't'\boldsymbol{k}'\\ l\ t\ \boldsymbol{k}}}\right|^2. \tag{32.42}$$

Similarly, the total probability of transition from a state with energy $E_l(\boldsymbol{k})$ to a state $E_{l'}(\boldsymbol{k}')$ with emission of an acoustical phonon is

$$P^{\text{ac}}_{\substack{l',\,\boldsymbol{k}-\boldsymbol{q}\\ l,\,\boldsymbol{k}}} = \frac{2\pi}{\hbar}\left(\frac{\hbar(\bar{n}_{q\nu}+1)}{2\rho\omega_{q\nu}\mathcal{V}}\right) W^{\text{ac}}_{\substack{l',\,\boldsymbol{k}-\boldsymbol{q}\\ l,\,\boldsymbol{k}}}(\boldsymbol{e}'_{q\nu})\,\delta(E_l(\boldsymbol{k}) - E_{l'}(\boldsymbol{k}-\boldsymbol{q}) - \hbar\omega_{q\nu}). \tag{32.41b}$$

The total probability of transitions with absorption and emission of optical phonons is derived in analogous fashion:

$$P^{\text{opt}}_{\substack{l',\,\boldsymbol{k}+\boldsymbol{q}\\ l,\,\boldsymbol{k}}} = \frac{2\pi}{\hbar}\left(\frac{\hbar\bar{n}^{\text{opt}}_{\nu}}{2\rho\omega^{\text{opt}}_{\nu}\mathcal{V}}\right) W^{\text{opt}}_{\substack{l',\,\boldsymbol{k}+\boldsymbol{q}\\ l,\,\boldsymbol{k}}}(\boldsymbol{e}^{\nu}_{\text{opt}}(\boldsymbol{q}))\times\ \delta(E_l(\boldsymbol{k}) - E_{l'}(\boldsymbol{k}+\boldsymbol{q}) + \hbar\omega^{\text{opt}}_{\nu}), \tag{32.43a}$$

$$P^{\text{opt}}_{\substack{l',\,\boldsymbol{k}-\boldsymbol{q}\\ l,\,\boldsymbol{k}}} = \frac{2\pi}{\hbar}\left(\frac{\hbar(\bar{n}^{\text{opt}}_{\nu}+1)}{2\rho\omega^{\text{opt}}_{\nu}\mathcal{V}}\right) W^{\text{opt}}_{\substack{l',\,\boldsymbol{k}-\boldsymbol{q}\\ l,\,\boldsymbol{k}}}(\boldsymbol{e}^{\nu}_{\text{opt}}(\boldsymbol{q}))\times\ \delta(E_l(\boldsymbol{k}) - E_{l'}(\boldsymbol{k}-\boldsymbol{q}) - \hbar\omega^{\text{opt}}_{\nu}), \tag{32.43b}$$

where $\omega^{\text{opt}}_{\nu}$ is the limiting frequency for the ν-th branch of optical modes:

$$W^{\text{opt}}_{\substack{l'\boldsymbol{k}'\\ l\,\boldsymbol{k}}} = \frac{1}{2}\sum_{tt'}\left|\mathcal{H}^{\text{opt}}(\boldsymbol{e}^{\nu}_{\text{opt}})_{\substack{l't'\boldsymbol{k}'\\ l\,t\,\boldsymbol{k}}}\right|^2, \tag{32.44}$$

and the matrix elements of $\mathcal{H}^{\text{opt}}(\boldsymbol{e}^{\nu}_{\text{opt}})$ are, by (32.36b),

$$\mathcal{H}^{\text{opt}}(\boldsymbol{e}^{\nu}_{\text{opt}})_{m'm} = \frac{1}{2}\sum_{\varkappa\varkappa'}(e^{\nu}_{\varkappa q} - e^{\nu}_{\varkappa' q})\,V^{\varkappa\varkappa'}_{m'm\,\text{opt}}. \tag{32.45}$$

If the band at $\boldsymbol{k}_0$ is degenerate only counting spin, by (29.28),

$$W^{a\kappa}_{\boldsymbol{k}\pm\boldsymbol{q},\,\boldsymbol{k}} = \left[D_{xx}(e^{\nu}_{qx}q_x) + D_{yy}(e^{\nu}_{qy}q_y) + D_{zz}(e^{\nu}_{qz}q_z)\right]^2, \tag{32.46}$$

i.e., $W^{\text{ac}}_{\boldsymbol{k}'\boldsymbol{k}}$ depends only on the difference $\boldsymbol{k}'-\boldsymbol{k}=\boldsymbol{q}$.

In cubic crystals, in the elastic continuum approximation, acoustical modes separate into one purely longitudinal mode with $\boldsymbol{e}_{qL}=\boldsymbol{q}/q$ and two purely transverse modes, for which $\boldsymbol{e}_q$ may be taken as

$$\boldsymbol{e}_{qT_1} = \frac{1}{(q_x^2+q_y^2)^{1/2}}\begin{cases} q_y,\\ -q_x,\\ 0;\end{cases}\qquad \boldsymbol{e}_{qT_2} = \frac{1}{q(q_x^2+q_y^2)^{1/2}}\begin{cases} q_xq_z,\\ q_yq_z,\\ -(q_x^2+q_y^2).\end{cases} \tag{32.47}$$

Accordingly, for the longitudinal mode,

$$W^{\text{ac}}_{L,\,\boldsymbol{k}\pm\boldsymbol{q},\,\boldsymbol{k}} = q^2\left[D_{zz} + (D_{xx}-D_{zz})\sin^2\vartheta\cos^2\varphi + (D_{yy}-D_{zz})\sin^2\vartheta\sin^2\varphi\right]^2, \tag{32.48a}$$

where ϑ and φ are the polar angles, determining the direction of the vector $\boldsymbol{q}$, where the polar axis is the principal axis Oz of the ellipsoid. The total $W_{T,\,\boldsymbol{k}\pm\boldsymbol{q}}$ for both transverse modes is

$$W^{\text{ac}}_{T,\,\boldsymbol{k}\pm\boldsymbol{q},\,\boldsymbol{k}} = \frac{1}{4}q^2\left[(D_{xx}-D_{yy})^2\sin^4\vartheta\sin^2 2\varphi + \right.$$
$$\left. + (D_{xx}-D_{zz})^2\sin^2 2\vartheta\cos^2\varphi + (D_{yy}-D_{zz})^2\sin^2 2\vartheta\sin^2\varphi\right]. \tag{32.48b}$$

For groups $G_{\boldsymbol{k}_0}$ with n-fold axes, $n>2$, it follows from (29.29) that $D_{xx}=D_{yy}=D_{\perp}$, $D_{zz}=D_{\parallel}$, and

$$W^{\text{ac}}_{L,\,\boldsymbol{k}\pm\boldsymbol{q},\,\boldsymbol{k}} = q^2\left[D_{\parallel} + (D_{\perp}-D_{\parallel})\sin^2\vartheta\right]^2, \tag{32.49a}$$

$$W^{\text{ac}}_{T,\,\boldsymbol{k}\pm\boldsymbol{q},\,\boldsymbol{k}} = \frac{1}{4}q^2(D_{\parallel}-D_{\perp})^2\sin^2 2\vartheta. \tag{32.49b}$$

For cubic groups $G_{\boldsymbol{k}_0}$, by (29.33), $D_{\parallel}=D_{\perp}=c$, and in this case scattering in nondegenerate bands is due only to longitudinal acoustical modes:

$$W_{L,\,\boldsymbol{k}\pm\boldsymbol{q},\,\boldsymbol{k}} = C^2q^2,\qquad W_{T,\,\boldsymbol{k}',\,\boldsymbol{k}} = 0. \tag{32.50}$$

In cubic crystals, the optical branches at $q = 0$ are threefold degenerate (if we neglect the long-range forces arising in polar crystals), i.e., the corresponding normal modes transform according to a three-dimensional representation, whereas in the case of nondegenerate representations $\mathscr{H}^{\text{opt}}$ can contain only modes which transform according to the identity representation. Thus, for cubic groups G_{k_0}, scattering by optical modes associated with short-range forces is absent in nondegenerate representations.

If the group G_{k_0} has lower symmetry, the three-dimensional representation according to which the optical modes transform is reducible in the corresponding point group. If one of its irreducible constituents is the identity representation, the optical modes which transform according to this representation will appear in $\mathscr{H}^{\text{opt}}$, i.e., these modes will cause scattering of electrons.

For example, in the diamond lattice the representation Γ'_{25} corresponds to the limiting optical mode (see Table 23.4, p. 227). In C_{4v}, which is the point group for Δ, we have $\Gamma'_{25} \to B_2^+ + E^+$ (see Table 11.1, p. 73). Consequently, in Si, where the conduction band has an extremum Δ, electrons are not scattered by optical modes. In $D_{3d} = C_{3v} \times C_i$, which is the point group for L, $\Gamma'_{25} = A_1^+ + E^+$. Thus, in Ge, where the conduction band has an extremum at L, electrons are scattered by optical modes with displacements $u_{1z} = -u_{2z} = u_{0z}$, which transform according to the representation A_1^+, and

$$\mathscr{H}^{\text{opt}}_{m'm}(u) = u_{0z} V^{\text{opt}} \delta_{mm'}, \text{ where } V^{\text{opt}} = 2V^{\text{opt}}_{zmm}. \tag{32.51}$$

Here the z-axis is along the [111] direction or an equivalent direction. Consequently,

$$\mathscr{H}^{\text{opt}}(e^{\nu}_{\text{opt}}) = (e^{\nu}_{1z} - e^{\nu}_{2z}) V^{\text{opt}}_{zmm} = e^{\nu}_{1z} V^{\text{opt}},$$

since, if both lattice atoms have the same mass, then $e_1 = -e_2$ for the limiting optical modes, where $|e_1|^2 = |e_2|^2 = 1$.

Accordingly, for the longitudinal mode

$$W^{\text{opt}}_{L,\, k \pm q,\, k} = V^2_{\text{opt}} \cos^2 \vartheta, \tag{32.52a}$$

and the total W_T for the two transverse modes is

$$W^{\text{opt}}_{T,\, k \pm q,\, k} = V^2_{\text{opt}} \sin^2 \vartheta, \tag{32.52b}$$

where ϑ is the angle between the direction of the vector q and the z-axis [111].

Since the frequencies of transverse and longitudinal optical modes in nonpolar lattices coincide, we can at once sum the scattering probabilities in (32.43) over all polarizations, setting $W^{\text{opt}}_{k \pm q,\, k} = V^2_{\text{opt}}$ in accordance with (32.44).

It is clear from the above equations that in the case of nondegenerate bands the probability (32.42), (32.44) of scattering from state k to k' depends only on the direction of the vector $q = k - k'$. The situation is more complicated in the case of degenerate bands. As an example let us find the scattering probabilities for holes in Ge and Si. The functions F_{lk} and the energy $E_l(k)$ for holes in Ge and Si are given by (24.19) and (24.13a), and the matrix $\mathscr{H}(\varepsilon)$ by (30.3), (30.4). The operator V^{opt} has one linearly independent nonzero matrix element

$$V^{\text{opt}}_{zxy} = \langle X | V^{\text{opt}}_z | Y \rangle = \frac{\sqrt{3}}{2} d_{\text{opt}}. \tag{32.53}$$

The operator $\mathscr{H}^{\text{opt}}(e_v^{\text{opt}})$ can be determined by the theory of invariants. Since the displacements $u_i^{1,2}$ transform according to the representation F_2^+ of the group $O_h = T_d \times C_i$, this operator is

$$\mathscr{H}^{\text{opt}}(u) = \frac{2}{\sqrt{3}} d_{\text{opt}} \left(u_x^{\text{опт}} [J_y J_z] + u_y^{\text{opt}} [J_x J_z] + u_z^{\text{opt}} [J_x J_y]\right). \tag{32.54}$$

We have here used the fact that $u^{\text{opt}} = \frac{1}{2}(u_1 - u_2) = u_1 = -u_2$, i.e., $\mathscr{H}^{\text{opt}}(e_v)$ is similar in form to (30.3), with

$$f^{\text{opt}} = g^{\text{opt}} = 0, \quad h^{\text{opt}} = -d_{\text{opt}}(ie_y^v + e_x^v), \quad j = -d_{\text{opt}} ie_z^v, \tag{32.55}$$

where

$$e^v = e_1^v = -e_2^v.$$

By (32.40), in order to calculate $W^{\text{ac}}_{l'k', lk}$, which determines the probability of scattering by acoustical modes, we multiply the matrices $\mathscr{T}^+_{l'l'k'}$, $\mathscr{H}(e)$, $\mathscr{T}_{llk}$ and sum over the degenerate states. After some rather tedious calculations, the result is found to be

$$W^{\text{ac}}_{\substack{mk' \\ lk}}(e') = \delta E_l(e', k)\, \delta E_m(e', k') - \delta E_1^0(e')\, \delta E_2^0(e')\, \Psi^{ml}_{k'k}. \tag{32.56}$$

Here $l, m = 1$ denote light holes, $l, m = 2$ heavy holes; $\delta E_l(e, k)$ are the energy changes of the holes under the strain e at high energies, defined by (30.34), and $\delta E_l^0(e)$ the changes in the energy of the holes at $k = 0$. By (30.5) and (30.8), $\delta E^0_{1,2}(e) = ae \pm \mathscr{E}_e^{1/2}$ and

$$\delta E_1^0(e)\, \delta E_2^0(e) = (a^2 - b^2) \sum_i e_{ii}^2 + \left(a^2 + \frac{b^2}{2}\right) \sum_{i \neq j} e_{ii} e_{jj} - \frac{d^2}{2} \sum_{i \neq j} e_{ij}^2. \tag{32.57}$$

The function $\Psi^{ml}_{k'k}$ in (32.56) is defined by

$$\Psi^{ml}_{k'k} = \frac{1}{2}\left\{1 \pm \frac{1}{2(\mathscr{E}_k \mathscr{E}_{k'})^{1/2}} \left[D^2 (kk')^2 - B^2 k^2 k'^2 + (3B^2 - D^2) \sum_i k_i^2 k_i'^2\right]\right., \tag{32.58}$$

where, according to (30.6),

$$\mathscr{E}_k = B^2 k^4 + \frac{1}{2}(D^2 - 3B^2) \sum_{i \neq j} k_i^2 k_j^2.$$

The plus sign in (32.58) corresponds to intraband transitions ($l = m$), the minus sign to interband transitions ($l \neq m$).

In this case, both $\Psi^{ml}_{k'k}$ and $W^{\text{ac}}_{mk', lk}$ depend on the directions of the vectors k and k'. The quantity $W^{\text{opt}}_{mk', lk}$, which determines the probability of scattering by optical modes, is similar to (32.56):

$$W^{\text{opt}}_{\substack{mk' \\ lk}}(e_v) = \delta E_l(e_v, k)\, \delta E_m(e_v, k') - \delta E_1^0(e_v)\, \delta E_2^0(e_v)\, \Psi^{ml}_{k'k}. \tag{32.59}$$

Here $\delta E_l(u^{\text{opt}}, k)$ is the change in the energy of the holes when each of the sublattices is subjected to a displacement $u^{\text{opt}} = u_1 = -u_2$, at energies significantly exceeding the band splitting $\delta E_1^0(u) - \delta E_2^0(u)$ at the point $k = 0$.

As (30.34)

$$\delta E_l(u^{\text{opt}}, k) = \pm \frac{D d_{\text{opt}}}{2\mathscr{E}_k^{1/2}} (k_x k_y u_z^{\text{opt}} + k_y k_z u_x^{\text{opt}} + k_x k_z u_y^{\text{opt}}), \tag{32.60}$$

$$\delta E_1^0(u^{\text{opt}})\, \delta E_2^0(u^{\text{opt}}) = -d_{\text{opt}}^2 u_{\text{opt}}^2. \tag{32.61}$$

Recall that the constant d_{opt} in (32.54) has dimensions of energy per unit length, and the quantities $\delta E_l(\boldsymbol{e}_\nu, \boldsymbol{k})$ and $\delta E_l^0(\boldsymbol{e}_\nu)$, as opposed to $\delta E_l(\boldsymbol{u}^{\text{opt}}, \boldsymbol{k})$ and $\delta E^0(\boldsymbol{u}^{\text{opt}})$, have the same dimensions as d_{opt}.

Intervalley scattering

When there are several equivalent extrema, scattered electrons may jump from an extremum located near $\boldsymbol{k}_{01}$ to an extremum $\boldsymbol{k}_{02}$. To calculate the probabilities of such transitions, we use the general equation (32.1). Using (25.25), we expand the displacement in normal modes $a_{q\nu}$ and rewrite (32.1) as

$$\delta V(\boldsymbol{x}) = \sum_{q\nu} [V^*_{q\nu}(\boldsymbol{x}) a_{q\nu} + V_{q\nu} a^+_{q\nu}], \tag{32.62}$$

where

$$V^*_{q\nu} = \sum_{f\varkappa} \boldsymbol{V}_\varkappa(\boldsymbol{x} - \boldsymbol{X}^\varkappa_f) \boldsymbol{e}^\nu_\varkappa(\boldsymbol{q}) e^{-iq\boldsymbol{X}^\varkappa_f}. \tag{32.63}$$

It follows from equations (32.62) and (15.26) that the probability of transition of an electron from state $\boldsymbol{k}_1$ to state $\boldsymbol{k}_2$ with absorption of a phonon $\boldsymbol{q}\nu$ is

$$P_{\boldsymbol{k}_1+\boldsymbol{q},\,\boldsymbol{k}_2} = 2\pi\left(\frac{n_{q\nu}}{2\rho\omega_{q\nu}}\right)\frac{1}{\mathcal{V}^2} |\langle \psi_{\boldsymbol{k}_2} | V^*_{q\nu} | \psi_{\boldsymbol{k}_1} \rangle|^2 \delta_{\boldsymbol{k}_1+\boldsymbol{q},\,\boldsymbol{k}_2} \delta(E_{\boldsymbol{k}_1} + \hbar\omega_q - E_{\boldsymbol{k}_2}). \tag{32.64}$$

By (15.26), for a transition with emission of a phonon we need only replace $\bar{n}_{q\nu}$ by $\bar{n}_{q\nu}+1$ and $V^*_{q\nu}$ by $V_{q\nu}$. The selection rules for the matrix element $V_{\boldsymbol{k}_1+\boldsymbol{q},\,\boldsymbol{k}_2} = \frac{1}{\mathcal{V}} \langle \psi_{\boldsymbol{k}_2} | V^*_{q\nu} | \psi_{\boldsymbol{k}_1} \rangle$ depend on the transformation rule of the operator $V_{q\nu}$. The invariance of the Hamiltonian (32.62) under the space group operations implies that if the components $a_{q\nu}$ transform under operations $g \in G_q$ according to a representation $\mathcal{D}$ of G_q, then the components $V^*_{q\nu}$ transform according to the complex conjugate representation $\mathcal{D}^*$. Under other operations of the space group, which take the vector $\boldsymbol{q}$ to an inequivalent point $g\boldsymbol{q}$, the component $a_{q\nu}$ goes into $a_{gq\nu}$ or into a combination of components $a_{gq\nu'}$ (a similar situation was observed for the Bloch functions). It follows from the definition of $V_{q\nu}$ (equation (32.63)) that in the latter case $V_{q\nu}$ also goes into $V_{gq\nu}$. Consequently, the components $V_{q\nu}(\boldsymbol{x})$ transform according to the same representations as the normal modes $a_{q\nu}$.

Knowing these representations and using the equations of §19, we can determine whether transitions from state $\boldsymbol{k}_1$ to $\boldsymbol{k}_2$ are allowed or forbidden and which phonons can cause such transitions. For arbitrary points $\boldsymbol{k}_1$ and $\boldsymbol{k}_2$, these transitions are always allowed, but if the points are near extrema $\boldsymbol{k}_{01}$ and $\boldsymbol{k}_{02}$ of sufficiently high symmetry and transitions from $\boldsymbol{k}_{01}$ to $\boldsymbol{k}_{02}$ are forbidden, the probability of transitions from $\boldsymbol{k}_1$ to $\boldsymbol{k}_2$ will be small. Selection rules must therefore be determined specifically for extremum points $\boldsymbol{k}_0$.

Below we shall discuss selection rules for intervalley transitions between points of the stars X, Δ and L in cubic crystals of the Ge, InSb and PbS types. Transitions between points of the stars X and L are induced by phonons of

the star X. For example, for the star X

$$\boldsymbol{k}_{0x}-\boldsymbol{k}_{0y}=\frac{2\pi}{a}(100)-\frac{2\pi}{a}(010)=\frac{2\pi}{a}(1\bar{1}0)=\frac{2\pi}{a}(001)+\frac{2\pi}{a}(1\bar{1}\bar{1})=\boldsymbol{k}_{0z}-\boldsymbol{b}_3.$$

Transitions between points of $\Delta(\boldsymbol{k}=(00k_0))$ are caused by phonons of Σ; when $k_0=\frac{3}{2}\frac{\pi}{a_0}$ the point Σ with $\boldsymbol{k}=(k_0k_00)$ goes into the point K or the equivalent point K' with $\boldsymbol{k}=\frac{2\pi}{a_0}\left(\frac{\bar{1}}{4}\frac{\bar{1}}{4}1\right)$; when $k_0>\frac{3}{2}\frac{\pi}{a_0}$ it goes into the point Σ' with $\boldsymbol{k}=\left(k_0'k_0'\frac{2\pi}{a_0}\right)$, where $k_0'=\frac{2\pi}{a_0}-k_0<\frac{3\pi}{2a_0}$.

All the points X, Δ and L belong to case (a_2), and the selection rules at these points are determined by equation (19.41), according to which the number of nonzero matrix elements for the transition from state $\psi^{\mu}_{\boldsymbol{k}_0}$ to $\psi^{\mu}_{-g_s\boldsymbol{k}_0}$ with phonon emission in the branch ν with wave vector $\boldsymbol{q}=\boldsymbol{k}_0+g_s\boldsymbol{k}_0$ is

$$N_1=\frac{1}{2h_0}\left\{\sum_{g_0}\chi^{q}_{\nu}(g_0)\chi^{k_0}_{\mu}(g_0)\chi^{k_0}_{\mu}(g_s^{-1}g_0g_s)+K^2\sum_{g_r}\chi^{q}_{\nu}(g_rg_s^{-1})\chi^{k_0}_{\mu}((g_rg_s^{-1})^2)\right\}. \qquad (32.65)$$

Here g_0 is an element of a group G_0 defined as the intersection of $G_{\boldsymbol{k}_0}$, $G_{-g_s\boldsymbol{k}_0}$ and $G_{\boldsymbol{q}}$, and h_0 is the order of this group. Note that any element common to two of these groups is always a member of the third. The only nonzero terms in the second sum are the characters of elements $(g_rg_s^{-1})^2$ of $G_{\boldsymbol{k}_0}$. In that case, $g_rg_s^{-1}\in G_{\boldsymbol{q}}$; and conversely, if $g_rg_s^{-1}\in G_{\boldsymbol{q}}$, then $(g_rq_s^{-1})^2\in G_{\boldsymbol{k}_0}$. In all cases considered, such elements exist (if there are none, it follows from (19.42) that we must replace $2h_0$ by h_0 in (32.65)). For transitions between points of the star X, when the phonons also belong to the star X,

$$\chi^{q}_{\nu}(g_0)=\chi^{k_0}_{\nu}(g_l^{-1}g_0g_l),$$

where g_l is an element which takes $\boldsymbol{k}_0$ into $\boldsymbol{q}$. We must remember here that the elements $g_l^{-1}g_0g_l$, like $g_s^{-1}g_0g_s$ and $(g_rg_s^{-1})^2$ in (32.65), may also contain primitive translations. This is an essential factor in determining selection rules for transitions between points L and X for Ge-type crystals.

TABLE 32.1. Selection rules for intervalley transitions

Type of crystal	Ge				InSb						PbS			
Positions of extrema	Δ	X	L		Δ	X			L		Δ	X	L	
Representation	Δ_{1-4}	X_{1-4}	$L_{1,2}$, $L'_{1,2}$	L_3, L'_3	Δ_{1-4}	X_1, X_3	X_2, X_4	X_5	$L_{1,2}$	L_3	Δ_{1-4}	$X^{\pm}_{1-5}$	L_{1-3}, L'_{1-3}	
Transitions allowed with phonons of representations	Σ_1 (or K_1, Σ'_1)	X_2, X_3	X_1	$2X_2$, X_3	Σ_1 or K_1, Σ'_1	X_1	X_4	X_1, X_4, X_5	X_1, X_4	$2X_1$, X_4, X_5	Σ_1 (or K_1, Σ'_1)	—	—	

Table 32.1 presents the results of the calculations and indicates which phonons can cause transitions between the corresponding electron states. It is evident from the table that in PbS-type crystals intervalley transitions between points of the stars X and L involving phonons of X are forbidden, since at X the phonons transform according to the odd representations X^-, whereas the product of the electronic functions may correspond only to even representations. In the other cases intervalley transitions are allowed. Time reversal symmetry forbids some of the possible transitions, such as transitions between points of the stars X and L in Ge with absorption or emission of phonons of X_1.

Chapter VI

EFFECT OF STRAIN ON FREE CARRIERS

§33. CYCLOTRON AND COMBINED RESONANCES IN STRAINED GERMANIUM AND SILICON

In the last chapter we discussed the effect of a strain on the spectrum of the current carriers – electrons and holes. In this chapter and the next we shall consider the physical effects associated with these spectral phenomena.

Cyclotron resonance, i.e., resonant UHF absorption due to electron transitions between Landau levels, is the most direct method to determine how the spectrum changes under a strain. The resonant frequency, usually called the cyclotron frequency, is determined by the carrier spectrum in a magnetic field. To determine this spectrum we must solve the Schrödinger equation in a magnetic field:

$$(\mathcal{H}(\boldsymbol{K}) + \mathcal{H}_s - E)F = 0, \tag{33.1}$$

where $\boldsymbol{K} = \boldsymbol{k} + \frac{e}{c\hbar}\mathcal{A}$ is the generalized momentum, $\boldsymbol{H} = \operatorname{rot}\mathcal{A}$, and F is the wave function in the effective mass approximation.

We first consider cyclotron resonance in strained crystals with germanium-type valence band. In germanium and silicon, the operator $\mathcal{H}(\boldsymbol{K})$ for one of the strain-split valence bands is given in the quadratic k approximation by equations (30.14)–(30.20). To determine the operator $\mathcal{H}_s$, describing the spin splitting, we write the spin Hamiltonian in the unstrained crystal, defined by equation (26.14), in the representation (24.19) which diagonalizes the Hamiltonian $\mathcal{H}(\varepsilon, \boldsymbol{k})$ in the strained crystal. (A similar procedure was adopted in Sec. 30 to determine the linear k terms; see equation (30.40)). For the upper split-off band, this gives

$$\mathcal{H}_s = \mathcal{H}_{11}\sigma_z + \mathcal{H}_{12}\sigma_+ + \mathcal{H}_{12}^*\sigma_-; \tag{33.2}$$

here

$$\begin{aligned}\mathcal{H}_{11} &= \mu_0 g |c_1|^2 \left\{ \frac{1}{2} H_z [3(|h|^2 - |j|^2) + (E_1 - f)^2] + \right. \\ &\left. + \frac{i\sqrt{3}}{2}(E_1 - f)(h^* H_- - h H_+) \right\}, \\ \mathcal{H}_{12} &= \mu_0 g c_1^* c_2 \{3H_z j h^* - i\sqrt{3}(E_1 - f) j H_+ + i(E_1 - f)^2 H_-\}.\end{aligned} \tag{33.3}$$

where

$$H_\pm = H_x \pm iH_y, \quad |c_{1,2}|^2 = (E_{1,2} - f)(E_{1,2} - E_{2,1}),$$

f, h, and j are defined by equation (30.4), and $g = g_0 \not{\varepsilon}$ (for $\varepsilon = 0$). The spin splitting $\Delta E_s = \hbar\omega_s$ for an arbitrary strain is determined by

$$\hbar\omega_s = \mu_0 \Big\{ \sum_{ij} g_{ij}^2 H_i H_j \Big\}^{1/2}, \tag{33.4}$$

where

$$\begin{aligned} g_{xx}^2 &= \frac{g^2}{\mathscr{E}_\varepsilon} \{[\mathscr{E}_\varepsilon^{1/2} + b(\varepsilon - 3\varepsilon_{xx})]^2 + 3d^2(\varepsilon_{xy}^2 + \varepsilon_{xz}^2)\}, \\ g_{xy}^2 &= \frac{g^2\sqrt{3}\,d}{\mathscr{E}_\varepsilon} \{\sqrt{3}\,d\varepsilon_{xz}\varepsilon_{yz} - \varepsilon_{xy}[2\mathscr{E}_\varepsilon^{1/2} - b(\varepsilon - 3\varepsilon_{zz})]\}; \end{aligned} \tag{33.5}$$

$\mathscr{E}_\varepsilon$ is given by (30.8). (The remaining components are obtained by a cyclic permutation $x \to y \to z$.) In particular, if the strain is applied along principal axes [001] or [111],

$$\hbar\omega_s = \mu_0 (g_\parallel^2 H_z^2 + g_\perp^2 H_\perp^2)^{1/2}, \tag{33.6}$$

where $H_\perp^2 = H_x^2 + H_y^2$, the z-axis lying along [001] or [111], respectively, and

$$g_\parallel^2 = g^2(1 \pm 2)^2, \quad g_\perp^2 = g^2(1 \pm 1)^2. \tag{33.7}$$

The upper sign refers to $b\varepsilon' > 0$ or $d\varepsilon' > 0$, the lower sign to $b\varepsilon' < 0$ or $d\varepsilon' < 0$.

Classical cyclotron resonance

If we restrict ourselves to terms quadratic in K in $\mathscr{H}(K)$ in (33.1), there is no need to allow for the dependence of the g-factor on K. Since cyclotron transitions take place without spin flip, it follows that in this approximation, according to which the cyclotron frequency is the same for all electrons, there is no need to include the spin explicitly; referred to the principal axes of the effective mass tensor, equation (33.1) reduces to

$$\Big(\sum_i \frac{\hbar^2}{2m_i} K_i^2 - E \Big) F = 0. \tag{33.8}$$

Going over to the variables

$$x_i' = x_i (m_i/m)^{1/2}, \quad \text{where } m = (m_{xx} m_{yy} m_{zz})^{1/3}, \tag{33.9}$$

and accordingly

$$k_i' = k_i (m/m_i)^{1/2}, \quad \mathscr{A}_i' = \mathscr{A}_i (m/m_i)^{1/2}, \quad H_i' = H_i (m_i/m)^{1/2}, \tag{33.10}$$

we can reduce $\mathcal{H}(K)$ in (33.8) to spherical form. Now let the z' -axis point in the direction of the field H', whose magnitude is

$$H' = \left(\sum_i (m_i/m) H_i^2\right)^{1/2}, \tag{33.11}$$

and choose $\mathcal{A}'_{x'} = -\mathcal{H}' y''$, $\mathcal{A}'_{y'} = 0$, $\mathcal{A}'_{z'} = 0$; then equation (33.8) is written

$$\left\{\frac{\hbar^2}{2m}\left[\left(k_x + \frac{eH'}{\hbar c} y\right)^2 + k_y^2 + k_z^2\right] - E\right\} F = 0 \tag{33.12}$$

(we have written k_i and x_i without primes). As is known /I.7/, the solution of this equation is

$$F_n = e^{i(k_x x + k_z z)} \Phi_n (y + y_0), \tag{33.13}$$

where

$$y_0 = s^2 k_x, \quad s^2 = \hbar c/eH', \tag{33.14}$$

and $\Phi_n(y + y_0)$ are the harmonic oscillator functions, i. e., the eigenfunctions of the operator

$$\mathcal{H} = \frac{\hbar^2}{2m}\left[s^{-4}(y + y_0)^2 - \frac{\partial^2}{\partial y^2}\right]. \tag{33.15}$$

We introduce the operators

$$a = \frac{s}{\sqrt{2}}(K_x + iK_y), \quad a^+ = \frac{s}{\sqrt{2}}(K_x - iK_y), \tag{33.16}$$

which, by (22.19), satisfy the relation

$$\{aa^+\} = 1. \tag{33.17}$$

Then the operator $K_x^2 + K_y^2$ is written

$$K_x^2 + K_y^2 = s^{-2}(aa^+ + a^+a) = 2s^{-2}\left(a^+a + \frac{1}{2}\right). \tag{33.18}$$

The functions F_n satisfy the relations

$$aF_n = \sqrt{n}\, F_{n-1}, \quad a^+F_n = \sqrt{n+1}\, F_{n+1}, \tag{33.19}$$

whence

$$a^+aF_n = nF_n. \tag{33.20}$$

It follows from (33.12), (33.18), (33.20) that

$$E_n = \frac{\hbar^2 k_z^2}{2m} + \frac{\hbar^2 s^{-2}}{m}\left(n + \frac{1}{2}\right) = \frac{\hbar^2 k_z^2}{2m} + \hbar\omega_c\left(n + \frac{1}{2}\right), \tag{33.21}$$

where the cyclotron frequency is

$$\omega_c = \frac{\hbar s^{-2}}{m} = \frac{eH'}{mc}. \tag{33.21a}$$

In the presence of a variable electric field $\mathcal{E}(t) = 2\mathcal{E}\sin\omega t$, the Hamiltonian (33.1) must include $\mathcal{A}(t) = 2\mathcal{E}\frac{c}{\omega}\cos\omega t$ in $\mathcal{A}$. In the linear field approximation, this produces an additional term in (33.8):

$$\mathcal{H}_{\mathcal{E}} = 2\frac{e\hbar}{\omega}\sum_i \frac{1}{m_{ii}}(k_i\mathcal{E}_i)\cos\omega t. \tag{33.22}$$

The transformation (33.9) takes $\mathcal{E}_i$ into $\mathcal{E}'_i = \mathcal{E}_i(m/m_i)^{1/2}$, and $\sum_i \frac{1}{m_{ii}}(K_i\mathcal{E}_i)$ into $\frac{1}{m}(K'\mathcal{E}')$, and in terms of the variables (33.16) the operator $\mathcal{H}_{\mathcal{E}}$ is

$$\mathcal{H}_{\mathcal{E}} = \frac{2e\hbar s^{-1}}{\omega m}(a\mathcal{E}'_- + a^+\mathcal{E}'_+ + \sqrt{}k_z\mathcal{E}'_z). \tag{33.23}$$

Here $\mathcal{E}'_\pm = \frac{1}{\sqrt{2}}(\mathcal{E}'_x \pm i\mathcal{E}'_y)$, and $\mathcal{E}'_x$, $\mathcal{E}'_y$, $\mathcal{E}'_z$ are the projections of the vector $\mathcal{E}'$ on the x'', y'' and z'' -axes. By (33.19), $\mathcal{H}_{\mathcal{E}}$ has nonzero matrix elements between states n and $n \pm 1$, provided the field $\mathcal{E}'$ has components $\mathcal{E}'_x$ and $\mathcal{E}'_y$. Consequently, a variable electric field $\mathcal{E}'$ induces cyclotron transitions if it has components normal to H'. However, this does not imply that transitions are always forbidden if $\mathcal{E}$ is parallel to H, for if $\mathcal{E}$ and H do not point along one of the principal axes of the ellipsoid, the fact that $\mathcal{E} \parallel H$ does not imply that $\mathcal{E}'$ is parallel to H'.

Going back to the original variables (33.10), (33.11) in (33.21a), we find ω_c as a function of the orientation of the magnetic field relative to the principal axes of the ellipsoid x, y and z:

$$\omega_c = \frac{eH}{m_c c}, \text{ where } \frac{1}{m_c^2} = \frac{\sin^2\vartheta\cos^2\varphi}{m_{xx}m_{zz}} + \frac{\sin^2\vartheta\sin^2\varphi}{m_{yy}m_{zz}} + \frac{\cos^2\vartheta}{m_{xx}m_{yy}}. \tag{33.24}$$

Here ϑ is the angle between the magnetic field H and the z-axis, and φ the angle between the zH and zx planes. In particular, if the strain is applied along the principal [001] or [111] axes, when the constant energy surfaces are ellipsoids of revolution, the cyclotron mass m_c depends only on the angle ϑ between the magnetic field and the strain direction:

$$\frac{1}{m_c^2} = \frac{\sin^2\vartheta}{m_\parallel m_\perp} + \frac{\cos^2\vartheta}{m_\perp^2}, \tag{33.25}$$

where $m_{\parallel}$ and $m_{\perp}$ are defined by (30.19) or (30.20), respectively.

Hensel and Feher (29.1) have measured cyclotron resonance in strained p-Si. Figure 34 shows that with an increase in strain the resonant lines of the light and heavy holes disappear, and a new line appears, which corresponds to the holes in the upper of the split valence bands. In addition, there is a marked change in the intensities of the electron lines, caused by transfer of electrons from the extrema on the [100] and [010] axes to the extremum on [001], which is shifted downward under the strain.

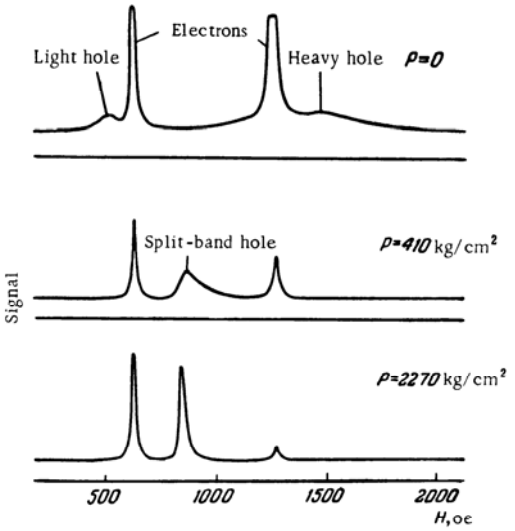

FIGURE 34. Cyclotron resonance in strained p-Si /29.1/. Horizontal axis: magnetic field in oersteds. $\nu \approx 8{,}900$ MHz.

It is clear from Figure 35 that the dependence of the cyclotron mass on the angle θ is adequately described by equation (33.25) for the split-band hole. The values of $m_{\parallel}$ and $m_{\perp}$ may be determined from the $m_c(\theta)$ curves and the values of the constants A, B, D found from equations (30.19) or (30.20).*

Measurements of this type yield the sign of the products bB or dD but not the sign of B and D separately, since the sign in the formulas (30.19) and (30.20) for $m_{\parallel}$ and $m_{\perp}$ depends on the sign of the deformation potential constants b and d.

As shown in /29.3/, the sign and magnitude of these constants can be determined by measuring the strain dependence of the effective masses. In silicon, which has a large spin-orbit splitting ($\Delta_{so} = 0.0441$ ev), one can reliably measure the change in the effective masses due to the effect of the split-off band, as given by (30.24) – (30.26), and for [001] and [111] strains by equations (30.30) and (30.31).

* Note that all the above equations refer to electrons. If the current carriers are holes, $\mathcal{H}$ must be replaced by $-\mathcal{H}$ and e by $-e$. This is equivalent to changing the sign of the effective mass and the magnetic field.

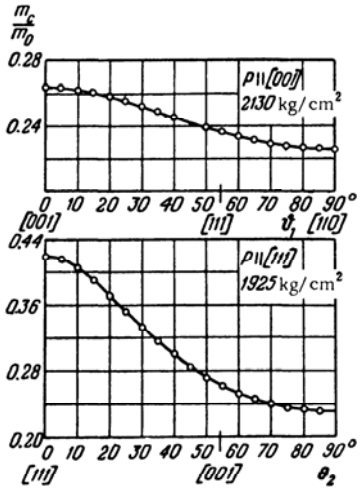

FIGURE 35. Cyclotron mass in p-Si vs. angle between magnetic field and strain direction /29.1/. ϑ_1 is the angle between the magnetic field and the [001] axis in the (110) plane (degrees); ϑ_2 is the angle between the magnetic field and the [111] axis in the (110) plane.

Figure 36 is a plot of m_c as a function of stress P ($\boldsymbol{H} \| P$). It is evident that δm^* depends linearly on ε only for large strains. The nonlinear behavior of δm^* for small ε is due to the nonparabolic nature of the bands when the splitting Δ_ε is small. If the ratio kT/Δ_ε is not too small, terms of fourth or higher orders in k, defined by equations (30.5) and (30.21), become significant. When these terms are included, the cyclotron frequency depends on the number n of the level; this brings about a shift of the line with increase in temperature or decrease in stress, and the dependence of ω_c on k_z^2 causes the so-called k_z line broadening, which increases with decreasing ε.

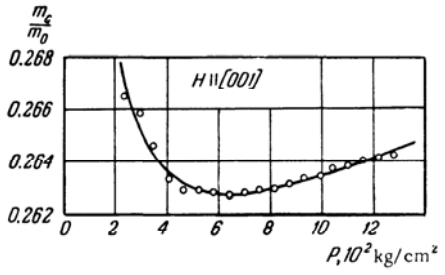

FIGURE 36. Cyclotron mass in p-Si vs. stress /29.1/.

The increase in effective mass due to terms $\sim k^4$ is also inversely proportional to the strain, whereas according to (30.24)–(30.26) δm^* is proportional to ε'_{zz}. The general behavior of $m_c(\varepsilon)$ is reasonably approximated by the function

$$\frac{1}{m_c(\varepsilon)} = \frac{1}{m_c^0} + \frac{\gamma}{\varepsilon'_{zz}} + \alpha\varepsilon'_{zz}.$$

Here the constant α for a [100] or [111] strain is determined from equations (30.30) and (30.31). Once values of γ have been derived from experimental data, we can find the constants b and d appearing in (30.30) and (30.31), and then, on the basis of their signs and the signs of bB and dD, determine the signs of B and D. The value of the ratio b/d has been determined independently from similar measurements, for a [110] strain. Table 40.2 (p. 468) presents values of the constants A, B, D, b and d* determined in this manner.

Note that if the sign of the strain is reversed, so that the crystal undergoes tension instead of compression, no marked changes in cyclotron mass are observed for large strains /30.1/. As pointed out in §30, this effect should indeed be absent for a strain along the principal [100] or [111] axes when $b\varepsilon' < 0$ or $d\varepsilon' < 0$.

Quantum cyclotron resonance

In p-Ge, which has a large spin-orbit splitting, the above method for measuring the deformation potential constants fails, since the contribution of the split-off band is comparable with that of the other close-lying bands, such as the conduction band. Another method, quantum cyclotron resonance in a strained crystal, is applicable for Ge. As noted previously, the cyclotron frequency $\omega_{n+1,n} = (E_{n+1} - E_n)/\hbar$, which is proportional to the energy difference $\Delta E_{n+1,n}$ between levels $n+1$ and n, decreases with increasing n because of the nonparabolic nature of the strain-split bands. In strong magnetic fields, at low temperatures and not too large strains, the individual lines corresponding to different n values can be resolved and their shift under the strain measured. To calculate the position of these lines for large n values it is sufficient to include in $\mathcal{H}(\boldsymbol{K})$ the terms $\sim K^4$ defined by equation (30.21). However, under conditions of quantum cyclotron resonance, when $\hbar\omega_c$ is of the order of kT, levels with small n are significant, and this equation is no longer applicable, since we must now take into account the noncommutativity of the operators K_i and the magnetic field. In order to determine the Hamiltonian $\mathcal{H}(\boldsymbol{K})$ in a magnetic field in a strained crystal to an approximation of higher order in K, we must first diagonalize the matrix $\mathcal{H}(\boldsymbol{\varepsilon})$ by using functions similar to (24.19). In this representation the blocks $\mathcal{H}_{\mathrm{I\,I}}(\boldsymbol{K},\boldsymbol{\varepsilon})$ and $\mathcal{H}_{\mathrm{II\,II}}(\boldsymbol{K},\boldsymbol{\varepsilon})$ are diagonal:

$$\mathcal{H}_{\mathrm{I\,I}} = \boldsymbol{I}E_1(\boldsymbol{K},\boldsymbol{\varepsilon}), \qquad \mathcal{H}_{\mathrm{II\,II}} = \boldsymbol{I}E_2(\boldsymbol{K},\boldsymbol{\varepsilon}),$$

where $E_{1,2}(\boldsymbol{K},\boldsymbol{\varepsilon})$ is defined by (30.14) and $\boldsymbol{I}$ is the 2×2 identity matrix. Next, using equation (15.49), we must eliminate the off-diagonal terms

* In the notation of /29.3, 40.3/, $a = -\frac{2}{3}D_d^v$, $b = -\frac{2}{3}D_u$, and $d = -\frac{2}{\sqrt{3}}D'_u$.

$\mathcal{H}_{I\,II}$ and $\mathcal{H}_{II\,I}$, allowing for the noncommutativity of the operator $\boldsymbol{K}$. In so doing, we must remember that, by (22.20), the original matrix $\mathcal{H}(\boldsymbol{K})$ includes the symmetrized products $[K_\alpha K_\beta]$, whose commutator is

$$\{[K_\alpha K_\beta][K_\gamma K_\delta]\} = \tfrac{1}{2}([K_\alpha K_\gamma]\{K_\beta K_\delta\}+[K_\beta K_\delta]\{K_\alpha K_\gamma\}+[K_\alpha K_\delta]\{K_\beta K_\gamma\}+[K_\beta K_\gamma]\{K_\alpha K_\delta\}).$$

We must also allow for the dependence of the g-factors on the wave vector $\boldsymbol{K}$, introducing a matrix $\mathcal{H}_s$ similar to (33.2) with f, g, h, j replaced by $F+f$, $\mathcal{G}+g$, $H+h$, $J+j$, respectively, where F, $\mathcal{G}$, H, J are defined by (24.11). If the strain and the magnetic field are applied along the principal [001] or [111] axes, there is no need to use the general method outlined above, which is applicable to any orientation of the strain and magnetic field; in these cases, we can use a representation in which the matrices $\mathcal{H}(\varepsilon)$ and $\mathcal{H}_s = \mu_0 g_0 \mathfrak{K}(\boldsymbol{JH})$ are diagonal, thereby eliminating two steps of the general procedure. For the first case, this is the representation (24.12), (26.12), (30.3), (30.9). For the second case the operator $\mathcal{H}(\boldsymbol{K}, \varepsilon)$ may be derived from (26.12) and (30.9) by transforming to a coordinate system with axes z' [111], x' [112], y' [110], as done in the transition from (31.9) to (31.11) in § 31.

According to (31.10a), the Hamiltonian $\mathcal{H}(\boldsymbol{K}, \varepsilon)$ defined by equations (26.12), (26.14), (30.9), (27.62) has the following form relative to the new axes (for holes, $\varphi = 0$)

$$\begin{aligned}\mathcal{H}(\boldsymbol{K},\ \varepsilon,\ \boldsymbol{H}) = {}& \left(\gamma_1 - \tfrac{5}{4}\gamma_3\right)K^2 + \tfrac{15}{4}\gamma_3 K_z^2 + \gamma_3 J_z^2 K^2 - 3\gamma_3 J_z^2 K_z^2 + \\ & + \tfrac{1}{3}(\gamma_2 + 2\gamma_3)(J_+^2 K_-^2 + J_-^2 K_+^2) + \\ & + \tfrac{l2\sqrt{2}}{3}(2\gamma_2 + \gamma_3)([J_z J_+]K_z K_- - [J_z J_-]K_z K_+) - \\ & - \tfrac{2\sqrt{2}}{3}(\gamma_2 - \gamma_3)(J_+^2 K_+ K_z + J_-^2 K_- K_z) - \\ & - \tfrac{l2}{3}(\gamma_2 - \gamma_3)([J_z J_+]K_+^2 - [J_z J_-]K_-^2) + \left(D_1 - \tfrac{5}{4}D_3\right)\varepsilon + \\ & + \tfrac{15}{4}D_3\varepsilon_{zz} + D_3 J_z^2 \varepsilon - 3D_3 J_z^2 \varepsilon_{zz} + \tfrac{1}{3}(D_2 + 2D_3)(J_+^2 \varepsilon_- + J_-^2 \varepsilon_+) + \\ & + \tfrac{l2\sqrt{2}}{3}(2D_2 + D_3)([J_z J_+]\varepsilon_{z-} - [J_z J_-]\varepsilon_{z+}) - \\ & - \tfrac{2\sqrt{2}}{3}(D_2 - D_3)(J_+^2 \varepsilon_{z+} + J_-^2 \varepsilon_{z-}) - \\ & - \tfrac{l2}{3}(D_2 - D_3)([J_z J_+]\varepsilon_+ - [J_z J_-]\varepsilon_- + g_0\mu_0 \mathfrak{K}(\boldsymbol{JH}),\end{aligned} \tag{33.26}$$

where $D_1 = -a$, $D_2 = -\frac{1}{2}b$, $D_3 = -\frac{d}{2\sqrt{3}}$. The remaining notation follows that in Table 31.4 (p. 324). If both strain and magnetic field are applied along [111], i. e., the only nonzero components in (33.26) are ε_{zz} and H_z, the matrix $\mathcal{H}(\boldsymbol{K}, \varepsilon, \boldsymbol{H})$ is

$$\mathcal{H}_{II} = -\left(a - \frac{d}{\sqrt{3}}\right)\varepsilon_{zz} + (\gamma_1 + \gamma_3)(2a^+a + 1)s^{-2} + (\gamma_1 - 2\gamma_3)k_z^2 + \tfrac{3}{2}\mu_0 g_0 \mathfrak{K} H\sigma_z, \tag{33.27a}$$

$$\mathcal{H}_{II\,II} = -\left(a + \frac{d}{\sqrt{3}}\right)\varepsilon_{zz} + (\gamma_1 - \gamma_3)(2a^+a + 1)s^{-2} + (\gamma_1 + 2\gamma_3)k_z^2 + \tfrac{1}{2}\mu_0 g_0 \mathfrak{K} H\sigma_z, \tag{33.27b}$$

$$\mathcal{H}_{I\,II} = \begin{Vmatrix} h_{13} & h_{14} \\ h_{14}^+ & -h_{13}^+ \end{Vmatrix}, \tag{33.27c}$$

where

$$h_{13} = -2\left(\frac{2}{3}\right)^{1/2}[(\gamma_3-\gamma_2)\,a^{+2}s^{-2}+(\gamma_3+2\gamma_2)\,as^{-1}k_z],$$
$$h_{14} = -2\left(\frac{1}{3}\right)^{1/2}[(\gamma_2+2\gamma_3)\,a^2s^{-2}+2(\gamma_3-\gamma_2)\,a^+s^{-1}k_z].$$

We have written these equations in terms of the operators a and a^+, replacing K_+ by $\sqrt{2}\,s^{-1}a$ and K_- by $\sqrt{2}\,s^{-1}a^+$ (see (33.16)). Next, eliminating the off-diagonal terms, we find

$$\tilde{\mathcal{H}}_{1\,1} = \mathcal{H}_{1\,1} + \frac{\mathcal{H}_{1\,11}\mathcal{H}_{11\,1}}{\Delta_g}, \qquad \tilde{\mathcal{H}}_{11\,11} = \mathcal{H}_{11\,11} - \frac{\mathcal{H}_{11\,1}\mathcal{H}_{1\,11}}{\Delta_g}. \tag{33.28}$$

Here $\Delta_g = (2/\sqrt{3})\,d\varepsilon'_{zz}$ and, in contrast to (30.13), this term may be either positive or negative. In addition to the diagonal terms, the matrix $\mathcal{H}_{1\,11}\mathcal{H}_{11\,1}$ includes terms of fourth order in k or a, which may be determined at once from equation (30.21), and terms of second order in k or a, arising from the noncommutativity of the operators a, a^+.

Substituting (33.27) into (33.28), we obtain

$$\begin{aligned}
\tilde{\mathcal{H}}_{1\,1} = {}& \tfrac{1}{2}\Delta_g + 2(\gamma_1+\gamma_3)\,s^{-2}[a^+a] + (\gamma_1-2\gamma_3)\,k_z^2 + \\
& + \frac{4}{\Delta_g}\Big[(\gamma_2^2+2\gamma_3^2)\,s^{-4}[a^{+2}a^2] + 2(\gamma_3^2-\gamma_2^2)\,s^{-1}k_z(a^3+a^{+3}) + \\
& + 2(\gamma_3^2+2\gamma_2^2)\,s^{-2}k_z^2[a^+a]\Big] + \sigma_z\Big\{\tfrac{3}{2}\mu_0 g_0 \beta H + \\
& + \frac{8}{3\Delta_g}[(\gamma_2+2\gamma_3)^2 - 2(\gamma_3-\gamma_2)^2]\,s^{-4}[a^+a] + \\
& + \frac{4}{3\Delta_g}[(\gamma_3+2\gamma_2)^2 - 2(\gamma_3-\gamma_2)^2]\,s^{-2}k_z^2\Big\} + \\
& + \sigma_x\Big\{\frac{8\sqrt{2}}{3\Delta_g}(\gamma_2-\gamma_3)[2(\gamma_2+2\gamma_3)\,s^{-4}[a^+a] - (\gamma_3+2\gamma_2)\,s^{-2}k_z^2]\Big\},
\end{aligned} \tag{33.29}$$

$$\begin{aligned}
\tilde{\mathcal{H}}_{11\,11} = {}& -\tfrac{1}{2}\Delta_g + 2(\gamma_1-\gamma_3)\,s^{-2}[a^+a] + (\gamma_1+2\gamma_3)\,k_z^2 - \\
& - \frac{4}{\Delta_g}[(\gamma_2^2+2\gamma_3^2)\,s^{-4}[a^{+2}a^2] + 2(\gamma_3^2-\gamma_2^2)\,s^{-1}k_z(a^3+a^{+3}) + \\
& + 2(\gamma_3^2+2\gamma_2^2)\,s^{-2}k_z^2[a^+a]\Big] + \sigma_z\Big\{\tfrac{1}{2}\mu_0 g_0 \beta H - \\
& - \frac{8}{\Delta_g}[(\gamma_2^2+2\gamma_3^2)\,s^{-4}[a^+a] + \frac{4}{\Delta_g}(2\gamma_2^2+\gamma_3^2)\,s^{-2}k_z^2\Big\} + \\
& + \frac{1}{\Delta_g}24\sqrt{2}\,\gamma_2\gamma_3 s^{-3}k_z(\sigma_+a + \sigma_-a^+).
\end{aligned} \tag{33.30}$$

As a trial solution of the system of Schrödinger equations with the Hamiltonian (33.29) or (33.30) we take $\boldsymbol{F}_n = \begin{Vmatrix} c_1F_n \\ c_2F_n \end{Vmatrix}$, where F_n are the functions defined by (33.13). In so doing, we may treat the terms containing Δ_g in the denominator as a perturbation. If $kT \ll \hbar\omega_c$, we can omit terms containing k_z in these perturbations, since $\hbar^2k_z^2/2m^*_{zz} \approx kT$. To this approximation, the function $\boldsymbol{F}_n$ is an exact solution of the corresponding Hamiltonian, since by (33.20) and (33.17)

$$[a^{+2}a^2]\,F_n = ((a^+a)^2 + (a^+a) + 1)\,F_n = (n^2+n+1)\,F_n. \tag{33.31}$$

It is now convenient to express the constants γ_1, γ_2, γ_3 in units of $\hbar^2/2m$, where m is the mass of a free electron, i.e., we go over to dimensionless constants /20.1/, noting that

$$\frac{\hbar^2 s^{-2}}{m} = \frac{e\hbar H}{mc} = \hbar\omega_0, \qquad \mu_0 g_0 H = \frac{e\hbar H}{mc} = \hbar\omega_0. \tag{33.32}$$

If we omit the terms containing k_z, the hole spectrum will have the form

$$E^{\mathrm{I}}_{\pm} = \frac{\Delta_g}{2} + \hbar\omega_0(\gamma_1+\gamma_3)\left(n+\frac{1}{2}\right) + \frac{(\hbar\omega_0)^2}{\Delta_g}\left[(\gamma_2^2+2\gamma_3^2)(n^2+n+1)\right] \pm$$
$$\pm\left\{\frac{3}{2}\hbar\omega_0 \not{\kappa} + \frac{2}{3}\frac{(\hbar\omega_0)^2}{\Delta_g}\left[(\gamma_2+2\gamma_3)^2 - 2(\gamma_3-\gamma_2)^2\right]\left[n+\frac{1}{2}\right]\right\}, \tag{33.33}$$

$$E^{\mathrm{II}}_{\pm} = -\frac{\Delta_g}{2} + \hbar\omega_0(\gamma_1-\gamma_3)\left(n+\frac{1}{2}\right) -$$
$$-\frac{(\hbar\omega_0)^2}{\Delta_g}\left[(\gamma_2^2+2\gamma_3^2)(n^2+n+1)\right] \pm$$
$$\pm\left\{\frac{1}{2}\hbar\omega_0 \not{\kappa} - 2\frac{(\hbar\omega_0)^2}{\Delta_g}(\gamma_2^2+2\gamma_3^2)\left(n+\frac{1}{2}\right)\right\}. \tag{33.34}$$

The contribution of the off-diagonal elements in (33.30) to E^{II} may be ignored, since it is of the order of $(\hbar\omega_0)^3/\Delta_g^2$ and terms of this order were omitted in the expansion (33.28).

It follows from equation (33.32) that for the series of levels $E^{\mathrm{II}}_{\pm}$, which are the lower levels of the holes if $\Lambda_g = 2\,d\varepsilon_{zz}/\sqrt{3} > 0$. the cyclotron frequencies for $n+1 \to n$ transitions

$$\hbar\omega^{\pm}_{n+1,\,n} = E^{\pm}_{n+1} - E^{\pm}_{n}$$

are defined by

$$\frac{\omega_{n+1,\,n}}{\omega_0} = \gamma_1 - \gamma_3 - \frac{2\hbar\omega_0}{\Delta_g}(\gamma_2^2+2\gamma_3^2)(n+1\pm 1), \tag{33.35}$$

i.e., the strain-induced change in the cyclotron frequency is, for the upper spin level,

$$\frac{\Delta\omega^{\mathrm{II}+}_{n+1,\,n}}{\omega_0} = -\frac{2\hbar\omega_0}{\Delta_g}(\gamma_2^2+2\gamma_3^2)(n+2), \tag{33.36a}$$

and for the lower spin level,

$$\frac{\Delta\omega^{\mathrm{II}-}_{n+1,\,n}}{\omega_0} = -\frac{2\hbar\omega_0}{\Delta_g}(\gamma_2^2+2\gamma_3^2)\,n. \tag{33.36b}$$

It is clear from (33.36) that for a $1^- \to 0^-$ transition the frequency is independent of the strain, but for all other transitions ω_c decreases, and so m_c increases, with decreasing strain.

For the series of levels $E^{\mathrm{I}}_{\pm}$, which are the lower levels for the holes if $d\varepsilon < 0$,

$$\frac{\omega^{\mathrm{I}\pm}_{n+1,\,n}}{\omega_0} = \gamma_1 + \gamma_3 + \frac{2\hbar\omega_0}{\Delta_g}\left[(\gamma_2^2+2\gamma_3^2)\left(n+1\pm\frac{1}{3}\right) \mp \frac{2}{3}(\gamma_3-\gamma_2)^2\right], \tag{33.37}$$

in other words, if $d\varepsilon < 0$ then ω_c decreases with decreasing strain for all levels.

Equations (33.35), (33.37) imply that for large n values the change in cyclotron frequency for both spin levels is the same, while for the terms E_I and E_{II}, it differs only in sign (this is also clear from equation (30.21)).

Cyclotron resonance has been observed experimentally by Hensel /30.2/ in strained germanium at low temperatures. Figure 37 shows curves of $\omega_0/\omega^{\pm}_{n+1,n}$ for transitions between the various levels shown in the inset. The solid lines are theoretical curves, obtained by computer solution of the system of equations (33.27) for the spectrum under an arbitrary strain. The parameter d, chosen to ensure the best fit between the theoretical and experimental curves, was $d = -4.4 \pm 0.3$ ev, and the value of $\gamma_1 - \gamma_3 = -A + D/2\sqrt{3}$, determined from the position of the unshifted line in units of $\hbar^2/2m_0$, was 7.745 ± 0.012. This is in good agreement with the other data in Table 40.2 (p. 468).

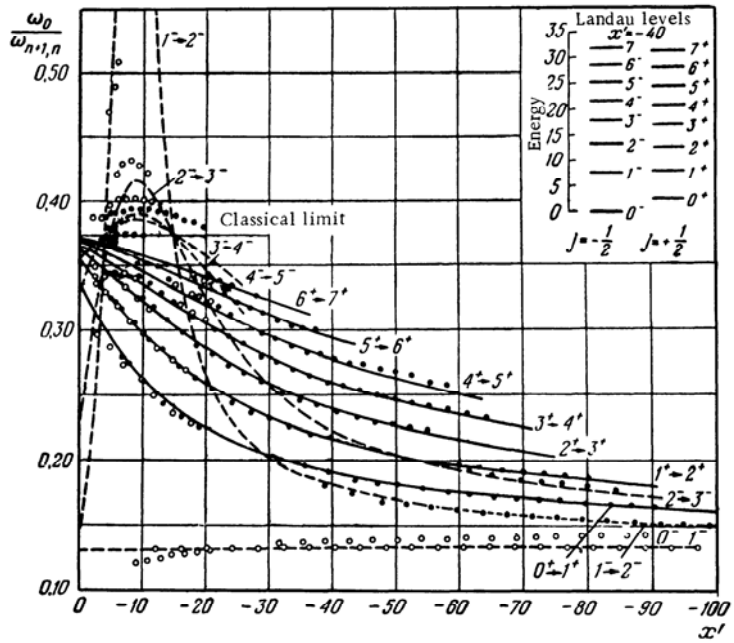

FIGURE 37. Cyclotron frequency in p-Ge vs. strain parameter $x' = \frac{e'}{\hbar eH/mc}$ /30.2/. The energy in the Landau ladder is in units of $\hbar eH/mc$.

Combined resonance

The off-diagonal matrix elements in (33.29) and (33.30) do not contribute to the spectrum in this approximation, but they may give rise to transitions with spin flip in a variable electric field. Analogous to ordinary

paramagnetic resonance, when such transitions are caused by a magnetic field, this effect, first predicted by Rashba /31.1/, is known as combined resonance.

As shown above, the transition probabilities in a variable electric field are determined by the operator $\mathcal{H}_{\mathcal{E}} = (e/\hbar c)[\nabla_k \mathcal{H}(k) \mathcal{A}]$. If the original matrix $\mathcal{H}(k)$ contains only quadratic k terms, the matrix $\mathcal{H}_{\mathcal{E}}$, which is similar to (33.23), is derived from $\mathcal{H}(k)$ via the substitutions

$$a \to a + s\frac{e\mathcal{E}_+(t)}{\hbar\omega}, \quad a^+ \to a^+ + s\frac{e\mathcal{E}_-(t)}{\hbar\omega}, \quad k_z \to k_z + s^{-2}\frac{e\mathcal{E}_z(t)}{\hbar\omega}.$$

It follows via (33.29) that the off-diagonal elements of the matrix $\mathcal{H}^{\mathrm{I}}_{\mathcal{E}}$, which determine the probability of a transition between states E^{I}_+ and E^{I}_-, is

$$\mathcal{H}^{\mathrm{I}}_{\mathcal{E}\pm} = \frac{4\sqrt{2}}{3}\frac{(\hbar\omega_0)^2}{\Delta_e}\frac{e}{\hbar\omega}(\gamma_2 - \gamma_3)[(\gamma_2 + 2\gamma_3)s(a^+\mathcal{E}_+ + a\mathcal{E}_-) - s^2(\gamma_3 + 2\gamma_2)k_z\mathcal{E}_z]\sigma_x. \tag{33.28}$$

Here, as in (33.33) and (33.34), the constants γ_1 and γ_3 are expressed in units of $\hbar^2/2m_0$. It is evident that a field $\mathcal{E} \parallel H$ causes transitions between spin states on the same Landau level, but a field $\mathcal{E} \perp H$ causes transitions with a unit change in n: $\mathcal{E}_-$ downward and $\mathcal{E}_+$ upward.

The off-diagonal elements of the matrix $\mathcal{H}^{\mathrm{II}}_{\mathcal{E}}$, which determine the probability of a transition between states E^{II}_+ and E^{II}_- are, by (33.30),

$$\mathcal{H}^{\mathrm{II}}_{\mathcal{E}\pm} = 6\sqrt{2}\frac{(\hbar\omega_0)^2}{\Delta_e}\frac{e}{\hbar\omega}\gamma_2\gamma_3[s^2k_z(\sigma_+\mathcal{E}_+ + \sigma_-\mathcal{E}_-) + s\mathcal{E}_z(\sigma_+a + \sigma_-a^+). \tag{33.29}$$

The situation here is evidently reversed: a field $\mathcal{E} \perp H$ induces transitions involving only spin flip, while a field $\mathcal{E} \parallel H$ causes transitions between different spin levels belonging to neighboring Landau levels. Comparing (33.38) and (33.39) with (33.23), we see that the intensity of these combined transitions is a factor of approximately $(\hbar\omega_0/\Delta_e)^2$ lower than that of the cyclotron transitions, but it is usually much higher than the intensity of paramagnetic resonance, which has not yet been observed for free holes.

Figure 38 illustrates the results of an experimental study of combined resonance in strained germanium /31.3/. Arrows indicate transitions observed for compression along [111] ($d\varepsilon > 0$), $H \parallel [111]$ and $\mathcal{E} \parallel H$. According to (33.39), only transitions $(n, +) \to (n+1, -)$ are observed in these conditions. Curves of $\omega_0/\omega_{n+1,n}$ plotted against ε are shown, where $\omega_{n+1,n}$ is the frequency corresponding to the transition $\hbar\omega_{n+1,n} = E^-_{n+1} - E^+_n$. The solid lines are theoretical curves obtained by computer solution of equations (33.27). The parameters d and f were chosen so as to assure the best fit between the experimental and theoretical curves: $d = -4.5 \pm 0.3$ ev, $f = -3.60 \pm 0.04$. Later measurements of paramagnetic resonance in free carriers in strained p-Ge /31.4/ have produced a more precise value of the constant f, namely -3.41 ± 0.03, and also a value of $g = 0.06 \pm 0.01$* (see (26.14)).

* Values of the constants γ more precise than those in /31.3/ are also given in this paper.

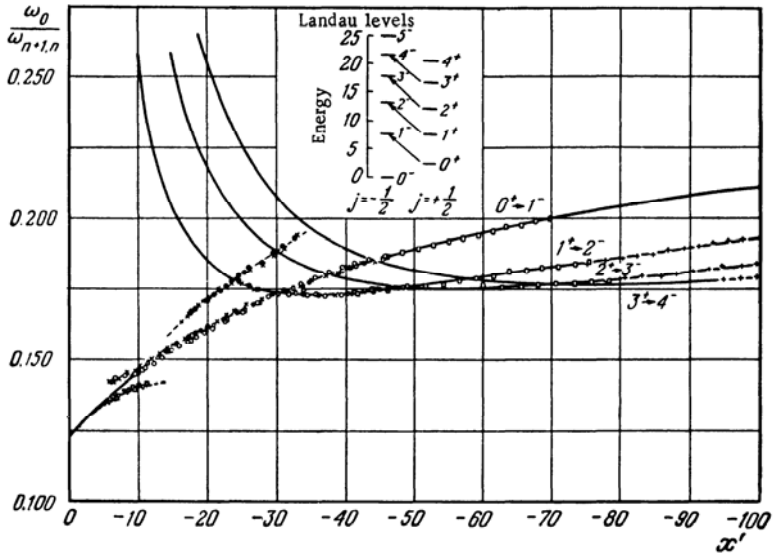

FIGURE 38. Combined resonance in strained p-Ge /31.3/.

Change of effective masses in nondegenerate bands

Cyclotron resonance enables one to observe not only "large" variations of effective masses in semiconductors with degenerate bands, but also "small" effects, due to the effect of the neighboring bands on effective masses in nondegenerate bands. As mentioned in §§ 29 and 30, when a shear strain is applied to n-Si, the transverse masses $1/m_{y'y'}$ and $1/m_{z'z'}$ must differ by the quantity $4\frac{m_\perp C' e_{yz}}{m'\Delta}$ (equation (29.45)).

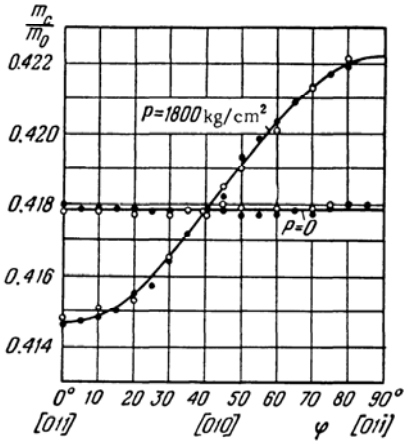

FIGURE 39. Cyclotron mass in n-Si vs. angle φ between magnetic field and [011] axis ([001] strain) /29.7/.

If the magnetic field is normal to the principal x-axis, it follows from (33.25) that the cyclotron mass m_c in the unstrained crystal is $m_c^0 = (m_\perp m_\parallel)^{1/2}$ and does not depend on the orientation of the magnetic field in the $y'z'$ - plane. By (29.45) and (33.25), this mass varies under strain as a function of the angle φ between $\boldsymbol{H}$ and the y'-axis (i.e., the [011] axis), according to the equation

$$m_c^2 = m_\perp m_\parallel \left(1 + \frac{2m_\perp}{m'} \frac{C' e_{yz}}{\Delta} \cos 2\varphi\right)^{-1}, \tag{33.40}$$

whence

$$m_c(\varepsilon) = m_c(0)\left(1 - \frac{m_\perp}{m'} \frac{C' e_{yz}}{\Delta} \cos 2\varphi\right). \tag{33.41}$$

Figure 39 plots m_c/m_0 as a function of φ, as observed in strained and unstrained crystals /29.7/. The solid curve is

$$\frac{m_c}{m_0} = a - b \cos 2\varphi$$

where

$$a = 1.4 \cdot 10^{-3},$$
$$b = (9.1 \pm 0.4) \cdot 10^{-3}.$$

The constant component a, which is absent in (33.41), is due to the effect of the other bands. The above value of b corresponds to

$$\alpha = \frac{m_\perp}{m'} \frac{C'}{\Delta} = 8.3.$$

The separation Δ to the nearest band at the point $\boldsymbol{k}_0$ is about 0.5 ev, while theoretical estimates /29.7/ give a value 1.32 for the ratio $m'/m_\perp$; this yields the value 5.6 ev for the constant C'.

§34. EFFECT OF STRAIN ON KINETIC PHENOMENA

In this section we shall consider the variation of electric conductivity in semiconductors under an anisotropic strain – the piezoresistance effect. Discovered in 1954 by Smith in Ge and Si /32.1/, this phenomenon marked the first research into the effect of uniaxial strains on the physical properties of semiconductors.

Phenomenological description of the piezoresistance effect

Application of a strain to a crystal causes a change in the electric conductivity tensor $\Delta\sigma_{\alpha\beta}$, which in the linear strain approximation may be

written

$$\frac{\Delta\sigma_{\alpha\beta}}{\bar{\sigma}} = \sum_{\gamma\delta} m_{\alpha\beta,\,\gamma\delta} e_{\gamma\delta}, \tag{34.1}$$

where $m_{\alpha\beta,\,\gamma\delta}$ is a dimensionless fourth rank tensor symmetric with respect to inversion of indices within each pair:

$$m_{\alpha\beta,\,\gamma\delta} = m_{\beta\alpha,\,\gamma\delta} = m_{\beta\alpha,\,\delta\gamma} = m_{\alpha\beta,\,\delta\gamma}, \tag{34.2}$$

and $\bar{\sigma}$ is the average conductivity of the crystal:

$$\bar{\sigma} = \frac{1}{3}\mathrm{Tr}\,\sigma = \frac{\sigma_{xx} + \sigma_{yy} + \sigma_{zz}}{3}.$$

The tensor $m_{\alpha\beta,\,\gamma\delta}$ is known as the elastoresistance tensor. Its form and the number of independent components depend on the crystal symmetry and on the symmetry (34.2) of the tensor itself relative to permutation of indices. By (20.18), the number of independent components is

$$N = \frac{1}{4h}\sum_{g\in F}[\chi_1^2(g)]^2, \tag{34.3}$$

where χ_1 is the character of a vector representation and h the order of the group F characterizing the crystal class. Equation (34.3) implies, for instance, that in cubic crystals three of the elastoresistance tensor components differ from zero: $m_{zz,\,zz}$, $m_{xx,\,yy}$ and $m_{xy,\,xy}$.

Experimentally, one usually measures the emf at a given point, i. e., determines the change in the resistivity $\rho = \sigma^{-1}$ under a strain.

The strain-induced change in resistivity, $\Delta\rho_{\alpha\beta}/\bar{\rho}$, is described as in (34.1) by a fourth rank tensor $m^{(\rho)}_{\alpha\beta,\,\gamma\delta}$ which has the same symmetry as the tensor $m^{(\sigma)}$. In cubic crystals, $m^{(\sigma)}_{\alpha\beta,\,\gamma\delta} = -m^{(\rho)}_{\alpha\beta,\,\gamma\delta}$, but in crystals with lower symmetry the connection between the components of $m^{(\sigma)}$ and $m^{(\rho)}$ also involves the quotients of the components of the conductivity (or resistivity) tensor of the unstrained crystal.

Since all the components of the tensors m, σ, ε depend only on the pair of indices $\alpha\beta$, it is convenient to adopt an abbreviated notation, denoting each pair of indices by one number. The strain tensor components $\varepsilon_{\alpha\beta}$ are now characterized by a single index,

$$\begin{gathered}\varepsilon_{xx}\to\varepsilon_1,\quad \varepsilon_{yy}\to\varepsilon_2,\quad \varepsilon_{zz}\to\varepsilon_3,\quad 2\varepsilon_{yz}\to\varepsilon_4,\quad 2\varepsilon_{xz}\to\varepsilon_5,\quad 2\varepsilon_{xy}\to\varepsilon_6;\\ \sigma_{xx}\to\sigma_1,\quad \sigma_{yy}\to\sigma_2,\quad \sigma_{zz}\to\sigma_3,\quad \sigma_{yz}\to\sigma_4,\quad \sigma_{xz}\to\sigma_5,\quad \sigma_{xy}\to\sigma_6,\end{gathered}$$

and the tensor $m_{\alpha\beta,\,\gamma\delta}$ becomes a 6×6 matrix. Thus, instead of 81 components symmetric with respect to inversion of indices within each pair, the tensor $m_{\alpha\beta,\,\gamma\delta}$ is defined in the general case by 36 values of m_{ij}.

Relation (34.1) may be written in matrix form:

$$\frac{\Delta\sigma_i}{\bar{\sigma}} = \sum_j m_{ij}\varepsilon_j. \tag{34.4}$$

In a cubic crystal, with the x-, y-, and z-axes taken along the fourfold axes, the elastoresistance matrix has the form

$$\begin{Vmatrix} m_{11} & m_{12} & m_{12} & 0 & 0 & 0 \\ m_{12} & m_{11} & m_{12} & 0 & 0 & 0 \\ m_{12} & m_{12} & m_{11} & 0 & 0 & 0 \\ 0 & 0 & 0 & m_{44} & 0 & 0 \\ 0 & 0 & 0 & 0 & m_{44} & 0 \\ 0 & 0 & 0 & 0 & 0 & m_{44} \end{Vmatrix} \tag{34.5}$$

and is characterized by three independent constants:

$$m_{11} = m_{xx,\,xx}, \quad m_{12} = m_{xx,\,yy}, \quad m_{44} = m_{xy,\,xy}.$$

These constants are easily determined experimentally by considering different orientations of the current, stress and strain. Using different relative orientations of the strain, field and current, one can in principle determine all components of the elastoresistance tensor.

Any small strain can be expressed as the sum of a strain which preserves the crystal symmetry and a strain which breaks the symmetry. An example of a strain preserving crystal symmetry is an isotropic strain $e_{xx} = e_{yy} = e_{zz} = \frac{1}{3}\frac{\Delta\mathcal{V}}{\mathcal{V}}$, where $\frac{\Delta\mathcal{V}}{\mathcal{V}}$ is the relative change in volume.

In noncubic crystals there are other types of symmetry-preserving strain. In uniaxial crystals, this is the case for a strain along the symmetry axis. Therefore, the coefficients m_{ij} are conveniently replaced by suitable linear combinations, corresponding to strains which preserve the crystal symmetry, known as the volume elastoresistance coefficients, and combinations of m_{ij}'s defined only by strains which reduce the crystal symmetry. The latter are known as the shear elastoresistance coefficients. The physical justification for this division of the coefficients into "volume" coefficients, not associated with a change in symmetry, and shear coefficients is that, as we shall show below, they generally depend on different mechanisms

For cubic crystals, the change in conductivity under an isotropic strain is a volume coefficient.

$$\frac{\Delta\sigma}{\sigma_0\,(\Delta\mathcal{V}/\mathcal{V})} = \frac{m_{11} + 2m_{12}}{3}. \tag{34.6}$$

The shear coefficients in cubic crystals are $(m_{11} - m_{12})/2$, which describes the change in conductivity along the x-axis under a strain $e_{xx} = -e_{yy}$, and m_{44}, which determines the component $\Delta\sigma_{xy}$ for a strain e_{xy} varying the angle between the x- and y-axes.

The elastoresistance coefficients are dimensionless; they determine the relative change in conductivity per unit strain, each for a specific type of strain. They are more convenient for a theoretical interpretation of piezoresistance effects.

In practice, however, one applies a stress to the crystal, and the relative change in conductivity is measured per unit stress in a given direction.

The relative change in conductivity, which is proportional to the stress, is defined by a fourth-rank tensor $\pi_{\alpha\beta,\,\gamma\delta}$ defined by a relation similar to (34.1):

$$\frac{\Delta\sigma_{\alpha\beta}}{\tilde{\sigma}} = \sum_{\gamma\delta} \pi_{\alpha\beta,\,\gamma\delta} P_{\gamma\delta}, \tag{34.7}$$

where $P_{\gamma\delta}$ is the stress tensor. The tensor $\pi_{\alpha\beta,\,\gamma\delta}$ is called the piezoresistance tensor. It has dimensions cm^2/dyne and possesses the same symmetry properties as the tensor $m_{\alpha\beta,\,\gamma\delta}$.

Introducing the notation

$$P_{xx} = P_1, \quad P_{yy} = P_2, \quad P_{zz} = P_3, \quad P_{yz} = P_4,$$
$$\pi_{xx,\,xx} = \pi_{11}, \quad 2\pi_{xy,\,xy} = \pi_{66}, \text{ etc.},$$

we write (34.7) as

$$\frac{\Delta\sigma_i}{\tilde{\sigma}} = \sum_j \pi_{ij} P_j. \tag{34.8}$$

The piezoresistance matrix π_{ij} is analogous to the matrix m_{ij} and has the form (34.5) for cubic crystals.

The coefficients $(\pi_{11} + 2\pi_{12})/3$ describe the change in conductivity under an isotropic pressure, while $(\pi_{11} - \pi_{12})/2$ and π_{44} describe the change in conductivity under shear stresses.

The stress tensor $P_{\alpha\beta}$ may be expressed in terms of the strain tensor by means of the tensor of elastic moduli $C_{\alpha\beta,\,\gamma\delta}$, which is the inverse of the tensor $S_{\alpha\beta,\,\gamma\delta}$. We may write this relation in matrix form as

$$\boldsymbol{P} = \boldsymbol{C}e, \tag{34.9}$$

where $C_{ij} \to C_{\alpha\beta,\,\gamma\delta}$, $i = (\alpha\beta)$ and $j = (\gamma\delta)$.

The matrix $\boldsymbol{C}$, which is analogous to the matrix $\boldsymbol{m}$ or $\boldsymbol{\pi}$, depends on three constants: $C_{11} = C_{xx,\,xx}$, $C_{12} = C_{xx,\,yy}$, $C_{44} = C_{yz,\,yz}$.

Equation (34.9) implies a relation between the matrices $\boldsymbol{m}$ and $\boldsymbol{\pi}$:

$$\boldsymbol{m} = \boldsymbol{\pi}\boldsymbol{C}, \tag{34.10}$$

so that the elastoresistance and piezoresistance coefficients for cubic crystals satisfy the following relations:

$$\begin{aligned} \frac{m_{11} + 2m_{12}}{3} &= \frac{\pi_{11} + 2\pi_{12}}{3}(C_{11} + 2C_{12}), \\ \frac{m_{11} - m_{12}}{2} &= \frac{\pi_{11} - \pi_{12}}{2}(C_{11} - C_{12}), \\ m_{44} &= \pi_{44} C_{44}. \end{aligned} \tag{34.11}$$

These relations enable us to determine the elastoresistance coefficients from experimental values of the piezoresistance coefficients.

A phenomenological description of piezoresistance effects makes it possible to derive the form of the elastoresistance matrix from symmetry considerations, and also to find the relative orientation of the electric field,

current and stress necessary for experimental determination of the elastoresistance tensor.

Volume piezoresistance effects

The electric conductivity tensor $\sigma_{\alpha\beta}$ of a crystal is the sum of the electric conductivity $\sigma^i_{\alpha\beta}$ of the carriers near each extremum:

$$\sigma_{\alpha\beta} = \sum_i \sigma^i_{\alpha\beta}. \tag{34.12}$$

If the band is degenerate at the extremum point $\boldsymbol{k}_0$ and the energy spectrum has several branches, each corresponding to a particular species of current carrier, the conductivity (34.12) is the sum of conductivities of the different species of carriers. But if there are electrons and holes in the semiconductor, its conductivity is composed of the electron and hole conductivities.

In the general case, the conductivity tensor $\sigma^i_{\alpha\beta}$ for carriers of species i, in the case of nondegenerate statistics, may be written

$$\sigma^i_{\alpha\beta} = \frac{e^2}{kT} \int f_0 \tau^i_{\alpha\beta} v^i_\alpha v^i_\beta \, d^3\boldsymbol{k}, \tag{34.13}$$

where f_0 is the equilibrium distribution function $f_0 = e^{(\zeta - E_i)/kT}$, ζ the chemical potential, v^i_α the group velocity of the current carriers:

$$v^i_\alpha = \frac{1}{\hbar} \frac{\partial E_i}{\partial k_\alpha},$$

and $\tau^i_{\alpha\beta}$ the relaxation time, which generally depends on $\boldsymbol{k}$ as well as on the direction of the current and the electric field. The relaxation time is determined both by scattering of current carriers due to phonons and impurities within the band i and by transitions between different branches of the spectrum.

Upon application of a strain, the energy spectrum E_i changes, inducing changes in the distribution function f_0 at the given point of $\boldsymbol{k}$-space, and in the group velocity; the relaxation time τ^i also changes.

As shown in §§29 and 30, the nature of the change in the energy spectrum is essentially bound up with the band structure in the unstrained crystal.

In the case of a nondegenerate band, the strain displaces the extremum by a quantity ΔE_i proportional to the strain, and changes the effective masses of the ellipsoid. The correction to the energy due to the change in the effective masses, $\Delta E \sim D\varepsilon \frac{\hbar^2 k^2}{2m^* E_g}$, is significantly less than $\Delta E_i \sim D\varepsilon$; as a first approximation, then, we shall disregard the strain-induced change in effective mass. In this approximation the group velocity for a nondegenerate band does not change.

As shown in §30, the change in the spectrum in a degenerate band, induced by a strain which removes the degeneracy, is more complicated:

there is a sharp change near the point of degeneracy, where the carrier kinetic energy, measured from the extremum point, is comparable with or less than the strain-induced band splitting, while in regions of $\boldsymbol{k}$-space sufficiently remote from the extremum point the energy correction ΔE_i is proportional to the strain but depends on the direction of the vector $\boldsymbol{k}$.

If the strain does not alter the crystal symmetry, each extremum is shifted by the same amount ΔE_c. The degeneracy is not removed and the current carrier relaxation time τ_i does not change.

In an impurity semiconductor, in the exhaustion region, the current carrier concentration remains the same when a strain is applied, and all the volume piezoresistance coefficients are small.

The volume piezoresistance coefficients in impurity semiconductors may be large when there are several species of current carriers with the same sign, i. e., in semiconductors which have close-lying inequivalent extrema. In this case an isotropic strain induces a redistribution of the current carriers among the extrema and consequently a change in conductivity.

The volume piezoresistance coefficients may be large in the region of intrinsic conductivity, where conduction is due to electrons and holes. The conductivity tensor in this case is:

$$\sigma_{\alpha\beta} = en\mu^n_{\alpha\beta} + ep\mu^p_{\alpha\beta}, \tag{34.14}$$

where n, p are the total concentrations of electrons and holes and $\mu^n_{\alpha\beta}$, $\mu^p_{\alpha\beta}$ their mobilities, averaged over all extrema. The electron and hole concentrations satisfy the neutrality condition $\mu^p_{\alpha\beta}$

$$p - n = N_a - N_d \equiv N, \tag{34.15}$$

where N_a and N_d are the concentrations of the acceptors and donors, which are assumed to be completely ionized. In a nondegenerate semiconductor,

$$pn = n_0^2 = N_c N_v e^{-E_g/kT}, \tag{34.16}$$

where n_0 is the intrinsic carrier concentration (that of an undoped semiconductor at the given temperature), N_c and N_v the effective density of states in the conduction and valence bands, and E_g the band gap.

The concentrations p and n are easily found from (34.15) and (34.16):*

$$p = \frac{N + \sqrt{N^2 + 4n_0^2}}{2} = \frac{N}{2}(R+1), \quad n = \frac{\sqrt{N^2 + 4n_0^2} - N}{2} = \frac{N}{2}(R-1), \tag{34.17}$$

where

$$R = \sqrt{1 + 4n_0^2/N^2}.$$

Under a strain which preserves the crystal symmetry, the bottom of the conduction band is shifted by ΔE_c and that of the valence band by ΔE_v. As a result, the band gap changes, by $\Delta E_g = \Delta E_c - \Delta E_v$, and hence, by (34.16), so does the intrinsic concentration n_0. According to (34.15) and (34.16), if we

* To fix ideas, we assume that $N_a - N_d = N > 0$.

disregard the change of the effective masses, i. e., assume that $\Delta N_c = \Delta N_v = 0$, then

$$\Delta p = \Delta n = -\frac{\Delta E_g}{kT}\frac{n_0}{p+n} = -\frac{\Delta E_g}{kT}\frac{n_0^2}{NR}. \tag{34.18}$$

Since the mobilities $\mu^n_{\alpha\beta}$ and $\mu^p_{\alpha\beta}$ are invariant under strain, the relative variation $\Delta\sigma_{\alpha\beta}/\bar{\sigma}$ is

$$\frac{\Delta\sigma_{\alpha\beta}}{\bar{\sigma}} = -\frac{\Delta E_g}{2kT}\frac{R^2-1}{R}\frac{\mu^n_{\alpha\beta}+\mu^p_{\alpha\beta}}{(R-1)\bar{\mu}^n+(R+1)\bar{\mu}^p}, \tag{34.19}$$

where $\bar{\sigma} = en\bar{\mu}^n + ep\bar{\mu}^p$ is the average conductivity of the unstrained crystal, $\bar{\mu}^n = \frac{1}{3}\mathrm{Tr}\mu^n$ and $\bar{\mu}^p = \frac{1}{3}\mathrm{Tr}\mu^p$ are the average electron and hole mobilities. For cubic crystals, where $\bar{\mu}^n_{\alpha\beta} = \mu^n\delta_{\alpha\beta}$ and $\bar{\mu}^p_{\alpha\beta} = \mu^p\delta_{\alpha\beta}$, equation (34.19) yields:

$$\frac{m_{11}+2m_{12}}{3} = -\frac{E_{1g}}{2kT}\frac{R^2-1}{R}\frac{1+b}{R-1+(R+1)b}, \tag{34.20}$$

where $b = \mu^n/\mu^p$, and E_{1g} is the deformation potential constant, which defines the change in the band gap E_g under an isotropic strain: $\Delta E_g = E_{1g}\mathrm{Tr}\varepsilon$.

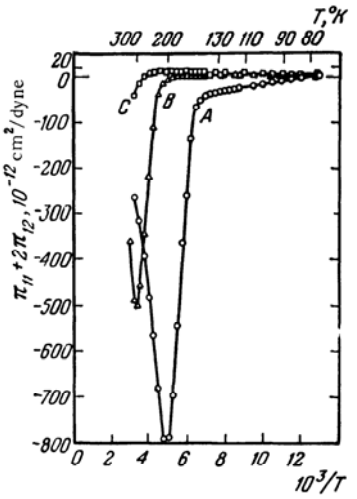

FIGURE 40. Temperature dependence of the volume piezoresistance coefficient in InSb /33.2/. The concentration $N_a - N_d$ in samples A, B, C is $3\cdot10^{15}$, $6.3\cdot10^{16}$, $6.6\cdot10^{17}$ cm^{-3}, respectively.

At low temperatures, when $n_0 \ll N$, i. e., in the region of impurity conductivity, we have $R \approx 1$, and the volume coefficients are small, in agreement

with the above result. With increasing temperature, n_0 increases exponentially and the piezoresistance effect becomes stronger. At high temperatures, when $R \gg 1$, $\Delta\sigma_{\alpha\beta}/\bar{\sigma}$ is the order of $\Delta E_g/2kT$ and decreases like $1/T$ with further increase in temperature.

The volume coefficient reaches a maximum at a temperature T_0, near which the intrinsic concentration n_0 and impurity concentration N become equal. At this maximum, the value of $(m_{11} + 2m_{12})/3$ is of the order of $E_{1g}/2kT_0$. Since E_{1g} is of the order of 5 to 10 ev, the value of $(m_{11} + 2m_{12})/3$ at the maximum may reach a few hundred in adequately pure specimens.

Thus, volume effects may be large in the intrinsic conductivity region for semiconductors with a narrow band gap.

Figure 40 illustrates the temperature dependence of the volume coefficient in InSb / 33.2/ . It is clear that the temperature and concentration dependence of the volume coefficient is described satisfactorily by equation (34.20).

Shear piezoresistance coefficients in many-valley semiconductors

In this case, each extremum is shifted by a quantity ΔE_i which differs for different extrema, removing the many-valley degeneracy of the spectrum. Since ΔE_i is independent of $\boldsymbol{k}$ when the change in effective mass is ignored, there is no change in group velocity.

Electrons may be scattered in a many-valley semiconductor because of either transitions within one ellipsoid or transitions between different extrema. Intravalley scattering is not affected by strain, but intervalley scattering may change. Under normal conditions, however, intervalley scattering makes only a small contribution to the relaxation time of the conduction electrons, which determines the conductivity, and we shall therefore neglect it, assuming that the relaxation time of the electrons (and hence also their mobility) remains unchanged under a strain.*

The mobility tensor is diagonal relative to the principal axes of the ellipsoid:

$$\mu_{st} = \mu_s \delta_{st},$$

where μ_s are the principal values of the mobility tensor, which are the same for all ellipsoids.

The carrier conductivity $\sigma^i_{\alpha\beta}$ in the i-th ellipsoid, relative to the crystal axes, is

$$\sigma^i_{\alpha\beta} = en_i\mu^i_{\alpha\beta}, \quad n_i = N_i e^{(\zeta - E_i)/kT}, \tag{34.21}$$

where n_i is the carrier concentration in one ellipsoid (the same for all ellipsoids in the unstrained crystal) and $\mu^i_{\alpha\beta}$ the carrier mobility tensor of

* The contribution to piezoresistance effects from strain-induced changes in intervalley scattering has been discussed in /32.2/.

the i-th ellipsoid relative to the crystal axes. Equations (34.12) and (34.21) give the strain-induced change in conductivity:

$$\Delta\sigma_{\alpha\beta}=\sum_i \Delta\sigma^i_{\alpha\beta}=e\sum_l \Delta n_l\mu^i_{\alpha\beta}=-\frac{en_l}{kT}\sum_i(\Delta E_l-\Delta\zeta)\,\mu^i_{\alpha\beta}.$$

Since the concentration is assumed constant, we have

$$\Delta n=-\frac{n_l}{kT}\sum_i(\Delta E_l-\Delta\zeta)=0;\qquad \Delta\zeta=\frac{1}{N_0}\sum_i \Delta E_i=\Delta E_c,$$

where N_0 is the number of extrema. Thus the relative change in conductivity is

$$\frac{\Delta\sigma_{\alpha\beta}}{\bar\sigma}=-\frac{1}{kT}\left(\frac{1}{N_0}\sum_i\frac{\Delta E_l}{\bar\mu}\mu^i_{\alpha\beta}-\Delta E_c\frac{\mu_{\alpha\beta}}{\bar\mu}\right), \tag{34.22}$$

where $\bar\mu=\frac{1}{3}\mathrm{Tr}\,\mu^i_{\alpha\beta}$ is the average current carrier mobility near one of the ellipsoids, which is the same for all the ellipsoids and thus coincides with the average mobility in the crystal, and $\mu_{\alpha\beta}=\frac{1}{N_0}\sum_i\mu^i_{\alpha\beta}$ is the mobility tensor in the unstrained crystal. In a nondegenerate band,

$$\Delta E_l=\sum_{\gamma\delta}D^i_{\gamma\delta}\,\varepsilon_{\gamma\delta}, \tag{34.23}$$

where $\varepsilon_{\gamma\delta}$ are the components of the strain tensor referred to the crystal axes, and $D_{\gamma\delta}$ is the tensor of deformation potential constants of the i-th ellipsoid in the same reference system. Substituting (34.23) into (34.22), we obtain an expression for the tensor $m_{\alpha\beta,\,\gamma\delta}$:

$$m_{\alpha\beta,\,\gamma\delta}=-\frac{1}{kT}\left(\frac{1}{N_0}\sum_i\frac{\mu^i_{\alpha\beta}D^i_{\gamma\delta}}{\bar\mu}-\frac{\mu_{\alpha\beta}}{\bar\mu}\frac{1}{N_0}\sum_i D^i_{\gamma\delta}\right). \tag{34.24}$$

This expression for $m_{\alpha\beta,\,\gamma\delta}$, in terms of the mobility components and deformation potential constants relative to the crystal axes, is sometimes conveniently rewritten in terms of the principal values of the mobilities μ_s $(s=1,2,3)$ and of the deformation potential constants D_t $(t=1,2,3)$ relative to the principal axes of each ellipsoid, x^i_t $(t=1,2,3)$, since these values are the same for all the ellipsoids. Since

$$\begin{aligned}\mu^i_{\alpha\beta}&=\sum_s\mu_s\cos(x_\alpha,\,x^i_s)\cos(x_\beta,\,x^i_s),\\ D^i_{\gamma\delta}&=\sum_t D_t\cos(x_\gamma,\,x^i_t)\cos(x_\delta,\,x^i_t),\end{aligned} \tag{34.25}$$

it follows from (34.24) that

$$m_{\alpha\beta,\,\gamma\delta}=-\frac{1}{kT}\sum_{st}\frac{\mu_s D_t}{\bar\mu}\left(R^{st}_{\alpha\beta,\gamma\delta}-R^s_{\alpha\beta}R^t_{\gamma\delta}\right), \tag{34.26}$$

where

$$\begin{aligned}R^{st}_{\alpha\beta,\,\gamma\delta}&=\frac{1}{N_0}\sum_i\cos(x_\alpha,\,x^i_s)\cos(x_\beta,\,x^i_s)\cos(x_\gamma,\,x^i_t)\cos(x_\delta,\,x^i_t),\\ R^s_{\alpha\beta}&=\frac{1}{N_0}\sum_i\cos(x_\alpha,\,x^i_s)\cos(x_\beta,\,x^i_s).\end{aligned} \tag{34.27}$$

Since $R^{st}_{\alpha\beta,\,\gamma\delta}$ and $R^{s}_{\alpha\beta}$ are symmetric with respect to permutation of the inner pair of indices, it follows that $m_{\alpha\beta,\,\gamma\delta}$ (34.26) also possesses the required symmetry (34.2) with respect to index permutation.

The quantities $R^{st}_{\alpha\beta,\,\gamma\delta}$ and $R^{s}_{\alpha\beta}$ satisfy the relations

$$\sum_t R^{st}_{\alpha\beta,\,\gamma\delta} = R^{s}_{\alpha\beta}\delta_{\gamma\delta}, \qquad \sum_s R^{st}_{\alpha\beta,\,\gamma\delta} = \delta_{\alpha\beta}R^{t}_{\gamma\delta}, \qquad \sum_t R^{t}_{\gamma\delta} = \delta_{\gamma\delta}. \tag{34.28}$$

Equation (34.26) expresses the elastoresistance tensor components in terms of the principal values of the mobility tensors and the deformation potential constants at one of the extrema, and in terms of the positions of the extrema in $\boldsymbol{k}$-space. It may be simplified if the energy ellipsoids are ellipsoids of revolution.

Indeed, if we assume that the axis of revolution of the ellipsoid is the x_1-axis, then $\mu_1 = \mu_\parallel$, $\mu_2 = \mu_3 = \mu_\perp$, $D_1 = D_\parallel$, $D_2 = D_3 = D_\perp$; using (34.28), we obtain

$$m_{\alpha\beta,\,\gamma\delta} = -\frac{\mu_\parallel - \mu_\perp}{\bar{\mu}}\left(\frac{D_\parallel - D_\perp}{kT}\right)\left(R^{11}_{\alpha\beta,\,\gamma\delta} - R^{1}_{\alpha\beta}R^{1}_{\gamma\delta}\right). \tag{34.29}$$

As follows from equation (34.29), the shear elastoresistance coefficients are proportional to the anisotropy $(\mu_\parallel - \mu_\perp)/\bar{\mu}$ of the carrier mobility at each extremum and to the deformation potential constant $\Xi_u = D_\parallel - D_\perp$, which determines the relative shift of the extrema under a shear strain. For the case of a cubic crystal with extrema on the [100] and [111] axes, equation (34.29) yields

$$\begin{aligned} &\frac{m_{11} - m_{12}}{2} = -\frac{1}{2}\frac{1-K}{1+2K}\frac{\Xi_u}{kT}, \quad m_{44} = 0 && \text{for extrema on [100],} \\ &\frac{m_{11} - m_{12}}{2} = 0, \quad m_{44} = -\frac{1}{3}\frac{1-K}{1+2K}\frac{\Xi_u}{kT} && \text{for extrema on [111],} \end{aligned} \tag{34.30}$$

where $K = \mu_\perp/\mu_\parallel$ is the anisotropy of the current carrier mobility at each extremum.

Thus, the magnitude of the shear effects is essentially determined by the positions of the extrema in $\boldsymbol{k}$-space.

The source of these effects is that, under a strain which destroys the equivalence of the extrema, some of the electrons transfer from one extremum to another (with conservation of total concentration), and the resultant mobility in the strained crystal becomes anisotropic.

From the standpoint of group theory, determination of the extrema whose equivalence is destroyed by a strain involves decomposition of an irreducible star $\{\boldsymbol{k}\}$ in the group F into irreducible stars $\{\boldsymbol{k}\}$ in the group F' into which the strain transforms the group F.

The piezoresistance effects associated with carrier transfer have a characteristic temperature dependence, which is determined primarily by a Boltzmann factor and also by the temperature dependence of the mobility anisotropy $(\mu_\parallel - \mu_\perp)/\bar{\mu}$. The magnitude of the piezoresistance effect is of the order of Ξ_u/kT, where Ξ_u is the deformation potential constant, usually about 1–10 ev. Therefore, at relatively low temperatures the shear piezoresistance effects associated with carrier transfer may have values of 10^2–10^3.

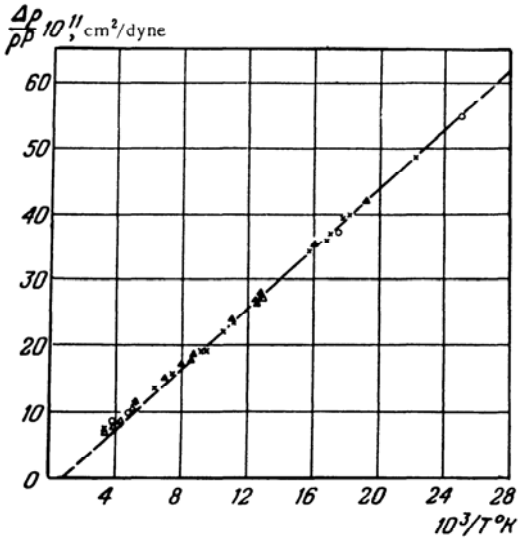

FIGURE 41. Temperature dependence of piezoresistance in n-Ge strained along [110] /32.2/.

Figure 41 illustrates the relative change in resistivity for n-Ge strained along [100]; it is evident that the coefficient π_{11} in n-Ge increases proportionally to $1/T$ over a wide temperature range and is practically independent of the carrier concentration. The small deviation from linearity at high temperatures is due to the contribution of intervalley scattering.

Piezoresistance effects in semiconductors with degenerate bands

Large piezoresistance effects also arise in the case of degenerate bands, for strains which remove the degeneracy.

Let us consider a degenerate band having s branches $E_i(\mathbf{k})$ $(i=1, 2, \ldots, s)$. If the temperature is sufficiently high most of the current carriers will be in a region quite remote from the degeneracy point, where the energy corrections are linear functions of the strain. In this case the conductivity change is also proportional to the strain.

In the case of a degenerate band, the conductivity $\sigma^i_{\alpha\beta}$ of each species of carrier is affected by the change in the distribution function f_0, the variation of the group velocity $\Delta v^i_\alpha = \frac{1}{\hbar}\frac{\partial E_i}{\partial k_\alpha}$, and also the change in the relaxation time τ^i.

As remarked in §32, scattering theory of current carriers in a degenerate band is more complicated than in the case of a nondegenerate band, since scattering may involve transitions both within and between different spectrum branches, and the transition probabilities are fairly

complicated functions of the scattering angle. It is even more difficult to determine the change $\Delta\tau$ in the relaxation time, since the strain causes τ to change not only via the difference in the carrier energy spectrum from the initial to the final states, but also owing to the change in the scattering matrix element due to the effect of strain on the wave functions.

If the transition probabilities are isotropic, it can be shown that the relaxation time is also isotropic, depending only on the energy:

$$\Delta\tau_i = \frac{\partial\tau_i}{\partial E}\Delta E_i. \tag{34.31}$$

In the case of anisotropic scattering, equality (34.31) is strictly speaking not valid, but we can reasonably assume that it accounts for the major part of the strain-induced change in the relaxation time, and we shall use it to calculate the piezoresistance effect in a degenerate band.

In calculating the shear piezoresistance coefficients, we shall assume that only the shear components of the strain tensor are nonzero, while the components ε_{ij} which transform according to the identity representation and determine the shift of the band as a whole vanish.

We claim in this case

$$\sum_i \Delta E_i(\boldsymbol{k}, \varepsilon) = 0 \text{ and } \int \Delta E_i(\boldsymbol{k}, \varepsilon)\, d\Omega_{\boldsymbol{k}} = 0, \tag{34.32}$$

where $d\Omega_{\boldsymbol{k}}$ is the solid angle element in $\boldsymbol{k}$-space.

Indeed, since $E_i(\boldsymbol{k}, \varepsilon)$ is a solution of the equation $|\mathcal{H}(\boldsymbol{k}) + \mathcal{H}(\varepsilon) - IE(\boldsymbol{k}, \varepsilon)| = 0$ where $\mathcal{H}(\boldsymbol{k})$ and $\mathcal{H}(\varepsilon)$ are the matrices determining the spectrum in the unstrained crystal and the strain-induced splitting of the bottom of the band, it follows that

$$\sum_i E_i(\boldsymbol{k}, \varepsilon) = \mathrm{Tr}\,\mathcal{H}(\boldsymbol{k}) + \mathrm{Tr}\,\mathcal{H}(\varepsilon).$$

Expanding $E_i(\boldsymbol{k}, \varepsilon)$ in series in ε, we obtain

$$\sum_i \Delta E_i(\boldsymbol{k}, \varepsilon) = \mathrm{Tr}\ \mathcal{H}(\varepsilon) = 0.$$

The second equality in (34.32) follows from the fact that $\int \Delta E_i(\boldsymbol{k}, \varepsilon)\, d\Omega_{\boldsymbol{k}}$ is an invariant combination of the strain tensor components, and is thus proportional to those of the components which we have assumed to be zero.

It follows from (34.32) that

$$\Delta n = \sum_i \Delta n_i = \frac{\Delta\zeta}{kT}\sum_i n_i = n\frac{\Delta\zeta}{kT}.$$

In an impurity semiconductor, in the exhaustion region $\Delta n = 0$, and so $\Delta\zeta = 0$.

Using (34.13) and (34.31), we obtain the correction $\Delta\sigma^i_{\alpha\beta}$ to the conductivity tensor of the carriers in the i-th band:

$$\Delta\sigma^i_{\alpha\beta} = \frac{e^2}{kT}\left\{\int \frac{\partial}{\partial E_i}\left(f_0\tau_i\right) v^i_\alpha v^i_\beta\, \Delta E_i\, d\boldsymbol{k} + \frac{1}{\hbar}\int f_0\tau_i\left(\frac{\partial\,\Delta E_i}{\partial k_\alpha} v^i_\beta + \frac{\partial\,\Delta E_i}{\partial k_\beta} v^i_\alpha\right) d\boldsymbol{k}\right\}.$$

Integrating by parts, we find

$$\Delta\sigma^i_{\alpha\beta} = -\frac{e^2}{kT}\left\{\int \frac{\partial}{\partial E_i}(f_0\tau_i)\, v^i_\alpha v^i_\beta\, \Delta E_i\, d\boldsymbol{k} + \frac{2}{\hbar^2}\int f_0\tau_i \frac{\partial^2 E_i}{\partial k_\alpha\, \partial k_\beta}\Delta E_i\, d\boldsymbol{k}\right\}. \tag{34.33}$$

Transforming from the variables k_x, k_y, k_z to the energy E_i and angles θ, φ, we write E_i, v^i_α and $\frac{\partial^2 E_i}{\partial k_\alpha\, \partial k_\beta}$*

$$E_i = \frac{\hbar^2 k^2}{2m^*_i(\theta,\varphi)}, \quad v^i_\alpha = \frac{\hbar k}{m^*_i}\Lambda^i_\alpha(\theta,\varphi) = \frac{(2E_i)^{1/2}}{m^{*1/2}_i}\Lambda^i_\alpha(\theta,\varphi),$$
$$\frac{\partial^2 E_i}{\partial k_\alpha\, \partial k_\beta} = \frac{\hbar^2}{m^*_i(\theta,\varphi)} B^i_{\alpha\beta}(\theta,\varphi). \tag{34.34}$$

In the quadratic k approximation, m^*, Λ_α and $B_{\alpha\beta}$ depend only on the angles θ and φ. It follows from (34.34) that

$$d\boldsymbol{k} = \frac{1}{2} dE_i\, E_i^{1/2}\, d\Omega_{\boldsymbol{k}} \frac{(2m^*_i)^{3/2}}{\hbar^3}.$$

and we can integrate separately in (34.33) over the energy E_i and over the angles θ and φ:

$$\Delta\sigma^i_{\alpha\beta} = \frac{e^2}{kT}\frac{2^{3/2}}{\hbar^3}\int_0^\infty f_0\tau_i E_i^{1/2} dE_i \int d\Omega_{\boldsymbol{k}}\left(\frac{3}{2}\Lambda^i_\alpha\Lambda^i_\beta\,\Delta E_i - B^i_{\alpha\beta}\,\Delta E_i\right). \tag{34.35}$$

For $\Delta\sigma^i_{\alpha\beta}/\bar{\sigma}$, we obtain

$$\frac{\Delta\sigma^i_{\alpha\beta}}{\bar{\sigma}} = \sum_i \frac{\langle\tau_i\rangle}{\langle\tau_i E_i\rangle}\frac{\bar{\sigma}_i}{\bar{\sigma}}\Gamma^i_{\alpha\beta}, \tag{34.36}$$

where

$$\langle\tau_i\rangle = \frac{\int_0^\infty f_0\tau_i E_i^{1/2}\, dE_i}{\int_0^\infty f_0 E^{1/2}\, dE}$$

is the Maxwellian average of τ_i and $\bar{\sigma}_i$ the average carrier conductivity in the i-th band:

$$\bar{\sigma}_i = \frac{2}{3}\frac{e^2}{kT}\frac{\langle\tau_i E_i\rangle}{\bar{m}_i}; \tag{34.37}$$

$$\frac{1}{\bar{m}_i} = \frac{\int d\Omega_{\boldsymbol{k}}\left(\Lambda^2_{xi} + \Lambda^2_{yi} + \Lambda^2_{zi}\right) m^{*1/2}_i}{\int m^{*3/2}_i\, d\Omega_{\boldsymbol{k}}}; \tag{34.38}$$

* In (34.34) the effective mass $m^*(\theta, \varphi)$ is assumed to be positive for both electrons and holes. This means that for the valence band, E_i and ΔE_i in (34.33)–(34.35) denote the hole energy, which is opposite in sign to the energy of electrons in the valence band.

$\bar{\sigma}$ is the average conductivity of the crystal, $\bar{\sigma} = \sum_i \bar{\sigma}_i$. The quantities $\Gamma^i_{\alpha\beta}$ are proportional to the deformation potential constants:

$$\Gamma^i_{\alpha\beta} = \frac{3 \int d\Omega_k \, \Delta E_i m_i^{*1/2} \left({}^3/_2 \, \Lambda^i_\alpha \Lambda^i_\beta - B^i_{\alpha\beta} \right)}{\int d\Omega_k \left(\Lambda^2_{xi} + \Lambda^2_{yi} + \Lambda^2_{zi} \right) m_i^{*1/2}}. \tag{34.39}$$

The value of $\frac{\langle \tau \rangle}{\langle \tau E \rangle}$ depends on the function $\tau(E)$. If $\tau(E) \sim E^n$, then

$$\frac{\langle \tau \rangle}{\langle \tau E \rangle} = \frac{1}{kT} \frac{1}{n + 3/2}.$$

As in many-valley semiconductors, the shear coefficients in a degenerate band are of the order of D/kT, where D denotes the deformation potential constants.

The temperature dependence of piezoresistance effects in a degenerate band is more complicated. It depends on the Boltzmann factor D/kT, on the temperature variation of the conduction mechanisms which determine the average $\frac{\langle \tau_i \rangle}{\langle E_i \tau_i \rangle}$, and on the temperature variation of the contribution of different species of carriers to the conductivity $\bar{\sigma}_i/\bar{\sigma}$.

For subsequent calculations of the elastoresistance coefficients $m_{\alpha\beta,\gamma\delta}$, we shall need the coefficients $\Gamma^i_{\alpha\beta}$; these may be determined only in each specific case, since by (34.29) the coefficients depend on the shape of the spectrum in the unstrained crystal and on the form of ΔE_i.

We can nevertheless state that in the degenerate model the piezoresistance coefficients will be large for shear strains which remove the band degeneracy at an extremum point, since only for such shear strains does ΔE_i fail to vanish.

The previous discussion of piezoresistance effects in many-valley and degenerate semiconductors implies that the shear elastoresistance coefficients will be large for strains which completely or partially lift the degeneracy of the band structure. From the group-theoretic standpoint, these are strains which reduce the crystal symmetry to the degree that the representation $\mathfrak{D}_\nu^{\{k_0\}}$ of the space group for the unstrained crystal corresponding to the star $\{k_0\}$ of the extremum positions becomes reducible in the symmetry group of the strained crystal.

Let us consider piezoresistance effects in a degenerate Γ_8 band of the type of the valence band in p-Ge and p-Si.

The integrals in (34.39) cannot be calculated explicitly for the Γ_8 band, and computers must be used. The calculations can be done if the surfaces of constant energy $E_{1,2}(k)$ of the heavy and light holes (24.13a) are approximated by suitable average spheres:

$$E_{1,2}(k) = \frac{\hbar^2 k^2}{2m^*_{1,2}}, \text{ where } \frac{\hbar^2}{2m^*_{1,2}} = |A \pm \bar{B}|, \; \bar{B} = \sqrt{B^2 + \frac{C^2}{5}}. \tag{34.40}$$

In this approximation $\Lambda_\alpha = k_\alpha/k$, $B_{\alpha\beta}^{(1,2)} = \delta_{\alpha\beta}/m_{1,2}$, and from (34.35) and (30.34) for $\Delta E_{1,2}(\boldsymbol{k})$ we obtain the shear piezoresistance coefficients for the Γ_8 band:

$$\frac{m_{11}-m_{12}}{2} = -\frac{9}{20}\frac{Bb}{\bar{B}}\left[\frac{\langle\tau_1\rangle}{\langle\tau_1 E\rangle}\frac{\sigma_1}{\sigma_1+\sigma_2} - \frac{\sigma_2}{\sigma_1+\sigma_2}\frac{\langle\tau_2\rangle}{\langle E\tau_2\rangle}\right],$$
$$m_{44} = -\frac{3}{20}\frac{Dd}{\bar{B}}\left[\frac{\langle\tau_1\rangle}{\langle E\tau_1\rangle}\frac{\sigma_1}{\sigma_1+\sigma_2} - \frac{\sigma_2}{\sigma_1+\sigma_2}\frac{\langle\tau_2\rangle}{\langle E\tau_2\rangle}\right]. \qquad (34.41)$$

The indices 1 and 2 in (34.41) designate heavy and light holes respectively. It follows from equation (34.41) that neither of the shear components $(m_{11}-m_{12})/2$ and m_{44} of the piezoresistance vanishes in the band Γ_8. Data on piezoresistance effects enable one to determine only the sign of the products Bb and Dd, but not the deformation potential constants b and d themselves.

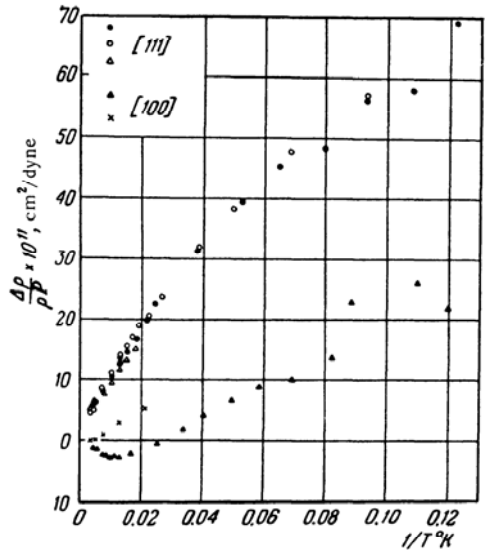

FIGURE 42. Temperature dependence of piezoresistance in p-Ge /32.2/.

Figure 42 illustrates the change in resistivity in p-Ge induced by strains along the [100] and [111] axes. One sees from the figure that although the piezoresistance coefficient increases sharply with decreasing temperature, nevertheless, as opposed to n-Ge and n-Si, the temperature dependence is markedly different from $1/T$. The value of π_{11} depends essentially on the carrier concentration.

Figure 43 shows a similar, even more marked dependence in p-Si: the coefficient $m_{11}-m_{12}$ changes sign with decreasing temperature and passes through a minimum. With increasing concentration, the position of the point

at which $m_{11} - m_{12} = 0$ is displaced toward higher temperatures. Underlying this behavior is the change in the relative contribution of the light and heavy holes, as well as the complicated temperature dependence of $\frac{\langle\tau\rangle}{\langle\tau E\rangle}$ when there are several scattering mechanisms. The nonspherical nature of the band, which increases the contribution of the light holes to $m_{11} - m_{12}$ and decreases it in m_{44}, is a decisive factor in p-Si.

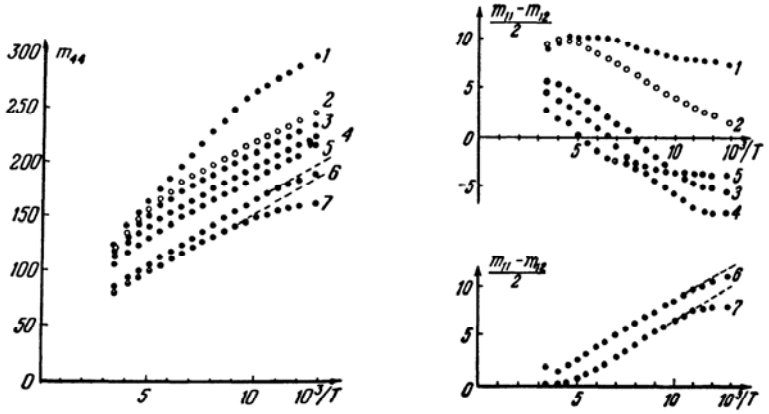

FIGURE 43. Temperature dependence of piezoresistance coefficients in p-Si for samples with different impurity concentrations /32.6/. The curves are numbered in order of increasing concentration.

Since light holes are more strongly scattered than heavy holes by impurities, the contribution of the former to the electrical conductivity increases with increasing temperature and decreasing impurity concentration; this is the reason for the change of sign in the coefficient $m_{11} - m_{12}$ with increasing temperature /32.6/. At even higher temperatures, the relatively large change in effective mass determined by equation (24.21) assumes a significant role and, as we show below, leads to temperature-independent strain-induced effects.

We have assumed hitherto that the electron (or hole) gas is not degenerate. Expressions for the piezoresistance coefficients allowing for Fermi degeneracy are readily obtained.

Allowance for Fermi degeneracy

In case of Fermi degeneracy, the current carrier conductivity for each ellipsoid or for each species of carrier in a degenerate band is

$$\sigma_{\alpha\beta} = -e^2 \int \frac{\partial f_0}{\partial E} \tau_{\alpha\beta} v_\alpha v_\beta \, dk, \qquad (34.42)$$

where f_0 is the Fermi equilibrium distribution function,

$$f_0 = \frac{1}{1 + e^{(E-\zeta)/kT}}, \tag{34.43}$$

and ζ is the chemical potential.

Expression (34.13) differs from (34.42) in that $\partial f_0/\partial E$ is replaced by f_0/kT. Duplicating the derivation of equation (34.26), we easily verify that in the case of an arbitrary electron degeneracy all the previous equations for piezoresistance effects in many-valley semiconductors remain valid, provided we replace $\mu_s/\bar{\mu}$ by the product $(\mu_s/\bar{\mu})\lambda_s$ in equations (34.24) – (34.30), where $\mu_s/\bar{\mu}$ is the ratio of mobilities in the degenerate case:

$$\frac{\mu_s}{\bar{\mu}} = \frac{\int \frac{\partial f_0}{\partial E} v_s^2 \tau_s \, dk}{\frac{1}{3}\int \frac{\partial f_0}{\partial E} \sum_a v_a^2 \tau_a \, dk}, \tag{34.44}$$

and

$$\lambda_s = -\frac{kT \int_0^\infty \frac{\partial^2 f_0}{\partial E^2} \tau_s v_s^2 \, dk}{\int_0^\infty \frac{\partial f_0}{\partial E} \tau_s v_s^2 \, dk}. \tag{34.45}$$

If $\tau_s(E) = \tau_s^0 E^n$, then

$$\lambda_s = -\frac{kT \int_0^\infty \frac{\partial^2 f_0}{\partial E^2} E^{n+3/2} \, dE}{\int_0^\infty \frac{\partial f_0}{\partial E} E^{n+3/2} \, dE}.$$

Integrating by parts and assuming that $n > -3/2$ (this assumption is valid in semiconductors for the known scattering mechanisms), we obtain

$$\lambda = \begin{cases} \dfrac{1}{(1 + e^{-\zeta^*}) \ln (1 + e^{\zeta^*})} & \text{if} \quad n = -1/2, \\ \dfrac{F_{n-1/2}(\zeta^*)}{F_{n+1/2}(\zeta^*)} & \text{if} \quad n > -1/2. \end{cases} \tag{34.46}$$

Here $\zeta^* = \zeta/kT$ is the reduced chemical potential, and

$$F_n(\zeta^*) = \frac{1}{\Gamma(n+1)} \int_0^\infty \frac{x^n \, dx}{1 + e^{x - \zeta^*}}. \tag{34.47}$$

In the case of nondegenerate statistics, when $e^{-\zeta^*} \gg 1$, we have $F_n(\zeta^*) = e^{\zeta^*}$ and $\lambda = 1$ regardless of the nature of the energy dependence of the relaxation time. In the case of strong degeneracy, when $e^{\zeta^*} \gg 1$, the elastoresistance coefficients are of the order of D/ζ, where D is the shear deformation

potential constant and ζ the value of the chemical potential. Thus, for a degenerate electron gas the magnitude of the piezoresistance effects decreases and they become less dependent on temperature.

Repeating the appropriate derivations for degenerate bands, we easily verify that $\Delta\sigma_{\alpha\beta}/\bar{\sigma}$ is given by an equation similar to (34.36), with $\frac{\langle\tau_i\rangle}{\langle\tau_i E\rangle}$ replaced by

$$\frac{\int_0^\infty \frac{\partial f_0}{\partial E}\tau E^{1/2}\,dE}{\int_0^\infty \frac{\partial f_0}{\partial E}\tau E^{3/2}\,dE} = \begin{cases} \frac{1}{kT}\frac{1}{(1+e^{-\zeta^*})\ln(1+e^{\zeta^*})}, & n=-1/2, \\ \frac{1}{kT}\frac{1}{n+3/2}\frac{F_{n-1/2}(\zeta^*)}{F_{n+1/2}(\zeta^*)}, & n>-1/2, \end{cases} \tag{34.48}$$

provided $\tau\sim E^n$.

As in the case of many-valley semiconductors, for strong degeneracy, the elastoresistance coefficients in a degenerate band are of the order of D/ζ

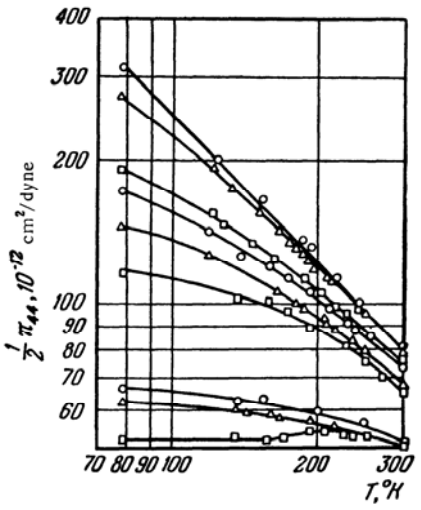

FIGURE 44. Temperature dependence of piezoresistance in heavily doped n-Ge /32.10/.

The decrease in the piezoresistance coefficient and the weakening of the temperature dependence with increasing degeneracy are quite noticeable in Figure 44, which shows the temperature dependence of π_{44} for samples with different concentrations. Since the value of ζ at a given concentration depends on the density of states, i. e., on the number of equivalent extrema N, the variation of π_{44} with concentration, as is evident from Figure 45, must be different for the point L, where $N=4$, and for the point Λ, where $N=8$. The agreement of the experimental data with the calculated curve for

$N = 4$ served as proof that the extrema in n-Ge are located on the edge of the Brillouin zone.

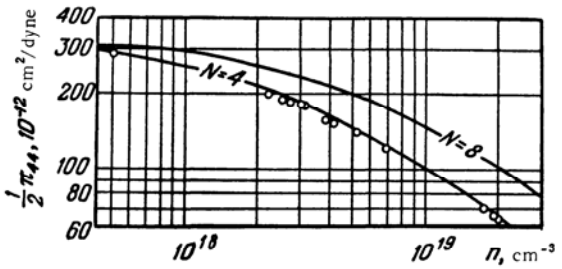

FIGURE 45. Piezoresistance vs. carrier concentration in heavily doped n-Ge /32.10/.

Nonlinear effects

The expressions we have derived for the shear piezoresistance coefficients, according to which the conductivity varies linearly in the strain, are valid provided $\Xi_u \varepsilon/kT \ll 1$ or $\Xi_u \varepsilon/\zeta \ll 1$ (when $\zeta > kT$). If the strain is sufficiently large and these conditions are not fulfilled, nonlinear effects become significant. In the many-valley model, the nonlinear effects are simple in nature. When the energy gap between different ellipsoids becomes comparable with kT, the linear approximation $\Delta n_i = n_i(\Delta\zeta - \Delta E_i)/kT$ underlying the linear theory of piezoresistance effects in many-valley semiconductors is no longer valid for change in carrier concentration in each of the valleys.

For a strain of arbitrary magnitude, it follows from (34.21) that for Boltzmann statistics the conductivity $\sigma_{\alpha\beta}(\varepsilon)$ of the strained crystal is

$$\sigma_{\alpha\beta}(\varepsilon) = e \sum_i \mu^i_{\alpha\beta} n_i(\varepsilon) = e e^{\zeta(\varepsilon)/kT} \sum_i \mu^i_{\alpha\beta} e^{-\Delta E_i/kT}.$$

The chemical potential $\zeta(\varepsilon)$ in the strained crystal is determined from the condition that the total electron concentration be constant:

$$\sum_i n_i(\varepsilon) = N n_0,$$

whence

$$e^{\zeta(\varepsilon)/kT} = \frac{1}{\frac{1}{N}\sum_i e^{-\Delta E_i/kT}},$$

and so

$$\sigma_{\alpha\beta}(\varepsilon) = \frac{1}{\frac{1}{N}\sum e^{-\Delta E_i/kT}} \sum_i \sigma^i_{\alpha\beta} e^{-\Delta E_i/kT}, \qquad (34.49)$$

where $\sigma^i_{\alpha\beta} = en\mu^i_{\alpha\beta}$ is the carrier conductivity of the i-th ellipsoid.

It follows from (34.49) that the average conductivity of the strained crystal, $\bar{\sigma}(\varepsilon) = \frac{1}{3}\mathrm{Tr}\,\sigma(\varepsilon)$, is independent of the strain and equal to the conductivity of the unstrained crystal, $\bar{\sigma}(0) = \frac{1}{3}\mathrm{Tr}\,\sigma(0)$.

Let us consider the strain dependence of the conductivity in cubic semiconductors with extrema on the fourfold and threefold axes, i. e., semiconductors with band structure of the n-Si and n-Ge type.

For n-Si, strained along the z-axis,*

$$\Delta E_1 = \Delta E_2 = \left(\Xi_d + \frac{1}{3}\Xi_u\right)\varepsilon - \frac{1}{3}\Xi_u e'_{zz},$$
$$\Delta E_3 = \left(\Xi_d + \frac{1}{3}\Xi_u\right)\varepsilon + \frac{2}{3}\Xi_u e'_{zz},$$

where $\varepsilon = \mathrm{Tr}\,\varepsilon$ and $\varepsilon'_{zz} = \varepsilon_{zz} - \varepsilon_{xx}$.

In n-Ge, where there are four valleys at the point L, for a [111] strain with $\varepsilon_{xy} = \varepsilon_{xz} = \varepsilon_{yz} = \varepsilon'_{111}/3$ and $\varepsilon'_{111} = \varepsilon_{111} - \varepsilon_{1\bar{1}0}$,

$$\Delta E_1 = \left(\Xi_d + \frac{1}{3}\Xi_u\right)\varepsilon + \frac{2}{3}\Xi_u e'_{111},$$
$$\Delta E_2 = \Delta E_3 = \Delta E_4 = \left(\Xi_d + \frac{1}{3}\Xi_u\right)\varepsilon - \frac{2}{9}\Xi_u e'_{111}$$

(the index 1 refers to the extremum on the [111] axis).

For n-Si and n-Ge, equation (34.49) yields

$$\sigma_\parallel - \sigma_\perp = \frac{3\sigma_0}{1+2K}(1-K)\frac{n_1 - n_2}{n}, \quad \frac{\sigma_\parallel + 2\sigma_\perp}{3} = \sigma_0, \tag{34.50}$$

where σ_0 is the conductivity of the unstrained crystal, K the ratio of mobilities, $K = \mu_\perp/\mu_\parallel$; $(n_1 - n_2)/n$ is the relative variation of current carrier concentration in the first and second ellipsoids, where n is the total current carrier concentration:

$$\frac{n_1 - n_2}{n} = \frac{e^{-\Delta E/kT} - 1}{2 + e^{-\Delta E/kT}}, \quad \Delta E = \Xi_u e'_{zz} \text{ (extrema at } \Delta),$$
$$\frac{n_1 - n_2}{n} = \frac{e^{-\Delta E/kT} - 1}{3 + e^{-\Delta E/kT}}, \quad \Delta E = \frac{8}{3}\Xi_u \varepsilon_{111} \text{ (extrema at } L). \tag{34.51}$$

For small strains, when $|\Delta E/kT| \gg 1$, equations (34.50) and (34.51) imply (34.30).

In the case of large strains, when one of the groups of ellipsoids is completely "emptied," if $\Delta E/kT \gg 1$, we have $(n_1 - n_2)/n = -1/2$ for extrema at Δ, and $(n_1 - n_2)/n = -1/3$ for extrema at L. If $\Delta E/kT \gg 1$, $(n_1 - n_2)/n = 1$ in both cases, i. e., all electrons are located in the first ellipsoid. The limiting

* In n-Si there are six equivalent extrema at the point Δ, but since the valleys at $\boldsymbol{k}_0$ and $-\boldsymbol{k}_0$ are uniformly shifted under a strain we may confine ourselves to three extrema, on the $\boldsymbol{k}_z$, $\boldsymbol{k}_x$ and $\boldsymbol{k}_y$ axes, respectively.

conductivities in the case of large strains are, respectively,

$$\sigma_\parallel - \sigma_\perp = -\frac{3\sigma_0(1-K)}{2(1+2K)} \quad \left(\text{if } \frac{\Delta E}{kT} \gg 1\right),$$
$$\sigma_\parallel - \sigma_\perp = \frac{3\sigma_0(1-K)}{1+2K} \quad \left(\text{if } -\frac{\Delta E}{kT} \gg 1\right) \text{ (point } \Delta\text{);} \tag{34.52a}$$

$$\sigma_\parallel - \sigma_\perp = -\frac{\sigma_0(1-K)}{1+2K} \quad \left(\text{if } \frac{\Delta E}{kT} \gg 1\right),$$
$$\sigma_\parallel - \sigma_\perp = \frac{3\sigma_0(1-K)}{1+2K} \quad \left(\text{if } -\frac{\Delta E}{kT} \gg 1\right) \text{ (point } L\text{).} \tag{34.52b}$$

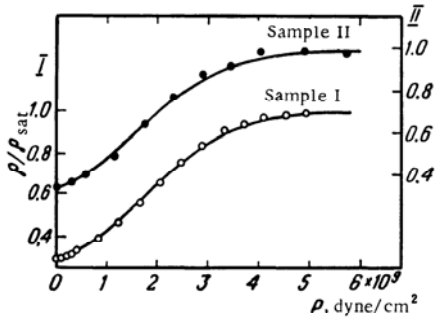

FIGURE 46. Saturation of piezoresistance in *n*-Ge under a large strain /32.9/.

Figure 46 plots resistivity in *n*-Ge for large strains at low temperatures. The curves show very clearly that for large strains, when all the electrons transfer to the lower of the split extrema, resistivity ceases to depend on strain. By (34.52), the limiting value

$$\rho_0/\rho_{sat} = (\rho_0/\rho_\parallel)_{\varepsilon\to\infty}$$

is $3/(1+2K)$. In n-Ge, $m_\parallel/m_\perp = 20$; when scattering is by lattice vibrations, $(\rho_0/\rho_\parallel)_{\varepsilon\to\infty} = 0.09$ for $\tau_\parallel/\tau_\perp = 1.24$. When scattering is due to ionized impurities, $(\rho_0/\rho_\parallel)_{\varepsilon\to\infty} = 0.3$. According to Figure 46, the experimental value of $\rho_0/\rho_\parallel$ is 0.35–0.37, pointing to the predominant role of impurity scattering under these conditions.

Effects which depend nonlinearly on the strain are more complicated in the degenerate model, for then a large strain may also cause rearrangement of the energy spectrum near the point of degeneracy.

Under strains for which the band splitting as given by (30.11) for the Γ_8 band exceeds the average current carrier energy, only carriers in the lower split-band hole contribute to the conductivity. The constant energy surfaces for the bulk of the carriers in this band will be ellipsoids. Therefore, for large strains the conductivity depends not on the magnitude of the strain but only on its direction and sign, being determined by the effective masses of the ellipsoids (given by (30.18) for the Γ_8 band) and the current carrier scattering mechanism.

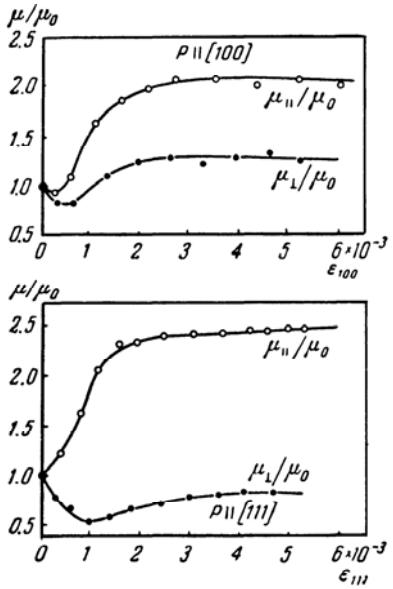

FIGURE 47. Saturation of Hall mobility in p-Ge for large [100] and [111] strains /32.4/. T = 6.19°K.

Figure 47 shows the change in the mobilities $\mu_\parallel$ and $\mu_\perp$ in p-Ge for dilation along the [100] and [111] axes under large strains, at low temperatures. According to these data, the value of $K=(\sigma_\perp/\sigma_\parallel)_{\varepsilon\to\infty}$ is 0.62 and 0.33, respectively, while according to (30.19) and (30.20) the ratio of the effective masses $m_\parallel/m_\perp$ for the lower hole band under these conditions, with $bB>0$ and $Dd>0$, should be 0.23 and 0.13, respectively. Consequently, the relaxation time anisotropy $\tau_\parallel/\tau_\perp$ is 0.4 in both cases, indicating the major role of impurity scattering.

Let us briefly consider the contribution to the piezoresistance effect due to strain-induced changes in effective mass.

According to the discussion in §29, in the case of a nondegenerate band application of a strain affects the nonzero effective mass tensor components and also gives rise to new components, equal to zero in the unstrained crystal. In a degenerate band, strain will influence the constants determining the band in the unstrained crystal (similar to the constants A, B and D for the Γ_8 band) and will also lead to the appearance of new terms of order εk^2, not present in the unstrained crystal, in the matrix $\mathcal{H}(k, \varepsilon)$. As shown in §29, the relative change in effective masses and band constants under strain is of the order of $D\varepsilon/E$, where D is the deformation potential constant and E the separation to the nearest band contributing to the relevant effective mass tensor component or band constant. Accordingly, the contribution of the change in effective masses and band constants to piezoresistance effects is of the order of D/E, i. e., usually much less than the shear piezoresistance coefficients, which are of the order of D/kT.

The elastoresistance coefficients associated with the strain-induced variation of effective masses are thus smaller and have a far weaker temperature dependence, conditioned chiefly by the change of scattering mechanisms. In the general case, the strain-induced change in effective masses contributes to all components m_{ij} of the elastoresistance tensor which differ from zero owing to specific symmetry considerations. In particular, they contribute to the valume elastoresistance coefficients.

Thus, in the general case, the piezoresistance coefficients associated with the strain-induced change in effective masses are not affected by specific features of the band structure.

However, if the semiconductor has close-lying bands, as in the case of semiconductors with a narrow bandgap in which the extrema lie at one point of the Brillouin zone (e.g., InSb), or if there are close-lying bands split by spin-orbit coupling (e.g., p-Si or crystals of the PbSe, PbTe types /34.6/), the piezoresistance constants associated with changes in effective mass may be quite large, reaching values of 10–20.

Even then, though, not all the elastoresistance coefficients will be large, but only those associated with the interaction of the close-lying bands. In certain cases, therefore, experimental data on piezoresistance effects due to changes in effective mass will yield information on the symmetry of close-lying bands /34.6/.

In conclusion, we note that corrections of the same order must be made to the large piezoresistance coefficients as well if the nonparabolic nature of the band is taken into account. Indeed, for nondegenerate statistics, the change in effective mass with energy due to the nonparabolic nature of the band is of the order of

$$\frac{\delta m^*(E)}{m^*} \sim \frac{kT}{E},$$

implying corrections to large piezoresistance effects of the order of

$$\frac{D}{kT}\frac{kT}{E} \sim \frac{D}{E}.$$

Therefore, when such corrections to large piezoresistance effects are included, we must take into account both strain-induced changes in effective masses (or in band parameters) and the nonparabolic nature of the band.

In several papers, study of piezoresistance effects is accompanied by theoretical and experimental investigations of the influence of uniaxial strain on other kinetic effects: Hall effect /32.3/, magnetoresistance /32.3, 36.1/, thermal emf /36.2, 36.3/, thermomagnetic effects /36.5, 36.6, 36.7/. These tensor effects are similar in nature to piezoresistance and are associated with carrier transfer (many-valley model) or with changes in the spectrum (degenerate model).

The change in all these kinetic coefficients under a strain is of the same order $D\varepsilon/kT$ (or $D\varepsilon/\zeta$ for a degenerate semiconductor) as the strain-induced change in conductivity.

§ 35. ABSORPTION AND REFLECTION OF LIGHT BY FREE CARRIERS IN STRAINED CRYSTALS

One of the effective methods of investigating semiconductors is to study their optical properties. The optical properties of a crystal are fully determined by its complex conductivity $\tilde{\sigma}$. The real part of $\tilde{\sigma}$ is related to the light absorption coefficient α.

In cubic crystals

$$\alpha = \frac{4\pi \operatorname{Re} \tilde{\sigma}(\omega)}{cn}, \tag{35.1}$$

where c is the velocity of light and n the refractive index. The imaginary part of $\tilde{\sigma}$ determines the contribution $\varkappa^e$ of the current carriers to the dielectric constant:

$$\varkappa^e_{ik} = -\frac{4\pi}{\omega} \operatorname{Im} \tilde{\sigma}_{ik}(\omega). \tag{35.2}$$

The dielectric constant $\varkappa(\omega)$ determines the refractive index n. If the tensor $\varkappa$ is anisotropic, n depends on the direction of light propagation; this produces the phenomonen of birefringence.

In the transparency region of the crystal, this effect makes it possible to measure the very small anisotropy of the dielectric constant: we can detect an anisotropy $\Delta\varkappa \sim \lambda\alpha$, where λ is the wavelength of the light.

In cubic crystals, the tensor is isotropic: $\varkappa_{ij} = \varkappa_0 \delta_{ij}$. Application of a strain gives rise to an anisotropic increment $\Delta\varkappa_{ij}$, which can be detected by the appearance of birefringence.

In the linear strain approximation the change in $\varkappa_{\alpha\beta}$ is determined by a fourth-rank tensor $\mathcal{P}_{\alpha\beta,\gamma\delta}$, similar to the tensor m describing the strain-induced change in static conductivity (see (34.1) and (34.2)):

$$\Delta\varkappa_{\alpha\beta} = \sum_{\gamma\delta} \mathcal{P}_{\alpha\beta,\gamma\delta} e_{\gamma\delta}. \tag{35.3}$$

It follows from the kinetic equation that

$$\tilde{\sigma}_{\alpha\beta}(\omega) = -e^2 \int \frac{\partial f_0}{\partial E} v_\alpha v_\beta \frac{\tau}{1 + i\omega\tau} dk. \tag{35.4}$$

If $\omega\tau \ll 1$, equation (35.4) reduces to (34.42), which determines the static conductivity $\sigma_{\alpha\beta}$. In the optical range $\omega\tau \gg 1$, the conductivity in a nondegenerate semiconductor is

$$\sigma^\infty_{\alpha\beta} = \frac{e^2}{kT\omega^2} \int \frac{f_0 v_\alpha v_\beta}{\tau} dk, \tag{35.5}$$

and it follows from (35.2) and (35.4) that the contribution $\varkappa^e_{\alpha\beta}$ of the free carriers to the dielectric constant is

$$\varkappa^e_{\alpha\beta} = -\frac{4\pi e^2}{\omega^2 kT} \int f_0 v_\alpha v_\beta dk. \tag{35.6}$$

Equation (35.5) is valid at relatively low frequencies ω, less than $kT/\hbar$. When $\hbar\omega > kT$, a quantum-mechanical calculation of the absorption coefficient α is necessary; the calculation should take into account processes of absorption, spontaneous and induced photon emission, and scattering by phonons at impurities.

For nondegenerate bands, equation (35.6) for the dielectric constant $\varkappa^e_{\alpha\beta}$ is valid provided $\hbar\omega/E_g \ll 1$. If $\hbar\omega$ is comparable with the band gap E_g at the extremum point k_0, we must allow for the contribution of interband virtual transitions; this necessitates quantum-mechanical corrections to $\varkappa$, of the order of $(\hbar\omega/E_g)^2$. * For degenerate bands, if $\hbar\omega \gtrsim kT$, virtual transitions between the branches of the spectrum become significant, and so we must take into account the interband components of the velocity operator. Thus, equation (35.6), like (35.5), is valid for degenerate bands provided $\hbar\omega \ll kT$.

Equations (35.5) and (35.6) show that the conductivity $\sigma^\infty_{\alpha\beta}$ depends on the shape of the energy spectrum and the nature of the current carrier relaxation, but the electronic contribution $\varkappa^e$ to the dielectric constant is determined only by their spectrum.

As in §34, we examine the strain-induced changes in σ^∞ and $\varkappa^e$ for our two models – the many-valley and degenerate models.

Many-valley model

In a many-valley semiconductor, the tensors σ^∞ and $\varkappa^e$ are the sums of the respective tensors over all the extrema. The main effect conditioning the changes in σ^∞ and $\varkappa^e$ under a strain is carrier transfer between different extrema. As mentioned in §34, the strain-induced changes in group velocity and relaxation time associated with the change in effective masses and intervalley scattering, cause extremely small changes in σ^∞ and $\varkappa^e$ under normal conditions, and we shall disregard them.

By (35.5) and (35.6), the components of σ^∞ and $\varkappa^e$ for each ellipsoid, referred to the principal axes of the ellipsoid, are defined by

$$\sigma^\infty_s = en_1\mu^\infty_s, \qquad \varkappa^e_s = -\frac{4\pi e^2 n_1}{\omega^2 m_s}, \tag{35.7}$$

where n_1 is the electron concentration in each ellipsoid, μ^∞_s and m_s the principal values of the mobility for $\omega\tau \gg 1$ and the effective mass. If we

* Thus, in the case of the simple two-band model /39.10/, when $\hbar\omega < E_g$

$$\varkappa_{qu} = \frac{\varkappa_{cl}}{1-(\hbar\omega/E_g)^2},$$

where $\varkappa_{cl}$ is defined by (35.7).

include only carrier-transfer effects, we have formulas similar to (34.24) and (34.26) for the tensor components $m^{\infty}_{\alpha\beta,\gamma\delta}$ and $\mathscr{P}_{\alpha\beta,\gamma\delta}$:

$$\begin{aligned} m^{\infty}_{\alpha\beta,\gamma\delta} &= -\frac{1}{kT}\sum_{st}\frac{\mu^{\infty}_{s}D_{t}}{\bar{\mu}^{\infty}}\left(R^{st}_{\alpha\beta,\gamma\delta}-R^{s}_{\alpha\beta}R^{t}_{\gamma\delta}\right), \\ \mathscr{P}_{\alpha\beta,\gamma\delta} &= \frac{4\pi e^{2}n}{kT\omega^{2}\bar{m}}\sum_{st}\frac{\bar{m}D_{t}}{m_{s}}\left(R^{st}_{\alpha\beta,\gamma\delta}-R^{s}_{\alpha\beta}R^{t}_{\gamma\delta}\right), \end{aligned} \tag{35.8}$$

where

$$\frac{1}{\bar{m}}=\frac{1}{3}\left(\frac{1}{m_{1}}+\frac{1}{m_{2}}+\frac{1}{m_{3}}\right),$$

$n=n_{1}N_{0}$ is the total current carrier concentration, $R^{st}_{\alpha\beta,\gamma\delta}$ and $R^{s}_{\alpha\beta}$ are coefficients which depend on the positions of the extrema in k-space, defined by (34.27).

If the constant energy surfaces near each extremum are ellipsoids of revolution, equations (35.8) reduce to a form similar to (34.29):

$$\begin{aligned} m^{\infty}_{\alpha\beta,\gamma\delta} &= -3\,\frac{1-K^{\infty}}{1+2K^{\infty}}\,\frac{\Xi_{u}}{kT}\left(R^{11}_{\alpha\beta,\gamma\delta}-R^{1}_{\alpha\beta}R^{1}_{\gamma\delta}\right), \\ K^{\infty} &= \frac{\mu^{\infty}_{\perp}}{\mu^{\infty}_{\parallel}}, \\ \mathscr{P}_{\alpha\beta,\gamma\delta} &= \frac{4\pi e^{2}n}{\omega^{2}}\,\frac{m_{\perp}-m_{\parallel}}{m_{\perp}m_{\parallel}}\,\frac{\Xi_{u}}{kT}\left(R^{11}_{\alpha\beta,\gamma\delta}-R^{1}_{\alpha\beta}R^{1}_{\gamma\delta}\right). \end{aligned} \tag{35.9}$$

For n-Si, in which the extrema are on the [100] axes,

$$\begin{aligned} \frac{m^{\infty}_{11}-m^{\infty}_{12}}{2} &= \frac{1}{2}\,\frac{1-K^{\infty}}{1+2K^{\infty}}\,\frac{\Xi_{u}}{kT}, \qquad m^{\infty}_{44}=0, \\ \frac{\mathscr{P}_{11}-\mathscr{P}_{12}}{2} &= \frac{2}{3}\,\frac{\pi e^{2}n}{\omega^{2}}\,\frac{m_{\perp}-m_{\parallel}}{m_{\perp}m_{\parallel}}\,\frac{\Xi_{u}}{kT}, \qquad \mathscr{P}_{44}=0. \end{aligned} \tag{35.10}$$

For n-Ge, in which the conduction band minima are on the [111] axes,

$$\begin{aligned} m^{\infty}_{44} &= \frac{1}{3}\,\frac{1-K^{\infty}}{1+2K^{\infty}}\,\frac{\Xi_{u}}{kT}, \qquad \frac{m^{\infty}_{11}-m^{\infty}_{12}}{2}=0, \\ \mathscr{P}_{44} &= \frac{4}{9}\,\frac{\pi e^{2}n}{\omega^{2}}\left(\frac{m_{\perp}-m_{\parallel}}{m_{\perp}m_{\parallel}}\right)\frac{\Xi_{u}}{kT}, \qquad \frac{\mathscr{P}_{11}-\mathscr{P}_{12}}{2}=0. \end{aligned} \tag{35.11}$$

Since m, m^{∞} and $\mathscr{P}$ are determined by different combinations of m^{*}_{i} and τ_{i} simultaneous measurement of these quantities makes it possible to determine the ratios of effective masses and relaxation times separately. Thus the magnitude of the components of the tensor m depends on the anisotropy of the low frequency mobility $K=\mu_{\perp}/\mu_{\parallel}$, which in the case that τ is a tensor is equal to $m_{\parallel}\tau_{\perp}/m_{\perp}\tau_{\parallel}$. The components of m^{∞} involve the ratio $K^{\infty}=\mu^{\infty}_{\perp}/\mu^{\infty}_{\parallel}=m_{\parallel}\tau_{\parallel}/m_{\perp}\tau_{\perp}$ while the magnitude of the components of the tensor $\mathscr{P}$ depends only on the effective mass anisotropy. Note that in the many-valley model the phenomenological equations (35.8)–(35.11) are valid

whatever the relationship of $\hbar\omega$ and kT, but when $\hbar\omega > kT$ the classical formula for K^∞ is no longer valid.

Degenerate model

For a degenerate band, the components of the tensors $\boldsymbol{m}^\infty$ and $\boldsymbol{\mathscr{P}}$ are calculated in the same way as the components of the tensor $\boldsymbol{m}$ in §34. If we assume, as in §34, that the relaxation time depends only on the energy and its behavior under strain is described by (34.31), then $\Delta\sigma^\infty_{\alpha\beta}/\bar{\sigma}^\infty$ is given by a formula similar to (34.36):

$$\frac{\Delta\sigma^\infty_{\alpha\beta}}{\bar{\sigma}^\infty} = \sum_i \frac{\langle 1/\tau_i\rangle}{\langle E/\tau_i\rangle}\frac{\bar{\sigma}_i}{\bar{\sigma}^\infty}\Gamma^i_{\alpha\beta}, \tag{35.12}$$

where $\Gamma^i_{\alpha\beta}$ is defined by (34.39), $\bar{\sigma}^\infty_i$ is the average mobility of a carrier of the i-th species, and $\bar{\sigma}^\infty = \sum_i \bar{\sigma}^\infty_i$. The change $\Delta\varkappa^{ei}_{\alpha\beta}$ in the dielectric constant, which depends only on the behavior of the spectrum, is given by

$$\Delta\varkappa^e_{\alpha\beta} = -\frac{8\pi e^2}{3\omega^2 kT}\sum_i \frac{n_i}{\bar{m}_i}\Gamma^i_{\alpha\beta}, \tag{35.13}$$

where

$$\frac{1}{\bar{m}_i} = \frac{\int m_i^{*1/2}(\theta,\varphi)\left(\Lambda^2_{xi}+\Lambda^2_{yi}+\Lambda^2_{zi}\right)d\Omega_k}{\int m_i^{*3/2}(\theta,\varphi)\,d\Omega_k}; \tag{35.14}$$

Λ_α and $m_i^*(\theta,\varphi)$ are defined by (34.34).

For the Γ_8 band in cubic crystals, in the spherical approximation (34.40), the components of the tensors $\boldsymbol{m}^\infty$ and $\boldsymbol{\mathscr{P}}$ are given by a formula similar to (34.41):

$$\begin{aligned}
\frac{m^\infty_{11}-m^\infty_{12}}{2} &= -\frac{9}{20}\frac{Bb}{\bar{B}}\left[\frac{\langle 1/\tau_1\rangle}{\langle E/\tau_1\rangle}\frac{\sigma^\infty_1}{(\sigma^\infty_1+\sigma^\infty_2)} - \frac{\langle 1/\tau_2\rangle\,\sigma^\infty_2}{\langle E/\tau_2\rangle(\sigma^\infty_1+\sigma^\infty_2)}\right],\\
m^\infty_{44} &= -\frac{3}{20}\frac{Dd}{\bar{B}}\left[\frac{\langle 1/\tau_1\rangle}{\langle E/\tau_1\rangle}\frac{\sigma^\infty_1}{(\sigma^\infty_1+\sigma^\infty_2)} - \frac{\langle 1/\tau_2\rangle}{\langle E/\tau_2\rangle}\frac{\sigma^\infty_2}{(\sigma^\infty_1+\sigma^\infty_2)}\right],
\end{aligned} \tag{35.15}$$

$$\begin{aligned}
\frac{\mathscr{P}_{11}-\mathscr{P}_{12}}{2} &= \frac{6}{5}\frac{\pi e^2 n}{\omega^2}\frac{m_1^{1/2}-m_2^{1/2}}{m_1^{3/2}+m_2^{3/2}}\frac{Bb}{\bar{B}kT},\\
\mathscr{P}_{44} &= \frac{2}{5}\frac{\pi e^2 n}{\omega^2}\frac{m_1^{1/2}-m_2^{1/2}}{m_1^{3/2}+m_2^{3/2}}\frac{Dd}{\bar{B}kT}.
\end{aligned} \tag{35.16}$$

The indices 1 and 2 in these formulas refer to heavy and light holes, respectively.

Expressions (35.8) – (35.16), which determine the strain-induced change in the real and imaginary parts of the dielectric constant, have been derived for a nondegenerate electron gas. If Fermi degeneracy is taken into account, as is the case for piezoresistance effects, additional factors must

be introduced. These factors are given by equations (34.46) and (34.48) for the many-valley and degenerate models, respectively. In this context, when high-frequency conductivity is being considered n must be replaced by $-n$ in (34.46) and (34.48), since the expression for high-frequency conductivity involves τ^{-1}. For the imaginary part of the dielectric constant, n must be set equal to zero.

Nonlinear effects

The equations we have derived for the change in the real and imaginary parts of the high-frequency conductivity, like the expressions (34.24) and (34.36) for the piezoresistance constants, are valid provided $\Xi_u \varepsilon / kT \ll 1$ (or $\Xi_u \varepsilon < \zeta$). For sufficiently large strains, when these conditions are no longer fulfilled, the strain-dependence of σ^∞ and $\varkappa^e$ becomes nonlinear. In the many-valley model, expressions for σ^∞ and $\varkappa^e$ may be obtained for any value of $\Xi_u \varepsilon / kT$, using an equation similar to (34.49).

Thus, for n-Si and n-Ge, $\sigma^\infty(\varepsilon)$ and $\varkappa^e(\varepsilon)$ are given by equations (34.50) with σ_0 and K replaced by σ_0^∞ and K^∞ for σ^∞, by $-4\pi e^2 n/\omega^2 \bar{m}$ and $m_\parallel/m_\perp$ for $\varkappa^e$. If the extrema lie on the [100] and [111] axes, we thus obtain for $\varkappa^e$:

$$\Delta\varkappa^e = \varkappa_\parallel^e - \varkappa_\perp^e = -\frac{4\pi e^2 n}{\omega^2}\left(\frac{1}{m_\parallel} - \frac{1}{m_\perp}\right)\left(\frac{n_1 - n_2}{n}\right), \tag{35.17}$$

where $(n_1 - n_2)/n$ is given by (34.51).

In the limiting case of large strains $|\Delta E/kT| \gg 1$, when all the electrons are concentrated at the lowest extrema, we obtain from (35.17) and (34.51):

extrema at the point Δ:

$$\begin{aligned} \Delta\varkappa^e &= \frac{2\pi e^2 n}{\omega^2}\left(\frac{1}{m_\parallel} - \frac{1}{m_\perp}\right) \quad \left(\text{if} \quad \frac{\Delta E}{kT} \gg 1\right), \\ \Delta\varkappa^e &= -\frac{4\pi e^2 n}{\omega^2}\left(\frac{1}{m_\parallel} - \frac{1}{m_\perp}\right) \quad \left(\text{if} \quad -\frac{\Delta E}{kT} \gg 1\right); \end{aligned} \tag{35.18}$$

extrema at the point L

$$\begin{aligned} \Delta\varkappa^e &= \frac{4}{3}\frac{\pi e^2 n}{\omega^2}\left(\frac{1}{m_\parallel} - \frac{1}{m_\perp}\right) \quad \left(\text{if} \quad \frac{\Delta E}{kT} \gg 1\right), \\ \Delta\varkappa^e &= -\frac{4\pi e^2 n}{\omega^2}\left(\frac{1}{m_\parallel} - \frac{1}{m_\perp}\right) \quad \left(\text{if} \quad -\frac{\Delta E}{kT} \gg 1\right). \end{aligned} \tag{35.19}$$

Formulas (35.18) and (35.19) are also valid in the case of Fermi degeneracy provided $\Delta E/\zeta \gg 1$.

In the degenerate model the nonlinear effects are more complicated. Here we shall consider the nonlinear effects for degenerate bands if the type of the valence band in Ge and Si. We restrict ourselves to the effect of a strain on the dielectric constant, since this effect is independent of the scattering mechanisms and therefore yields direct information about the band structure.

In principle, equation (35.6) and the general expression (30.5) for $E(\boldsymbol{k}, \varepsilon)$ in the strained crystal provide the means for finding the function $\varkappa^\varepsilon(\varepsilon)$,

whatever the magnitude of the strain. However, this calculation may be carried out only by numerical methods. We therefore restrict ourselves to a discussion of two limiting cases in which explicit expressions may be derived for the function $\varkappa^e(\varepsilon)$: small strains $\Delta_\varepsilon/kT \ll 1$, for which we shall find corrections to $\varkappa^e$ of second order in Δ_ε/kT, and large strains $|\Delta_\varepsilon/kT| \gg 1$. In the latter case we shall determine the limiting values for [100] and [111] strains as $|\Delta_\varepsilon/kT| \to \infty$, together with corrections of the order of kT/Δ_ε. Here $\Delta_\varepsilon = \delta E_{1,2}$ is the band splitting at $k = 0$ (see (30.11)).

Quadratic effects. It follows from equation (35.6) that in order to calculate effects which are quadratic in the strain we must introduce both quadratic ε corrections to the energy, $\Delta E^{(2)}(\varepsilon)$, and squares of the linear ε correction $\Delta E(k, \varepsilon)$, which is determined by relation (30.34). In addition, we must allow for the change $\Delta\zeta$ in the chemical potential, which is quadratic in the strain. The correction $\Delta\varkappa^{(2)}_{\alpha\beta}$ quadratic in the strain is thus

$$\Delta\varkappa^{(2)}_{\alpha\beta} = -\frac{4\pi e^2}{\omega^2 kT}\Big\{\int f_0\Big[\frac{1}{2}\Big(\frac{\Delta E}{kT}\Big)^2 v_\alpha v_\beta - \Big(\frac{\Delta E}{kT}\Big)(v_\alpha \Delta v_\beta + v_\beta \Delta v_\alpha) + \Delta v_\alpha \Delta v_\beta\Big]\,dk + \int f_0\Big(-\frac{\Delta E^{(2)}}{kT} v_\alpha v_\beta + \Delta v^{(2)}_\beta v_\alpha + \Delta v^{(2)}_\alpha v_\beta\Big)\,dk + \frac{\Delta\zeta}{kT}\int f_0 v_\alpha v_\beta\,dk\Big\}, \tag{35.20}$$

where

$$\Delta v^{(2)}_\alpha = \frac{1}{\hbar}\frac{\partial \Delta E^{(2)}}{\partial k_\alpha}.$$

By (30.5),

$$\Delta E^{(2)} = \pm\Big(\frac{1}{2}\frac{\mathscr{E}_\varepsilon}{\sqrt{\mathscr{E}_k}} - \frac{1}{8}\frac{\mathscr{E}^2_{\varepsilon k}}{\mathscr{E}^{3/2}_k}\Big). \tag{35.21}$$

Noting that

$$\Delta E\,\Delta v_\alpha = \frac{1}{2\hbar}\frac{\partial}{\partial k_\alpha}(\Delta E)^2,$$

we integrate (35.20) by parts and bring the result to the form

$$\Delta\varkappa^{(2)}_{\alpha\beta} = -\frac{4\pi e^2}{\omega^2 kT}\Big\{-\frac{1}{2(kT)^2}\int f_0 (\Delta E)^2 v_\alpha v_\beta\,dk + \frac{1}{\hbar^2 kT}\int (\Delta E)^2 \frac{\partial^2 E}{\partial k_\alpha \partial k_\beta} f_0\,dk + \int f_0 \Delta v_\alpha \Delta v_\beta\,dk + \frac{1}{kT}\int f_0 \Delta E^{(2)} v_\alpha v_\beta\,dk - \frac{2}{\hbar^2}\int f_0 \Delta E^{(2)} \frac{\partial^2 E}{\partial k_\alpha \partial k_\beta}\,dk + \frac{\Delta\zeta}{kT}\int f_0 v_\alpha v_\beta\,dk\Big\}. \tag{35.22}$$

To calculate $\Delta\varkappa^{(2)}_{\alpha\beta}$, we shall proceed as in the case of the linear corrections, using the spherical approximation (34.40). In this case $\frac{\partial^2 E}{\partial k_\alpha \partial k_\beta} \sim \delta_{\alpha\beta}$, and therefore the corresponding terms in (35.22) do not result in anisotropy

of $\Delta\varkappa_{\alpha\beta}^{(2)}$. The first term of $\Delta E^{(2)}$ (35.21) and the term proportional to $\Delta\zeta/kT$ in (35.22) always give an isotropic contribution to $\Delta\varkappa_{\alpha\beta}^2$, and so we may disregard them when calculating anisotropic effects.

Since $\Delta E_1 = -\Delta E_2$, the $(\Delta E)^2$ terms bring in contributions of the same sign to the anisotropic component from both light and heavy holes, while the contributions from the $\Delta E^{(2)}$ terms have opposite signs.

For a [001] strain,

$$\mathscr{E}_e = b^2\varepsilon_{zz}'^2, \quad \mathscr{E}_{ek} = Bb\left(3k_z^2 - k^2\right)\varepsilon_{zz}',$$

and in this case

$$\Delta\varkappa_{\parallel}^{(2)} - \Delta\varkappa_{\perp}^{(2)} = \Delta\varkappa_{zz}^{(2)} - \Delta\varkappa_{xx}^{(2)} =$$

$$= -\frac{48}{35}\frac{\pi e^2 n}{\omega^2\left(m_1^{3/2} + m_2^{3/2}\right)}\left(\frac{bB\varepsilon_{zz}'}{\bar{B}kT}\right)^2\left\{m_1^{1/2} + m_2^{1/2} + \frac{\hbar^2}{12\bar{B}}\left(\frac{1}{m_1^{1/2}} - \frac{1}{m_2^{1/2}}\right)\right\}. \qquad (35.23)$$

By (34.40), in the spherical approximation,

$$\frac{\hbar^2}{\bar{B}} = \frac{4m_1m_2}{m_1 - m_2}.$$

By (35.16) and (35.23), for small strains the anisotropic component of the dielectric constant $\Delta\varkappa = \Delta\varkappa_{\parallel} - \Delta\varkappa_{\perp}$, counting linear and quadratic terms, may be written

$$\Delta\varkappa = \Delta\varkappa_{\parallel} - \Delta\varkappa_{\perp} = \frac{12}{5}\frac{\pi e^2 n}{\omega^2}\left(\frac{Bb\varepsilon_{zz}'}{\bar{B}kT}\right)\left(\frac{m_1^{1/2} - m_2^{1/2}}{m_1^{3/2} + m_2^{3/2}}\right)\left\{1 - \frac{4}{7}\frac{m_1 + m_2 + \frac{5}{3}m_1^{1/2}m_2^{1/2}}{m_1 - m_2}\left(\frac{Bb\varepsilon_{zz}'}{\bar{B}kT}\right)\right\}. \qquad (35.24)$$

In (35.23) and (35.24) m_1 and m_2 are the effective masses of the heavy and light holes respectively.

Under a [111] strain, by (30.14) and (30.37),

$$\mathscr{E}_e = \frac{1}{3}d^2\varepsilon_{z'z'}'^2, \quad \mathscr{E}_{ek} = \frac{1}{3}Dd\left(3k_{z'}^2 - k^2\right)\varepsilon_{z'z'}',$$

where the z'-axis lies along [111]. Therefore, the expression for $\Delta\varkappa$ in the case of a [111] strain differs from (35.24) in the substitution of

$Bb\varepsilon_{zz}'$ for $\frac{1}{3}Dd\varepsilon_{z'z'}'$.

Large strains. In the limiting case of large strains $\Delta_\varepsilon/kT \gg 1$ the constant energy surfaces are ellipsoids (see §30). Therefore, the tensor $\varkappa_{\alpha\beta}^e$ referred to the principal axes of the ellipsoid, for $\Delta_\varepsilon/kT \to \infty$, is given by equation (35.7):

$$\varkappa_s^e = -\frac{4\pi e^2 n}{\omega^2}\frac{1}{m_s}. \qquad (35.25)$$

The effective masses m_s depend on the strain direction and are given by (30.18). To calculate the corrections to $\varkappa^e$ of the order of kT/Δ_ε, we must include in the expansion (30.21) of $E(\boldsymbol{k}, \varepsilon)$ terms δE of the order of $k^4/\sqrt{\mathscr{E}_e}$

which describe the nonparabolic nature of the bands under the strain. By (35.6), the contribution to $\varkappa_s$ from these terms is

$$\delta\varkappa_s = -\frac{4\pi e^2}{\omega^2 kT}\left\{-\int f_0\left(\frac{\delta E-\Delta\zeta}{kT}\right)v_s^2\,dk + 2\int f_0 v_s\,\Delta v_s\,dk\right\}. \tag{35.26}$$

If the carrier concentration $n = \int f_0\,dk$ is independent of the strain, the change in chemical potential is

$$\Delta\zeta = \frac{1}{n}\int f_0\,\delta E\,dk.$$

Integrating the second term in (35.26) by parts and using the fact that for an ellipsoidal constant energy surface

$$\int f_0 v_s^2\,dk = (n/m_s)kT,$$

we obtain

$$\delta\varkappa_s = -\frac{4\pi e^2}{kT\omega^2}\left\{\int f_0 v_s^2\,\frac{\delta E}{kT}\,dk - \frac{1}{m_s}\int f_0\,\delta E\,dk\right\}. \tag{35.27}$$

By (30.21) and (30.5), for a [100] strain, we have for the lower hole band:

$$\delta E = -\frac{1}{8|be'_{zz}|}\left\{3B^2\left(k_x^4+k_y^4\right)+2\left(2D^2-3B^2\right)k_x^2k_y^2+4D^2\left(k_x^2k_z^2+k_y^2k_z^2\right)\right\}. \tag{35.28}$$

Calculation of $\delta\varkappa_s$ for δE as given by (35.28) reduces to evaluation of integrals of the type

$$I^{\alpha\beta\gamma} = \int f_0 k_x^\alpha k_y^\beta k_z^\gamma\,dk =$$
$$= n m_1^{\alpha/2} m_2^{\beta/2} m_3^{\gamma/3}\left(\frac{2kT}{\hbar^2}\right)^{(\alpha+\beta+\gamma)/2}\frac{\Gamma\left(\frac{\alpha+1}{2}\right)\Gamma\left(\frac{\beta+1}{2}\right)\Gamma\left(\frac{\gamma+1}{2}\right)}{\Gamma^3(1/2)}, \tag{35.29}$$

where $\Gamma(z)$ is the gamma-function. The calculation gives

$$\begin{aligned}\delta\varkappa_\parallel &= \frac{8\pi e^2 n m_\perp}{\omega^2\hbar^4}\,\frac{kTD^2}{|be'_{zz}|},\\ \delta\varkappa_\perp &= \frac{4\pi e^2 n}{\omega^2\hbar^4}\,\frac{kT}{|be'_{zz}|}\left\{\left(D^2+3B^2\right)m_\perp + D^2 m_\parallel\right\}.\end{aligned} \tag{35.30}$$

Hence, in view of (35.25) and (30.19), if $|be'_{zz}| > kT$, the anisotropic part of the dielectric constant $\varkappa_\parallel^e - \varkappa_\perp^e$ is

$$\Delta\varkappa^e = \varkappa_\parallel^e - \varkappa_\perp^e = \frac{6\pi e^2 n}{\omega^2 m}\,\gamma|B_0|\left\{1+\frac{kT}{6mbB_0e'_{zz}}\left[m_\perp\left(D_0^2-3B_0^2\right)-D_0^2m_\parallel\right]\right\}, \tag{35.31}$$

where

$$\gamma = \frac{Bb\varepsilon'_{zz}}{|Bb\varepsilon'_{zz}|},$$

and B_0, D_0 are dimensionless coefficients:

$$B = \frac{\hbar^2}{2m} B_0, \quad D = \frac{\hbar^2}{2m} D_0.$$

Under a [111] strain, the constant energy surfaces are ellipsoids of revolution, the axis of revolution being [111]. Referred to the coordinate system (30.20a) for the principal axes of the ellipsoid, the z-axis lying along [111], the δE for a [111] strain is

$$\delta E = \frac{-\sqrt{3}}{8|d\varepsilon'_{z'z'}|}\left\{(k_x^2+k_y^2)^2\left(B^2+\frac{2}{3}D^2\right)+4k_z^2(k_x^2+k_y^2)\left(2B^2+\frac{D^2}{3}\right)-\right.$$
$$\left.-4\sqrt{2}\,k_xk_y\left(k_x^2-\frac{1}{3}k_y^2\right)(D^2-3B^2)\right\}. \qquad (35.32)$$

Note that the last term in (35.32), which depends on the choice of the k_x and k_y axes, does not contribute to $\delta\varkappa$, since it contains odd powers of k. The calculation yields

$$\delta\varkappa_\parallel = \frac{8\sqrt{3}\,\pi e^2 n}{\omega^2|d\varepsilon'_{zz}|}\,m_\perp\frac{kT}{\hbar^4}\left(2B^2+\frac{D^2}{3}\right),$$
$$\delta\varkappa_\perp = \frac{4\pi e^2 n\sqrt{3}}{|d\varepsilon'_{zz}|\omega^2}\frac{kT}{\hbar^4}\left\{2m_\perp\left(B^2+\frac{2}{3}D^2\right)+m_\parallel\left(2B^2+\frac{D^2}{3}\right)\right\}. \qquad (35.33)$$

whence, in view of (30.20), we obtain the following equation for the anisotropic part $\varkappa^e_\parallel - \varkappa^e_\perp$ of the dielectric constant under a [111] strain:

$$\Delta\varkappa^e = \varkappa^e_\parallel - \varkappa^e_\perp =$$
$$= \frac{2\sqrt{3}\pi e^2 n|D_0|\gamma}{\omega^2 m_0}\left\{1-\frac{kT}{2m_0D_0\,d\varepsilon'_{z'z'}}\left[m_\parallel\left(2B_0^2+\frac{D_0^2}{3}\right)+2m_\perp\left(\frac{D_0^2}{3}-B_0^2\right)\right]\right\}, \qquad (35.34)$$

where $\gamma = \frac{D\,d\varepsilon'_{zz}}{|D\,d\varepsilon'_{zz}|}$.

It is noteworthy that the calculation of $\varkappa^e$ for large strains does not assume that the band in the unstrained crystal is spherical. In the spherical approximation $D = \sqrt{3}B$, equations (35.32) and (35.34) yield the same value for $\Delta\varkappa^e$ for the same band splitting:

$$\Delta_\varepsilon = 2b\varepsilon'_{zz} = \frac{2d}{\sqrt{3}}\varepsilon'_{z'z'}.$$

In semiconductors with small spin-orbit splitting Δ (e.g., p-Si), we must introduce a correction to $\varkappa^e$ of the order of $\Delta_\varepsilon/\Delta$. For large strains, this contribution is due to the changes in effective mass, given by (30.24), (30.30)–(30.32a). When these corrections are taken into account, the expression

for $\Delta\varkappa^e$ when $\Delta_g \gg kT, \zeta$ is:

for [100] strains, $be'_{zz} > 0$

$$\Delta\varkappa^e = \varkappa^e_{\parallel} - \varkappa^e_{\perp} = \frac{6\pi e^2 n \mid B_0 \mid \gamma}{\omega^2 m}\left(1 + \frac{4}{\Delta} be'_{zz}\right); \tag{35.35}$$

for [111] strains, $de'_{111} > 0$

$$\Delta\varkappa^e = \varkappa^e_{\parallel} - \varkappa^e_{\perp} = \frac{6\pi e^2 n \mid D_0 \mid \gamma}{\omega^2 m \sqrt{3}}\left(1 + \frac{4}{\sqrt{3}} \frac{de_{111}}{\Delta}\right). \tag{35.36}$$

If $be'_{zz} < 0$ or $de'_{111} < 0$ there are no corrections linear in ε.

The effect of strain on light absorption and birefringence has been studied most thoroughly in n-Ge and n-Si. When analyzing the experimental data, one must remember that these effects may be caused not only by free electrons but also by the lattice, by impurities, and by interband transitions of electrons.

Since by (35.5) the absorption coefficient for free electrons, α^e, is proportional to λ^2, it may be determined by subtracting the limiting value $\alpha(\lambda \to 0)$ (found by extrapolating the straight line $\alpha = f(\lambda^2)$ to zero) from the experimental value of $\alpha(\lambda)$.

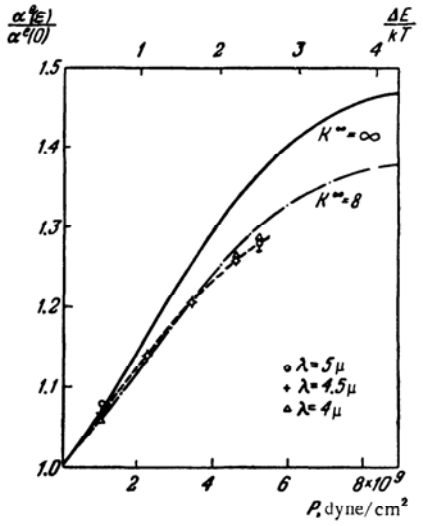

FIGURE 48. Light absorption by free electrons in strained Ge /37.1/. Solid curve: theoretical.

Figure 48 illustrates the behavior of $\alpha^e(\varepsilon)/\alpha^e(0)$ for n-Ge compressed along the [111] direction, with the light propagating in the same direction. By (34.50), under such conditions

$$\frac{\alpha^e(\varepsilon)}{\alpha^e(0)} = \frac{\sigma_\perp}{\sigma_0} = 1 - \frac{1 - K^\infty}{1 + 2K^\infty} \frac{n_1 - n_2}{n}. \tag{35.37}$$

Theoretical $\alpha^e(\varepsilon)/\alpha^e(0)$ curves based on this equation for $\Xi_u = 18$ ev, $K^\infty = 8$ and $K^\infty = \infty$ are shown in the same figure. The $K^\infty = 8$ curve gives the best fit to the experimental curve. Since $m_\parallel/m_\perp = 20$ for n-Ge, this value of K^∞ gives $\tau_\parallel^\infty/\tau_\perp^\infty = 0.4$, whereas the ratio of low-frequency relaxation times $\tau_\parallel/\tau_\perp$ is 1.24 for scattering due to lattice vibrations and 4.5 for impurity scattering. The reason for this discrepancy is apparently that at the light frequencies ω used in /37.1/ the condition $\hbar\omega < \zeta$ for applicability of the classical theory is not fulfilled.

As noted above, measurement of piezo-absorption does not yield the deformation potential constants directly, and here measurement of strain-induced birefringence is more convenient. Based on such measurements, we can directly determine the tensor of piezo-optical constants $\boldsymbol{Q}$, which relates the change in the dielectric constant $\Delta\varkappa$ to the applied stress:

$$\Delta\varkappa_{\alpha\beta} = \frac{\lambda n_0}{\pi} \sum_{\gamma\delta} Q_{\alpha\beta\gamma\delta} P_{\gamma\delta} \tag{35.38}$$

or

$$\Delta\varkappa = \frac{\lambda n_0}{\pi} \boldsymbol{QP}. \tag{35.39}$$

Here λ is the wavelength of light in vacuum, $n_0 = \varkappa_0^{1/2}$ the refractive index of the unstrained crystal.

The tensor $\boldsymbol{Q}$ is related to the tensor $\boldsymbol{\mathcal{P}}$ of (35.3), whose components may be called the elasto-optical constants, by an equation similar to (34.10):

$$\boldsymbol{\mathcal{P}} = \frac{\lambda n_0}{\pi} \boldsymbol{QC},$$

where $\boldsymbol{C}$ is the matrix of elastic constants.

As in §34, we introduce a two-index notation for the tensors $\boldsymbol{\mathcal{P}}$ and $\boldsymbol{Q}$, denoting

$$\varkappa_{xx} = \varkappa_1, \quad \varkappa_{xy} = \varkappa_6, \quad \ldots, \quad \mathcal{P}_{xxxx} = \mathcal{P}_{11}, \quad \mathcal{P}_{xy,\,xy} = \mathcal{P}_{66}, \quad \ldots,$$
$$Q_{xxxx} = Q_{11}, \quad 2Q_{xy,\,xy} = Q_{66}, \quad \ldots,$$

and then the above relation yields, for cubic crystals, formulas similar to (34.11):

$$\begin{aligned} \frac{\mathcal{P}_{11} + 2\mathcal{P}_{12}}{3} &= \frac{\lambda n_0}{\pi} \frac{Q_{11} + 2Q_{12}}{3} (C_{11} + 2C_{12}), \\ \frac{\mathcal{P}_{11} - \mathcal{P}_{12}}{2} &= \frac{\lambda n_0}{\pi} \frac{Q_{11} - Q_{12}}{2} (C_{11} - C_{12}), \\ \mathcal{P}_{44} &= \frac{\lambda n_0}{\pi} Q_{44} C_{44}. \end{aligned} \tag{35.40}$$

The tensor $\boldsymbol{Q}$ is usually determined by the phase shift between two beams of light polarized parallel and perpendicular to the strain. In cubic

crystals strained along [100], this phase shift, relative to the length d of the sample, is

$$\Delta\varphi/d = (Q_{11} - Q_{12}) P_{100}. \tag{35.41}$$

Similarly, for a [111] strain,

$$\Delta\varphi/d = Q_{44} P_{111}. \tag{35.42}$$

The following method is usually used to measure the phase shift $\Delta\varphi$. Light, linearly polarized at 45° to the strain direction, is focused on the sample. An analyzer at the output passes plane polarized light rotated through 90° with respect to the polarization plane at the incident beam. The output intensity is then a function of the phase shift:

$$I = I_0 \sin^2(\Delta\varphi/2), \tag{35.43}$$

where I_0 is the intensity of the incident beam.

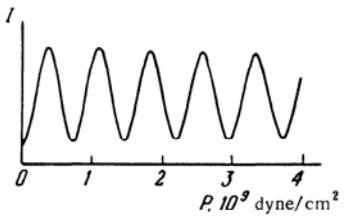

FIGURE 49. Light modulation in strained Ge due to change in dielectric constant /38.3/. I is the intensity in arbitrary units. $P \parallel [111]$, $T = 4.2°K$, $\lambda = 2.1\ \mu$.

Figure 49 is a plot of the intensity of the radiation emerging from the n-Ge sample as a function of stress.

The contribution $\varkappa^e$ to $\Delta\varkappa$ due to the free carriers is usually comparable with the contribution $\varkappa^{ib}$ due to interband transitions. The latter can be determined independently by measurements on pure samples. However, a high impurity concentration may somewhat alter the probabilities of interband transitions. Thus, the interband contribution is more reliably detected by measurements under large strains, when $\varkappa^e$ reaches saturation.

Figures 50 and 51 illustrate the behavior of $\frac{\Delta\varphi^e}{\lambda\, dn}$ as a function of the stress P, obtained in this way at different wavelengths n and different carrier concentrations n. It is clear that, as predicted by the theory, $\Delta\varphi^e$ is proportional to the impurity concentration and increases linearly with increasing λ.

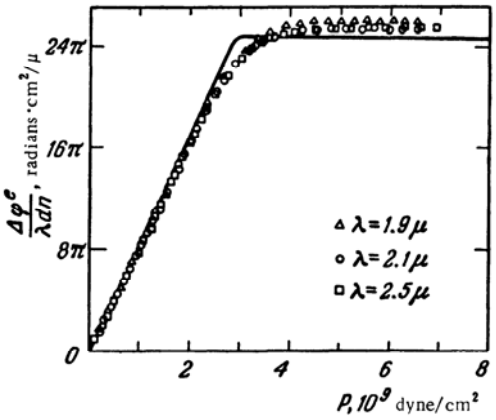

FIGURE 50. Birefringence in n-Ge vs. stress at different wavelengths /38.3/. $n = 3.12 \cdot 10^{8}$ cm^{-3} (As). $T = 1.4$°K. $P \parallel [111]$.

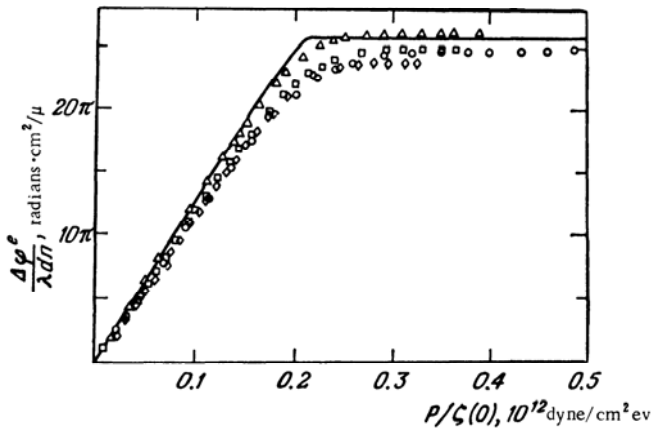

FIGURE 51. Birefringence in n-Ge at different impurity concentrations /38.3/. $\zeta(0)$ is the Fermi energy at $P = 0$. Circles — $n = 1.24 \cdot 10^{18}$ cm^{-3} (As), squares — $n = 3.67 \cdot 10^{18}$ cm^{-3} (As), diamonds — $7.14 \cdot 10^{18}$ cm^{-3} (As), triangles — $n = 4.66 \cdot 10^{18}$ cm^{-3} (Sb).

To determine the deformation potential constants from these data, we need a sufficiently accurate value of the carrier concentration. This concentration may be determined from the value of Δx^{∞}. In the case of Ge and Si, for which effective masses are readily available, this method is more accurate than Hall effect measurements. Here the deformation potential constants are most conveniently determined from a stress value P_0 corresponding to the intersection of a straight line, extending the initial

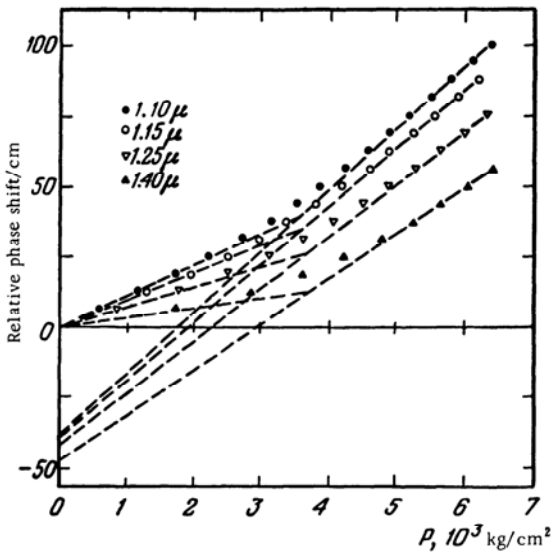

FIGURE 52. Birefringence coefficient in *n*-Si (ρ = 0.01 ohm·cm) vs. stress /38.4/. $P \parallel [100]$, T = 77°K.

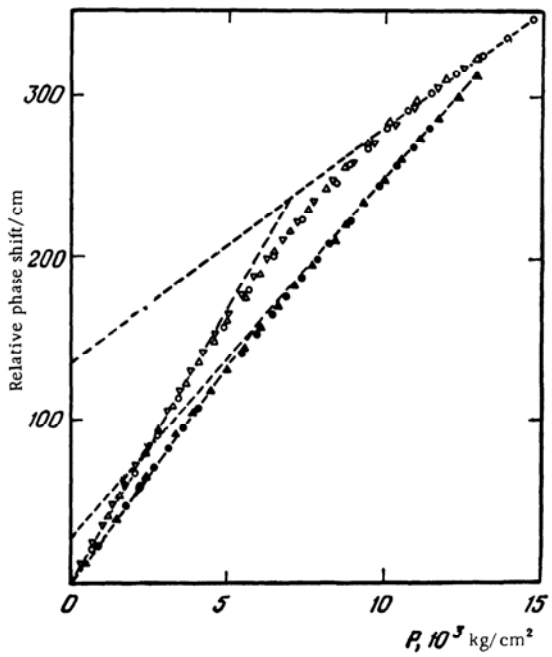

FIGURE 53. Birefringence coefficient in *p*-Si (ρ = 0.006 ohm·cm) vs. stress /38.4/. $P \parallel [111]$, T = 77°K, λ = 1.15 μ.

linear part of the curve, and the straight line corresponding to saturation of the electronic part $\varkappa^e$ (Figures 52 and 53).

By (35.10), (35.11), and (35.31), the condition for these lines to intersect, for n-Si compressed along [100], is

$$-\frac{3kT}{(S_{11}-S_{12})P_0\Xi_u}\frac{F_{1/2}}{F_{-1/2}}=1. \tag{35.44}$$

For n-Ge compressed along [111],

$$-\frac{9kT}{S_{44}P_0\Xi_u}\frac{F_{1/2}}{F_{-1/2}}=1. \tag{35.45}$$

Knowing P_0, we can determine Ξ_u from (35.44) and (35.45). In this method the concentration is needed only to determine the value of ζ in the unstrained crystal, which enters into the integrals $F_{1/2}$ and $F_{-1/2}$. The method is convenient in that there is no need for direct inclusion of the interband contribution, since the position of the point P_0 is independent of whether there is such a contribution linear in the strain.

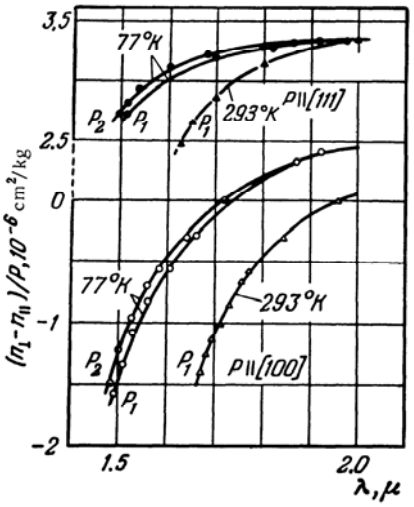

FIGURE 54. Elasto-optical constants in Ge /39.4/ vs. light wavelength.

P_1 = 3,000 kg/cm², P_2 = 6,000 kg/cm².

The resulting values of the deformation potential constants are: germanium $\Xi_u = 18.0 \pm 0.5$ ev, silicon $\Xi_u = 8.5 \pm 0.4$ ev.

Strain-induced birefringence has also been observed in p-Ge and p-Si /38.4/, /39.4/. As figure 53 shows, in this case too there is an initial segment, determined by free carriers and interband transitions, and a linear

segment corresponding to large ε, which in this case may be caused not only by interband transitions but also by the change in $\varkappa^e$ due to comparatively large effective mass changes. This contribution is determined by equation (35.35) or (35.36). By (35.35) and (35.36), the ratio of the $\varkappa^e_{(\varepsilon\to\infty)}$ values for [111] and [100] strains is $D/\sqrt{3}B$.

Because of the large anisotropy of the band constants and the small spin-orbit splitting, when calculating the initial segment and the nonlinear region for Si we must take into account the nonspherical and nonparabolic nature of the bands.

§36. ABSORPTION AND REFLECTION OF LIGHT IN INTERBAND TRANSITIONS IN STRAINED CRYSTALS

As mentioned in §35, the optical properties of a substance are completely determined by the complex conductivity tensor $\tilde{\sigma}$, or by two real tensors: the conductivity tensor $\sigma = \mathrm{Re}\,\tilde{\sigma}$ and the dielectric constant tensor $\varkappa = -(4\pi/\omega)\,\mathrm{Im}\,\tilde{\sigma}$. The contribution to these tensors from interband transitions (and transitions between local levels), allowing for spatial dispersion, is given by /39.1./*

$$\sigma^{\mathrm{ib}}_{\alpha\beta}(\omega, q) = -\frac{\pi}{\hbar\omega\mathscr{V}}\sum_{m,\, n\neq m} F^0_m \{j^\alpha_{mn}(-q)\, j^\beta_{nm}(q)\,\delta(\omega-\omega_{mn}) - \\ - j^\alpha_{nm}(-q)\, j^\beta_{mn}(q)\,\delta(\omega+\omega_{mn})\}, \tag{36.1a}$$

$$\varkappa^{\mathrm{ib}}_{\alpha\beta}(\omega, q) = \frac{4\pi}{\hbar\omega^2\mathscr{V}}\,\mathscr{P}\sum_{m,\, n\neq m} F^0_m \left\{\frac{j^\alpha_{mn}(-q)\, j^\beta_{nm}(q)}{\omega-\omega_{mn}} - \right. \\ \left. - \frac{j^\alpha_{nm}(-q)\, j^\beta_{mn}(q)}{\omega+\omega_{mn}} + \frac{j^\alpha_{mn}(0)\, j^\beta_{nm}(0) + j^\alpha_{nm}(0)\, j^\beta_{mn}(0)}{\omega_{mn}}\right\}. \tag{36.1b}$$

The summation extends over all quantum states m and n. For Bloch electrons, these indices include the band number, the spin states and the set of wave numbers k. F^0_m denotes the distribution function

$$F^0_m = \left(e^{(-\zeta+E_m)/kT}+1\right)^{-1},$$

ω is the frequency of the light, q its wave vector, $\hbar\omega_{mn} = E_m - E_n$; $\mathscr{P}$ denotes the principal value of the integral.

When the spin-orbit coupling is included, the current operator j has the form**

$$j(q) = \frac{e}{2m}(\pi e^{-iqx} + e^{-iqx}\pi) - \frac{e^2}{cm}\mathscr{A}, \quad j(0) = \frac{e\pi}{m} - \frac{e^2}{cm}\mathscr{A}, \tag{36.2}$$

* $\tilde{\sigma}(\omega, q)$ is defined as the ratio of the total current $j(\omega, q)$ including the magnetization current $j = \mathrm{rot}\, M$, to the field of the electromagnetic wave $\mathscr{E} = \sqrt{\mu/\varkappa}\,H$. Equations (36.1) therefore fail at $\omega = 0$, where $\tilde{\sigma}$ and the magnetic susceptibility $\mu = 1 + 4\pi M/cH$ must be introduced separately /39.1/.

** To allow for spatial dispersion, we must include the contribution of quadrupole and the magnetic dipole transitions to σ and $\varkappa$. These effects may usually be neglected for interband transitions, since even if dipole transitions at the extremum point k_0 are forbidden, they become allowed when higher order terms in $k = K - k_0$ are included.

where, by (17.15),

$$\pi = p + \frac{\hbar}{4mc^2}[\sigma \nabla V].$$

In the multiband model, in which the energy operator is $\mathcal{H}_{m'm}(k)$ (22.27), the current operator matrix in the same representation is

$$j_{m'k',\,mk}(0) = ev_{m'k',\,mk} = \frac{e}{\hbar}\nabla_k \mathcal{H}_{m'm}(k)\,\delta_{kk'}, \tag{36.3}$$

i. e., by (22.27),

$$j^{\alpha}_{m'k,\,mk} = \frac{e\pi^{\alpha}_{m'm}}{m} + \frac{e\hbar}{2m^2}\sum_{s\beta} k_{\beta}\left(\pi^{\alpha}_{m's}\pi^{\beta}_{sm} + \pi^{\beta}_{m's}\pi^{\alpha}_{sm}\right)\left(\frac{1}{E_m - E_s} + \frac{1}{E_{m'} - E_s}\right). \tag{36.3a}$$

As mentioned in §22, this equation is valid at frequencies $\hbar\omega$ which are small compared with the separations to the bands not included in $\mathcal{H}(k)$, since the derivatives $\partial S/\partial t$ were neglected in its derivation. We may thus use the equation for degenerate bands provided $\hbar\omega \ll E_g$, and for the multiband model if $\hbar\omega$ is much smaller than the separation to other bands E_s, i. e., $\hbar\omega \ll E_m - E_s, E_{m'} - E_s$. Since $\hbar\omega \gtrsim E_g$ in interband transitions, this means equation (36.3) is applicable if $E_m - E_s \gg E_g$ when $E_m - E_s \approx E_{m'} - E_s$. If this condition is not fulfilled, we must replace (36.3a) by the exact expression, which may be derived from the general equation (15.51) by the substitution $\mathcal{H}' = \hbar k\pi/m$:

$$j^{\alpha}_{m'k,\,mk} = \frac{e\pi^{\alpha}_{m'm}}{m} + \frac{e\hbar}{m^2}\sum_{s\beta} k_{\beta}\left(\frac{\pi^{\alpha}_{m's}\pi^{\beta}_{sm}}{E_m - E_s} + \frac{\pi^{\beta}_{m's}\pi^{\alpha}_{sm}}{E_{m'} - E_s}\right). \tag{36.3b}$$

The first terms in (36.3a) and (36.3b) are obviously identical, but the second terms coincide only if $E_g \ll E_s - E_m$. Equation (36.3b) is applicable at frequencies for which $|\hbar\omega - E_g| \ll |E_g - E_m|$. By (26.34) and (26.35), in the simplest case, the two-band spherical model,

$$j^{\alpha} = es\rho_y\sigma_{\alpha} + \frac{e\hbar}{m^*}\theta\rho_x(\sigma_{\alpha+1}k_{\alpha+2} + \sigma_{\alpha+2}k_{\alpha+1}), \tag{36.4}$$

where $\theta = A_1 m^*/\hbar^2$ is a dimensionless constant. Similarly, for the two-band ellipsoidal model

$$j^{\alpha} = es_{\alpha}\rho_y\sigma_{\alpha} + \frac{e\hbar}{m^*}\rho_x(\theta_{\alpha+1}\sigma_{\alpha+1}k_{\alpha+2} + \theta_{\alpha+2}\sigma_{\alpha+2}k_{\alpha+1}). \tag{36.5}$$

For biaxial ellipsoids, two of the constants s_{α} and θ_{α} coincide (for example, when $m^*_{xx} = m^*_{yy}$ we have $s_x = s_y$ and $\theta_x = \theta_y$).

If the corresponding little group contains inversion, one of the constants s or θ vanishes, depending on the parity of the representations corresponding to the two bands. In the absence of inversion, as in crystals of class T_d, both constants may be nonzero.

When calculating the effect of strain on optical phenomena, we must bear in mind that strain-induced changes in σ and $\varkappa$ may result both from changes in the spectrum and from changes in the matrix elements of the current operator $\boldsymbol{j}$ or the velocity $\boldsymbol{v}$.

Nondegenerate bands

For nondegenerate bands near the absorption edge, i. e., when $|\hbar\omega - E_g| \ll E_g$, the major factor is the shift of the bottom of the bands; the change in the matrix elements and the change in the effective masses may both be neglected. Only when the selection rules dictate that a dipole transition at an extremum point is forbidden in the unstrained crystal but allowed in the strained crystal (due to reduction of symmetry) must we include the strain-induced change in the matrix element.

If $|\hbar\omega - E_g|$ is much less than E_g and the separation to other bands, in calculating σ and $\varkappa$ we may disregard the nonparabolic nature of the bands and the contribution of all the other bands to $\varkappa$.

If transitions occur between two nondegenerate bands whose extrema lie at the same point of $\boldsymbol{k}$-space and for which the principal axes of the ellipsoids coincide, the components σ^i_{ss} and $\varkappa_{ss}$ for each of the extrema, referred to its principal axes, are determined according to (36.1) and (36.2) by

$$\sigma^i_{ss} = \frac{e^2(\tilde{m}_1\tilde{m}_2\tilde{m}_3)^{1/2}}{4\pi m^2\hbar^3\omega} P_s \times \begin{cases} (\hbar\omega - E_g)^{1/2} & \text{if} \quad \hbar\omega > E_g, \\ 0 & \text{if} \quad \hbar\omega < E_g; \end{cases} \tag{36.6}$$

$$\varkappa^i_{ss} = \frac{e^2(\tilde{m}_1\tilde{m}_2\tilde{m}_3)^{1/2}}{\hbar^3\omega^2 m^2} P_s \left[2E_g^{1/2} - (\hbar\omega + E_g)^{1/2} - \begin{cases} 0 & \text{if} \quad \hbar\omega > E_g \\ (E_g - \hbar\omega)^{1/2} & \text{if} \quad \hbar\omega < E_g \end{cases} \right], \tag{36.7}$$

where

$$\frac{2}{\tilde{m}_i} = \frac{1}{m_{ci}} + \frac{1}{m_{vi}}, \quad P_s = \sum_{\alpha_c, \alpha_v} |p_{s\alpha_c\alpha_v}|^2.$$

Here α_v and α_c denote the sets of spin states of the valence and conduction bands, respectively. The valence band is assumed to be completely filled and the conduction band empty. The strain-induced change in σ^i_{ss} and $\varkappa^i_{ss}$ is determined by the change in the band gap E_g at $\boldsymbol{k}_0$: by (29.28),

$$\delta E^i_g = \sum_t E_{1t} e_{tt}, \tag{36.8}$$

where e_{tt} are the components of the strain tensor referred to the principal axes of the extremum, $E_{1t} = D_{tc} - D_{tv}$, and accordingly

$$\delta\sigma^i_{ss} = -\frac{1}{2}\sigma^i_{ss}\frac{\delta E^i_g}{(\hbar\omega - E_g)^{1/2}}. \tag{36.9}$$

As in (34.1), (35.3) we introduce tensors $m^{ib}_{\alpha\beta\gamma\delta}$ and $\mathscr{P}^{ib}_{\alpha\beta\gamma\delta}$ which determine the change in σ^{ib} and $\varkappa^{ib}$ under strain:

$$\frac{\delta\sigma^{ib}_{\alpha\beta}}{\sigma^{ib}_0}=\sum_{\gamma\delta} m^{ib}_{\alpha\beta\gamma\delta}\,e_{\gamma\delta},\quad \delta\varkappa_{\alpha\beta}=\sum_{\gamma\delta}\mathscr{P}^{ib}_{\alpha\beta\gamma\delta}\,e_{\gamma\delta}, \tag{36.10}$$

where

$$\sigma^{ib}_0=\frac{1}{3}N_0\,\mathrm{Tr}\,\sigma^{l}_{ss}=\frac{N_0 e^2(\bar m_1\bar m_2\bar m_3)^{1/2}}{4\pi m^2\hbar^3\omega}(\hbar\omega-E_g)^{1/2}\,\bar P, \tag{36.11}$$

N_0 is the number of extrema, $\bar P=\frac{1}{3}\sum_s P_s$. The components $m^{ib}_{\alpha\beta\gamma\delta}$ and $\mathscr{P}^{ib}_{\alpha\beta\gamma\delta}$ are determined by expressions similar to (35.9). However, as opposed to (35.9), there is no analog of the second term in (35.9), which is associated with the condition that the free carrier concentration is constant. In this case, then, not only the shear coefficients but also the volume coefficients will differ from zero. The general expressions for $m^{ib}_{\alpha\beta\gamma\delta}$ and $\mathscr{P}^{ib}_{\alpha\beta\gamma\delta}$ are

$$m^{ib}_{\alpha\beta\gamma\delta}=-\frac{1}{2(\hbar\omega-E_g)}\sum_{st}E_{1t}\frac{P_s}{\bar P}R^{st}_{\alpha\beta\gamma\delta}, \tag{36.12}$$

$$\mathscr{P}^{ib}_{\alpha\beta\gamma\delta}=-\frac{e^2(\bar m_1\bar m_2\bar m_3)^{1/2}}{2\hbar^3\omega^2m^2(E_g-\hbar\omega)^{1/2}}\sum_{st}E_{1t}P_sR^{st}_{\alpha\beta\gamma\delta}. \tag{36.13}$$

For cubic crystals, the volume coefficients are

$$\frac{m^{ib}_{11}+2m^{ib}_{12}}{3}=-\frac{E_{1g}}{2(\hbar\omega-E_g)}\qquad(\hbar\omega>E_g) \tag{36.14}$$

$$\frac{\mathscr{P}^{ib}_{11}+2\mathscr{P}^{ib}_{12}}{3}=-N_0\frac{e^2(\bar m_1\bar m_2\bar m_3)^{1/2}\bar P}{2\hbar^3\omega^2m^2}\frac{E_{1g}}{(E_g-\hbar\omega)^{1/2}}\qquad(\hbar\omega<E_g), \tag{36.15}$$

where

$$E_{1g}=\frac{1}{3}\sum_t E_{1t}.$$

If the extremum is at $k=0$, the shear coefficients vanish in this approximation, for they depend only on the changes in the effective masses and matrix elements and are smaller by a factor $\left|\frac{\hbar\omega-E_g}{E_g}\right|$ than the volume coefficients.

The shear coefficients for crystals in which the extrema are at the point L (111) (such as PbS, PbSe, PbTe) are given by expressions similar to (34.30):

$$m^{ib}_{11}-m^{ib}_{12}=0,\quad m^{ib}_{44}=-\frac{1}{6}\frac{P_\parallel-P_\perp}{P_\parallel+2P_\perp}\frac{\Xi^c_u-\Xi^v_u}{(\hbar\omega-E_g)}, \tag{36.16}$$

$$\mathscr{P}^{ib}_{11}-\mathscr{P}^{ib}_{12}=0,\ \mathscr{P}^{ib}_{44}=-\frac{1}{18}\frac{e^2(\bar m_\parallel\bar m_\perp^2)^{1/2}}{\hbar^3\omega^2m^2}\frac{P_\parallel-P_\perp}{(E_g-\hbar\omega)^{1/2}}(\Xi^c_u-\Xi^v_u). \tag{36.17}$$

Similarly, for nondegenerate bands with extrema at the point $X(100)$,

$$m_{44}^{ib}=0,\quad \frac{m_{11}^{ib}-m_{12}^{ib}}{2}=-\frac{1}{4}\frac{P_\parallel-P_\perp}{P_\parallel+2P_\perp}\frac{\Xi_u^c-\Xi_u^v}{(\hbar\omega-E_g)}, \tag{36.18}$$

$$\mathcal{P}_{44}^{ib}=0,\quad \frac{\mathcal{P}_{11}^{ib}-\mathcal{P}_{12}^{ib}}{2}=-\frac{1}{12}\frac{e^2(\bar{m}_\parallel\bar{m}_\perp^2)^{1/2}}{\hbar^3\omega^2m^2}\frac{P_\parallel-P_\perp}{(E_g-\hbar\omega)^{1/2}}(\Xi_u^c-\Xi_u^v). \tag{36.19}$$

If the selection rules forbid dipole transitions at an extremum point for all polarizations, and the probability of these transitions is proportional to k^2, the conductivity σ_s is of the order of $(\hbar\omega-E_g)^{3/2}$. In this case the strain-induced change $\delta\sigma$, like $\delta\varkappa$, has no singularities as $\hbar\omega\to E_g$, and

$$m_{\alpha\beta\gamma\delta}^{ib}=-\frac{3}{2}\frac{1}{\hbar\omega-E_g}\sum_{st}E_{1t}\frac{\sigma_{ss}}{\bar{\sigma}_{ss}}R_{\alpha\beta\gamma\delta}^{st},\ \text{where}\ \bar{\sigma}_{ss}=\frac{1}{3}\sum_s\sigma_{ss}. \tag{36.20}$$

If an extremum in a cubic crystal is at the point $\boldsymbol{k}=0$ and the bands are not degenerate, then, as noted above, the shear coefficients are determined by comparatively small changes in the effective masses and in the matrix elements that determine the transition probability. But if the band is degenerate at $\boldsymbol{k}=0$ the shear effects will also be large.

Degenerate bands

As an example, let us consider the band structure characteristic for most crystals of groups III–V and for Ge: the valence band at Γ is fourfold degenerate counting spin and corresponds to the representation Γ_8 (or $\Gamma_8^\pm$); the conduction band at Γ is degenerate only counting spin and corresponds to the representations Γ_6 or Γ_7 (or $\Gamma_6^\mp$ and $\Gamma_7^\mp$). The two-band Hamiltonian $\mathcal{H}(\boldsymbol{k},\varepsilon)$ for these bands is given in Table 24.2* (p. 238).

In this case, therefore, the interband matrix elements of the velocity operator (relative to the basis $Y_{1/2}^{1/2}$, $Y_{-1/2}^{1/2}$ and $Y_{3/2}^{3/2}$, $Y_{1/2}^{3/2}$, $Y_{-1/2}^{3/2}$, $Y_{-3/2}^{3/2}$) are

$$\begin{aligned}
v_x&=\frac{\partial\mathcal{H}^{ib}}{\partial p_x}=\frac{s}{2}\begin{Vmatrix}0&-1&0&-\sqrt{3}\\ i\sqrt{3}&0&i&0\end{Vmatrix},\\
v_y&=\frac{\partial\mathcal{H}^{ib}}{\partial p_y}=\frac{s}{2}\begin{Vmatrix}0&-i&0&i\sqrt{3}\\ -\sqrt{3}&0&1&0\end{Vmatrix},\\
v_z&=\frac{\partial\mathcal{H}^{ib}}{\partial p_z}=\frac{s}{2}\begin{Vmatrix}0&0&2i&0\\ 0&2&0&0\end{Vmatrix},
\end{aligned} \tag{36.21}$$

where

$$s=\sqrt{\frac{2}{3}}\left\langle Y_0^0\left|\frac{p_z}{m}\right|Y_0^1\right\rangle.$$

* If $|\hbar\omega-E_g|$ is greater than or comparable with the spin-orbit splitting Δ_{SO}, we must allow both for transitions from the split-off band and for the nonparabolic nature of the valence band. In this case (36.21) must be replaced by the complete Hamiltonian for all three bands, determined from Table 24.2.

In the Kane approximation, in which only the interaction of the two nearest bands is considered, $2m_n^* s^2 = E_g$, where m_n^* is the effective mass of the electrons and the light holes. By (24.6) and (24.34), in this approximation

$$A = B = \frac{D}{\sqrt{3}} = -\frac{\hbar^2}{2m_n^*}. \tag{36.22}$$

To calculate σ and $\varkappa$ from equations (36.1a) and (32.1b), we must go over to the representation (24.19) in which the intraband matrix (30.3), (24.13) is diagonal. Next, we sum the product $v^{\alpha}_{mn} v^{\beta}_{nm}$ over both states of the conduction band n and the two states of the valence band m corresponding to light and heavy holes with energy $E_l(\varepsilon, k)$ $(l = 1, 2)$. As a result we find the values of $\Theta^l_{\alpha\beta} = \sum_{mn} v^{\alpha}_{mn} v^{\beta}_{nm}$: if $\alpha = \beta$

$$\Theta^l_{\alpha\alpha} = \frac{s^2}{E_l - E_{l'}} \{2E_l - (L+M)k^2 + (L-M)k_\alpha^2 - (l+m)\varepsilon + (l-m)\varepsilon_{\alpha\alpha}\}, \tag{36.23a}$$

and if $\alpha \neq \beta$

$$\Theta^l_{\alpha\beta} = \frac{3s^2}{E_l - E_{l'}} (Nk_\alpha k_\beta + n\varepsilon_{\alpha\beta}). \tag{36.23b}$$

Here $l \neq l'$. It follows from equation (36.23) that, in the notation of (24.12) and (30.8),

$$\frac{1}{3}\mathrm{Tr}\,\Theta^l = \frac{1}{3}\sum_{\alpha} \Theta^l_{\alpha\alpha} = s^2, \tag{36.24a}$$

$$\Theta^l_{\alpha\alpha} - \Theta^l_{\beta\beta} = \frac{3s^2}{E_l - E_{l'}} [B(k_\alpha^2 - k_\beta^2) + b(\varepsilon_{\alpha\alpha} - \varepsilon_{\beta\beta})], \tag{36.24b}$$

$$\Theta^l_{\alpha\beta} = \frac{\sqrt{3}\, s^2}{E_l - E_{l'}} (Dk_\alpha k_\beta + d\varepsilon_{\alpha\beta}). \tag{36.24c}$$

Substituting (36.24a) into (36.1), we find that in the unstrained crystal

$$\sigma_0^{\mathrm{ib}} = \frac{e^2 s^2}{4\pi\omega\hbar^3} (\hbar\omega - E_g)^{1/2} (\tilde{m}_1^{3/2} + \tilde{m}_2^{3/2}), \tag{36.25}$$

$$\varkappa_0^{\mathrm{ib}} = \frac{e^2 s^2 (\tilde{m}_1^{3/2} + \tilde{m}_2^{3/2})}{\hbar^3\omega^2} \times \begin{cases} 2E_g^{1/2} - (E_g + \hbar\omega)^{1/2} & \text{if} \quad \hbar\omega > E_g, \\ 2E_g^{1/2} - (E_g + \hbar\omega)^{1/2} - (E_g - \hbar\omega)^{1/2} & \text{if} \quad \hbar\omega < E_g, \end{cases} \tag{36.26}$$

where

$$\tilde{m}^r_{1,2} = \frac{1}{4\pi} \int d\Omega\, \tilde{m}^r_{1,2}(\vartheta, \varphi), \tag{36.27a}$$

$$\frac{2}{\tilde{m}_{2,1}(\vartheta, \varphi)} = \frac{1}{m} + \frac{2}{\hbar^2} (|A| \pm \bar{B}(\vartheta, \varphi)), \tag{36.27b}$$

$$\bar{B}(\vartheta, \varphi) = \left(B^2 + C^2 \frac{k_x^2 k_y^2 + k_x^2 k_z^2 + k_y^2 k_z^2}{k^4} \right)^{1/2}. \tag{36.27c}$$

The change in σ^{ib} and $\varkappa^{ib}$ under an isotropic strain depends only on the change in the band gap: in this case we must replace E_g by $E_g + E_{1g}\varepsilon$ in equations (36.25) and (36.26). Substituting (36.24b, c) into (36.1), we obtain the shear constants m^{ib} and $\mathscr{P}^{ib}$, which describe the change in σ^{ib} and $\varkappa^{ib}$ under an anisotropic strain in the linear ε approximation:

$$m_{11}^{ib} - m_{12}^{ib} = \frac{\sigma_{xx}^{ib} - \sigma_{yy}^{ib}}{\sigma_0^{ib}\varepsilon'_{xx}} = \frac{3}{2}\frac{b}{\hbar\omega - E_g}\frac{\Phi_1}{\bar{m}_1^{3/2} + \bar{m}_2^{3/2}} \quad (\text{if} \quad \hbar\omega > E_g), \tag{36.28}$$

$$m_{44}^{ib} = \frac{\sigma_{xy}^{ib}}{2\sigma_0^{ib}\varepsilon_{xy}} = \frac{\sqrt{3}}{4}\frac{d}{\hbar\omega - E_g}\frac{\Phi_2}{\bar{m}_1^{3/2} + \bar{m}_2^{3/2}}, \tag{36.29}$$

$$\mathscr{P}_{11}^{ib} - \mathscr{P}_{12}^{ib} = \frac{\varkappa_{xx}^{ib} - \varkappa_{yy}^{ib}}{\varepsilon'_{xx}} = \frac{3}{2}\frac{e^2s^2b}{\hbar^3\omega^2(\hbar\omega - E_g)^{1/2}}\Phi_1, \tag{36.30}$$

$$\mathscr{P}_{44}^{ib} = \frac{\varkappa_{xy}^{ib}}{2\varepsilon_{xy}} = \frac{\sqrt{3}}{4}\frac{e^2s^2d}{\hbar^3\omega^2(\hbar\omega - E_g)^{1/2}}\Phi_2, \tag{36.31}$$

where

$$\begin{aligned}
\Phi_1 = \frac{\hbar^2}{4\pi}\Bigg\{\int d\Omega\Bigg[&\frac{\bar{m}_1^{1/2}(\vartheta,\varphi) - \bar{m}_2^{1/2}(\vartheta,\varphi)}{\bar{B}(\vartheta,\varphi)} + \\
&+ \frac{3}{2}\frac{B^2k_x^2(k_x^2 - k_y^2)}{\bar{B}^3(\vartheta,\varphi)k^4}\left(\bar{m}_2^{1/2}(\vartheta,\varphi) - \bar{m}_1^{1/2}(\vartheta,\varphi)\right) + \\
&+ \frac{3}{4}\frac{B^2k_x^2(k_x^2 - k_y^2)}{\hbar^2\bar{B}^2(\vartheta,\varphi)k^4}\left(\bar{m}_2^{3/2}(\vartheta,\varphi) + \bar{m}_1^{3/2}(\vartheta,\varphi)\right)\Bigg]\Bigg\}, \\
\Phi_2 = \frac{\hbar^2}{4\pi}\Bigg\{\int d\Omega\Bigg[&\frac{\bar{m}_1^{1/2}(\vartheta,\varphi) - \bar{m}_2^{1/2}(\vartheta,\varphi)}{\bar{B}(\vartheta,\varphi)} + \\
&+ \frac{D^2k_x^2k_y^2}{\bar{B}^3(\vartheta,\varphi)k^4}\left(\bar{m}_2^{1/2}(\vartheta,\varphi) - \bar{m}_1^{1/2}(\vartheta,\varphi)\right) + \\
&+ \frac{1}{2}\frac{D^2k_x^2k_y^2}{\hbar^2\bar{B}^2(\vartheta,\varphi)k^4}\left(\bar{m}_2^{3/2}(\vartheta,\varphi) + \bar{m}_1^{3/2}(\vartheta,\varphi)\right)\Bigg]\Bigg\}.
\end{aligned} \tag{36.32}$$

In the spherical approximation, in which $\bar{B}(\vartheta, \varphi)$ is replaced by the constant

$$\bar{B} = \left[\frac{1}{5}(2B^2 + 3D^2)\right]^{1/2} = \frac{\hbar^2(\bar{m}_1 - \bar{m}_2)}{4\bar{m}_1\bar{m}_2},$$

which is independent of the angles, the effective masses $\bar{m}_1$ and $\bar{m}_2$ are also independent of the angles and the constants Φ_1 and Φ_2 are:

$$\begin{aligned}
\Phi_1 &= \frac{2\bar{m}_1\bar{m}_2}{\bar{m}_2^{1/2} + \bar{m}_1^{1/2}}\left(1 - \frac{1}{5}\frac{B^2}{\bar{B}^2}\right) + \frac{1}{10}\frac{B^2}{\bar{B}^2}\left(\bar{m}_1^{3/2} + \bar{m}_2^{3/2}\right), \\
\Phi_2 &= \frac{2\bar{m}_1\bar{m}_2}{\bar{m}_2^{1/2} + \bar{m}_1^{1/2}}\left(1 - \frac{1}{15}\frac{D^2}{\bar{B}^2}\right) + \frac{1}{30}\frac{D^2}{\bar{B}^2}\left(\bar{m}_1^{3/2} + \bar{m}_2^{3/2}\right).
\end{aligned} \tag{36.33}$$

In the Kane approximation, $\bar{m}_1 = 2m_c$, $\bar{m}_2 = m_c$, $B = D/\sqrt{3} = \bar{B}$, we have

$$\Phi_1 = \Phi_2 = 1.7m_c^{3/2}, \quad m_{11}^{ib} - m_{12}^{ib} = \frac{2\sqrt{3}b}{d}m_{44}^{ib} = \frac{0.67b}{\hbar\omega - E_g}.$$

The above equations are valid at frequencies for which $|\hbar\omega - E_g|$ significantly exceeds the strain-induced band splitting.* On the other hand, $|\hbar\omega - E_g|$ must be much less than E_g and Δ_{so}.

For sufficiently large strains, near the band edge when $|\hbar\omega - E_g| < \Delta_s$, the opposite approximation (large strains) is valid. In this case we see from (36.24b, c) that for the upper of the split-off p-bands, under a strain e_{xx},

$$\Theta_{xx} - \Theta_{yy} = \frac{3}{2} s^2 \gamma, \text{ where } \gamma = \frac{be_{xx}}{|be_{xx}|}; \tag{36.34}$$

under a strain e_{xy}

$$\Theta_{xy} = \frac{\sqrt{3}}{2} s^2 \gamma, \text{ where } \gamma = \frac{de_{xy}}{|de_{xy}|} \tag{36.35}$$

Substituting these values into (36.1), we find that for a strain e_{xx}

$$\sigma_{xx} - \sigma_{yy} = \frac{3e^2 (\bar{m}_\parallel \bar{m}_\perp^2)^{1/3} s^2}{8\pi\omega\hbar^3} \gamma (\hbar\omega - E_g(\varepsilon))^{1/2}, \tag{36.36a}$$

and for a strain e_{xy}

$$\sigma_{xy} = \frac{\sqrt{3} e^2 (\bar{m}_\parallel \bar{m}_\perp^2)^{1/3} s^2}{2\pi\omega\hbar^3} \gamma (\hbar\omega - E_g(\varepsilon))^{1/2}. \tag{36.36b}$$

Similarly, when $\Delta_e > E_g - \hbar\omega > 0$, for a strain e_{xx},

$$\varkappa_{xx}^{ib} - \varkappa_{yy}^{ib} = \frac{3}{2} \frac{e^2 (\bar{m}_\parallel \bar{m}_\perp^2)^{1/2} s^2 \gamma}{\hbar^3 \omega^2} \{2E_g^{1/2}(\varepsilon) - (\hbar\omega + E_g(\varepsilon))^{1/2} - (E_g(\varepsilon) - \hbar\omega)^{1/2}\}, \tag{36.37a}$$

and for a strain e_{xy},

$$\varkappa_{xy}^{ib} = \frac{\sqrt{3} e^2 (\bar{m}_\parallel \bar{m}_\perp^2)^{1/2} s^2 \gamma}{2\hbar^3 \omega^2} \{2E_g^{1/2}(\varepsilon) - (\hbar\omega + E_g(\varepsilon))^{1/2} - (E_g(\varepsilon) - \hbar\omega)^{1/2}\}. \tag{36.37b}$$

Here

$$\frac{2}{\bar{m}_t} = \frac{1}{m_{ct}} + \frac{1}{m_{vt}}.$$

The effective masses of the holes near the band edge, which depend on the sign of $bB\varepsilon$ or $dD\varepsilon$, were given in §30 (equations (30.18) – (30.20)), and $E_g(\varepsilon)$ is the band gap including its change under a strain: $E_g(\varepsilon) = E_g^0 + E_{1g}\varepsilon - \mathscr{E}_\varepsilon^{1/2}$.

It is evident from our equations that the sign of the effect of both small and large strains depends only on the sign of the constants b and d (and on the sign of the strain), as opposed to the effects associated with free carriers, whose sign depends on the sign of the product $bB\varepsilon$ or $dD\varepsilon$.

* The difference $|\hbar\omega - E_g|$ must also exceed the exciton binding energy, since the interaction of an electron-hole pair excited by light was neglected in the derivation of these equations. The effect of strains on the exciton spectrum will be discussed in the following chapter.

Chapter VII

EFFECT OF STRAIN ON IMPURITY CENTERS AND EXCITONS

§37. SPECTRUM OF IMPURITY CENTERS IN A STRAINED CRYSTAL

We saw in §27 that in the effective mass approximation the energy levels and wave functions of a shallow impurity center are given by an equation (27.1) whose form depends on the band structure at the extremum point. Under a strain, the band structure changes, causing a change in the energy and wave functions of the ground state and excited states of the impurity center. In this section we consider the strain-induced change in the states of a shallow impurity center for various band structures: nondegenerate bands, many-valley bands and bands which are degenerate at an extremum point.

Nondegenerate bands

In a nondegenerate band, a strain induces a shift ΔE of the band edge and a change in effective masses. Thus the equation (27.1) for a shallow impurity center will include terms of the order of εk^2 describing the change in the effective masses of the band carriers.

The band edge shift ΔE results only in a corresponding energy shift for all the impurity states, and thus does not affect the ionization energy, which is measured from the band edge. The change in ionization energy E_i in this case is due only to the strain-induced change in the effective masses; it is of the order of $\delta E_i/E_i \sim \Delta m^*/m^* \sim D\varepsilon/E_g$. Under an anisotropic strain, when the change in effective masses is anisotropic, the degeneracies of excited states may be removed. The splitting of a degenerate level with energy E_n, caused by the change in effective mass, is also of the order of $E_n D\varepsilon/E_g$.

The nature of the splitting may be determined in the usual manner from symmetry considerations.

Many-valley bands

Let us consider a band with several extrema, at each of which the band is nondegenerate. As shown in §27, in the effective mass approximation

the ground state of the impurity center is n-fold degenerate, where n is the number of extrema, and the wave functions are arbitrary combinations of the impurity center functions $\Psi_l = \psi_{k_l} f^l$ corresponding to the states near the l-th extremum. Here ψ_{k_l} is the Bloch function at the l-th extremum, and $f^l(x)$ is a smooth function (the envelope function) satisfying equation (27.1).

If we neglect the overlapping (in k-space) of wave functions belonging to different extrema, a homogeneous strain will not cause mixing of states belonging to different extrema but will merely shift the energy of the state at each extremum by a quantity δE_l, which is equal to the band shift ΔE_l at the extremum if the effective mass changes under the strain are neglected. Since different extrema are generally shifted by different amounts under a strain, the strain removes the many-valley degeneracy of the impurity center ground state to the same degree that it removes the degeneracy of the bottom of the band.

As an example, let us consider donor levels in Si and Ge. In the effective mass approximation, the shallow donor center ground state in Si is sixfold degenerate. Under a strain along the z-axis, $e'_{zz} \neq 0$, the impurity center levels corresponding to extrema on the k_z axis are shifted by $\Delta E_3 = \frac{2}{3} \Xi_u e'_{zz}$, while for extrema on the k_x and k_y axes they are shifted by $\Delta E_2 = -\frac{1}{3} \Xi_u e'_{zz}$. Thus the sixfold degenerate state splits into fourfold and twofold degenerate states separated by $\Xi_u e'_{zz}$, which is just the strain-induced splitting of the conduction band bottom.

In n-Ge, where the ground state of the impurity center is fourfold degenerate, the impurity center state corresponding to an extremum on the [111] axis is shifted under a [111] strain by $\Delta E_1 = \frac{2}{3} \Xi_u e'_{111}$, and the remaining three states are shifted by $\Delta E_2 = \Delta E_3 = \Delta E_4 = -\frac{2}{9} \Xi_u e'_{111}$,* i.e., the ground state splits into onefold and threefold degenerate states with splitting $\frac{8}{9} \Xi_u e'_{111}$. This splitting of an impurity state in a many-valley band occurs only in the effective mass approximation, which ignores the splitting of the impurity state in the unstrained crystal due to the departure from effective mass theory. As noted in §27, it is these corrections that cause the removal of many-valley degeneracy characteristic of effective mass theory.

If these corrections are small compared to the ionization energy, the wave functions may be derived from group-theoretic considerations as linear combinations of the impurity center functions corresponding to each valley. The correct linear combinations of functions for shallow donors in Ge and Si were indicated in §27 (equations (27.20), (27.22)).

To determine the ground state energy and the wave functions of an impurity center in the strained crystal we must diagonalize the perturbation matrix, which is made up of the strain and the corrections to effective mass theory for all states which are degenerate in the effective mass approximation. Relative to the basis of correct functions, incorporating the corrections to effective mass theory, the strain matrix is no longer diagonal. If the strain splitting of the bottom of the band is small compared to the

* From now on we omit the term $\left(\Xi_d + \frac{1}{3} \Xi_u\right) \mathrm{Tr}\, \varepsilon$ describing the uniform shift of all the impurity levels.

chemical shift, we can consider the strain splitting of each degenerate level separately.

If we take as basis the functions Ψ_l, so that the strain matrix is diagonal, the chemical shift matrix has off-diagonal matrix elements. Thus, for n-Ge the perturbation matrix relative to the basis Ψ_l is, by (27.22),*

$$\begin{Vmatrix} \Delta E_1 - \Delta/4 & -\Delta/4 & -\Delta/4 & -\Delta/4 \\ -\Delta/4 & \Delta E_2 - \Delta/4 & -\Delta/4 & -\Delta/4 \\ -\Delta/4 & -\Delta/4 & \Delta E_3 - \Delta/4 & -\Delta/4 \\ -\Delta/4 & -\Delta/4 & -\Delta/4 & \Delta E_4 - \Delta/4 \end{Vmatrix}, \tag{37.1}$$

where $\Delta E_l(\mathbf{e})$ ($l = 1, 2, 3, 4$) is the band shift at the l-th extremum and Δ is the splitting between the triplet and singlet states in the unstrained crystal; the zero of energy is taken to be the triplet energy in the unstrained crystal. By (37.1), the energy E in the strained crystal is determined by the equation

$$\begin{aligned} &(\Delta E_1 - E)(\Delta E_2 - E)(\Delta E_3 - E)(\Delta E_4 - E) - \\ &-\frac{\Delta}{4}\{(\Delta E_1 - E)(\Delta E_2 - E)(\Delta E_3 - E) + (\Delta E_1 - E)(\Delta E_2 - E)(\Delta E_4 - E) + \\ &+ (\Delta E_1 - E)(\Delta E_3 - E)(\Delta E_4 - E) + (\Delta E_2 - E)(\Delta E_3 - E)(\Delta E_4 - E)\} = 0. \end{aligned} \tag{37.2}$$

For a [111] strain,

$$\Delta E_1 = \frac{2}{3}\Xi_u e'_{111}, \quad \Delta E_2 = \Delta E_3 = \Delta E_4 = -\frac{2}{9}\Xi_u e'_{111},$$

and from equation (37.2) we obtain

$$E_3 = E_4 = -\frac{2}{9}\Xi_u e'_{111} = -\frac{\Delta}{4}x, \tag{37.3}$$

$$E_{1,2} = \frac{\Delta}{2}\left\{-1 + \frac{x}{2} \mp \sqrt{1 + x^2 + x}\right\}, \tag{37.4}$$

where

$$x = \frac{8}{9}\frac{\Xi_u e'_{111}}{\Delta}.$$

Figure 55 plots the energy of an impurity center in n-Ge as a function of x for different signs of the strain.

It follows from (37.4) that a strain induces splitting of a degenerate state, but the degeneracy is not completely removed.

If $e'_{111} = 0$, the terms E_2, E_3, E_4 coincide, corresponding to a threefold degenerate state, while $E_1 = -\Delta$ corresponds to the singlet state of the impurity center. Under small strains, with $\left|\frac{8}{9}\Xi_u e'_{111}\right| \ll \Delta$,

$$E_1 = -\Delta, \quad E_2 = \frac{4}{9}\Xi_u e'_{111}. \tag{37.5}$$

* Owing to the deviation from effective mass theory there is another diagonal increment which shifts all the levels by Λ; this correction is neglected here.

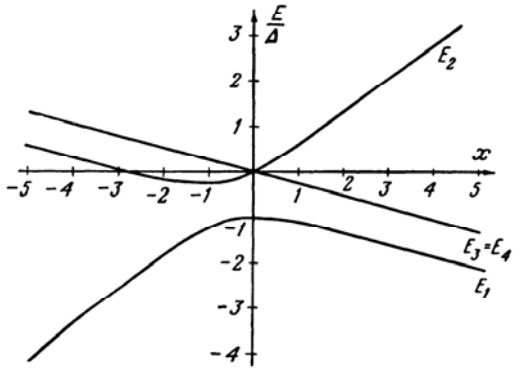

FIGURE 55. Strain splitting of donor ground state in Ge.

Under large strains, when the induced splitting exceeds the chemical shift, $\left|\frac{8}{9}\Xi_u\varepsilon'_{111}\right| \gg \Delta$ or $|x| \gg 1$,

$$E_{1,2} = -\frac{\Delta}{4}(2 \pm \gamma) + \frac{2}{9}\Xi_u\frac{\varepsilon'_{111}}{3}(1 \mp 2\gamma), \tag{37.6}$$

where

$$\gamma = \frac{x}{|x|} = \frac{\Xi_u\varepsilon'_{111}}{|\Xi_u\varepsilon'_{111}|}.$$

If $\gamma = 1$

$$E_1 = -\frac{3}{4}\Delta - \frac{2\Xi_u\varepsilon'_{111}}{9}, \quad E_2 = -\frac{\Delta}{4} + \frac{2}{3}\Xi_u\varepsilon'_{111}; \tag{37.7a}$$

if $\gamma = -1$

$$E_1 = -\frac{\Delta}{4} + \frac{2}{3}\Xi_u\varepsilon'_{111}, \quad E_2 = -\frac{3}{4}\Delta - \frac{2}{9}\Xi_u\varepsilon'_{111}. \tag{37.7b}$$

Using the matrix (37.1), we easily find the wave functions corresponding to the eigenvalues E_l; they are determined by the coefficients of the expansion in terms of the impurity center functions near each extremum.

For degenerate states with energy $E_3 = E_4$ the two wave functions may be taken as

$$\Psi_3 = \frac{1}{\sqrt{2}}(010\bar{1}), \quad \Psi_4 = \frac{1}{\sqrt{6}}(01\bar{2}1)$$

or any linear combination of these functions. It is sometimes convenient to take the functions

$$\Psi'_3 = \frac{1}{\sqrt{2}}(\Psi_3 - i\Psi_4), \quad \Psi'_4 = \frac{1}{\sqrt{2}}(\Psi_3 + i\Psi_4),$$

which are multiplied by $e^{\pm 2\pi i/3}$ when rotated about the [111] axis through $2\pi/3$.

For states with energies E_1 and E_2 the wave functions are

$$\Psi_1 = \frac{1}{\sqrt{3+\alpha^2}}(\alpha 111), \quad \Psi_2 = \frac{1}{\sqrt{3+\beta^2}}(\beta 111), \tag{37.8}$$

where

$$\alpha = -1-2x+2\sqrt{1+x+x^2}, \quad \alpha\beta = -3. \tag{37.8a}$$

For a [110] strain,

$$\Delta E_1 = \Delta E_2 = -\frac{1}{3}\Xi_u e'_{110}, \quad \Delta E_3 = \Delta E_4 = -\frac{1}{3}\Xi_u e'_{110},$$
$$e'_{110} = \varepsilon_{110} - \varepsilon_{1\bar{1}0} = 2\varepsilon_{xy},$$

where the indices 1, 2, 3, 4 designate extrema on the [111], [11$\bar{1}$], [1$\bar{1}$1], [$\bar{1}$11] axes, respectively, and from (37.2) we obtain

$$E_1 = \frac{1}{3}\Xi_u e'_{110}, \quad E_2 = -\frac{1}{3}\Xi_u e'_{110},$$
$$E_{3,4} = -\frac{\Delta}{2} \pm \frac{1}{2}\sqrt{\Delta^2 + \left(\frac{2}{3}\Xi_u e'_{110}\right)^2}. \tag{37.9}$$

If $\varepsilon'_{110} = 0$, the terms E_1, E_2, E_3 coincide and correspond to the triplet state; E_4 is the singlet.

The impurity center wave functions in the strained crystal, for a [110] strain, are

$$\Psi_1 = \frac{1}{\sqrt{2}}(1\bar{1}00), \quad \Psi_2 = \frac{1}{\sqrt{2}}(001\bar{1}),$$
$$\Psi_3 = \frac{1}{\sqrt{2(1+\alpha^2)}}(\bar{\alpha}\bar{\alpha}11), \quad \Psi_4 = \frac{1}{\sqrt{2(1+\beta^2)}}(\beta\beta 11), \tag{37.10}$$

where

$$\alpha = x+\sqrt{1+x^2}, \quad \beta = \sqrt{1+x^2}-x, \quad x = \frac{2\Xi_u e'_{110}}{3}, \quad \alpha\beta = 1. \tag{37.11}$$

We now consider the effect of a strain on a donor ground state in silicon.

The energy levels in the unstrained crystal will be measured from the lowest state – the singlet. We denote the energies of the triplet and doublet states by Δ_1 and Δ_2. Then the matrix of the interaction with the strain, relative to the basis (27.20), is

$$\begin{Vmatrix}
\frac{1}{3}(\Delta E_1+\Delta E_2+\Delta E_3) & \frac{1}{\sqrt{6}}(\Delta E_1-\Delta E_2) & \frac{1}{3\sqrt{2}}(2\Delta E_3-\Delta E_1-\Delta E_2) & 0 & 0 & 0 \\
\frac{1}{\sqrt{6}}(\Delta E_1-\Delta E_2) & \frac{\Delta E_1+\Delta E_2}{2}+\Delta_2 & \frac{1}{2\sqrt{3}}(\Delta E_1-\Delta E_2) & 0 & 0 & 0 \\
-\frac{1}{3\sqrt{2}}(2\Delta E_3-\Delta E_1-\Delta E_2) & \frac{1}{2\sqrt{3}}(\Delta E_1-\Delta E_2) & \frac{\Delta E_1+\Delta E_2}{6}+\frac{2}{3}\Delta E_3+\Delta_2 & 0 & 0 & 0 \\
0 & 0 & 0 & \Delta E_1+\Delta_1 & 0 & 0 \\
0 & 0 & 0 & 0 & \Delta E_2+\Delta_1 & 0 \\
0 & 0 & 0 & 0 & 0 & \Delta E_3+\Delta_1
\end{Vmatrix} \tag{37.12}$$

It follows from (37.12) that under a strain the triplet states are shifted by ΔE_1, ΔE_2 and ΔE_3, so that in the general case the degeneracy is removed; the correct wave functions of the triplet level in the strained crystal are again given by (27.20). Under a [001] strain, $\Delta E_1 = \Delta E_2 = -\frac{1}{3}\Xi_u \varepsilon'_{zz}$, $\Delta E_3 = \frac{2}{3}\Xi_u \varepsilon'_{zz}$ and equation (37.12) yields the energies for the states arising from the doublet and singlet levels in the unstrained crystal:

$$E_1 = \Delta_2 - \tfrac{1}{3}\Xi_u \varepsilon'_{zz},$$
$$E_{2,3} = \frac{\Xi_u \varepsilon'_{zz}}{6} + \frac{\Delta_2}{2} \pm \frac{1}{2}\sqrt{(\Xi_u \varepsilon'_{zz})^2 + \Delta_2^2 + \frac{2}{3}\Delta_2 \Xi_u \varepsilon'_{zz}}. \tag{37.13}$$

The states with energies E_1, E_2 correspond to doublets, the state with energy E_3 to the singlet state of the unstrained crystal $\Delta_2 > 0$.

The state with energy E_1 corresponds to the wave function $\frac{1}{2}(11\bar{1}\bar{1}00)$, the states with energies E_2 and E_3 to the functions

$$\Psi'_2 = \frac{1}{\sqrt{1+\alpha^2}}(\alpha\Psi_1 + \Psi_3),$$
$$\Psi'_3 = \frac{1}{\sqrt{1+\alpha^2}}(\Psi_1 - \alpha\Psi_3), \tag{37.14}$$

where

$$\alpha = \frac{-2\sqrt{2}\,x/3}{1 + \frac{x}{3} + \sqrt{1 + x^2 + \frac{2}{3}x}}, \qquad x = \frac{\Xi_u \varepsilon'_{zz}}{\Delta_2},$$
$$\Psi_1 = \frac{1}{\sqrt{6}}(111111), \qquad \Psi_3 = \frac{1}{2\sqrt{3}}(\bar{1}\bar{1}\bar{1}\bar{1}22). \tag{37.14a}$$

For a [110] strain, the nonzero strain tensor components are $\varepsilon_{xx} = \varepsilon_{yy}$, ε_{zz}, ε_{xy}, and since the shear strain ε_{xy} does not affect the positions of the extrema in Si equations (37.13) and (37.14) remain valid, with $\varepsilon'_{zz} = \varepsilon_{zz} - \varepsilon_{xx}$.

The excited states of a shallow impurity center have a considerably larger radius than the ground state, and therefore, as noted in §27, we may expect the chemical shift for excited states to be small.

If we neglect chemical shifts, the strain splitting of the excited states of a shallow impurity center coincides with the splitting of the band bottom.

Degenerate bands

To determine the energy and wave functions of an impurity center in a degenerate band, we must solve the system of equations (27.1), augmented by adding, besides the operator $\mathcal{H}(k)$(21.19), an operator $\mathcal{H}(\varepsilon)$which determines the splitting of the bottom of the band. Under a strain, therefore, the spectrum and wave functions of the impurity center are determined by the system of equations

$$\sum_s \mathcal{H}_{ts} f_s = E f_t, \quad \mathcal{H} = \mathcal{H}(k) + V(r) + \mathcal{H}(\varepsilon). \tag{37.15}$$

As opposed to the nondegenerate band, a strain may significantly alter the electron spectrum in the band near an extremum. This results in considerable rearrangement of the impurity center spectrum and the wave functions under large strains, when the valence band splitting Δ_ε becomes comparable with the impurity ionization energy E_i.

Equations (37.15) cannot usually be solved in closed form for an arbitrary strain. We shall therefore consider two limiting cases: small strains $\Delta_\varepsilon \ll E_i$ and large strains $\Delta_\varepsilon \gg E_i$.

In the case of small strains the operator $\mathcal{H}(\varepsilon)$ may be treated as a perturbation, and so the splitting of a degenerate state is determined by a perturbation matrix $\mathcal{H}'(\varepsilon)$ with elements

$$\mathcal{H}'_{ij}(\varepsilon) = \sum_{st} \int f_s^{i*} \mathcal{H}_{st}(\varepsilon) f_t^j \, dx = \sum_{st} \mathcal{H}(\varepsilon)_{st} \int f_s^{i*} f_t^j \, dx, \tag{37.16}$$

evaluated between the envelope functions f^i of the impurity center, with components f_s^i (see § 27).

For the impurity center ground state, which has the symmetry of the band bottom, the matrix $\mathcal{H}'(\varepsilon)$ has the same form as $\mathcal{H}(\varepsilon)$ for a band which differs from the ground state only in the values of the deformation potential constants. These constants b' and d' generally differ from b and d: they depend on the form of the wave functions and may be expressed in terms of b and d via (37.16).

Let us consider the deformation potential constants for acceptor states in Ge and Si.

Suppose we let the f^i's be the trial functions (27.23) or (27.25), corresponding to the approximation $\Delta \to \infty$ or $\Delta = 0$, where Δ is the valence band spin-orbit splitting; then we obtain (provided $c_4 = 0$)

$$\begin{aligned} &\Delta = 0: \quad b' = \left(1 - \frac{3}{2} c_3^2\right) b, \quad d' = \left(1 - \frac{c_3^2}{2}\right) d; \\ &\Delta = \infty: \quad b' = (c_1^2 - c_3^2) b, \quad d' = \left(c_1^2 - c_2^2 - \frac{c_3^2}{3}\right) d. \end{aligned} \tag{37.17}$$

Using the values of the constants defining the wave functions for Ge and Si in (27.25) and (27.23) as indicated in Tables 27.3 and 27.5 (pp. 276 and 277), we obtain the following values for b'/b and d'/d:

TABLE 37.1

		b'/b	d'/d
$\Delta = \infty$	Ge	0.56	0.61
	Si	0.77	0.82
$\Delta = 0$	Si, $B<0$	0.84	0.93
	Si, $B>0$	0.73	0.75

As seen in the table, the shear deformation potential constants b' and d' for an impurity center may differ considerably from the constants b and d,

coinciding only if $c_2 = c_3 = 0$ in (27.23). The deformation potential constant a' is always equal to a if terms of the order of εk^2 are neglected in the matrix $\mathcal{H}(\varepsilon, k)$. In the general case this is valid for all deformation potential constants which do not cause band splitting at the extremum point.

Note that the ratio of the deformation potential constants for band and impurity center depends sensitively on the form of the functions, and so it is difficult to estimate the accuracy of the data in Table 37.1.

Thus, the strain-induced splitting of an impurity level is determined by the same equation as the splitting of the band bottom, provided we replace the band deformation potential constants by corresponding constants for the impurity center. The impurity center wave functions for the strained crystal are linear combinations of ground state functions which diagonalize the matrix $\mathcal{H}'(\varepsilon)$. For example, in p-Ge and p-Si these combinations are determined by equations (24.19) with $k_\alpha k_\beta$ replaced by $\varepsilon_{\alpha\beta}$ and $B \to b'$, $D \to d'$.

In the case of large strains, when the strain splitting Δ_ε of the band bottom is greater than the ionization energy E_i of the impurity center, we must first diagonalize the matrix $\mathcal{H}(\varepsilon)$ in equation (37.15). In the new representation, the matrix $\mathcal{H}(k)$ becomes $\mathcal{H}'(k)$, which determines the spectrum in the strained crystal in the vicinity of the degeneracy point. Thus, for large strains $\Delta_\varepsilon \gg E_i$ the energy and wave functions of the impurity center in the strained crystal are again given by equation (27.1), in which $\mathcal{H}(k)$ determines the carrier spectrum in the strained crystal.

In a degenerate band of the type of the valence band in Ge and Si, the constant energy surfaces become ellipsoids under a strain, and so, in the limiting case of large strains, the problem of determining the energy and wave functions of an impurity center ground state for Ge and Si reduces to solving the corresponding problem for a simple band, as discussed in §27.

Under a [001] or [111] strain, when the constant energy surfaces are ellipsoids of revolution with effective masses (30.19), (30.20), we may use the trial function (27.17), which gives equations (27.18) and (27.19) for the ionization energy.

For large but finite strains corrections must be made to the ionization energy, of the order of E_i/Δ_ε; these are due to the nonparabolic nature of the split-off band.

If we transform equations (27.1) to the representation based on functions of the band bottom in the strained crystal which diagonalize the matrix $\mathcal{H}(\varepsilon)$, equation (27.15) becomes

$$\begin{Vmatrix} I\left(E_1(k) - \frac{e^2}{\varkappa r}\right) & \mathcal{H}_{1\,II} \\ \mathcal{H}_{1\,II}^{+} & I\left(E_2(k) - \frac{e^2}{\varkappa r}\right) \end{Vmatrix} \begin{Vmatrix} f_1 \\ f_2 \end{Vmatrix} = E \begin{Vmatrix} f_1 \\ f_2 \end{Vmatrix}, \tag{37.18}$$

where I is the 2×2 identity matrix, $\mathcal{H}_{1\,II}$ and $\mathcal{H}_{1\,II}^{+}$ are 2×2 matrices of second order in k, dependent on the strain direction, and $E_1(k)$, $E_2(k)$ are given by equations (30.14) – (30.17).

To calculate the energy corrections to first order in E_i/Δ_ε, we can transform the Hamiltonian as in (15.49a).* As a result we obtain the transformed

* To introduce corrections of higher orders in E_i/Δ_ε, the Hamiltonian $\Delta\mathcal{H}$ can no longer be obtained by simply expanding $E(\varepsilon, k)$ in higher powers of k^2/Δ_ε, because of the noncommutivity of the operators $k = -i\nabla$ and $V(x)$.

Hamiltonian for the upper of the split-off levels:

$$\tilde{\mathcal{H}}_{\mathrm{I\,I}} = I\left(E_1(k) - \frac{e^2}{\varkappa r}\right) - \frac{\mathcal{H}_{\mathrm{I\,II}}\mathcal{H}^{+}_{\mathrm{I\,II}}}{2\Delta_e}. \tag{37.19}$$

On the other hand, the operator $\Delta\mathcal{H} = -\mathcal{H}_{\mathrm{I\,II}}\mathcal{H}^{+}_{\mathrm{I\,II}}/2\Delta_e$ determines energy corrections of the order of k^4/Δ_e; by (30.21),

$$\Delta\mathcal{H} = I\Delta_4 E = I\left(\frac{1}{2}\frac{\mathcal{E}_k}{\mathcal{E}_e^{1/2}} - \frac{1}{8}\frac{\mathcal{E}_{ek}^2}{\mathcal{E}_e^{3/2}}\right), \tag{37.20}$$

where $\mathcal{E}_k$, $\mathcal{E}_{ek}$, $\mathcal{E}_e$ are given by equations (30.6) – (30.8).

The corrections to the ionization energy are

$$\delta E_i = \int f^* \Delta_4 E f \, dx, \tag{37.21}$$

where f is the envelope function of the ground state, defined by (27.17).

Under a [001] strain, by (37.20),

$$\Delta_4 E = \left\{\frac{3}{4}B^2(k^4 + 2k^2k_z^2 - 3k_z^4) + C^2(k_x^2k_y^2 + k_x^2k_z^2 + k_y^2k_z^2)\right\}/\Delta_e. \tag{37.22}$$

if the trial function is taken as

$$f = (\pi a_x a_y a_z)^{-1/2}\exp\left\{-\left(\frac{x^2}{a_x^2} + \frac{y^2}{a_y^2} + \frac{z^2}{a_z^2}\right)^{1/2}\right\}$$

the integrals defining the correction δE_i are

$$\int f^* k_x^4 f \, dx = \frac{1}{a_x^4}; \quad \int f^* k_x^2 k_y^2 f \, dx = \frac{1}{3}\frac{1}{a_x^2 a_y^2}. \tag{37.23}$$

Therefore, for a [001] strain,

$$\delta E_i = \frac{\Xi_0}{2|b e'_{001}|}, \text{ where } \Xi_0 = B^2 a_\perp^{-4} + \frac{D^2}{3}\frac{1}{a_\perp^2}\left(\frac{1}{a_\perp^2} + \frac{2}{a_\parallel^2}\right). \tag{37.24}$$

For a [111] strain, similar calculations yield

$$\delta E_i = \frac{\Xi_0}{2|d e'_{111}/\sqrt{3}|},$$
$$\Xi_0 = \frac{2}{3}B^2\frac{1}{a_\perp^2}\left(\frac{1}{a_\perp^2} + \frac{2}{a_\parallel^2}\right) + \frac{2}{9}\frac{D^2}{a_\perp^2}\left(\frac{2}{a_\perp^2} + \frac{1}{a_\parallel^2}\right). \tag{37.25}$$

The behavior of the ionization energy of the impurities in the large strain region is investigated experimentally in /32.4/. The change in ionization energy is determined by the change in hole concentration at low temperatures, $kT \ll \Delta_e$.

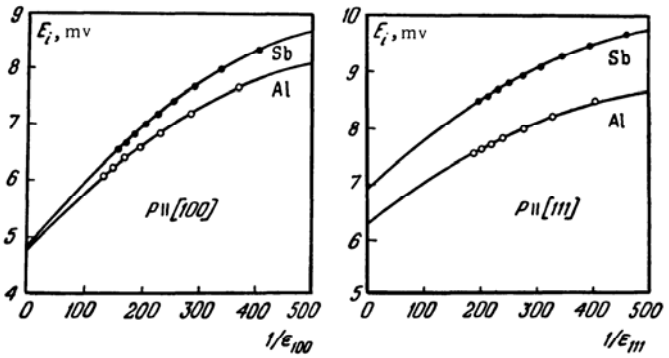

FIGURE 56. Ionization energy of acceptors (Sb and Al) in p-Ge under [100] and [111] /32.4/.

The function $E_i(\varepsilon)$ is shown in Figure 56 for [100] and [111] strains. Figure 56 shows that the ionization energy is different for different dopants this is because of chemical shift.

It is evident from Figure 56 that under the maximum strain attained in the experiment the value of $E_i(\varepsilon)$ does not yet reach saturation; the author therefore approximated $E_i(\varepsilon)$ by

$$E_i(\varepsilon) = E_{i\infty} + \frac{W_1}{\varepsilon} + \frac{W_2}{\varepsilon^2}, \tag{37.26}$$

choosing the constants $E_{i\infty}$, W_1, W_2 so as to guarantee the best fit.

§38. EFFECT OF STRAIN ON OPTICAL PROPERTIES OF IMPURITY CENTERS

In this section we shall discuss optical transitions between the ground and excited states of a shallow impurity center in a strained crystal.

We first consider the case of a many-valley band structure in which the constant energy surfaces are ellipsoids of revolution, as in the conduction bands of Ge and Si.

A perturbation producing optical dipole transitions is described by the operator

$$\mathcal{H}_\mathcal{E} = 2e(\mathcal{E}\boldsymbol{x})\cos\omega t, \tag{38.1}$$

where $\mathcal{E}$ is the electric field of the light wave, e the electron charge, and ω the frequency of the radiation. The impurity center wave function is a product of functions of the band bottom and envelope functions of effective mass theory.

In the effective mass approximation, transitions may occur only between states corresponding to the same extremum; thus the selection rules

depend on the coordinate matrix elements between the envelope functions of the ground and excited states of the impurity center. Moreover, transitions may occur only between states with unlike parities.

Let us consider in greater detail transitions between the different levels of the $1s$ ground state and the nearest excited states p_0 and $p_\pm$.

If the original state Ψ_s is a superposition of states belonging to different extrema,

$$\Psi_s = \sum_l C_l^s f_0^l \psi_{k_l},$$

and a transition occurs to an excited state

$$\Psi_{p_l} = f_p^l \psi_{k_l},$$

corresponding to the extremum l, the transition probability is proportional to

$$|\langle \Psi_s | (\mathscr{E}x) | \Psi_{p_l} \rangle|^2 = |C_l^s|^2 |\langle f_0^l | (\mathscr{E}x) | f_p^l \rangle|^2.$$

The scalar product $(\mathscr{E}x)$ may be written

$$(\mathscr{E}x) = \mathscr{E}_{z_l} z_l + \mathscr{E}_+^l x_-^l + \mathscr{E}_-^l x_+^l,$$

where

$$x_\pm^l = \frac{1}{\sqrt{2}}(x_l \pm i y_l), \quad \mathscr{E}_\pm^l = \frac{1}{\sqrt{2}}(\mathscr{E}_{x_l} \pm i \mathscr{E}_{y_l}),$$

and the x_l, y_l, z_l axes are taken along the principal axes of the ellipsoid l. The p-state wave functions in these axes transform thus: $f_{p_0}^l$ as z_l, $f_{p_\pm}^l$ as $x_\pm^l$ Thus the probability of a transition to the p_0 state is proportional to

$$|\langle \Psi_s | (\mathscr{E}x) | \Psi_{p_0 l} \rangle|^2 = |C_l^s|^2 A_\parallel^2 \mathscr{E}^2 \cos^2 \varphi_l; \tag{38.2a}$$

for a transition to the $p_\pm$ state,

$$|\langle \Psi_s | (\mathscr{E}x) | \Psi_{p_\pm l} \rangle|^2 = \frac{1}{2} |C_l^s|^2 A_\perp^2 \mathscr{E}^2 \sin^2 \varphi_l. \tag{38.2b}$$

Here φ_l is the angle between the direction of $\mathscr{E}$ and the z_l-axis of the extremum,

$$A_\parallel = \int f_0^l z_l f_{p_0}^l \, dr, \quad A_\perp = \int f_0^l x_+^l f_{p_-}^l \, dr.$$

If the final state is degenerate, the transition probability must be summed, as usual, over all final states.

In an unstrained cubic crystal, the total transition probability is of course independent of the direction of the electric field.

A strain induces splitting of the degenerate ground and excited states of a shallow impurity center. This in turn causes splitting of the optical lines and makes the absorption coefficient dependent on the direction of the electric field of the wave relative to the crystal axes.

Nondegenerate bands

Let us consider transitions between the ground and excited states in n-Ge under a strain along [111]. Figures 57 and 58 are energy level schemes for a strained Ge crystal with $\delta = \frac{2}{3}\Xi_u \varepsilon'_{111} < 0$, for small ($|\delta| \ll \Delta$) and large ($|\delta| \gg \Delta$) strains (where Δ is the valley-orbit splitting of the ground state.

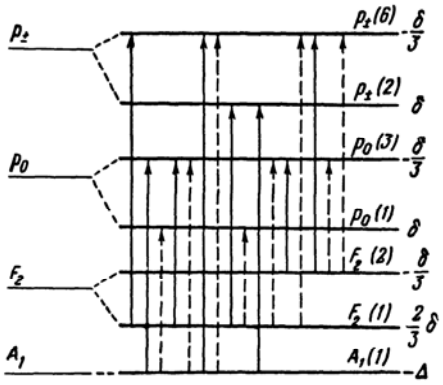

FIGURE 57. Energy level scheme of donor center, $\delta = \frac{2}{3}\Xi_u \varepsilon'_{111} < 0$. Germanium, small strains $|\delta/\Delta| \ll 1$.

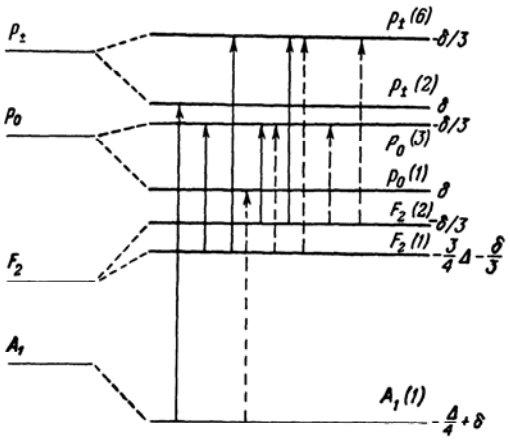

FIGURE 58. Same for Ge, large strains, $|\delta/\Delta| \gg 1$.

The probabilities of transition to the excited states p_0 and $p_\pm$ are given in Table 38.1, for a field $\mathcal{E}$ making an angle φ with the strain direction.

TABLE 38.1

	p_0 (1)	p_0 (3)	$p_\pm$ (2)	$p_\pm$ (6)
A_1 (1)	$\frac{\alpha^2}{3+\alpha^2} A_\parallel^2 \cos^2\varphi$	$\frac{A_\parallel^2}{3+\alpha^2} \times$ $\times\left(\frac{1}{3}+\sin^2\varphi\right)$	$\frac{\alpha^2}{3+\alpha^2} A_\perp^2 \sin^2\varphi$	$\frac{A_\perp^2}{3+\alpha^2} \times$ $\times\left(\frac{5}{3}+\cos^2\varphi\right)$
F_2 (1)	$\frac{3A_\parallel^2}{3+\alpha^2}\cos^2\varphi$	$\frac{\alpha^2 A_\parallel^2}{3(3+\alpha^2)} \times$ $\times\left(\frac{1}{3}+\sin^2\varphi\right)$	$\frac{3A_\perp^2}{3+\alpha^2}\sin^2\varphi$	$\frac{\alpha^2 A_\perp^2}{3(3+\alpha^2)} \times$ $\times\left(\frac{5}{3}+\cos^2\varphi\right)$
F_2 (2)	0	$\frac{2}{3} A_\parallel^2 \times$ $\times\left(\frac{1}{3}+\sin^2\varphi\right)$	0	$\frac{2}{3} A_\perp^2 \times$ $\times\left(\frac{5}{3}+\cos^2\varphi\right)$

φ — angle between field $\mathcal{E}$ and strain direction [111]; α is defined by (37.14a).

The dashed arrows in Figures 57 and 58 show the allowed transitions in a longitudinal electric field, the solid arrows the transitions in a transverse field. The degeneracies are indicated in parentheses.

Let us first consider small strains. In this case the line corresponding to the transition $A_1 \to p_0$ in the unstrained crystal splits into two lines, shifted by $-\frac{2}{9}\Xi_u \varepsilon'_{111} = -\frac{\delta}{3}$ (transition $A_1 \to p_0(3)$) and δ (transition $A_1 \to p_0(1)$).

When $\mathcal{E} \perp [111]$ only the transition $A_1 \to p_0$ (3) is observed, but when $\mathcal{E} \parallel [111]$ both components are observed. The line corresponding to $A_1 \to p_\pm$ also splits into two components, shifted by $-\frac{\delta}{3}$ ($A_1 \to p_\pm(6)$) and δ ($A_1 \to p_\pm(2)$). When $\mathcal{E} \parallel [111]$ only the transition $A_1 \to p_\pm(6)$ is observed, but when $\mathcal{E} \perp [111]$ both transitions are allowed. The lines corresponding to the transitions $F_2 \to p_0$ and $F_2 \to p_\pm$ in the unstrained crystal split into three components. One of these is not shifted and corresponds to the line position in the unstrained crystal – transitions $F_2(2) \to p_0(3)$, $F_2(2) \to p_\pm(6)$; the other two are shifted by $-\delta$ and $\frac{\delta}{3}$ ($F_2(1) \to p_0(3)$, $F_2(1) \to p_\pm(6)$ and $F_2(1) \to p_0(1)$, $p_\pm(2)$, respectively). When $\mathcal{E} \parallel [111]$ all three lines are observed for transitions $F_2 \to p$ and two lines for the transition $F_2 \to p_\pm$, namely $F_2(1)$, $F_2(2) \to p_\pm(6)$. When $\mathcal{E} \perp [111]$ all three lines are observed for the transition $F_2 \to p_\pm$ and two lines for transitions $F_2 \to p_0$: $F_2(1)$, $F_2(2) \to p_0(3)$.

Under a large strain, $|\delta| \gg \Delta$, the ground state changes considerably, and as a result the pattern of optical transitions from the ground state to the excited states is quite different. When $\mathcal{E} \parallel [111]$ the only possible transition

from A_1 is to $p_0(1)$ (see Figure 58, which shows all the allowed transitions under large strains), which is shifted from its position in the unstrained crystal by $\Delta/4$. The possible transitions from an F_2 state are $F_2(1) \to p_0(3)$, $p_\pm(6)$, shifted by $\frac{3}{4}\Delta$ relative to the unstrained crystal, and transitions $F_2(2) \to$ $\to p_0(3)$, $p_\pm(6)$, which are not shifted. In the transverse orientation $\mathscr{E} \perp [111]$, the transition $A_1 \to p_\pm(2)$ is shifted by $\Delta/4$, the transitions $F_2 \to p_0(3)$, $F_2 \to p_\pm(6)$ by $\frac{3}{4}\Delta$, and the positions of the lines corresponding to transitions $F_2(2) \to p_0(3)$, $p_\pm(6)$ coincide with their positions in the unstrained crystal.

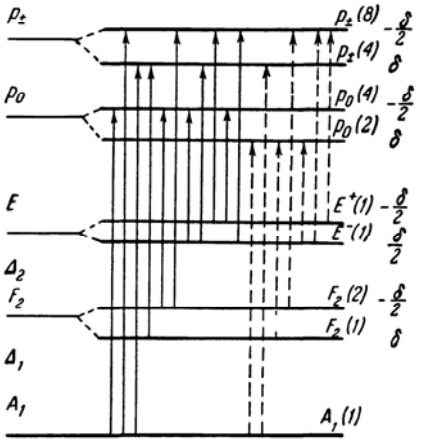

FIGURE 59. Same for Si, small strains, $|\delta/\Delta| \ll 1$: $\delta = \frac{2}{3}\Xi_u e'_{zz} < 0$.

We now consider optical transitions in n-Si under a strain along [001]. Figure 59 is a splitting diagram of the ground and excited p-states for shallow donor centers in Si (small strains). The figure indicates the degeneracy of the impurity center state and the energy shift for $\delta = \frac{2}{3}\Xi_u e'_{zz} < 0$. Equation (37.13) implies that under such a strain all the levels except A_1 split into two.

As in the case of n-Ge, selection rules for optical transitions between the ground and excited p_0, $p_\pm$ are readily established.

It follows from Table 38.2 and Figure 59 that the line corresponding to a transition $A_1 \to p_0$ in the unstrained crystal splits into two components shifted by δ and $-\delta/2$, the first line appearing when $\mathscr{E} \parallel [001]$ and the second when $\mathscr{E} \perp [001]$. Of the transitions $F_2 \to p_0$, only $F_2(1) \to p_0(2)$ is allowed in the strained crystal when $\mathscr{E} \parallel [001]$, and only $F_2(2) \to p_0(4)$ when $\mathscr{E} \perp [001]$. Both transitions correspond to an unshifted line. All the transitions $F_2(2) \to p_\pm(8)$ when $\mathscr{E} \parallel [001]$ and $F_2(1) \to p_\pm(4)$, $F_2(2) \to p_\pm(8)$ when $\mathscr{E} \perp [001]$ between the states $F_2 \to p_\pm$ in the strained crystal correspond to the line position in the unstrained crystal.

TABLE 38.2

	p_0 (2)	p_0 (4)	$p_\pm$ (4)	$p_\pm$ (6)
A_1 (1)	$\frac{(\alpha-\sqrt{2})^2}{3(1+\alpha^2)} A_\parallel^2 \cos^2\varphi$	$\frac{(\sqrt{2}\alpha+1)^2}{6(1+\alpha^2)} A_\parallel^2 \sin^2\varphi$	$\frac{(\alpha-\sqrt{2})^2}{3(1+\alpha^2)} A_\perp^2 \sin^2\varphi$	$\frac{(\sqrt{2}\alpha+1)^2}{6(1+\alpha^2)} A_\perp^2 (1+\cos^2\varphi)$
F_2 (2)	0	$A_\parallel^2 \sin^2\varphi$	0	$A_\perp^2 (1+\cos^2\varphi)$
F_2 (1)	$A_\parallel^2 \cos^2\varphi$	0	$A_\perp^2 \sin^2\varphi$	0
E^+ (1)	0	$\frac{A_\parallel^2}{2} \sin^2\varphi$	0	$\frac{A_\perp^2}{2}(1+\cos^2\varphi)$
E^- (1)	$\frac{(\sqrt{2}\alpha+1)^2}{3(1+\alpha^2)} A_\parallel^2 \cos^2\varphi$	$\frac{(\sqrt{2}-\alpha)^2}{6(1+\alpha^2)} A_\parallel^2 \sin^2\varphi$	$\frac{(\sqrt{2}\alpha+1)^2}{3(1+\alpha^2)} A_\perp^2 \sin^2\varphi$	$\frac{(\sqrt{2}-\alpha)^2}{6(1+\alpha^2)} A_\perp^2 (1+\cos^2\varphi)$

φ — angle between electric field $\mathscr{E}$ and strain direction [001]; α is defined by (37.14a).

The line corresponding to the transition $E \to p_0$ splits under a strain into two components. In a parallel field $\mathfrak{F} \parallel [001]$, the transition $E^-(1) \to p_0(2)$* is allowed; it corresponds to a line shifted by $\delta/2$; when $\mathfrak{F} \perp [001]$ transitions $E^+(1) \to p_0(4)$ and $E^- \to p_0(4)$, corresponding to an unshifted line and a line shifted by $-\delta$, are allowed.

The line corresponding to the transition $E \to p_\pm$ splits under a strain into three components. One of these coincides in position with the line in the unstrained crystal and is observed for both orientations of the field ($E^+(1) \to p_\pm(8)$), another is shifted by $-\delta$ ($E^-(1) \to p_\pm(8)$), and the third is shifted by $\delta/2$ ($E^-(1) \to p_\pm(4)$ when $\mathfrak{F} \perp [001]$).

The above selection rules and the nature of the line splitting under a [001] strain are also valid for transitions from the ground state to any excited np_0 and $np_\pm$ states.

The polarization dependence of the selection rules is similar in the case of a strain along [110], provided we continue to measure the angle φ in Table 38.2 from the [001] direction, which is now perpendicular to the strain.

Optical transitions from the ground to the excited p_0 and $p_\pm$ states for shallow donor centers in Ge and Si have been investigated in a number of papers. The line positions and polarization dependence of the line intensities are in good agreement with theory.

As noted in §27, if we introduce corrections to effective mass theory, the impurity center wave functions in Ge and Si are classified according to the representations of the local symmetry group T_d (rather than O_h) and do not possess a definite parity. From the group-theoretic viewpoint, therefore, transitions $A_1 \to F_2$ (and $E \to F_2$) are allowed; the intensities of these transitions, which are forbidden in the effective mass approximation, are necessarily higher for deeper centers.

Transitions $A_1 \to F_2$ for Bi impurities in Si were observed in /41.10/. The authors measured the spin-orbit splitting between the states E_2' and G', which, as noted in §27, split off from the state F_2.

The strain-induced splitting of the F_2 level for strains which are smaller than or comparable with the spin-orbit splitting presents a more complicated picture than indicated in §37; it is determined by an equation similar to (30.33).

Degenerate band

We now consider the case of a degenerate band of the Ge and Si valence band. The excited states of the acceptor center are now classified according to the representations of the entire cubic group $O_h = T_d \times C_i$, i.e., they may have the symmetry of $E_1'^{\pm}$, $E_2'^{\pm}$, $G'^{\pm}$. In the effective mass approximation, optical transitions may occur only between states of unlike parity, i.e., we may have transitions from the ground state $G'^{\pm}$ to states $E_1'^{-}$, E_2', G'. The probability of transitions to "even" states, which are allowed from the group-theoretic viewpoint, is small for shallow impurity centers.

In the unstrained crystal the intensities of these transitions are independent of the direction of the electric field vector of the wave. Under a

* Levels of the state E which increase (decrease) under a strain are denoted by $E^{\pm}(1)$. When $\delta < 0$, the solution E_3 of equation (37.13) defines the level $E^+(1)$.

strain, the $G'^{\pm}$ levels are shifted by $a\varepsilon$ and split into two. The splitting Δ_ε is given by (30.11) with b and d replaced by the correct deformation potential constants b' and d' for the level, which differ for different levels. Since the Kramers doublets E_1' and E_2' are also shifted by $a\varepsilon$, an isotropic strain does not affect the position of an optical transition line in the effective mass approximation.

An arbitrary strain splits the lines of the optical transitions from the ground to an excited state: lines corresponding to transitions $G'^{+} \to E_1'^{-}$, $E_2'^{-}$ are split into two components shifted by $\pm\Delta_\varepsilon/2$ relative to the unstrained crystal. The $G'^{+} \to G'^{-}$ line generally splits into four components, shifted by

$$\pm \tfrac{1}{2}(\Delta_\varepsilon^1 + \Delta_\varepsilon^2), \quad \pm \tfrac{1}{2}(\Delta_\varepsilon^1 - \Delta_\varepsilon^2),$$

where Δ_ε^1 and Δ_ε^2 are the splittings of the first and second levels.

Selection rules for optical transitions in the strained crystal are readily derived from group-theoretic considerations.

Let us consider strains along [001] and [111]. Under a [001] strain, the symmetry group $O_h = T_d \times C_i$ is reduced to D_{4h}, and the representations $E_1'^{-}$, $E_2'^{-}$, $G'^{\pm}$, respectively, become the following representations of $D_{4h} = D_{2d} \times C_i$:

$$E_1'^{-} \to E_2'^{-}, \quad E_2'^{-} \to E_1'^{-}, \quad G'^{\pm} \to E_1'^{\pm} + E_2'^{\pm}. \tag{38.3}$$

Of course, group theory does not tell us which level of the representations $E_1'^{\pm}$ or $E_2'^{\pm}$ that split off from $G'^{\pm}$ is the lower; this is determined by the sign of the deformation potential constants and the sign of the strain.

Use of character tables shows that

$$\begin{aligned} &E_1'^{-} \times E_1'^{+} = E_2'^{-} \times E_2'^{+} = A_1^{-} + A_2^{-} + E^{-}, \\ &E_1'^{+} + E_2'^{-} = B_1^{-} + B_2^{-} + E^{-}, \end{aligned} \tag{38.4}$$

where A_1^{-}, A_2^{-}, B_1^{-}, B_2^{-}, E^{-} are the corresponding single-valued odd representations of D_{4h} (Table 11.1). Since z transforms according to the representation A_2^{-} and x, y according to E^{-}, it follows from (38.3) and (38.4) that, for the longitudinal orientation, the only allowed transitions for $G'^{+} \to E_1'^{-}$, $E_2'^{-}$ occur from one of the split states, the corresponding lines for transitions $G'^{+} \to E_1'^{-}$, $G' \to E_2'^{-}$ being shifted in different directions relative to the line position of the unstrained crystal. In a transverse field, both transitions are allowed.

In a longitudinal field, the only allowed transitions $G'^{+} \to G'^{-}$ are $E_1'^{-} \to E_1'^{+}$ and $E_2'^{-} \to E_2'^{+}$; to these correspond two lines which are shifted relative to the unstrained crystal by $\pm \frac{1}{2}(\Delta_\varepsilon^1 - \Delta_\varepsilon^2)$ if the deformation potential constants b_1' and b_2' for levels G'^{+} and G'^{-} have the same sign and by $\pm \frac{1}{2}(\Delta_\varepsilon^1 + \Delta_\varepsilon^2)$ otherwise.

According to (38.3), all four transitions are allowed in the case of a transverse field.

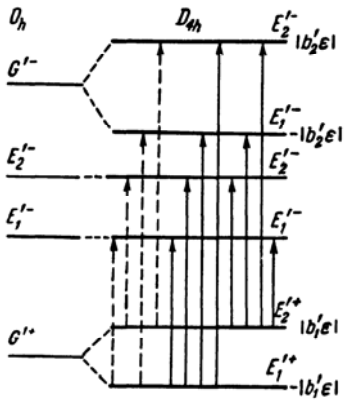

FIGURE 60. Splitting of acceptor levels under a [001] strain.

Figure 60 shows the impurity levels for a strain along [001], in the case that the deformation potential constants b_1' and b_2' have the same sign and the state E_1' is the lower of the split levels. The figure shows the allowed transitions in longitudinal and transverse fields.

Under a [111] strain, the O_h symmetry is reduced to $D_{3d}=D_3\times C_i$, and the representations of the group $O_h=T_d\times C_i$ $E_1'^-$, $E_2'^-$, $G'^\pm$ become double-valued representations of $D_{3d}=D_3\times C_i$:

$$E_1'^- \to E'^-,\ E_2'^- \to E^-,\ G'^\pm = E_1'^\pm + E_2'^\pm + E'^\pm, \tag{38.5}$$

where $E'^\pm$ is a two-dimensional double-valued representation of D_{3d}, $E_1'^\pm$ and $E_2'^\pm$ one-dimensional representations with complex conjugate characters.

As in the case of a [001] strain, the $G'^\pm$ level splits into two Kramers conjugate doublets, the representation E' and the representations $E_1'+E_2'$, separated by $\Delta_\varepsilon=(2d'/\sqrt{3})\varepsilon_{111}'$; in the general case, therefore, the absorption lines corresponding to transitions $G'^+\to E_1'^-$, $E_2'^-$ split into two components and the $G'^+\to G'^-$ line into four components.

It follows from character tables that

$$\begin{aligned} &E'^-\times E'^+ = A_1^- + A_2^- + E^-,\quad E^-\times(E_1'^+ + E_2'^+) = 2E^-,\\ &(E_2'^+ + E_1'^+)(E_1'^- + E_2'^-) = 2(A_1^- + A_2^-). \end{aligned} \tag{38.6}$$

Since a parallel strain of the x_{11} coordinate transforms according to the representation A_2^- and the perpendicular components according to E, (38.6) yields selection rules for transitions between the states G'^+ and $E_1'^-$, $E_2'^-$, G'^- under a [111] strain. For transitions $G^+\to E_1^-$, E_2^-, one line, corresponding to the transition $E'^+\to E'^-$, is observed in the parallel orientation, while both split-off lines are observed in the transverse orientation.

For the transition $G'^+\to G'^-$, with the field parallel to the strain, the allowed transitions $E'^-\to E'^+$ and $E_1'^+ + E_2'^+ \to E_1'^- + E_2'^-$, corresponding to lines shifted by $\pm\,{}^1/_2(\Delta_\varepsilon^2-\Delta_\varepsilon^1)$ from the line position in the unstrained crystal if

$d_2'/d_1' > 0$ (or by $\pm\,{}^1/_2(\Delta_e^2 + \Delta_e^1)$) if $d_2'/d_1' < 0$. In the transverse orientation three lines appear, corresponding to transitions $E'^+ \to E'^-$, $E'^+ \to E_1'^- + E_2'^-$ and $E_1'^+ + E_2'^+ \to E'^-$, shifted by $\pm\,{}^1/_2(\Delta_e^2 + \Delta_e^1)$ and ${}^1/_2(\Delta_e^2 - \Delta_e^1)$ if $d_2'/d_1' > 0$ (if $d_2'/d_1' < 0$ the line shifts are $\pm\,{}^1/_2(\Delta_e^2 - \Delta_e^1)$ and ${}^1/_2(\Delta_e^2 + \Delta_e^1)$).

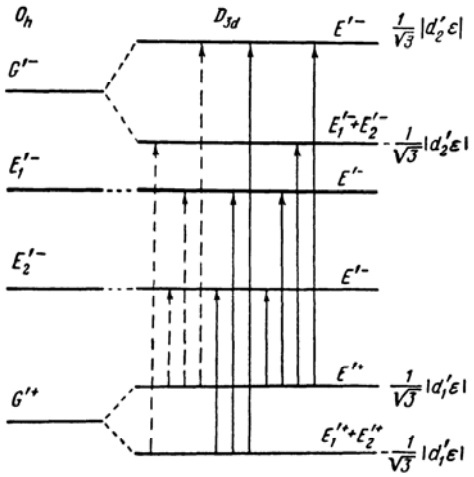

FIGURE 61. Splitting of acceptor levels under a [111] strain.

Figure 61 illustrates the splitting of acceptor levels under a [111] strain when $d_1'/d_2' > 0$ and shows the allowed transitions for longitudinal and transverse fields.

The above expressions for the nature of the line splitting and the probability of optical transitions were obtained under the assumption of a small strain, for which the strain-splitting and the level shift are small compared to the separation between the nearest excited states.

In Ge, which has close-lying excited acceptor states, this approximation is not always valid.

When there are close-lying levels and the strain splitting of the levels is comparable with or greater than their separation, one must consider the entire group of close-lying levels as a whole, using degenerate perturbation theory. In this case the energy and the wave functions in the strained crystal are determined by solving the characteristic equation, whose degree is equal to the number of close-lying levels.

Experimental investigations of optical transitions between ground and excited levels of shallow acceptor centers in strained crystals of Ge and Si are presented in /41.1–41.9/. Investigating the nature of the strain-induced line splitting and the polarization dependence of the intensities, one can identify most of the lines with the transitions from ground to excited states considered by Schechter /21.4/, Mendelson and James /21.5/.

§39. PARAMAGNETIC RESONANCE ARISING FROM SHALLOW IMPURITY CENTERS

In this section we discuss Zeeman splitting of shallow impurity centers in many-valley and degenerate semiconductors, and its behavior under a strain.

Many-valley bands

In a semiconductor whose constant energy surfaces near an extremum are ellipsoids of revolution, the energy levels and wave functions of an impurity center in a uniform magnetic field $\boldsymbol{H}$ are determined by equations (33.1), (22.21):

$$\left\{\frac{\hbar^2}{2m_\perp}(k_x^2+k_y^2)+\frac{\hbar^2k_z^2}{2m_\parallel}-\frac{e^2Z}{\varkappa r}+\frac{1}{2}(g_0\mu_0\sigma+2\boldsymbol{L})\boldsymbol{H}\right\}f=Ef, \tag{39.1}$$

where μ_0 is the Bohr magneton, $\mu_0=e\hbar/2mc$. In a nondegenerate band f is a two-component quantity, corresponding to two Kramers-conjugate functions of the band bottom. As shown in §22 (see (22.22)), the matrix $\boldsymbol{L}$ determines the correction to the g-factor of the band carriers due to the effect of the other bands. If the level splitting caused by the magnetic field is small compared to the ionization energy of the impurity (the case to be considered presently), the external magnetic field may be viewed as a perturbation. If the vector potential is taken to be $\mathcal{A}=\frac{1}{2}[\boldsymbol{H}\boldsymbol{x}]$, the perturbation operator

$$\mathcal{H}_H=\frac{1}{2}\mu_0(g_0\sigma+2\boldsymbol{L})\boldsymbol{H}-\frac{ie\hbar}{m_\perp c}\left(\mathcal{A}_x\frac{\partial}{\partial x}+\mathcal{A}_y\frac{\partial}{\partial y}\right)-\frac{ie\hbar}{m_\parallel c}\mathcal{A}_z\frac{\partial}{\partial z}$$

becomes

$$\mathcal{H}_H=\frac{1}{2}\mu_0(g_0\sigma+2\boldsymbol{L})\boldsymbol{H}+\mu_0\frac{m}{m_\perp}(\mathcal{L}\boldsymbol{H})+ \\ +\mu_0\left(H_+x_-\frac{\partial}{\partial z}-H_-x_+\frac{\partial}{\partial z}\right)m\left(\frac{1}{m_\parallel}-\frac{1}{m_\perp}\right), \tag{39.2}$$

where $H_\pm=\frac{1}{\sqrt{2}}(H_x\pm iH_y)$, $x_\pm=\frac{1}{\sqrt{2}}(x\pm iy)$, $\mathcal{L}$ is the orbital momentum operator, $\mathcal{L}_z=-i\left(x\frac{\partial}{\partial y}-y\frac{\partial}{\partial x}\right)$, etc.

The first term in (39.2) describes that part of the level splitting in the magnetic field associated with the wave functions of the band bottom; the second and third terms represent the contribution to this splitting due to the orbital motion of an impurity electron. To determine the splitting of the impurity levels in the magnetic field, we must find the matrix elements of $\mathcal{H}_H$ between the envelope functions of the impurity ground state. It is easy to see that symmetry considerations dictate the vanishing of the

contribution from the last two terms in (39.2) for the ground state, and consequently the Zeeman splitting of the ground state in the nondegenerate band coincides with the Zeeman splitting of the band carriers near the extremum.

The spin Hamiltonian for the l-th extremum may be written

$$\mathcal{H}_H = \tfrac{1}{2}\mu_0 \sum_{\alpha\beta} g^l_{\alpha\beta}\sigma_\alpha H_\beta, \quad \text{where } g^l_{\alpha\beta} = g_0\delta_{\alpha\beta} + \mathrm{Sp}\,(L^{(l)}_\beta \sigma_\alpha); \tag{39.3}$$

$g^l_{\alpha\beta}$ are the components of the g-factor of the free carriers of the l-th extremum. The symmetry of the g-factor is determined by the little group G_{k_l} and is analogous to the symmetry of the effective mass tensor. If the constant energy surfaces are ellipsoids of revolution, the g-factor is also determined by two components $g_\parallel$ and $g_\perp$.

The Zeeman interaction (39.31) of the impurity center is referred to the axes of the l-th ellipsoid. It is often convenient to go over to the coordinate system defined by the principal axes of the crystal. The Zeeman interaction operator will again have the form of (39.3), but the $g'^l_{\alpha\beta}$ are expressed relative to the crystal axes in terms of the principal components of the tensor g_s by

$$g'^l_{\alpha\beta} = \sum_s g_s \cos(x^l_s, x_\alpha)\cos(x^l_s, x_\beta), \tag{39.4}$$

where $\cos(x^l_s, x_\alpha)$ are the direction cosines of the principal axes of the l-th energy ellipsoid relative to the principal crystal axes x_α.

If the splitting of a many-valley impurity center degeneracy due to chemical shift is neglected, it follows from (39.3) and (39.4) that in general one should observe a number of paramagnetic resonance lines for each extremum, determined by the g-factor (39.4): these lines may coincide for certain magnetic field directions. If, however, the chemical shift is significantly greater than the Zeeman splitting (which is usually the case), one must consider paramagnetic resonance at each of the levels formed as a result of chemical shift. As is evident from (27.10), each such state is described by the expansion coefficients c_l of the impurity center functions in terms of the impurity states near the extremum k_l. If the state in question is m-fold degenerate, there are m columns c^s_l ($s = 1, 2, \ldots, m$) of coefficients.

The Zeeman interaction matrix for a onefold degenerate state has the form of (39.3), and the effective g-factor is

$$g_{\alpha\beta} = \sum_l |c_l|^2 g'^l_{\alpha\beta}. \tag{39.5}$$

The summation in (39.5) extends over all extrema. If the state is degenerate, the matrix elements of $\mathcal{H}_H$ are

$$\mathcal{H}^{ss'}_H = \frac{\mu_0}{2}\sum_{\alpha\beta} g^{ss'}_{\alpha\beta}\sigma_\alpha H_\beta, \tag{39.6}$$

where

$$g^{ss'}_{\alpha\beta} = \sum_l c^{*s}_l c^{s'}_l g'^l_{\alpha\beta}. \tag{39.7}$$

Let us consider the g-factor for donor centers in Si. For the singlet state A, it follows from (39.5) and (27.20) that the g-factor is isotropic:

$$g^A_{\alpha\beta} = \frac{1}{3}(g_\parallel + 2g_\perp)\delta_{\alpha\beta}, \tag{39.8}$$

as it must be for a symmetric state in a cubic crystal. The matrix $\mathcal{H}_H$ for the doublet state E, relative to the basis functions (27.20), is

$$\left\| \begin{array}{ll} \frac{g_\parallel+2g_\perp}{3}(\sigma H)+\frac{g_\parallel-g_\perp}{6}((\sigma H)-3\sigma_z H_z) & \frac{g_\parallel-g_\perp}{2\sqrt{3}}(\sigma_x H_x-\sigma_y H_y) \\ \frac{g_\parallel-g_\perp}{2\sqrt{3}}(\sigma_x H_x-\sigma_y H_y) & \frac{g_\parallel+2g_\perp}{3}(\sigma H)-\frac{g_\parallel-g_\perp}{6}((\sigma H)-3\sigma_z H_z) \end{array} \right\|, \tag{39.9}$$

where σ_i are the Pauli matrices. If $g_\parallel \neq g_\perp$, the Zeeman splitting depends on the direction of the magnetic field.

The matrix $\mathcal{H}_H$ for the threefold degenerate (neglecting spin) level F_2, relative to the basis functions $\Psi^1_{F_2}$, $\Psi^2_{F_2}$, $\Psi^3_{F_2}$ (27.20), is

$$\left\| \begin{array}{ccc} g_\perp(\sigma H)+(g_\parallel-g_\perp)\sigma_x H_x & 0 & 0 \\ 0 & g_\perp(\sigma H)+(g_\parallel-g_\perp)\sigma_y H_y & 0 \\ 0 & 0 & g_\perp(\sigma H)+(g_\parallel-g_\perp)\sigma_z H_z \end{array} \right\|. \tag{39.10}$$

Thus the Zeeman splitting of the F_2 level relative to the crystal axis is determined, as is that of the band carriers, by three anisotropic g-factors.

We now consider the g-factor for different levels of the ground state of shallow donors in Si, under a [001] strain such that the strain splitting significantly exceeds the Zeeman splitting. In this case we may consider the g-factor for each of the split levels.

According to (39.5) and (37.14), the g-factor for the ground state in the strained crystal becomes anisotropic and has two components $g^*_\parallel$ and $g^*_\perp$ relative to the strain direction:

$$\begin{aligned} g^*_\parallel &= \frac{1}{3(1+\alpha^2)}\left\{2g_\perp\left(1-\frac{\alpha}{\sqrt{2}}\right)^2 + g_\parallel(1+\alpha\sqrt{2})^2\right\}, \\ g^*_\perp &= \frac{1}{3(1+\alpha^2)}\left\{g_\perp\left[\left(1-\frac{\alpha}{\sqrt{2}}\right)^2+(1+\alpha\sqrt{2})^2\right]+g_\parallel\left(1-\frac{\alpha}{\sqrt{2}}\right)^2\right\}, \end{aligned} \tag{39.11}$$

where α is given (37.14). For large strains $x \gg 1$ we have $\alpha \to -1/\sqrt{2}$, but if $x \ll -1$ then $\alpha \to \sqrt{2}$ and from (39.11) we obtain

$$\begin{aligned} &g^*_\parallel \to g_\perp, \quad g^*_\perp \to \frac{g_\parallel + g_\perp}{2} && (x \gg 1), \\ &g^*_\parallel \to g_\parallel, \quad g^*_\perp \to g_\perp && (x \ll -1). \end{aligned} \tag{39.12}$$

The g-factor for the state with energy E_2 (37.13) is obtained from (39.11) by substituting $-1/\alpha$ for α. The g-factor for the second doublet level E_1 (37.13 is independent of the strain:

$$g^*_\parallel = g_\perp, \quad g^*_\perp = \frac{g_\parallel + g_\perp}{2}. \tag{39.13}$$

For a [001] strain, the Zeeman splitting for a triplet level is determined, as before, by (39.10). Similar expressions for g-factors hold in the case of a [110] strain, provided we replace x by $\Xi_u \frac{e_{zz}-e_{xx}}{\Delta_2}$ in the expression for α in (37.14).

We now consider shallow donors in germanium. The g-factor for the singlet state is again isotropic,

$$g^* = \frac{g_\parallel + 2g_\perp}{3}.$$

The Zeeman splitting matrix for the triplet state, relative to the basis functions $\Psi^1_{F_1}$, $\Psi^2_{F_1}$, $\Psi^3_{F_1}$ (27.22), is

$$\begin{Vmatrix} \frac{g_\parallel+2g_\perp}{3}(\sigma H) & \frac{g_\parallel-g_\perp}{3}(\sigma_z H_y+\sigma_y H_z) & \frac{g_\parallel-g_\perp}{3}(H_x\sigma_z+H_z\sigma_x) \\ \frac{g_\parallel-g_\perp}{3}(\sigma_z H_y+\sigma_y H_z) & \frac{g_\parallel+2g_\perp}{3}(\sigma H) & \frac{g_\parallel-g_\perp}{3}(H_x\sigma_y+\sigma_x H_y) \\ \frac{g_\parallel-g_\perp}{3}(H_x\sigma_z+H_z\sigma_x) & \frac{g_\parallel-g_\perp}{3}(H_x\sigma_y+\sigma_x H_y) & \frac{g_\parallel+2g_\perp}{3}(\sigma H) \end{Vmatrix} \tag{39.14}$$

As noted above, under a [111] strain the triplet state splits into a onefold state E_2 (37.4) and a twofold degenerate state with energy $E_3 = E_4$ (37.3), while the state with energy E_2 is mixed with the singlet state with energy E_1.

The g-factor for the singlet and onefold degenerate states has two components $g^*_\parallel$ and $g^*_\perp$ relative to the strain direction:

$$\left.\begin{aligned} g^*_\parallel &= \frac{4}{3+\alpha^2}\left(\frac{g_\parallel+2g_\perp}{3}\right)+\frac{\alpha^2-1}{3+\alpha^2}g_\parallel, \\ g^*_\perp &= \frac{4}{3+\alpha^2}\left(\frac{g_\parallel+2g_\perp}{3}\right)+\frac{\alpha^2-1}{3+\alpha^2}g_\perp; \end{aligned}\right\} \text{ (singlet state } E_1\text{)}$$

$$\left.\begin{aligned} g^*_\parallel &= \frac{4\alpha^2}{3+\alpha^2}\frac{g_\parallel+2g_\perp}{9}+\frac{9-\alpha^2}{3(3+\alpha^2)}g_\parallel, \\ g^*_\perp &= \frac{4\alpha^2}{3+\alpha^2}\frac{g_\parallel+2g_\perp}{9}+\frac{9-\alpha^2}{3(3+\alpha^2)}g_\perp, \end{aligned}\right\} \text{ (state } E_2\text{)} \tag{39.15}$$

and α is given by (37.8a). For a zero strain, $\alpha = 1$; for a large strain, if $x \to -\infty$ then $\alpha \to \infty$, and if $x \to \infty$ then $\alpha \to 0$. In this case, we obtain for the singlet state

$$\begin{aligned} &g^*_\parallel = g_\parallel, \quad g^*_\perp = g_\perp && (x \to -\infty), \\ &g^*_\parallel = \tfrac{1}{9}(g_\parallel + 8g_\perp), \quad g^*_\perp = \frac{4g_\parallel+5g_\perp}{9} && (x \to \infty). \end{aligned} \tag{39.16}$$

Corresponding expressions for the g-factor of the E_2 level may be obtained from (39.16) by reversing the sign of the strain.

Degenerate bands

To determine the Zeeman splitting of acceptor levels in a degenerate band, we must replace $k_\alpha k_\beta$ in the kinetic energy matrix $\mathcal{H}(\boldsymbol{k})$ by the symmetrized product $[K_\alpha K_\beta]$ and in addition, according to (26.14) we must include in $\mathcal{H}$ the term

$$g_0\mu_0\left(\varkappa(\boldsymbol{JH})+\varphi\sum_i J_i^3 H_i\right). \tag{39.17}$$

Thus the interaction matrix in the linear magnetic field approximation for the degenerate Γ_8 band has the form

$$\mathcal{H}_H=\mu_0 g_0\left(\varkappa(\boldsymbol{JH})+\varphi\sum_i J_i^3 H_i\right)+\mu_0\mathcal{H}'_H, \tag{39.18}$$

where $\mathcal{H}'_H$ is obtained from the operator $\mathcal{H}(\boldsymbol{k})$ describing the hole spectrum in an ideal crystal by the substitution $k_\alpha k_\beta \to -i(A_\alpha\nabla_\beta + A_\beta\nabla_\alpha)$. In a nondegenerate band, in the case of an ellipsoidal isoenergy surface, $\mathcal{H}'_H$ corresponds to the second and third terms in (39.2).

To determine the Zeeman splitting of an impurity level we must evaluate the matrix of the operator $\mathcal{H}_H$ between the impurity center wave functions. Symmetry considerations imply that the resulting perturbation matrix $\mathcal{H}_H^{\text{im}}$ may be written in a form similar to (39.17):

$$\mathcal{H}_H^{\text{im}}=\mu_0\left(g_1(\boldsymbol{JH})+g_2\sum_i J_i^3 H_i\right). \tag{39.19}$$

The constants g_1 and g_2 in this equation may be expressed in terms of $\varkappa$, φ and the band parameters A, B and D.

Two remarks are in order here.

First, the constant φ for band holes is relativistic and must be small /20.1/, whereas the constant g_2 in (39.19) is not relativistically small and differs from zero even at $\varphi = 0$.

Second, the Zeeman splitting constants g_1 and g_2 also depend on the orbital parameters A, B, D, so that they do not vanish even at $\varkappa=\varphi=0$. In this sense the situation for an acceptor center is analogous to the case of free holes, for which the g-factor is determined primarily by the band parameters A, B, D. The constants g_1 and g_2 for Ge and Si are evaluated in /42.9, 42.10/. Calculations using the trial functions for the impurity center ground state /21.4/ show that for Ge

$$g_1=-8.49, \quad g_2=0.6, \tag{39.20}$$

whereas $g_0\varkappa = -6.82$, $g_0\varphi = -0.12$. The deviation of g_1, g_2 from $\varkappa$, φ (like that of d', b' from b, d) is due to the fact that the impurity center wave functions depend on the angles, so that, if we set $c_2=c_3=0$ in (27.23), then $g_1=g_0\varkappa$ and $g_2=g_0\varphi$. However, as Mendelson and James have shown /21.5/, the angular dependence of the trial function is highly sensitive to the method of calculation, and it is therefore difficult to estimate the error in g_1 and g_2 when an approximate wave function is used.

Diagonalizing the matrix (39.19), we obtain the splitting energy of the acceptor center in a magnetic field:

$$E_{1,2}=\pm\mu_0\Big\{\frac{H^2}{8}\Big[9\Big(g_1+\frac{9}{4}g_2\Big)^2+\Big(g_1+\frac{g_2}{4}\Big)^2\Big]+ +\Big(g_1+\frac{7}{4}g_2\Big)\Big[\Big(g_1+\frac{13}{4}g_2\Big)^2H^4-9g_2\Big(g_1+\frac{5}{2}g_2\Big)\times \times(H_x^2H_y^2+H_x^2H_z^2+H_y^2H_z^2)\Big]^{1/2}\Big\}^{1/2}, \tag{39.21a}$$

$$E_{3,4}=\pm\mu_0\Big\{\frac{H^2}{8}\Big[9\Big(g_1+\frac{9}{4}g_2\Big)^2+\Big(g_1+\frac{g_2}{4}\Big)^2\Big]- -\Big(g_1+\frac{7}{4}g_2\Big)\Big[\Big(g_1+\frac{13}{4}g_2\Big)^2H^4-9g_2\Big(g_1+\frac{5}{2}g_2\Big)\times \times(H_x^2H_y^2+H_x^2H_z^2+H_y^2H_z^2)\Big]^{1/2}\Big\}^{1/2}. \tag{39.21b}$$

If $g_2=0$, the energies $E_{1,2}=\pm\frac{3}{2}|g_1|\mu_0H$ belong to states with $m=\pm 3/2$, the energies $E_{3,4}=\pm\frac{|g_1|}{2}\mu_0H$ to states with $m=\pm 1/2$; the energies do not depend on the direction of $\boldsymbol{H}$.

If $g_2\neq 0$, the Zeeman splitting of the acceptor center depends on the direction of the magnetic field H:

when the direction of $\boldsymbol{H}$ is along [001]

$$E_{1,2}=\pm\frac{3}{2}\mu_0H\Big(g_1+\frac{9}{4}g_2\Big),\quad E_{3,4}=\pm\frac{\mu_0H}{2}\Big(g_1+\frac{g_2}{4}\Big); \tag{39.22}$$

when the direction of $\boldsymbol{H}$ is along [111]

$$E_{1,2}=\pm\frac{\mu_0H}{2}\sqrt{6\Big(g_1+\frac{9}{4}g_2\Big)^2+3\Big(g_1+\frac{5}{4}g_2\Big)^2}, \qquad E_{3,4}=\pm\frac{\mu_0H}{2}(g_1+3g_2) \tag{39.23}$$

In the general case, when $g_2\neq 0$ and the direction of $\boldsymbol{H}$ is arbitrary, paramagnetic transitions are allowed between all the split levels. The probabilities of transitions with selection rules $\Delta m=\pm 1$ (transitions $E_1\to E_3$, $E_3\to E_4$, $E_4\to E_2$) are proportional to g_1^2; the probabilties of other transitions are proportional to g_2^2, so that if $|g_2|\ll|g_1|$ these lines are much weaker.

To date, no observations have been recorded of paramagnetic resonance due to degenerate impurity centers in unstrained crystals. The reason is apparently its short lifetime, due to strong interaction with acoustical lattice modes, the considerable line broadening caused by strains arising from dislocations and other defects, and the electric field of charged impurities.

In the presence of an external strain, the operator $\mathcal{H}_H$ (39.18) must incorporate an operator $\mathcal{H}'(\varepsilon)$ describing the interaction of the impurity center with the strain, which is similar to (30.9). Then, using (27.62), we find that the splitting of the acceptor levels in the strained crystal is determined by the operator

$$\mathcal{H}'=\mu_0\Big(g_1(\boldsymbol{JH})+g_2\sum_i J_i^3H_i\Big)-a\varepsilon I+b'\sum_i\Big(J_i^2-\frac{5}{4}\Big)e_{ii}+\frac{d'}{\sqrt{3}}\sum_{i\neq j}[J_iJ_j]e_{ij}. \tag{39.24}$$

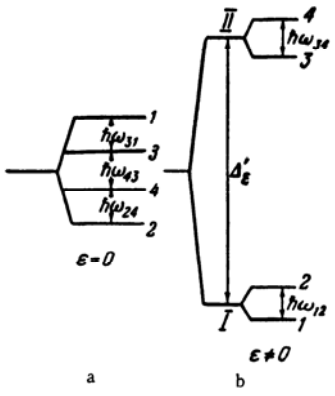

FIGURE 62. Splitting of the ground state of an acceptor center in a magnetic field: a) unstrained crystal, b) under large strains.

We first consider relatively small strains, when the strain-induced level splitting exceeds the spin splitting: $2\Delta_\varepsilon \gg \hbar\omega_s$ but $2\Delta_\varepsilon \ll E_i$. In this case the fourfold degenerate state of the acceptor center splits into two Kramers doublets. In a magnetic field, each of the Kramers doublets splits into two levels (see Figure 62b).

To determine the Zeeman splitting of each of the split-off Kramers doublets in the zeroth approximation with respect to $\hbar\omega_s/\Delta_\varepsilon$, we must evaluate the operator $\mathcal{H}_H$ (39.19) in a new representation which diagonalizes $\mathcal{H}'(\varepsilon)$. The calculation yields the following value of the Zeeman splitting $\Delta E_{1,2}$ in the strained crystal /40.4/:

$$\Delta E_{1,2} = \mu_0 \sum_{\alpha\beta} (H_\alpha g^{1,2}_{\alpha\beta} H_\beta)^{1/2}, \tag{39.25}$$

where

$$g^{1,2}_{xx} = \frac{1}{\mathscr{E}_\varepsilon}\left\{\left[\pm\sqrt{\mathscr{E}_\varepsilon}\left(g_1+\frac{13}{4}g_2\right)+b'(\mathrm{Tr}\,\varepsilon-3\varepsilon_{xx})\left(g_1+\frac{7}{4}g_2\right)\right]^2+\right.$$
$$\left.+3d'^2(\varepsilon_{xy}^2+\varepsilon_{xz}^2)\left(g_1+\frac{9}{4}g_2\right)\left(g_1+\frac{1}{4}g_2\right)\right\}, \tag{39.26a}$$
$$g^{1,2}_{xy} = \frac{\sqrt{3}d'}{\mathscr{E}_\varepsilon}\left\{\sqrt{3}d'\varepsilon_{xz}\varepsilon_{yz}\left(g_1+\frac{9}{4}g_2\right)^2+\right.$$
$$+\varepsilon_{xy}\left(g_1+\frac{7}{4}g_2\right)\left[\mp 2\sqrt{\mathscr{E}_\varepsilon}\left(g_1+\frac{7}{4}g_2\right)+\right.$$
$$\left.\left.+b'(\mathrm{Sp}\,\varepsilon-3\varepsilon_{zz})\left(g_1+\frac{13}{4}g_2\right)\right]\right\}. \tag{39.26b}$$

The other components $g^{1,2}_{\alpha\beta}$ are obtained from (39.26) by cyclic permutation of the indices x, y, z. The indices 1 and 2 in (39.25) and (39.26) refer to the states with hole energy $\mp\sqrt{\mathscr{E}_\varepsilon}$, respectively.

As follows from (39.26), in the strained crystal the g-factor of each of the split-off levels is anisotropic and depends sensitively on the direction

and sign of the strain. For a strain along [001] and [111], the g-factor has two components $g_\parallel$ and $g_\perp$ relative to the strain direction; their values for the lower level (level 1) are given in Table 39.1, depending on the sign of the strain. The g-factors for the upper level are obtained from these values by reversing the sign of the strain.

TABLE 39.1

	[001]		[111]	
	$b'e'_{zz}>0$	$b'e'_{zz}<0$	$d'e'_{111}>0$	$d'e'_{111}<0$
$g_\parallel$	$g_1+\frac{1}{4}g_2$	$3\left(g_1+\frac{9}{4}g_2\right)$	$g_1+\frac{13}{4}g_2$	$3\left(g_1^2+\frac{23}{6}g_1g_2+\frac{187}{48}g_2^2\right)^{1/2}$
$g_\perp$	$2g_1+5g_2$	$\frac{3}{2}g_2$	$2g_1+\frac{7}{4}g_2$	0

Using the acceptor center wave functions in the strained crystal, we can compute the squared absolute value of the matrix element of a paramagnetic transition caused by a high-frequency field $\boldsymbol{h}(t)=\boldsymbol{h}\cos\omega t$. The perturbation operator is

$$\mathcal{H}_h=\mu_0\cos\omega t\left[g_1(J\boldsymbol{h})+g_2\sum_i J_i^3h_i\right]. \tag{39.27}$$

The matrix element defining the transition probability is

$$|\mathcal{H}_{h,\,12}|^2=\frac{\mu_0^2}{4}\frac{(H_\alpha g^{1,2}_{\alpha\beta}H_\beta)(h_\alpha g^{1,2}_{\alpha\beta}h_\beta)-(H_\alpha g^{1,2}_{\alpha\beta}h_\beta)^2}{(H_\alpha g^{1,2}_{\alpha\beta}H_\beta)}. \tag{39.28}$$

The transition probabilities display a fairly complicated angular dependence, determined by the orientation of the constant and high-frequency magnetic fields relative to the crystal axes. In the case of a strain along the principal axes, (39.28) becomes

$$|\mathcal{H}_{h,\,12}|^2=\mu_0^2\frac{(g_\parallel^{1,2})^2[H\times h]_\perp^2+(g_\perp^{1,2})^2[H\times h]_\parallel^2}{(g_\parallel^{1,2})^2H_\parallel^2+(g_\perp^{1,2})^2H_\perp^2}(g_\perp^{1,2})^2. \tag{39.29}$$

This implies that the transition probability vanishes at $g_\perp=0$, as is the case, e.g., for a [111] strain with $d'e'_{111}<0$.

It is highly significant that the conditions for observation of paramagnetic resonance are considerably more favorable in a strained crystal than otherwise, since under a strain the line-broadening mechanisms are significantly weakened. Since the strain and the electric field alone cannot cause splitting of Kramers levels, their effect may be sensed only through consideration of another split-off level, which reduces the heterogeneous line broadening by a factor of $\Delta_s/\hbar\omega$ /40.4/.

Paramagnetic resonance at acceptor levels in strained crystals of Si was first observed in /42.1/, under a compression along [001]. Figure 63

shows the appearance of a paramagnetic resonance line when a strain is applied. The experimental dependence of the position of the line for different acceptors, as shown in Figure 64, is well described by the two components $g_\parallel$ and $g_\perp$ of the g-factor. To determine g_2 and g_1 from (39.25)–(39.26) using experimental data, we need the signs of the constant b' and of the ratio $g_\parallel/g_\perp$. Depending on these signs, one obtains four systems of values g_1 and g_2 from the known values of $|g_\parallel|$ and $|g_\perp|$.

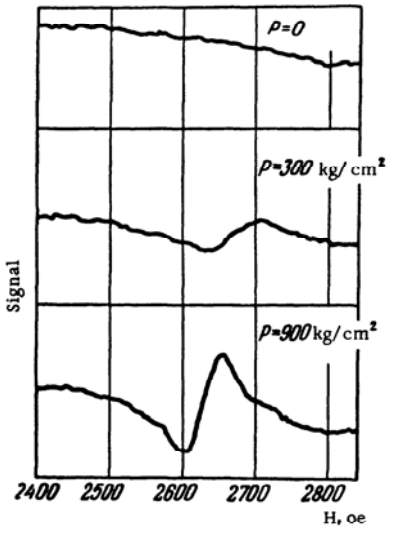

FIGURE 63. Paramagnetic resonance at acceptor centers in strained Si /42.1/. T = 1.3°K, ν = 9065 MHz.

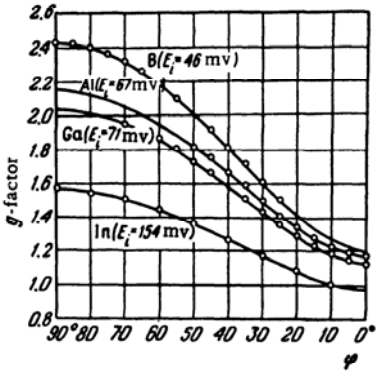

FIGURE 64. g-factor of acceptor center in strained Si vs. angle φ between magnetic field and strain direction /42.1/. T = 1.3 °K $\nu \approx$ 900 MHz.

If the values of $g_\parallel$ and $g_\perp$ for a [111] strain were known, it would be possible to determine g_1 and g_2 uniquely. These data are not given in /42.1/, but the authors note that the values of $g_\parallel$ and $g_\perp$ for a [111] strain are close to their values for a [001] strain. It follows from Table 39.1 that this situation is possible only if $b' < 0$, $d' < 0$, $g_\perp/g_\parallel > 0$ and $|g_2| \ll |g_1|$. These conditions agree with the theoretical estimates, since according to Table 37.1 the signs of b', d' coincide with those of b and d, and it is known from other experiments that $b < 0$ and $d < 0$ in Si. The inequality $|g_2| \ll |g_1|$ follows, as shown previously, from theoretical estimates using trial functions.

TABLE 39.2

	B	Al	Ga	In
g_1	−1.21	−1.19	−1.14	−1.00
g_2	0.002	0.047	0.051	0.087

Table 39.2 presents values of g_1 and g_2 calculated from the experimental data in /42.1/ for various acceptors in Si. The sign of g_1 cannot be determined from the experimental data, but we may expect it to coincide with the sign of κ; according to /20.1/, $\kappa < 0$ in silicon. The table shows that $|g_1|$ decreases and $|g_2|$ increases, with increasing ionization energy of the acceptors.

For large strains, $\Delta_s \gg E_l$, the acceptor center energy levels correspond, as noted in §26, to a simple ellipsoidal band, and the g-factor is given by (39.26) with g_1 and g_2 replaced by $g_{0\gamma}$ and $g_{0\delta}$, respectively.

§40. EFFECT OF STRAIN ON OPTICAL PROPERTIES OF EXCITONS IN SEMICONDUCTORS

One of the most effective methods of exciton research is to exploit the optical effects associated with the excitation of exictons. Measurement of the change in the absorption or reflection coefficient in the region of exciton transitions enjoys several advantages over direct observation of interband transitions, while yielding practically the same information about the band structure in the case of shallow excitons.

Since the original state of the crystal without the exciton is completely symmetric, the general selection rules for direct excitons allow optical dipole transitions to occur only to exciton states which transform like the components of the vector $\boldsymbol{p}$ (or $\boldsymbol{r}$), i. e., states belonging to the representation $\mathcal{D}_1^-$ in cubic groups or the representations split off from $\mathcal{D}_1^-$ in groups of lower symmetry. Similarly, magnetic dipole transitions are allowed to states which transform like the components of the pseudovector $[\boldsymbol{rp}]$ or $\boldsymbol{H}$, i. e., states belonging to representations which split off from $[\mathcal{D}_1^- \times \mathcal{D}_1^-] = -\mathcal{D}_1^+$. Quadrupole transitions are allowed to states which transform like symmetrized products $[r_\alpha p_\beta]$, i. e., to representations splitting off from the representations $\{\mathcal{D}_1^- \times \mathcal{D}_1^-\} = \mathcal{D}_1^+ + \mathcal{D}_3^+$. In the case of shallow excitons the probability of a transition to an allowed state depends essentially on whether the transition between the corresponding bands at the extremum point is allowed. If it is allowed, the line will be relatively strong. For this reason, quadrupole and magnetic dipole transitions, whose intensities are significantly lower than dipole transitions, may apparently be observed only when the corresponding interband transitions are allowed.*

If the interband transition is forbidden at the extremum, the matrix element of a transition between states with $\boldsymbol{k} \neq 0$ is proportional to the first (or higher) power of $\boldsymbol{k}$ (see (36.3)). Since exciton states are superpositions of states with $k \approx (2m^* E_0/\hbar^2)^{1/2}$, where E_0 is the exciton binding energy, the intensity of the transition will then be proportional to the first (or higher) power of E_0/E_g' where E_g' is the separation to the nearest band to which a transition is allowed from both the conduction and valence bands. In this case the excitation of an exciton may be regarded as a virtual transition through one or more intermediate bands.

The absorption coefficient or the corresponding conductivity tensor σ associated with exciton excitation may be calculated from the general formula (36.1a).

* To date, quadrupole transitions have been observed only in one crystal, cuprous oxide /43.1, 43.2/.

In the effective mass approximation, where the exciton function is expressed as a superposition of valence band hole states (n, k_2) and conduction band electron states (m, k_1), the matrix element of the current operator for a transition from the ground state of the crystal to a given exciton state l may be expressed as the corresponding superposition of matrix elements for the transition of an electron from state $K(n, k_2)$ to state (m, k_1), since, as seen in §27, the formation of a hole in state (n, k_2) is the excitation of an electron from the state $K\psi_{nk_2} = \psi_{K(nk_2)}$. As shown in the supplement to this section,

$$j_l(q) = \sum_{mnk_1} C^{*l}_{mk_1,\, n,\, q-k_1} j_{mKn}(k_1, q), \tag{40.1}$$

where

$$j_{mKn}(k, q) = j_{mk,\, K(n,\, q-k)} = \frac{1}{\mathcal{V}} \langle \psi_{mk} j(q) K\psi_{n,\, q-k} \rangle.$$

We have used the fact that, by (36.3), the interband matrix element of the current operator differs from zero only when $k_2 = q - k_1$, i. e., when the total momentum of the electron-hole pair is $\mathcal{K} = k_1 + k_2 = q$.

By (27.51), the coefficients $C_{mk_1,\, nk_2}$ are the expansion coefficients of the exciton function $F_{mn}(r_1, r_2)$ in the effective mass approximation:

$$F^l_{\mathcal{K},\, mn}(r_1, r_2) = \frac{1}{\sqrt{\mathcal{V}}} e^{i\mathcal{K}\mathcal{R}} f^l_{\mathcal{K},\, mn}(r) = \frac{1}{\mathcal{V}} \sum_{k_1 k_2} C^l_{mk_1,\, nk_2} e^{i(kr + \mathcal{K}\mathcal{R})} \tag{40.2}$$

and so

$$f^l_{0,\, mn}(r) = \frac{1}{\sqrt{\mathcal{V}}} \sum_k C^l_{mk,\, n-k} e^{ikr}. \tag{40.3}$$

By (36.1a),

$$\sigma^{ex}_{\alpha\beta}(\omega) = \frac{\pi}{\hbar\omega\mathcal{V}} \sum_l j^l_\alpha(-q)\, j^{*l}_\beta(q)\, \delta(\omega - \omega_l). \tag{40.4}$$

The summation is performed over all exciton states with the given energy $\hbar\omega_l = E_g - E_l$.

In the case of nondegenerate bands, when equations (27.63) reduce to one equation for the single function $f(r)$ (not counting the exchange interaction), the coefficients $C_{mk_1,\, nk_2}$ are independent of the indices m and n, and we may take each exciton state l to be the state corresponding to a definite pair m, n, and summation over l may be replaced by summation over m and Kn, which in this case is equivalent to summation over m and n:

$$\sigma^{ex}_{\alpha\beta}(\omega) = \frac{\pi}{\hbar\omega\mathcal{V}} \sum_{kk'} C_{k,\, -k} C^*_{k',\, -k'} \sum_{mn} j^\alpha_{mn}(k, -q)\, j^\beta_{nm}(k', q)\, \delta(\omega - \omega_l). \tag{40.5}$$

If interband transitions are allowed at the extremum point, the matrix elements j_{mn} may be viewed to a first approximation as constants which do

not depend on k, and then

$$\sigma_{\alpha\beta}^{ex}(\omega) = \frac{\pi}{\hbar\omega} |f^0(0)|^2 \sum_{mn} j_{mn}^{\alpha}(-q) j_{nm}^{\beta}(q) \delta(\omega - \omega_l), \tag{40.6}$$

since, by (40.3),

$$\frac{1}{V} \sum_{kk'} C_{k',-k'}^{*} C_{k,-k} = f^0(0) f^{0*}(0).$$

By (36.3b), for dipole transitions,

$$j_{mn}^{\alpha} = e\pi_{mn}^{\alpha}/m.$$

In the case of spherical bands it follows from (36.4) that $j^{\alpha} = es\rho_{\nu}\sigma_{\alpha}$, and

$$\sigma_{\alpha\beta}^{ex}(\omega) = \frac{2\pi}{\hbar\omega} e^2 s^2 |f(0)|^2 \delta_{\alpha\beta} \delta(\omega - \omega_l), \tag{40.7}$$

since

$$\sum_{mn} \sigma_{mn}^{\alpha} \sigma_{nm}^{\beta} = \mathrm{Tr}(\sigma_{\alpha}\sigma_{\beta}) = 2\delta_{\alpha\beta}. \tag{40.8}$$

In this approximation only excitons in the s-state may be excited, since only for these does $f(0)$ fail to vanish. For these states

$$|f_n(0)|^2 = \frac{1}{\pi a_0^3 n^3}, \text{ where } a_0 = \frac{\hbar^2 \varkappa}{me^2}, \tag{40.9}$$

and so

$$\sigma_{\alpha\beta}^{n}(\omega) = \frac{2e^2 s^2}{a_0^3 n^3 \hbar} \delta_{\alpha\beta} \delta(\omega - \omega_n). \tag{40.10}$$

If the constant energy surfaces are coaxial ellipsoids, the tensor $\sigma_{\alpha\beta}^{ex}$, referred to principal axes, also has only diagonal components; by (36.5), the constant s in (40.7) must then be replaced for each component by s_{α}.

Let us now consider the case that only transitions between states with $k \neq 0$ are allowed and the matrix element of the transition is proportional to k:

$$j_{amn}(k) = \sum_{\alpha'} R_{mn}^{\alpha\alpha'} k_{\alpha'}, \tag{40.11}$$

where, by (46.3b),

$$R_{mn}^{\alpha\alpha'} = \frac{e\hbar}{m^2} \sum_{s} \frac{\pi_{ms}^{\alpha} \pi_{sn}^{\alpha'}}{E_m - E_s} + \frac{\pi_{ms}^{\alpha'} \pi_{sn}^{\alpha}}{E_n - E_s}. \tag{40.11a}$$

Substituting (40.11) into (40.5), we obtain

$$\sigma_{\alpha\beta}^{ex}(\omega) = \frac{\pi}{\hbar\omega}\sum_{\alpha'\beta'}\frac{\partial f^*(0)}{\partial x_{\alpha'}}\frac{\partial f(0)}{\partial x_{\beta'}}\sum_{mn}R_{mn}^{\alpha\alpha'}R_{nm}^{\beta\beta'}\delta(\omega-\omega_l), \tag{40.12}$$

since, according to (40.3),

$$\frac{1}{V}\sum_{kk'}C_{k'}^{*}{}_{,\,-k'}k_\alpha' C_{k,\,-k}k_\beta = \left(\frac{\partial f^*}{\partial x_\alpha}\right)_{x=0}\left(\frac{\partial f}{\partial x_\beta}\right)_{x=0}.$$

In the case of spherical bands, we have from (36.4) that

$$j_\alpha = \frac{e\hbar}{m^*}\theta\rho_x(\sigma_{\alpha+1}k_{\alpha+2}+\sigma_{\alpha+2}k_{\alpha+1}),$$

and so, in view of (40.8), we find that

$$\begin{aligned}\sigma_{\alpha\beta}^{ex} = \frac{2\pi e^2\hbar^2\theta^2}{\hbar\omega m^{*2}}\Big[\delta_{\alpha\beta}\Big(\Big|\frac{\partial f(0)}{\partial x_{\alpha+1}}\Big|^2+\Big|\frac{\partial f(0)}{\partial x_{\alpha+2}}\Big|^2\Big)+\\ +\delta_{\alpha+1,\,\beta}\frac{\partial f^*(0)}{\partial x_\alpha}\frac{\partial f(0)}{\partial x_{\alpha+1}}+\delta_{\alpha+2,\,\beta}\frac{\partial f^*(0)}{\partial x_\alpha}\frac{\partial f(0)}{\partial x_{\alpha+2}}\Big]\delta(\omega-\omega_l).\end{aligned} \tag{40.13}$$

For hydrogenic functions, the derivative $\frac{\partial f(0)}{\partial x_\alpha}$ differs from zero only for p-like functions, and moreover, there is only one nonzero derivative for each of the three functions X, Y, Z: the derivative with respect to x, y, z, respectively. We than have

$$|\nabla f_n(0)|^2 = \left|\frac{\partial X_n}{\partial x}\right|^2_{x\to 0} = \frac{n^2-1}{3\pi a_0^5 n^5}. \tag{40.14}$$

Thus, only transitions to two of the three p-like functions, namely $X_{\alpha+1}$ and $X_{\alpha+2}$, contribute to each of the diagonal components $\sigma_{\alpha\alpha}$, and the off-diagonal components $\sigma_{\alpha\beta}$ vanish. Consequently, summing (40.13) over all p-states, we finally obtain

$$\sigma_{\alpha\beta}^{ex} = \frac{4\pi e^2\hbar^2\theta^2}{\hbar\omega m^{*2}}\delta_{\alpha\beta}|\nabla f(0)|^2\delta(\omega-\omega_l) \tag{40.15}$$

or, in view of (40.14),

$$\sigma_{\alpha\beta}^{n} = \frac{4}{3}\frac{e^2\hbar\theta^2}{\omega m^{*2}}\frac{n^2-1}{a_0^5 n^5}\delta_{\alpha\beta}\delta(\omega-\omega_n). \tag{40.15a}$$

If the constant energy surfaces are ellipsoids of revolution, the p-state splits into X, Y and Z states. The component σ_{zz} then differs from zero only for transitions to the X and Y states and is determined by a formula differing from (40.15) in the substitution of $\theta_y^2=\theta_x^2$ for θ^2 (see equation (36.5)); the component σ_{xx} (σ_{yy}) differs from zero for transitions to the Y or X state (Z state) and is determined by a formula differing from (40.5) in the substitution of $\theta_z^2+\theta_x^2$ for $2\theta^2$.

If the matrix element of a transition is proportional to k^2, only excitons in the d state for which the second derivative $\frac{\partial^2 f(0)}{\partial x_\alpha \partial x_\beta}$ differs from zero will be excited.

We shall now consider the effect of a strain on the exciton spectrum, and how it is manifested in optical effects. We shall first neglect exchange splitting, since, as will be seen further on, it appears only under special conditions.

Nondegenerate bands

In the case of nondegenerate bands, a shift of exciton lines corresponds to a change in the band gap, since the comparatively small change in effective mass has practically no effect on the activation energy of an exciton.*

As an example, Figure 65 illustrates how the activation energy of excitons in CdS changes for different strain directions /43.7/. The three lines A, B, C correspond to three excitons formed by an electron-hole pair in one of the three valence bands. If we neglect the strain-induced change in the exciton binding energy, the behavior of these lines corresponds to the relative change in the separation from the conduction band to the three valence bands and is described by equations (31.23), (31.24) and (31.15). The terms proportional to ε_{zz} and $\varepsilon_{xx}+\varepsilon_{yy}$ in these equations are accurate, but those proportional to $\varepsilon_{xx}-\varepsilon_{yy}$, ε_{xy}, ε_{xz} and ε_{yz} are accurate only up to ε^2. If the separation $E_A^0 - E_B^0$ of the two lowest-lying levels is much less than the separation $E_A^0 - E_C^0$ to the third level, which, by (31.16) and (31.17), is the case when

$$\frac{2\Delta_{cr}\Delta_{so}}{3(\Delta_{cr}+\Delta_{so})^2} \ll 1, \tag{40.16}$$

we can derive a more accurate expression for these low-lying levels, valid for any strain under which the shift of these levels remains small compared to the separation to the third level. If we omit the matrix elements associated with the third level in (31.19), the eigenvalues $E_{1,2}$ will be given by a formula similar to (24.14):

$$E_{1,2}=\frac{E_1^1+E_2^1}{2} \pm \left\{\left(\frac{E_1^1-E_2^1}{2}\right)^2+|\gamma|^2+|\delta|^2\right\}^{1/2}. \tag{40.17}$$

* When the exciton binding energy is comparable with the separations between the nearest bands, as is the case, for example, for many wurtzite-type crystals, the exciton state is a superposition of states of different bands. A change in the interband separation may then significantly alter their contribution to the state in question and consequently cause a change in the ionization energy. At such small interband separations, the strain-induced change in effective masses may also be significant. However, since the exciton binding energy in these crystals is determined as a rule by the effective electron mass, which is much smaller than effective hole mass, we may usually disregard the change in ionization energy for these crystals. As for the polarization dependence considered below, the contribution of several nearest bands to the exciton state cannot lead to forbidden transitions becoming allowed, since their being forbidden depends only on the symmetry of the exciton state; however, the ratio of the intensities for the allowed polarizations may then change.

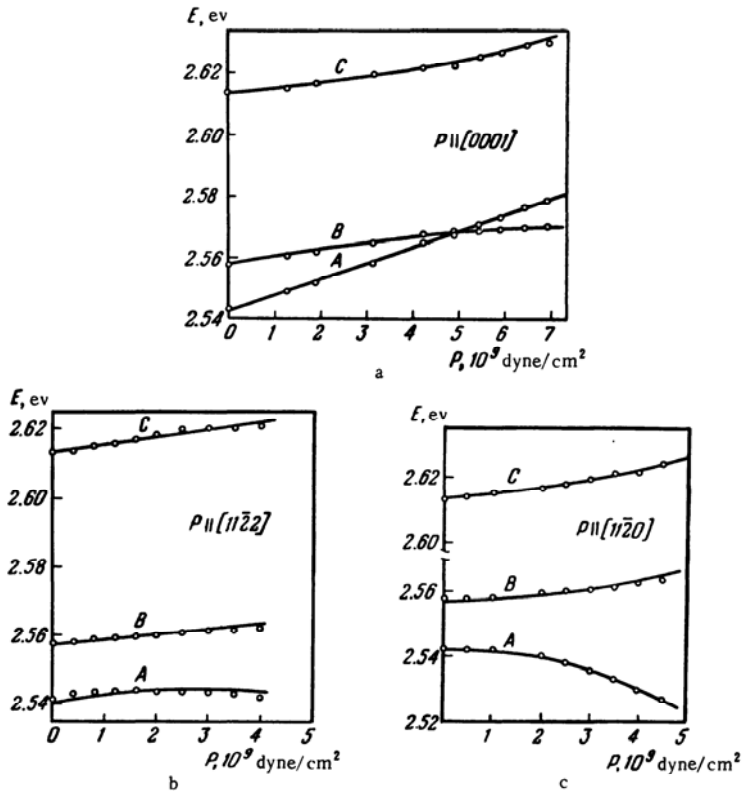

FIGURE 65. Exciton activation energy in CdS vs. stress for different stress directions /43.7/. T = 77°K.

We see from this formula that levels 1 and 2 may intersect, as is the case in Figure 65a, only for strains $\varepsilon_{zz} \neq 0$ or $\varepsilon_{xx} + \varepsilon_{yy} \neq 0$, when the values of E_1^1 and E_2^1 determined by (31.15), (31.14) are comparable. On the other hand, for strains corresponding to the curves in Figure 65b and c, when the components $\varepsilon_{xx} - \varepsilon_{yy}$, ε_{xy}, ε_{xz} or ε_{yz} do not vanish, the constants appearing in (40.17),

$$|\gamma|^2 = \frac{(G - E_2^1)^2 D_6^2 (\varepsilon_{xz}^2 + \varepsilon_{yz}^2)}{(G - E_2^1)^2 + \Delta^2}, \quad |\delta|^2 = \frac{\Delta D_6^2 [(\varepsilon_{xx} - \varepsilon_{yy})^2 + 4\varepsilon_{xy}^2]}{(G - E_2^1)^2 + \Delta^2}, \tag{40.18}$$

differ from zero and the terms cannot intersect.

The deformation potential constants for CdS may be determined from the curves in Figure 65. In so doing, though, one should remember that in the region where the energy spacing is comparable with exchange splitting the exchange interaction must be included in the calculation of strain-induced effects. The corresponding data in Table 40.3 were obtained in /43.17/, with allowance for the exchange interaction.

The strain-induced line shift is accompanied by a change in the transition intensities for different polarizations. As is clear from equation (40.6), the polarization dependence of σ^{ex} is determined by the polarization dependence of the interband transitions.

In the linear ε approximation the current operator matrix element $\tilde{f}_{mn}$, which determines the probability of a transition from a valence band state n to a conduction band state m in the strained crystal, is, by the general formula (15.51),

$$\tilde{f}^{\alpha}_{mn} = f^{\alpha}_{mn} + \sum_{n'} \frac{f^{\alpha}_{mn'} \mathcal{H}_{n'n}(\varepsilon)}{E_n - E_{n'}}. \qquad (40.19)$$

where f^{α}_{mn} is the matrix element in the unstrained crystal, which is, according to (36.3),

$$f^{\alpha}_{mn} = \frac{e}{\hbar} \frac{\partial}{\partial k_\alpha} \mathcal{H}_{mn}(k).$$

Here $\mathcal{H}(k)$ is the "interband" matrix (31.29) and the $\mathcal{H}_{n'n}(\varepsilon)$ in (40.19) are the matrix elements of the intraband matrix (31.19). For example, under strains which break the lattice symmetry the excitation of an exciton associated with the highest lattice band (A), which belongs to the representation Γ_9, is also possible for longitudinal polarization $\mathcal{E} \| C$. It is evident from Table 31.6 that in the unstrained crystal such transitions are forbidden. Substituting the matrix elements from (31.19), (31.29) into (40.6), (40.19) and using (31.21a), we find the relative intensity of such transitions in the strained crystal:

$$\frac{\sigma^{ex}_{zz}}{\sigma^{ex}_{xx}} = \frac{2P_1^2}{P_2^2} \frac{D_6^2 (E_1^0 - E_2^0 - E_3^0)^2 (\varepsilon_{xz}^2 + \varepsilon_{yz}^2) + D_5^2 \Delta^2 [(\varepsilon_{xx} - \varepsilon_{yy})^2 + 4\varepsilon_{xy}^2]}{[(E_1^0 - E_2^0)(E_1^0 - E_3^0)]^2}. \qquad (40.20)$$

Here E_i^0 is the position of the corresponding extremum in the unstrained crystal, given by (31.16).

Degenerate bands

In the degenerate model, determination of the exciton spectrum in strained crystals requires solution of the system of equations (27.63), with the operator $\mathcal{H}$ incorporating terms proportional to ε, as in the treatment of impurity centers in §37. Again, as in the latter case, we must distinguish two cases.

Under small strains the splitting of degenerate exciton states does not coincide with the band splitting, but is determined by a matrix $\mathcal{H}(\varepsilon)$ similar to (37.16).

If we use trial functions of the type (27.23) for the ground state of a direct exciton in Ge, the relationship of the constants b' and d', which determine the splitting of this state under small strains, to the band constants

b and d is described by equations similar to (37.17) ($c_4 = 0$ as $\Delta \to \infty$):

$$b' = b(c_1^2 - c_3^2), \quad d' = d\left(c_1^2 - c_2^2 - \frac{c_3^2}{3}\right). \tag{40.21}$$

The constant a' defining the exciton level shift under an isotropic strain is the sum of the constants $-a + c$ which determine the change in the band gap.

For large strains, when the band splitting exceeds the exciton binding energy, each of the split bands corresponds to a fixed group of exciton levels which are shifted together with the band. The binding energy of each of these levels is determined by the effective mass of the band, and therefore the ground state binding energies for the split excitons are generally different and differ from the binding energy in the unstrained crystal. If the anisotropy of the reduced mass tensor (27.85) is low (as it is in Ge, owing to the small effective electron mass compared to the hole masses), these energies are close together. Thus, for a trial function of type (27.17) it follows from equations (27.18), (27.19) that for a small anisotropy

$$x = \frac{\bar{m}_\parallel - \bar{m}_\perp}{\bar{m}} = \left(\frac{1}{\bar{m}}\right)^{-1}\left(\frac{1}{\bar{m}_\perp} - \frac{1}{\bar{m}_\parallel}\right)$$

the exciton binding energy is

$$E_0 = E_0(\bar{m})\left(1 - \frac{x^2}{10}\right) = E_0\left(\frac{\overline{1}}{\bar{m}}\right)\left(1 + \frac{x^2}{10}\right). \tag{40.22}$$

Here $E_0(\bar{m})$ and $E_0\left(\frac{\overline{1}}{\bar{m}}\right)$ are the "isotropic exciton" binding energies $e^4m/2\bar{\kappa}^2\hbar^2$ for $m = \bar{m}$ and $m = \left(\frac{\overline{1}}{\bar{m}}\right)^{-1}$, respectively, where

$$\bar{m} = \tfrac{1}{3}(\bar{m}_\parallel + 2\bar{m}_\perp), \quad \left(\frac{\overline{1}}{\bar{m}}\right) = \tfrac{1}{3}\left(\frac{1}{\bar{m}_\parallel} + \frac{2}{\bar{m}_\perp}\right).^*$$

Since, as we see from equation (30.18), the average inverse hole mass $(\overline{1/\bar{m}_n})$ in both split bands in strained Ge is $(2/\hbar^2)|A|$ for any strain, it follows that always

$$\left(\frac{\overline{1}}{\bar{m}}\right) = \frac{1}{m_e^*} + \frac{2}{\hbar^2}|A|$$

and if the anisotropy is $x \leqslant 0.5$ the binding energies in the two split-off bands differ by at most two to three percent. Hence, as is clear from

* If the dielectric constant is also anisotropic, as is the case, for example, in crystals with wurtzite structure, equation (40.22) is valid with

$$\left(\frac{\overline{1}}{\bar{m}}\right) = \frac{1}{3}\left(\frac{2}{\bar{m}_\perp} + \frac{\varkappa_\perp}{\varkappa_\parallel}\frac{1}{\bar{m}_\parallel}\right), \quad \bar{\varkappa} = (\varkappa_\parallel \varkappa_\perp^2)^{1/3}, \quad x = \left(\frac{\overline{1}}{\bar{m}}\right)^{-1}\left(\frac{1}{\bar{m}_\perp} - \frac{\varkappa_\perp}{\varkappa_\parallel}\frac{1}{\bar{m}_\parallel}\right). \tag{40.22a}$$

Figure 66 /43.8/, the straight lines representing the behavior of the exciton levels under a strain "nearly" intersect at $\varepsilon = 0$, and the experimental points lie on one straight line under both compression and tension; this would not have been the case had there been a significant change in the reduced effective masses.

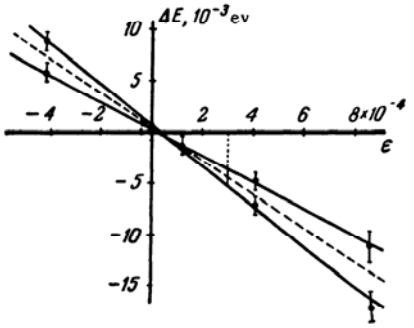

FIGURE 66. Splitting of the ground state of direct exciton in Ge under a [111] strain /43.8/.

For indirect excitons in Ge and Si we must also allow for the difference in the shifts experienced by different conduction band extrema, along with the valence band splitting. Therefore, under an arbitrary strain, the ground state in Ge splits into eight levels and in Si into six levels. Under a strain along the principal axes, when all or some of the extrema are shifted uniformly, the number of split levels is smaller. For sufficiently large strains, each pair of split-off bands corresponds to a specific exciton, whose shift is determined by the shift of the corresponding bands.

For example, for Ge strained along the [100] axis, when the conduction band does not split, there are two levels, whose splitting is determined by the valence band:

$$\Delta E_{1,2} = E_{1g}\varepsilon \pm b\varepsilon'_{zz}. \tag{40.23}$$

Under a [111] strain the conduction band splits: three extrema are shifted in one direction and one in the other. Thus four lines are observed, with

$$\Delta E_{1-4} = E_{1g}\varepsilon \pm \frac{d}{\sqrt{3}}\varepsilon'_{111} + \frac{2}{9}\Xi_u\varepsilon'_{111}(1 \pm 2). \tag{40.24}$$

A similar picture is observed under a strain along [110], when two conduction band extrema are shifted downward and two upward (Figure 67) /43.10/.

By contrast, the exciton level for Si splits under a [111] strain into two (Figure 68) /43.10/. Here

$$\Delta E_{1,2} = E_{1g}\varepsilon \pm \frac{d}{\sqrt{3}}\varepsilon'_{111}, \tag{40.25}$$

while a [100] strain gives rise to four levels with

$$\Delta E_{1-4} = E_{1g}\varepsilon \pm b\varepsilon'_{zz} + \frac{1}{6}\Xi_u\varepsilon'_{zz}(1 \pm 3). \qquad (40.26)$$

Under a [110] strain the exciton level splits into four, as in Ge.

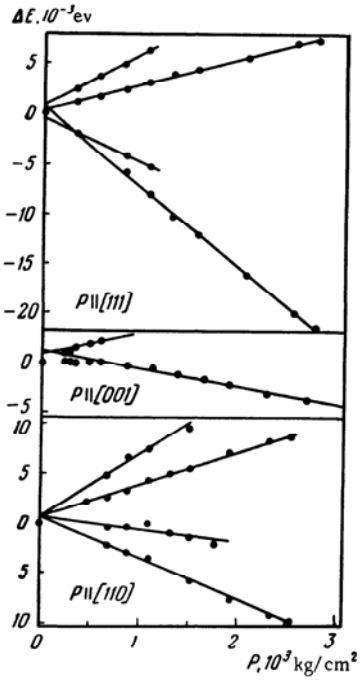

FIGURE 67. Splitting of ground state of indirect exciton in Ge under strains along [111], [001], [110] /43.10/. T = 80°K, $E_g - E_0$ = 0.761 ev.

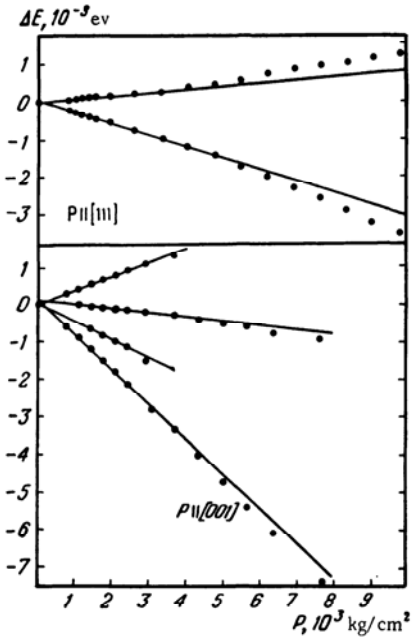

FIGURE 68. Splitting of ground state of indirect exciton in Si under strains along [111] and [001] /43.10/. T = 80°K, $E_g - E_0$ = 1.210 ev.

We reiterate that equations (40.23) – (40.26) are valid for those strains under which the band splitting considerably exceeds the exciton binding energy. The binding energies of excitons belonging to different bands may differ slightly.

Table 40.1 presents the binding energies of E_0 of excitons for different extrema of the conduction band and two valence subbands, calculated by means of equations (27.18). When all three masses were different, the two closest together were assumed equal and replaced by the average $\frac{1}{m} = \frac{1}{2}\left(\frac{1}{m_1} + \frac{1}{m_2}\right)$. The table also lists the deviations of these energies from their values according to the hydrogenic equation (27.14) with isotropic mass

$\frac{1}{m}=\frac{1}{3}\left(\frac{1}{m_1^e}+\frac{2}{m_\perp^e}+\frac{3}{m^h}\right)$, where $\frac{1}{m^h}=\frac{2}{\hbar^2}|A|$. In certain cases the ratio $\Delta E_0/E_0$ may reach 20%. Thus equations (40.23)–(40.26) determine the slope of each of the straight lines in Figures 67 and 68, but not the distance between different lines, which also includes the difference in binding energies. The difference in these energies is the reason that these straight lines intersect at different points and not at $\varepsilon = 0$.

TABLE 40.1

Substance		Si				Ge			
positions of minima		[001], [00$\bar{1}$]		[100], [010] [$\bar{1}$00], [0$\bar{1}$0]		[111]		[11$\bar{1}$], [$\bar{1}$11], [1$\bar{1}$1]	
shape of valence band ellipsoids		prolate	oblate	prolate	oblate	prolate	oblate	prolate	oblate
[001] strain	E_0, mev	12.3	12.0	12.4	12.1	2.6	2.5	2.6	2.5
	ΔE_0, mev	-0.4	-0.7	-0.3	-0.6	-0.4	-0.5	-0.4	-0.5
[111] strain	E_0, mev	12.5	12.0	12.5	12.0	3.4	2.5	2.5	2.7
	ΔE_0, mev	-0.2	-0.7	-0.2	-0.7	+0.4	-0.5	-0.5	-0.3

From the behavior of the exciton levels under large strains we can determine the deformation potential constants for both valence band and conduction band. The values of these constants according to the data in /43.8/ and /43.10/ are presented in Table 40.2 at the end of the section.

A characteristic feature of exciton lines in the degenerate case is the strong polarization dependence of the levels that split under the strain. This should be observed for both direct and indirect excitons, when the excitation includes two stages: a "vertical" transition without change in k, accompanied by absorption of a photon, and a transition with transfer of momentum to an impurity or a phonon. In the latter case the polarization depends significantly not only on the original and final states of the electron, but also on the intermediate state that participates in the transition. We shall therefore restrict ourselves here to a discussion of the simplest case – a direct exciton in Ge.

By (40.6), (36.3) and (36.23), for sufficiently large strains, so that the excitons associated with each of the split bands may be treated independently, the conductivity is given by

$$\sigma_{\alpha\beta}^{ex}=\frac{\pi e^2}{\hbar\omega}|f^0(0)|^2\Theta_{\alpha\beta}\delta(\omega-\omega_l), \tag{40.27}$$

where, by (36.24), relative to the principal crystal axes,

$$\mathrm{Tr}\,\Theta=3s^2,$$

$$\Theta_{\alpha\alpha}-\Theta_{\beta\beta}=\pm 3s^2\frac{b(e_{\alpha\alpha}-e_{\beta\beta})}{\Delta_e},\quad \Theta_{\alpha\beta}=\pm\sqrt{3}\,s^2\frac{de_{\alpha\beta}}{\Delta_e}\quad(\alpha\neq\beta). \tag{40.28}$$

The upper sign corresponds to the highest valence band, the lower sign to the lowest of the split-off bands; $\Delta_e = 2\mathscr{E}_e^{1/2}$.

For a stress P of arbitrary direction, it is convenient to determine the polarization for three directions: along the ξ axis parallel to P, and along the ζ and η axes in a plane perpendicular to P. The ζ axis is placed in the $z\xi$ plane and the η axis perpendicular to this plane. The angle between the z and ξ axes is denoted by ϑ, the angle between the zx and $z\xi$ planes by φ The tensor components $\Theta_{\alpha\beta}$ relative to the ξ, ζ, η axes, which determine the polarization dependence of $\sigma_{\alpha\beta}$ in these axes via (40.27), are

$$\begin{aligned}
\Theta_{\xi\xi} &= s^2 \pm \frac{s^2 P}{\Delta_e}\Big\{2b(S_{11}-S_{12})[1-3\sin^2\vartheta+3\sin^4\vartheta(1-\sin^2\varphi\cos^2\varphi)]+ \\
&\quad + \sqrt{3}\,dS_{44}[\sin^2\vartheta - \sin^4\vartheta(1-\sin^2\varphi\cos^2\varphi)]\Big\}, \\
\Theta_{\zeta\zeta} &= s^2 \mp \frac{s^2 P}{\Delta_e}\Big\{b(S_{11}-S_{12})[1-6\sin^2\vartheta\cos^2\vartheta(1-\sin^2\varphi\cos^2\varphi)]+ \\
&\quad + \sqrt{3}\,dS_{44}\sin^2\vartheta\cos^2\vartheta(1-\sin^2\varphi\cos^2\varphi)\Big\}, \\
\Theta_{\eta\eta} &= s^2 \mp \frac{s^2 P}{\Delta_e}\Big\{b(S_{11}-S_{12})(1-6\sin^2\vartheta\cos^2\varphi\sin^2\varphi)+ \\
&\quad + \sqrt{3}\,dS_{44}\sin^2\vartheta\cos^2\varphi\sin^2\varphi\Big\},
\end{aligned} \tag{40.29}$$

If the stress P is applied along the principal [100] or [111] axes, then

$$\Theta_{\xi\xi} = s^2(1 \pm \gamma), \quad \Theta_{\zeta\zeta} = \Theta_{\eta\eta} = s^2\left(1 \mp \frac{\gamma}{2}\right). \tag{40.30}$$

where $\gamma = \frac{bP}{|bP|}$ or $\gamma = \frac{dP}{|dP|}$, respectively. Here positive P corresponds to tension and negative P to compression. It is immediate that if $\gamma = -1$ absorption occurs for the upper band, only when the electric field $\mathscr{E}$ of the wave is perpendicular to P, i.e., $\sigma_\parallel = 0$, and $\sigma_\parallel/\sigma_\perp = 4$ for the lower band. If $\gamma = 1$, the bands are interchanged. Similar relations hold for an arbitrary direction of P in the spherical approximation, i.e., if $dS_{44} = 2\sqrt{3}\,b\,(S_{11} - S_{12})$. If this relation is not valid, the transverse components $\sigma_{\zeta\zeta}$ and $\sigma_{\eta\eta}$ are not the same for a strain along any direction other than [100] and [111].

Exchange interaction in semiconductors with simple bands

As noted in §27, the exchange interaction results in additional splitting of the exciton state. A strain which reduces the crystal symmetry will induce further splitting of exciton levels. The characteristic feature of the exchange interaction is that the strain-induced splitting also occurs when the exciton is associated with nondegenerate bands (neglecting spin) which cannot themselves split under a strain. This effect was first observed in cuprous oxide in 1960 /43.2/; it was then explained qualitatively by an exchange interaction /22.5/. In cuprous oxide the extrema of the conduction band and of several close-lying valence bands are located at the point Γ ($k=0$), where the little group is O_h.

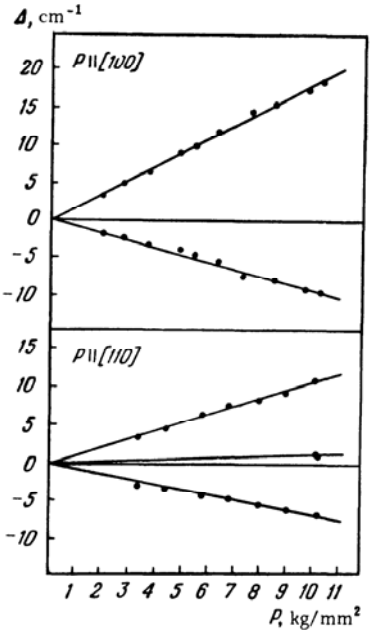

FIGURE 69. Splitting of exciton ground state in cuprous oxide under strains along [100] and [110] /43.2/.

Figure 69 illustrates the splitting of the exciton ground state associated with the nondegenerate bands Γ_6^+ and Γ_7^+ under strains along [100] and [110]. This state corresponds to the representation $\Gamma_6^+ \times \Gamma_7^+ = \Gamma_2 + \Gamma_{25}'$, so that it splits into a onefold and a threefold degenerate state. The basis functions of the state Γ_{25}' transform like XY, XZ, YZ and its strain splitting is determined by a matrix similar to (30.2): under a [100] strain it splits into two terms, corresponding to the functions XZ, YZ and XY; under a [110] strain the degeneracy is completely lifted, the three split-off states corresponding to the functions $(1/\sqrt{2})(XZ+YZ)$, $(1/\sqrt{2})(XZ-YZ)$ and XY. Quadrupole transitions are allowed to all these states; the matrix element of the transition to state XY is proportional to $\mathscr{E}_x q_y + \mathscr{E}_y q_x$, and soon. Both dipole and quadrupole transitions to the state Γ_2 are forbidden, and this line was not observed.

Later, splitting of exciton states associated with nondegenerate bands was observed in a number of crystals with wurtzite structure /43.12–43.17/. The line shifts in these experiments were determined from reflection spectra.

Figure 70 illustrates the line splitting for excitons A and B under a compression perpendicular to the principal axis C. The light propagated along this axis and was polarized parallel or perpendicular to the strain direction; one of the split lines was observed for each polarization.

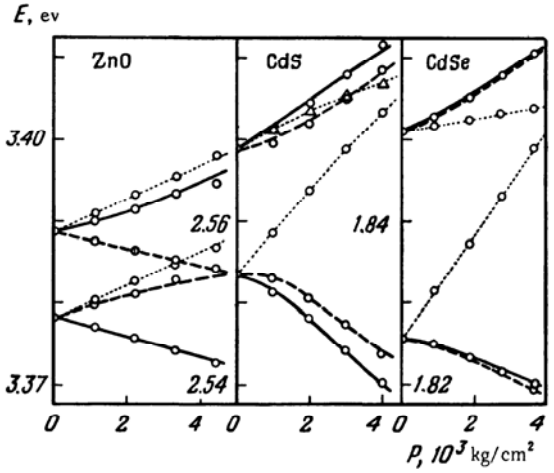

FIGURE 70. Splitting of exciton ground state in hexagonal ZnO, CdS and CdSe under a strain perpendicular to the principal axis /43.12/. Solid lines: $\mathfrak{s} \perp P, C$; $P \perp C$; dashed lines $\mathfrak{s} \parallel P$, $P \perp C$; dotted lines: $\mathfrak{s} \parallel C$, $P \parallel C$.

For an accurate calculation of nonlinear strain effects, we need the exchange interaction matrix $\mathcal{H}^{\text{exch}}$(27.77), (27.75) between the band functions, incorporating their change under the strain. We shall not present the rather tedious calculations here, but restrict ourselves to the linear case. We shall use the theory of invariants to construct $\mathcal{H}^{\text{exch}}(\varepsilon)$, and then estimate the constants entering into this Hamiltonian. The exchange interaction for an exciton A corresponding to the representation $\Gamma_7 \times \Gamma_9 = \Gamma_5 + \Gamma_6$ splits the ground state into two. $\mathcal{H}^{\text{exch}}(\varepsilon)$ may contain components of ε which transform according to the representations $\Gamma_5 \times \Gamma_5 = \Gamma_6 \times \Gamma_6 = \Gamma_1 + \Gamma_2 + \Gamma_6$ and $\Gamma_5 \times \Gamma_6 = \Gamma_3 + \Gamma_4 + \Gamma_{15}$, and relative to the basis $Y^{1-}_{\pm 1} = (1/\sqrt{2})(X \pm iY)(\Gamma_5)$, $Y^{2-}_{\pm 2}$ (Γ_6) the operator $\mathcal{H}^{\text{exch}}(\varepsilon)$ has the form

$$\mathcal{H}^{\text{exch}}_{A}(\varepsilon) = \begin{Vmatrix} E_0 + \Delta/2 & c_1\varepsilon_- & c_3\varepsilon_{z+} & 0 \\ c_1\varepsilon_+ & E_0 + \Delta/2 & 0 & c_3\varepsilon_{z-} \\ c_3\varepsilon_{z-} & 0 & E_0 - \Delta/2 & 0 \\ 0 & c_3\varepsilon_{z+} & c_2\varepsilon_+ & E_0 - \Delta/2 \end{Vmatrix} \tag{40.31}$$

Here E_0 is the exciton energy, not counting exchange splitting, including the strained-induced shift defined by (31.23), (31.24), (31.15) or (40.17), and Δ is the exchange splitting. For the other notation, see Table 31.4 (p. 324).

Of the two split states, only Γ_5 is optically active. It is clear from (40.31) that under strains $\varepsilon_{xx} - \varepsilon_{yy}$ or ε_{xy} it splits into two, with energies

$$E_{1,2} = E_0 + \frac{\Delta}{2} \pm c_1 \left[(\varepsilon_{xx} - \varepsilon_{yy})^2 + 4\varepsilon^2_{xy}\right]^{1/2}, \tag{40.32}$$

corresponding to the functions

$$\varphi_1=\frac{1}{\sqrt{2}}\begin{Vmatrix}-\chi\\1\end{Vmatrix},\quad \varphi_2=\frac{1}{\sqrt{2}}\begin{Vmatrix}\chi\\1\end{Vmatrix},\quad \text{where } \chi=\frac{\varepsilon_-}{|\varepsilon_-|}. \tag{40.33}$$

For a strain $\varepsilon_{xx}-\varepsilon_{yy}$, these are the functions X and Y; for ε_{xy} they are $(X+Y)/\sqrt{2}$ and $(X-Y)/\sqrt{2}$. In these cases the lines are completely polarized: when $\mathfrak{E}\parallel P$, one of the levels is excited, and when $\mathfrak{E}\perp P$ and $\mathfrak{E}\perp C$ the other.

The ground state for excitons B and C, which correspond to the representations $\Gamma_7\times\Gamma_7=\Gamma_1+\Gamma_2+\Gamma_6$, is split by the exchange interaction into three states, two nondegenerate (Γ_1 and Γ_2) and one twofold degenerate (Γ_6). In this case $\mathcal{H}^{\text{exch}}(\varepsilon)$ may contain components of ε which transform according to Γ_1, Γ_2, Γ_5, $\Gamma_2\times\Gamma_5=\Gamma_5$ and $\Gamma_5\times\Gamma_5=\Gamma_1+\Gamma_2+\Gamma_6$. If we take Y_0^{0-}, Y_0^{1-}, $Y_{\pm1}^{1-}$ as basis functions which transform according to the representations Γ_2, Γ_1, Γ_5 respectively, the matrix will be

$$\mathcal{H}^{\text{exch}}_{B,C}(\varepsilon)=\begin{Vmatrix} E_0-\frac{\Delta}{2}+\Delta' & 0 & c_3\varepsilon_{z+} & -c_3\varepsilon_{z-}\\ 0 & E_0-\frac{\Delta}{2}-\Delta' & c_2\varepsilon_{z+} & c_2\varepsilon_{z-}\\ c_3\varepsilon_{z-} & c_2\varepsilon_{z-} & E_0+\frac{\Delta}{2} & c_1\varepsilon_-\\ -c_3\varepsilon_{z+} & c_2\varepsilon_{z+} & c_1\varepsilon_+ & E_0+\frac{\Delta}{2}\end{Vmatrix} \tag{40.34}$$

Here Δ and Δ' are the exchange splittings.

It is clear from (40.34) that the state Γ_5 splits under strains $\varepsilon_{xx}\neq\varepsilon_{yy}$ and ε_{xy} in the same way as in the case of A. If $q\parallel C$, then here again the only excited states are Γ_5. Their splitting and polarization are defined by equations similar to (40.32) and (40.33), so that here again if $\mathfrak{E}\parallel P$ one of the levels is excited, and if $\mathfrak{E}\perp P$ (and $\mathfrak{E}\perp C$) the other level is excited. But when the polarization is $\mathfrak{E}\parallel C$, the state Γ_1 must also be excited. In (40.31) and (40.34) we have omitted the diagonal terms defining the change in the constants Δ and Δ' under the strain, which are proportional to ε_{zz} and $\varepsilon_\perp$. These components do not cause additional splitting or shifting of states

In the quasi-cubic model, in which the wave functions of the three bands Γ_8, Γ_7, Γ_7 are defined by equations (31.18), the constants Δ and Δ' for excitons A, B, C in (40.31) and (40.34) satisfy the following relations:

$$\begin{aligned}&\text{exciton } A\text{: } \Delta=-3\Delta_1,\\ &\text{exciton } B\text{: } \Delta=3\Delta_1(\sin^2\theta-\cos^2\theta),\ \Delta'=3\Delta_1\sin^2\theta,\\ &\text{exciton } C\text{: } \Delta=3\Delta_1(\cos^2\theta-\sin^2\theta),\ \Delta'=3\Delta_1\cos^2\theta,\end{aligned} \tag{40.35}$$

where $\tan\theta=(-E_3^0/E_2^0)^{1/2}$. Here E_2^0 and E_3^0 are defined by (31.16). When $\Delta_{SO}\gg\Delta_{CF}$, $\tan\theta=\sqrt{2}$. In this case the representations Γ_1 and Γ_5 for the exciton C are combined.

Formulas (40.35) are valid provided the contribution of the neighboring bands to the wave function of excitons A, B, C is not significant, and the value of $|f(0)|^2$ for the ground states of these excitons is the same as when $m_e^*\ll m_h^*$. Under these conditions, the constant Δ_1 in (40.35) coincides with the Δ_1 in equation (40.37) below.

According to the data in /43.17/ the value of the constant $3\Delta_1$ (in the notation of /43.17/, $3\Delta_1 = j$) is 5.7 mev for ZnO, 2.5 mev for CdS and 0.4 mev for CdSe.

Note that in crystals without an inversion center, the linear k terms (and odd terms of higher order in k) may contribute to the exchange splitting in the electron-hole spectrum. For the exciton $\Gamma_7 \times \Gamma_7$, when the electron-hole spectrum is given by (31.12), the corresponding contribution to Δ' is

$$\Delta' = 4(m_{\perp e} m_{\perp h})^{1/2}(m_{\perp e} + m_{\perp h})^{-1}(\Delta E_c \Delta E_v)^{1/2},$$

where $\Delta E_{c,v}$ is the downward shift of the extrema for electrons and holes due to the linear k terms (by (31.2), this shift is $-E(0) = \alpha_1^2/4A_2$) and $m_{\perp e}$, $m_{\perp h}$ are the transverse electron and hole masses: $m_{\perp}^{-1} = 2A_2/\hbar^2$.

The contribution of linear k terms to Δ for the exciton $\Gamma_7 \times \Gamma_7$, as for the exciton $\Gamma_9 \times \Gamma_7$, vanishes.

Relation (40.35) is no longer valid for the contributions to Δ and Δ' from linear k terms.

The constants c_i in (40.31) and (40.34) are proportional to the exchange splitting; in order of magnitude,

$$c_i \approx \frac{D_{12}}{E_1 - E_2}\Delta,$$

where D_{12} is the off-diagonal deformation potential constant which determines the strain-induced change in the separation of the band 1 from the neighboring band 2; here the constant is D_5 in (31.14), and $E_1 - E_2$ is the separation of the bands.

Using the values of the elastic constants from Figure 70, we can estimate the values of c_1: for ZnO ≈ 2 ev, for CdS ≈ 1 ev.

Equation (40.34) is valid only for strains so small that $D_5|e_+|$ is considerably less than the separation of the valence bands, so that $2c_1|e_+| < \Delta$. For large strains, the strain-induced splitting must be "saturated" and approach the exchange splitting in order of magnitude.

In conclusion, we note that, as is clear from (40.31) and (40.34), the states split off as a result of exchange splitting are mixed under shear strains e_{xz} and e_{yz}. This should activate optically inactive states.

Exchange interaction in semiconductors with degenerate bands

As we saw in §27, in cubic crystals with a fourfold degenerate valence band (Γ_8) and a nondegenerate conduction band (Γ_6 or Γ_7), the ground state of a direct exciton corresponds to the representation $\mathfrak{D}_{ex} = \Gamma_8 \times \Gamma_7$.

If one of the bands is simple, the wave function of the exciton may be written

$$\Psi_{m\mu} = \sum_n \mathcal{F}_n^{\mu}(r_1, r_2)\varphi_m u_n = \varphi_m \psi_{\mu}, \quad \text{where } \psi_{\mu} = \sum_{n=1}^{4} \mathcal{F}_n^{\mu}(r_1, r_2) u_n.$$

The envelope functions $\mathcal{F}_n^{\mu}(r_1, r_2) = f_{\mathcal{K}n}^{\mu}(r)\, e^{i\mathcal{K}R}$ are independent of the index of the conduction band functions, since the operator (27.63), defining these functions is independent of these indices, provided, of course, that the exchange interaction is not included in $\mathcal{H}^{eh}$. The functions ψ_μ for the exciton ground state at $k = 0$ transform according to the same representation Γ_8 as the functions u_n of the band bottom. It follows that some of the functions $f_n^{\mu}(r)$ corresponding to $\mathcal{K} = 0$ transform according to all the representations occurring in the product $\Gamma_8 \times \Gamma_8 = A_1 + A_2 + E + 2F_1 + 2F_2$, so that at least one of these functions transforms according to A_1 and does not vanish at $r = 0$. We shall designate this function by the index $f_1 = f_\mu^\mu$, assuming that the function ψ_μ transforms in the same way as the band bottom function u_μ. Accordingly, we may write the function $\Psi_{m\mu}$ at $\mathcal{K} = 0$ as

$$\Psi_{0m\mu} = \varphi_m \psi_{0\mu} = \varphi_m \Big[u_\mu f_1(r) + \sum_{n \neq \mu} f_n^{\mu}(r)\, u_n \Big]. \tag{40.36}$$

The representation $\mathcal{D}_{ex} = \Gamma_8 \times \Gamma_7 = E + F_1 + F_2$ is reducible, and the exchange splitting splits it into three terms. The operator $\mathcal{H}^{exch}$ describing the splitting must contain three constants, since $\mathcal{D}_{ex} \times \mathcal{D}_{ex}$ contains the identity representation three times; it may be written

$$\mathcal{H}^{exch} = \Delta_0 + \Delta_1 (J\sigma) + \Delta_2 (J_x^3 \sigma_x + J_y^3 \sigma_y + J_z^3 \sigma_z). \tag{40.37}$$

The operators J_i act on the wave functions ψ_μ, the operators σ_i on the conduction band functions φ_m. If the functions of the representation Γ_8 are built up from functions of only one representation F_2 or F_1, then $\Delta_2 = 0$ in this approximation, and

$$\Delta_0 = -\tfrac{3}{2}\Delta_1 = \tfrac{1}{2}\mathcal{V} |f_1(0)|^2 \int U(r_1 - r_2)\, S^*(r_1)\, S(r_2)\, X(r_1)\, X^*(r_2)\, dr_1\, dr_2,$$

where $X(r)$ is a function which transforms according to the representation F_2 (or F_1) and $S(r)$ a function which transforms according to the identity representation. It is obvious that in the spherical approximation the Hamiltonian (40.37) does not contain the last term, and $\mathcal{D}_{ex} = \mathcal{D}_{1/2} \times \mathcal{D}_{3/2} = \mathcal{D}_1 + \mathcal{D}_2$. When the symmetry is reduced to T_d, the representation $\mathcal{D}_1^-$ becomes Γ_2 ($\mathcal{D}_1^+$ goes into F_1), and $\mathcal{D}_2^-$ splits into $E + F_1$ ($\mathcal{D}_2^+$ into $E + F_2$). The operator $\mathcal{H}_{ex}$ describing the splitting of an exciton level under small strains, when this splitting is much less than the exciton binding energy, is determined by an equation similar to (30.9) with b and d replaced by b' and d' (see (40.21)). In this case the exciton level splits under a strain even in the absence of the exchange interaction, and so the Hamiltonian need not include the small terms that describe the strain-induced change in exchange splitting.

Since the constant Δ_2 vanishes in the spherical approximation, we may expect it to be much smaller than Δ_1. We therefore set $\Delta_2 = 0$, and it is thus possible to diagonalize $\mathcal{H}_{ex}$ whatever the direction of the strain. Below we shall discuss the qualitative features of the spectra when $\Delta_2 \neq 0$, using group-theoretic considerations, and show that the experimental data also confirm that Δ_2 is small.

We now introduce the reduced strain tensor, setting

$$\varepsilon'_{ij}=\begin{cases}\varepsilon_{ij} & \text{for } i=j,\\ \varepsilon_{ij}\dfrac{d}{\sqrt{3}\,b} & \text{for } i\neq j\end{cases}$$

and go over to a new coordinate system whose x'-, y'- and z'-axes are the principal axes of the reduced strain tensor ε'_{ij}, and the principal values of the tensor ε' are equal to ε_i $(i=1,2,3)$. The operator $\mathcal{H}_{ex}$ in this coordinate system is

$$\mathcal{H}_{ex}=\mathcal{H}^{exch}+\mathcal{H}_\varepsilon=b'\sum_i\left(J_i'^2-\frac{5}{4}\right)\varepsilon_{ii}+\Delta_1(\boldsymbol{J}'\sigma'). \tag{40.38}$$

Here we have incorporated the quantities Δ_0 and $E_{1\varepsilon}\varepsilon=(c-a)\,\varepsilon$ into the energy E_0, which will be the zero point for the energy E later.

We take the following functions $\Psi_i=\Psi_{m\mu}=\varphi_m\psi_\mu$ as basis:

$$\begin{array}{lll}\Psi_1=\varphi_{1/2}\psi_{3/2}, & \Psi_2=\varphi_{-1/2}\psi_{-3/2}, & \Psi_3=\varphi_{-1/2}\psi_{1/2},\\ \Psi_4=\varphi_{1/2}\psi_{-1/2}, & \Psi_5=\varphi_{-1/2}\psi_{3/2}, & \Psi_6=\varphi_{1/2}\psi_{1/2},\\ \Psi_7=\varphi_{1/2}\psi_{-3/2}, & \Psi_8=\varphi_{-1/2}\psi_{-1/2}.\end{array} \tag{40.39}$$

Here ψ_i are functions which transform like $Y_i^{3/2}$, and φ_m like $Y_m^{1/2}$. Relative to the basis (40.39), the matrix (40.38) becomes

$$\mathcal{H}_{ex}=\begin{vmatrix}\mathcal{H}_{II} & 0\\ 0 & \mathcal{H}_{II\,II}\end{vmatrix}; \tag{40.40}$$

$$\mathcal{H}_{II}=\begin{vmatrix}{}^3/_2\Delta_1-F & 0 & 0 & -I\\ 0 & {}^3/_2\Delta_1-F & -I & 0\\ 0 & -I & -(\Delta_1/2)+F & 2i\Delta_1\\ I & 0 & -2i\Delta_1 & -(\Delta_1/2)+F\end{vmatrix}, \tag{40.40a}$$

$$\mathcal{H}_{II\,II}=\begin{vmatrix}-{}^3/_2\Delta_1-F & i\sqrt{3}\,\Delta_1 & 0 & -I\\ -i\sqrt{3}\,\Delta_1 & (\Delta_1/2)+F & -I & 0\\ 0 & -I & -{}^3/_2\Delta_1-F & -i\sqrt{3}\,\Delta_1\\ -I & 0 & i\sqrt{3}\,\Delta_1 & (\Delta_1/2)+F\end{vmatrix} \tag{40.40b}$$

where $F=-\frac{b'}{2}(3\varepsilon_3-\varepsilon)$, $I=\frac{\sqrt{3}}{2}b'(\varepsilon_1-\varepsilon_2)$.

The solutions of the equation $|\mathcal{H}_{ex}-E\boldsymbol{I}|=0$ are

$$\begin{aligned}E_{1,2}&=E_\pm^{(s)}=\tfrac{3}{2}\Delta_1\pm\sqrt{\Delta_\varepsilon},\\ E_{3,4}&=E_\pm^{(z)}=-\tfrac{\Delta_1}{2}\pm\sqrt{\Delta_\varepsilon+4\Delta_1^2+2\Delta_1 b'(3\varepsilon_3-\varepsilon)},\\ E_{5,6}&=E_\pm^{(y)}=-\tfrac{\Delta_1}{2}\pm\sqrt{\Delta_\varepsilon+4\Delta_1^2+2\Delta_1 b'(3\varepsilon_2-\varepsilon)},\\ E_{7,8}&=E_\pm^{(x)}=-\tfrac{\Delta_1}{2}\pm\sqrt{\Delta_\varepsilon+4\Delta_1^2+2\Delta_1 b'(3\varepsilon_1-\varepsilon)},\end{aligned} \tag{40.41}$$

where

$$\Delta_\varepsilon = \frac{b'^2}{2}\{(\varepsilon_1-\varepsilon_2)^2+(\varepsilon_1-\varepsilon_3)^2+(\varepsilon_2-\varepsilon_3)^2\}, \quad \varepsilon = \sum_i \varepsilon_{ii}.$$

The eigenfunctions of the Hamiltonian (40.40) are superpositions of the functions (40.36), (40.39):

$$\Psi^\nu = \sum_l A_l^\nu \Psi_l = \sum_{m\mu n} A^\nu_{m\mu} f^\mu_n(r)\, u_n \varphi_m. \tag{40.42}$$

For states with $\nu = 1, 2, 3, 4$,

$$A_1^\nu = -\frac{I}{{}^3/_2\Delta_1 - F - E_\nu} A_4^\nu, \quad A_2^\nu = \pm i A_1^\nu, \quad A_3^\nu = \pm i A_4^\nu, \tag{40.042a}$$
$$|A_4^\nu|^2 = \frac{1}{2}\frac{{}^3/_2\Delta_1 - F - E_\nu}{(1\pm 2)\Delta_1 - 2E_\nu};$$

for states with $\nu = 5, 6, 7, 8$,

$$A_5^\nu = \frac{-I \pm \sqrt{3}\,\Delta_1}{{}^3/_2\Delta_1 + F + E} A_8^\nu, \quad A_6^\nu = \mp i A_8^\nu, \quad A_7^\nu = \mp i A_5^\nu,$$
$$|A_8^\nu|^2 = \frac{1}{4}\frac{{}^3/_2\Delta_1 + F + E_\nu}{(\Delta_1/2) + E_\nu}. \tag{40.42b}$$

The upper sign in (40.42a, b) corresponds to $\nu = 1, 2, 5, 6$, the lower sign to $\nu = 3, 4, 7, 8$.

If we expand the envelope functions $f^\mu_{mn}(r)$ in Fourier series, then in the general case, when both bands are degenerate and $f(r)$ depends on both indices m and n, the function Ψ^ν may be written

$$\Psi_0^\nu(r) = \frac{1}{\sqrt{\mathcal{V}}}\sum_{mn\mu} A^\nu_{mn\mu} f^\mu_{mn}(r)\varphi_m u_n = \frac{1}{\mathcal{V}}\sum_{mnk} C^\nu_{mk,\,n,\,-k} e^{ikr}\varphi_m u_n,$$

where

$$C^\nu_{mk,\,n,\,-k} = \sum_\mu A^\nu_{mn\mu} C^\mu_{mk,\,n,\,-k}.$$

Consequently, by (40.1), (40.36) the current operator matrix element is

$$j^\nu = \sum_{mnk} C^{*\nu}_{mk,\,n,\,-k} j_{mKn} = \sum_{\mu mnk} A^{\nu*}_{mn\mu} C^{\mu*}_{mk,\,n,\,-k} j_{mKn} =$$
$$= \sqrt{\mathcal{V}}\sum_{\mu mn} A^{\nu*}_{mn\mu} f^{\mu*}_{mn}(0)\, j_{mKn} = \sqrt{\mathcal{V}}\sum_{mn} f^{\nu*}_{mn}(0)\, j_{mKn}. \tag{40.43}$$

Here

$$f^\nu_{mn}(r) = \sum_\mu A^\nu_{mn\mu} f^\mu_{mn}(r).$$

In the case of a simple conduction band, when the only function not vanishing at $r = 0$ is $f^\mu_\mu = f_1$ and $f(r)$ is independent of m,

$$j^\nu = \sqrt{\mathcal{V}}\, f_1^*(0)\sum_{\mu m} A^{\nu*}_{m\mu} j_{mK\mu}. \tag{40.43a}$$

For the current operator we have $j_{m\kappa\mu}=ev_{m\kappa\mu}$, where $v_{m\mu}$ is the interband matrix of the velocity operator, defined by equations (36.21) for the band structure under consideration. Using this equation and noting that the functions $K\varphi_\mu$ are related to φ_μ by

$$K\varphi_{3/2}=\varphi_{-3/2},\quad K\varphi_{1/2}=-\varphi_{1/2},\quad K\varphi_{-1/2}=\varphi_{1/2},\quad K\varphi_{3/2}=-\varphi_{3/2},$$

we see that for states $\nu=1,\ldots,8$ with energies (40.41) the nonzero components of the complex dielectric constant $\tilde{\varkappa}_{ij}=-(4\pi/\omega)\tilde{\sigma}_{ij}$ are given, in accordance with (36.1), by*

$$\begin{aligned}
\tilde{\varkappa}_{zz} &= -4\pi\frac{e^2s^2}{\hbar\omega^2}|f_1(0)|^2\sum_{\nu=3,4}\frac{B_\nu^z}{\omega-\omega_\nu},\\
\tilde{\varkappa}_{yy} &= -4\pi\frac{e^2s^2}{\hbar\omega^2}|f_1(0)|^2\sum_{\nu=5,6}\frac{B_\nu^y}{\omega-\omega_\nu},\\
\tilde{\varkappa}_{xx} &= -4\pi\frac{e^2s^2}{\hbar\omega^2}|f_1(0)|^2\sum_{\nu=7,8}\frac{B_\nu^x}{\omega-\omega_\nu},
\end{aligned}\tag{40.44}$$

where

$$\begin{aligned}
B_\nu^z &= 1-\frac{2\Delta_1+(b'/2)(3\varepsilon_3-\varepsilon)}{E_\nu+(\Delta_1/2)} && (\nu=3,\ 4),\\
B_\nu^y &= 1-\frac{2\Delta_1+(b'/2)(3\varepsilon_2-\varepsilon)}{E_\nu+(\Delta_1/2)} && (\nu=5,\ 6),\\
B_\nu^x &= 1-\frac{2\Delta_1+(b'/2)(3\varepsilon_1-\varepsilon)}{E_\nu+(\Delta_1/2)} && (\nu=7,\ 8).
\end{aligned}\tag{40.45}$$

Here

$$\omega_\nu=(E_\nu/\hbar)+i\gamma_\nu.$$

The constant γ_ν defining the width of the exciton lines vanishes in this approximation. Since we have restricted ourselves to dipole transitions, the components $\tilde{\varkappa}_{ij}$ may be calculated from the start relative to the principal axes of the reduced strain tensor.

Equations (40.41) show that when there is no strain the eight levels defined by (40.41) merge into two levels, corresponding to the representations D_1 and D_2 which become F_2 and $E+F_1$ when $\Delta_2\neq 0$ (which of the levels coincide at $\varepsilon=0$ depends on the sign of the constant Δ_1). Under a strain along the z-axis, with $\varepsilon_1=\varepsilon_2=\varepsilon_{xx}$, $\varepsilon_3=\varepsilon_{zz}$, the crystal symmetry is reduced from T_d to D_{2d}, and these representations split as follows:

$$E\to B_1+A_1,\quad F_1\to E+A_2,\quad F_2\to E+B_2,$$

forming six different terms, two of which are twofold degenerate.

In the absence of a strain the only optically active level is F_2. It is readily verified from the character table of the representations of the group D_{2d} that under a strain the optically active terms are the two twofold

* We are neglecting the nonresonant terms whose denominators contain $\omega+\omega_\nu$.

degenerate terms (in an electric field perpendicular to the z-axis, i. e., in σ-polarization), which correspond to the levels $E_5=E_7$ and $E_6=E_8$ in (40.41), and the term B_2 (when $\mathscr{E} \parallel Oz$, i. e., in π-polarization), which corresponds to one of the levels E_3 or E_4. Two of these lines originate in the optically active term F_2, while one originates in the inactive term F_1 so that its intensity approaches zero when $\varepsilon'_{zz}=\varepsilon_{zz}-\varepsilon_{xx}=0$. Under a [111] strain, referred to the coordinate system $[1\bar{1}0]$, $[11\bar{2}]$, [111], and also under a [001] strain, we have $\varepsilon_1=\varepsilon_2$. Hence the expressions for E_v and B_v in this case differ from the equations for $P \parallel [001]$ and the same value of $\varepsilon_1-\varepsilon_2$ in that b' is replaced by $d'/\sqrt{3}$. In either case, as we see from (40.41), $E_5=E_7$ and $E_6=E_8$ and one of the levels $E_{1,2}$ coincides with one of the levels $E_{3,4}$. This identity of results for [001] and [111] strains is a consequence of the approximation $\Delta_2 = 0$.

Group-theoretic analysis reveals the difference between these cases and permits qualitative analysis of the role of the Δ_2 terms. When $P \parallel [111]$ and the symmetry is reduced from T_d to C_{3v}, the terms E, F_1, F_2 split, becoming representations of the group C_{3v}:

$$E \to E, \quad F_1 \to E + A_2, \quad F_2 \to E + A_1.$$

The states E of the group C_{3v} which arise from F_1 and F_2 correspond to the levels $E_{5,7}$ and $E_{6,8}$, and the state E arising from E of the group T_d corresponds to a pair of coinciding levels, one from each of $E_{1,2}$ and $E_{3,4}$.

The state A_2 corresponds to a nondegenerate term from the pair $E_{1,2}$, the state A_1 to a nondegenerate term from the pair $E_{3,4}$.

According to group theory, transitions are allowed to state A_1 in a longitudinal field and to state E in a transverse field. In contrast to the case $P \parallel [001]$, the degeneracy of levels arising from E (T_d) is not removed even when $\Delta_2 \neq 0$; a transition to these levels is allowed in a transverse field, its probability vanishing both as $\Delta_2 \to 0$ and as $\varepsilon \to 0$.

Under a [001] strain, referred to the system of axes [100], $[01\bar{1}]$, [011], where the tensor ε is diagonal and all three components ε_1, ε_2 and ε_3 are different, the degeneracy is completely removed. The symmetry is then reduced to C_{2v}, and the representations of the group T_d become representations of C_{2v}:

$$E \to A_1 + A_2, \quad F_2 \to A_1 + B_1 + B_2, \quad F_1 \to A_2 + B_1 + B_2.$$

By group theory the allowed transitions are: to B_1 in x-polarization, to B_2 in y-polarization, to A_1 in z-polarization.

Thus, the terms $E_{3,4}$ correspond to representations A_1, the terms $E_{7,8}$ to representations B_1, the terms $E_{5,6}$ to representations B_2, and the terms $E_{1,2}$ to representations A_2. This analysis shows that for a strain along [011] inclusion of the Δ_2 terms entails no new qualitative features of the spectrum.

Figures 71 and 72 show the change in the positions of the exciton lines in cubic ZnS under compression along the [001] and [011] axes. The line positions were determined from the position of the inflection point on the dispersion curve of the reflection coefficient.

According to the theory, under a strain along [001] three polarized lines appear in the spectrum: a strong π line and σ_1 and σ_2 lines. The σ_1 line weakens somewhat with increasing strain. The σ_1 line

is observed only under sufficiently large strains, and becomes stronger with increasing strain. Under a strain the π and σ_2 lines are shifted toward longer wavelengths. In the absence of the exchange interaction, these lines would merge into one line, corresponding to the lower sign in equations (40.30) with $\gamma = -1$. The σ_1 line is shifted under a strain toward shorter wavelengths – this is the line corresponding to the upper sign in (40.30) with $\gamma = -1$; $\sigma_{zz} \sim \Theta_{\xi\xi} = 0$.*

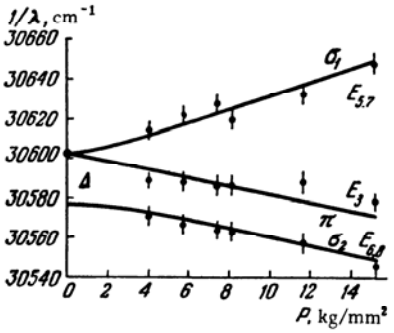

FIGURE 71. Splitting of exciton ground state in cubic ZnS under a [001] strain with reflection from the (100) and (011) faces /43.14/.

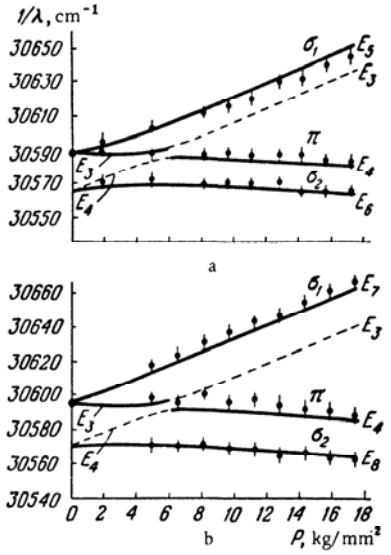

FIGURE 72. Splitting of exciton ground state in cubic ZnS under a [011] strain with reflection from the (100) (a) and (011) (b) faces /43.15/.

Under a strain along [011], when the levels E_5, E_7 and E_6, E_8 are non-degenerate, the lines E_5 and E_6 are observed in σ-polarization in reflection spectra measured from the (100) face when $\mathcal{E} = \mathcal{E}_y$, and the lines E_7 and E_8 in reflection spectra measured from $(01\bar{1})$ when $\mathcal{E} = \mathcal{E}_x$. In either case, one of the lines E_3 or E_4 is observed in π-polarization. As follows from (40.44) and (40.45), the intensity of the other line, although not zero for either $\boldsymbol{P} \parallel [001]$ or $\boldsymbol{P} \parallel [111]$, is very small. Both the intensity of the lines and the difference in the positions of the σ_1 and σ_2 lines in reflection spectra from inequivalent faces are determined by the anisotropy factor

$$\Theta = \frac{d'}{\sqrt{3}\, b'} \frac{S_{44}}{2(S_{11} - S_{12})} - 1.$$

* Equations (40.27)–(40.30) were derived on the assumption that the splitting Δ_ε exceeds the exciton binding energy E_0. However, they are also applicable to the reverse case $\Delta^{\text{exch}} \ll \Delta_\varepsilon \ll E_0$ (with b replaced by b' and d by d'), since the functions ψ_μ (40.36) for the exciton ground state transform like the functions u_μ of the valence band bottom.

In Figures 71 and 72 the solid lines indicate the theoretical curves $E^{\nu}(\varepsilon)$, calculated for levels $E_{5,6}$, $E_{7,8}$, $E_{3,4}$ from equations (40.41). The parameters Δ_1, b', d', E_{1g} were chosen to guarantee the best fit with the experimental points:

$$\Delta = 4\Delta_1 = -2.8 \cdot 10^{-3} \text{ ev}, \quad E_{1g} \simeq 4 \text{ ev},$$
$$b' = -1.5 \text{ ev}, \quad d' = -4.5 \text{ ev},$$

Throughout the foregoing computations, we neglected the contribution to the exciton energy associated with the annihilation or resonance interaction defined by (27.69). Indeed, in our application of the theory of invariants we did not include in the Hamiltonian terms depending on the direction of the exciton wave vector $\mathcal{K}$, so that we in effect considered only the terms (27.77). We shall show that the exciton spectrum allowing for the annihilation interaction coincides with the excitation spectrum obtained by solving Maxwell's equations and neglecting time lag, provided the dielectric constant in the equations is calculated without allowance for the annihilation interaction. The exciton spectrum based on (27.69) is determined by the equation

$$|E_i^0\delta_{ij} + \mathcal{H}_{ij}^{a} - E\delta_{ij}| = 0. \tag{40.46}$$

It is assumed here that the exchange interaction (27.77) is incorporated in the Hamiltonian $\mathcal{H}^{eh}$ and the energy eigenvalues and eigenfunctions are defined with this interaction taken into account. Since the matrix elements (27.69) may be written

$$\mathcal{H}_{ij}^{a} = R_i^* R_j, \tag{40.47}$$

where

$$R_j = \frac{2\hbar}{mE_g}\frac{\sqrt{\pi}\,e}{\sqrt{\varkappa}\,\mathcal{K}}\sum_{mn\alpha} f_{mn}^{j}(0)\, p_{Knm}^{\alpha}\mathcal{K}^{\alpha}, \tag{40.47a}$$

the determinant in (40.46) is similar to (32.18b), and (40.46) reduces to the equation

$$\prod_{l}(E_l - E)\left[1 + \frac{4\pi e^2}{\varkappa\mathcal{K}^2}\frac{\hbar^2}{m^2E_g^2}\sum_{\nu}(E_\nu - E)^{-1}\times\right.$$
$$\left.\times\sum_{\alpha m'n'} f_{m'n'}^{*\nu}(0)\, p_{m'Kn'}^{\alpha}\mathcal{K}^{\alpha}\sum_{\beta mn} f_{mn}^{\nu}(0)\, p_{Knm}^{\beta}\mathcal{K}^{\beta}\right] = 0. \tag{40.48}$$

For optically inactive terms, for which

$$\sum_{mn} f_{mn}^{\nu}(0)\, p_{Knm}^{\alpha} = 0,$$

the roots of equation (40.48) are $E_l = E_\nu$ for every α; similarly, for N-fold degenerate optically active terms, $N-1$ of the roots E_l are equal to E_ν.

The remaining roots are determined by the equation

$$\varkappa + \frac{4\pi e^2}{\mathcal{K}^2}\frac{\hbar^2}{m^2E_g^2}\sum_{\nu}(E_\nu - E)^{-1}\sum_{\alpha m'n'} f^{*\nu}_{m'n'}(0)\,p^{\alpha}_{m'Kn}\mathcal{K}_\alpha \sum_{\beta mn} f^{\nu}_{mn}(0)\,p^{\beta}_{Knm}\mathcal{K}_\beta = 0. \qquad (40.49)$$

Like (32.18c), this equation coincides with the phenomenological equation (32.18d):

$$\sum_{\alpha\beta}\varkappa_{\alpha\beta}\mathcal{K}_\alpha\mathcal{K}_\beta = 0, \qquad (40.50)$$

which follows from Maxwell's equation (neglecting time lag) if we include the contribution to the dielectric constant $\varkappa$ from exciton excitation. According to (36.1), this contribution is

$$\Delta\varkappa^{ex}_{\alpha\beta} = -\frac{4\pi}{\hbar\omega^2\mathcal{V}}\sum_{\nu}\frac{f^{\alpha}_{\nu}f^{\beta*}_{\nu}}{\omega - \omega_\nu}. \qquad (40.51)$$

By (40.43), the current operator matrix elements in the dipole approximation are

$$j^{\alpha}_{\nu} = \frac{\sqrt{\mathcal{V}}\,e}{m}\sum_{mn} f^{\nu*}_{mn}(0)\,p^{\alpha}_{mKn}. \qquad (40.52)$$

Substituting these into (40.51), we obtain from (40.50)–(40.52) an equation coinciding with (40.49). This phenomenological approach shows that the annihilation interaction is determined by a potential $U(r)$ with a dielectric constant $\varkappa(\omega_\nu)$ (minus the contribution to $\varkappa$ due to excitation of the exciton), in practice optical dielectric constant $\varkappa_\infty$, while the direct Coulomb interaction for the exciton of large radius is determined by the static dielectric constant $\varkappa_0$.

Analysis of optical data requires calculation of the reflection (or absorption) coefficient with the aid of Maxwell's equations, using the above values of the tensor $\varkappa$, calculated without allowance for the annihilation interaction. However, in all experimental situations considered above the stress P, the wave vector q of the light and the electric field $\mathcal{E}$ were directed along the principal axes of the strained crystal. Under these conditions, only "transverse" excitons, for which $\sum_\alpha j^{\alpha}_{\nu}q_\alpha = 0$, are excited, and therefore the positions of the absorption lines or of the inflection points on the dispersion curves of the reflection coefficient are at $\omega_\nu = E_\nu/\hbar$, where E_ν is determined by equations which neglect the contribution of long-range forces to the exciton energy.

Current operator matrix element for transition to an exciton state (supplement to §40)

In the second quantized formalism, the current operator is

$$\hat{j} = \sum_{m\mathbf{k}_1,\, n\mathbf{k}_2} j_{m\mathbf{k}_1,\, n\mathbf{k}_2}\, a^{+}_{m\mathbf{k}_1}a_{n\mathbf{k}_2}. \qquad (40.53)$$

Here a^+_{mk} and a_{mk} are the electron creation and destruction operators in the k-representation, related to the corresponding operators in the x-representation, $\psi^+_m(r)$ and $\psi_m(r)$, by

$$\psi^+_m(r) = \frac{1}{\sqrt{\mathcal{V}}}\sum_k a^+_{mk}e^{-ikr}, \qquad \psi_m(r) = \frac{1}{\sqrt{\mathcal{V}}}\sum_k a_{mk}e^{ikr}. \tag{40.54}$$

These operators satisfy cross relations similar to (27.90):

$$\{a^+_{mk}a_{m'k'}\} = \delta_{mm'}\delta_{kk'} \quad \{a^+_{mk}a^+_{m'k'}\} = \{a_{mk}a_{m'k'}\} = 0, \tag{40.55}$$

and the averages over the vacuum are

$$\langle 0|a_{mk}a^+_{m'k'}|0\rangle = \delta_{mm'}\delta_{kk'}, \qquad \langle 0|a^+_{mk}a_{m'k'}|0\rangle = 0. \tag{40.56}$$

Using (40.56), we easily see that the matrix element of the operator (40.53) between states $\psi_{nk_2} = a^+_{nk_2}|0\rangle$ and $\psi_{mk_1} = a^+_{mk_1}|0\rangle$ i. e., $\langle\psi^+_{mk_1}|j|\psi_{nk_2}\rangle$, is indeed $j_{mk_1,\,nk_2}$. Moreover, $\psi^+_{mk} = \langle 0|a_{mk}$.

Let $b^+_{nk_2}$ and b_{nk_2} denote the creation and destruction operators for a hole: they are related to the operators a_{nk} and $a^+_{nk_2}$ by relations similar to (27.87):

$$b^+_{nk_2} = a_{K(nk_2)}, \qquad b_{nk_2} = a^+_{K(nk_2)}. \tag{40.57}$$

These operators satisfy relations similar to (40.55), (40.56); the corresponding operators in the x-representation, $\varphi^+_n(r)$ and $\varphi_n(r)$ (27.92), possess expansions similar to (40.54) in terms of the b-operators. The operator j in the new notation is

$$j = \sum_{mk_1,\,nk_2} j_{mk_1,\,K(nk_2)}a^+_{mk_1}b^+_{nk_2}. \tag{40.58}$$

The matrix element of this operator between the ground state of the crystal and the state $a^+_{mk_1}b^+_{nk_2}|0\rangle$ corresponding to the creation of the electron-hole pair $(mk_1,\ nk_2)$ is

$$j_{mk_1,\,nk_2,\,0} = j_{mk_1,\,K(nk_2)}. \tag{40.59}$$

The exciton wave function in the k-representation is

$$\Psi_e = \sum_{mk_1,\,nk_2} C^e_{mk_1,\,nk_2}a^+_{mk_1}b^+_{nk_2}|0\rangle, \tag{40.60}$$

where the coefficients $C^e_{mk_1,\,nk_2}$ are defined by equations (40.2), (40.3). Calculating the matrix element of the operator (40.57) between the ground state $|0\rangle$ and the state Ψ^+_e, we obtain

$$j^e = \sum_{mk_1,\,nk_2} C^{*e}_{mk_1,\,nk_2}j_{mk_1,\,K(nk_2)}. \tag{40.61}$$

TABLE 40.2. Effective masses and deformation potential constants in Ge, Si and some A_3B_5 compounds. All effective masses are in units of the free electron mass m_0; A, B, D are in units of $\hbar^2/2m_0$; Δ_{so} and the deformation potential constants are in ev.

	Conduction band				Valence band		
	position of lowest extremum	m^*_Γ (at Γ)	$m^*_\parallel$ (at extremum points X, Δ or L)	$m^*_\perp$ (at extremum points X, Δ or L)	Δ_{so}	average hole masses	
						light	heavy
Ge	L	0.041[c]	1.588[c]	0.0815[c]	0.29[b]	0.045[c]	0.35[c]
Si	Δ	—	0.9163[c]	0.1905[c]	0.044[b]	0.12[c]	0.44[c]
InSb	Γ	0.014[d] 0.0145[g]	—		0.90[a] 0.81[d]	0.021[h]	0.39[h]
InP	Γ	0.067[d] 0.073[h]	—		0.21[d]	—	0.4[h]
InAs	Γ	0.022[d] 0.026[g]	—		0.41[a] 0.43[d]	0.025[h]	0,41[h]
GaSb	Γ	0.047[d, g]	—		0.80[a] 0.70[d]	0.06[h]	0.3[h]
GaP	X	0.12[d]	$(m^*_\parallel m^{*2}_\perp)^{1/3} = 0{,}35$[d]		0,13[d]	—	—
GaAs	Γ	0.068[d] 0.065[f]	—		0.35[d]	0.12[h]	0.68[h]
AlSb	X	0.09[d]	$(m^*_\parallel m^{*2}_\perp)^{1/3} = \begin{cases} 0.39^d \\ 0.25^f \end{cases}$		0.75[a] 0.60[d]	—	0.9[h]

Valence band parameters

	A	B	D	δ	φ
Ge	−13.2[l] −13.27[l] −13.38[m]	−8.2[l] −8.63[l] −8.5[m]	−19.5[l] −19.4[l] −19.8[m]	−3.29[d] −3.60[l] −3.41[m]	−0.06[m]
Si	−4.22[e] −4.28[l]	−1.00[e] −0.75[l]	−4.78[e] −5.4[l]	—	—
InSb	−25[g]	−21[g]	−40[g]	−10—13[l]	—
CaSb	−11[g]	−6[g]	−15[g]	—	—

TABLE 40.2 (continued)

Deformation potential constants

	$E_{1g}=\Xi_d+\frac{1}{3}\Xi_u-a$	Ξ_u	b	d
Ge	2.9[q]	16.0[q]	−2.8[k] −2.7[p] −2.4[q]	−5.7[k] −4.5[l] −4.7[p] −3.5[q]
Si	3.8[q]	8.6[q]	−1.4[j] −2.4[q]	−3.1[j] −5.3[q]
GaP	3.7[n]	6.2[n]	−1.3[n]	−4.0[n]

References

a	27.2	*e*	27.15	*i*	27.19	*m*	31.4
b	27.3	*f*	27.16	*j*	29.1	*n*	43.7
c	27.7	*g*	27.17	*k*	30.1	*p*	43.8
d	27.14	*h*	27.18	*l*	31.3	*q*	43.10

TABLE 40.3. Crystal and spin-orbit splitting, effective masses, g-factors and deformation potential constants in hexagonal CdS, CdSe, ZnS (/27.4, 27.5, 27.13, 43.17/)

	CdS	CdSe	ZnS
Δ_1, 10^{-3} ev	28.4	68.8	55
Δ_2, 10^{-3} ev	20.9	138.0	28 — 31
Δ_3, 10^{-3} ev	20.7	150.7	28 — 31
$m_{e\parallel}$	0.205±0.01	0.13±0.01	0.28±0.03
$m_{e\perp}$	0.205±0.01	0.13±0.01	0.28±0.03
$m_{h\parallel}(\Gamma_9)$	5	1	1.4
$m_{h\perp}(\Gamma_9)$	0.7±0.1	0.45±0.09	0.49±0.06
$g_{e\parallel}$	1.78±0.05	0.6±0.1	1.9
$g_{e\perp}$	1.72±0.1	0.51±0.05	2.2±0.2
$g_{h\parallel}(\Gamma_9)$	1.15±0.5	—	1.5
$D_1-D_\parallel$	−2.8	−0.76	—
$D_2-D_\perp$	−4.5	−3.7	—
D_3	−1.3	−4.0	—
D_4	2.9	2.2	—
$\lvert D_5\rvert$	1.5	1.2	—
$\lvert D_6\rvert$	1.2	1.5	—

$D_\parallel$ and $D_\perp$ are the deformation potential constants for the conduction band (Γ_7).

BIBLIOGRAPHY

I. TEXTBOOKS OF GROUP THEORY AND ITS PHYSICAL APPLICATIONS. TABLES

I.1. Wigner, E.P. Group Theory and its Application to the Quantum Mechanics of Atomic Spectra. — New York, Academic Press, 1959.

I.2. Murnaghan, F.D. The Theory of Group Representations. — New York, Dover, 1963.

I.3. Lyubarskii, G.Ya. Group Theory and its Application to Physics. — Moscow, Fizmatgiz. 1957. (Russian)

I.4. Van der Waerden, B.L. Die gruppentheoretische Methode in der Quantenmechanik. — Berlin, Springer, 1932.

I.5. Hamermesh, M. Group Theory and its Application to Physical Problems. — Reading, Mass., Addison-Wesley, 1962.

I.6. Heine, V. Group Theory in Quantum Mechanics. — London, Pergamon Press, 1960.

I.7. Landau, L.D. and E.M. Lifshits. Quantum Mechanics, Chap. XII. — Moscow, Fizmatgiz. 1963. (Russian)

I.8. Gel'fand, I.M., R.A. Minlos and Z.Ya. Shapiro. Representations of the Full Rotation Group and the Lorentz Group. — Moscow, Fizmatgiz. 1958. (Russian)

I.9. Petrashen', M.A. and E.D. Trifonov. The Application of Group Theory to Quantum Mechanics. — Moscow, Nauka. 1967. (Russian)

I.10. Delone, B.N., N.N. Padurov, and A.D. Aleksandrov. Mathematical Foundations of the Structural Analysis of Crystals. — Moscow, GTTI. 1934. (Russian)

I.11. Frobenius, G. Theory of Characters and Group Representations. — Khar'kov. 1937. [Russian translation of selected papers.]

I.12. Meijer, P.H.E. and E. Bauer. Group Theory. The Application to Quantum Mechanics. — Amsterdam, North-Holland. 1965.

I.13. Tinkham, M. Group Theory and Quantum Mechanics. New York, McGraw-Hill. 1964.

I.14. Jones, H. The Theory of Brillouin Zones and Electronic States in Crystals. — Amsterdam, North-Holland. 1960.

I.15. Curtis, C.W. and I. Reiner. Representation Theory of Finite Groups and Associative Algebras. — New York, Wiley (Interscience). 1962.

I.16. Slater, J.C. Quantum Theory of Molecules and Solids. — New York, McGraw-Hill. 1964.

I.17. Knox, R.S. and A. Gold. Symmetry in the Solid State. — New York, Benjamin. 1964.

I.18. International Tables for X-ray Crystallography. — Birmingham. 1952.

I.19. Landolt-Bornstein. Zahlenwerte und Funktionen aus Physik, Chemie, Astronomie, Geophysik und Technik, 6. Aufl., Bd. I, Teil 4: Kristalle. — Berlin, Springer. 1955.

I.20. Faddeev, D.K. Tables of the Basic Unitary Representations of the Fedorov Groups. — Moscow, Izdatel'stvo Akad. Nauk SSSR. 1961. (Russian)

I.21. Kovalev, O.V. Irreducible Representations of Space Groups. — Kiev, Izdatel'stvo Akad. Nauk. Ukr. SSR. 1961. (Russian)

I.22. Streitwolf, H.-W. Gruppentheorie in der Festkörperphysik. — Leipzig, Akademische Verlagsges. Geest and Portig K.-G. 1967. English translation: Group Theory in Solid-State Physics. — London, Macdonald. 1971.

II. LITERATURE BY SUBJECT

1. REPRESENTATIONS OF POINT GROUPS

1.1. McIntosh, H.V. – J. Mol. Spectr. **5** (1960), 269.
1.2. Koster, G.F., J.O. Dimmock, R.G. Wheeler and H. Statz. Properties of the Thirty-Two Point Groups. – Cambridge, Mass., MIT Press. 1963.

2. MATRIX-ALGEBRAIC DESCRIPTION OF SPACE GROUPS

2.1. Seitz, F. – Z. Kristallogr. **88** (1934), 433; **90** (1935), 289; **91** (1935), 336; **94** (1936), 100.

3. SEITZ METHOD FOR REPRESENTATIONS OF SPACE GROUPS

3.1. Seitz, F. – Ann. Math. **37** (1936), 17.

4. PROJECTIVE REPRESENTATIONS, GENERAL THEORY

4.1. Schur, I. – J. Reine Angew. Math. **127** (1904), 20; **132** (1907), 85; **139** (1911), 155.
See also /I.5/, Chap. XII; /I.15/.

5. PROJECTIVE REPRESENTATIONS OF THE 32 POINT GROUPS

5.1. Döring, W. – Z. Naturforsch. **142** (1959), 343.
5.2. Kudryavtseva, N.V. and V.A. Chaldyshev. – Izv. Vuzov, Fizika 3 (1962), 133; **4** (1962), 98.
5.3. Hurley, A.C. – Philos. Trans. Roy. Soc. London Ser. A1108, **260** (1966), 1.

6. PROJECTIVE OPERATORS FOR SPACE GROUPS

6.1. Döring, W. – Z. Naturforsch. **142** (1959), 343.
6.2. Raghavacharyulu, I.V.V. – Can. J. Phys. **39** (1961), 830.
6.3. Shur, M.S. – Kristallografiya, **12** (1967), 981.

7. APPLICATIONS OF GROUP THEORY TO SOLID STATE PHYSICS. REVIEWS

7.1. Sokolov, A.V. and V.P. Shirokovskii. – UFN **60** (1956), 617; **71** (1960), 485.
7.2. Johnston, D.F. – Rep. Progr. Phys. **26** (1960), 67.
7.3. Nussbaum, A. – Sol. St. Phys. **18** (1966), 165.
7.4. Brown, E. – Sol. St. Phys. **22** (1968), 313.
See also /I.3/, /I.6/, /I.7/, /I.9/, /I.12/, /I.17/, /I.22/.

8. SPLITTING OF TERMS IN A CRYSTAL FIELD

8.1. Bethe, H.A. - Ann. Physik 3 (1929), 133.
8.2. Hellwege, K. – Ann. Physik **4** (1948), 951.
8.3. Bell, D.G. – Rev. Mod. Phys. **26** (1954), 311.
8.4. Meijer, P.H.E. – Phys. Rev. **95** (1954), 1443.

9. VIBRATIONS OF MOLECULES AND CRYSTALS

General theory

9.1. Born, M. and Kun Huang. Dynamical Theory of Crystal Lattices. – Oxford, Clarendon Press. 1954.
9.2. Maradudin, A. Theory of Lattice Dynamics in the Harmonic Approximation. – New York, Academic Press. 1963.

Application of group theory to classification of molecular vibrations

9.3. Wigner, E.P. – Nachr. Ges. Wiss. Gottingen, Math.-Phys. Kl. (1930), 133.
9.4. Rosenthal, J.E. and G.M. Murphy. – Rev. Mod. Phys. 8 (1936), 317.

Application of group theory to classification of vibrational spectra in solids

9.5. Yanagawa, S. – Progr. Theor. Phys. (Kyoto) 10 (1953), 83.
9.6. Bell, D.G. – Rev. Mod. Phys. 26 (1954), 311.
9.7. Poulet, H. – Ann. Phys. (Paris) 10 (1955), 908.
9.8. Raghavacharyulu, I.V.V. – Can. J. Phys. 39 (1961), 1704.
9.9. Loudon, R. – Advances Phys. 13 (1964), 423.
9.10. Chen, S.H. – Phys. Rev. 163 (1967), 533.

10. DEGENERATE PERTURBATION THEORY

10.1. Bogolyubov, N.N. Lectures on Quantum Statistics. – Kiev, 1949. (Russian)
10.2. Löwdin, P.-O. – J. Chem. Phys. 19 (1951), 1396.
10.3. Price, P. – Proc. Phys. Soc. A 63 (1950), 25.

11. SPINOR REPRESENTATIONS

Spinor representations of point groups

11.1. Bethe, H.A. – Ann. Phys. 3 (1929), 133.

Projective representations of double groups

11.2. Burneika, I.P. and I.B. Levinson. – Trudy Akad. Nauk Lit. SSR, Ser. B, 4, No. 27 (1961), 3.
11.3. Kitz, A. – Phys. St. Sol. 8 (1965), 813.

12. ANALYTICAL PROPERTIES OF BLOCH FUNCTIONS

12.1. Blount, E.I. – Sol. St. Phys. 13 (1962), 305.
12.2. Krieger, J.B. – Phys. Rev. 156 (1967), 776.

13. TIME REVERSAL AND COREPRESENTATION THEORY

13.1. Wigner, E.P. – Nachr. Ges. Wiss. Göttingen, Math.-Phys. Kl. (1932), 546.
13.2. Herring, C. – Phys. Rev. 52 (1937), 361, 365.
13.3. Johnston, D.F. – Proc. Roy. Soc. Ser. A 243 (1958), 546.
13.4. Chaldyshev, V.A., N.V. Kudryavtseva and G.F. Karavaev. – Izv. Vuzov, Fizika 2 (1963), 46.
See also /I.1/, Chap. 26.

14. SELECTION RULES FOR SPACE GROUPS

14.1. Levinson, I.B. – Trudy Akad. Nauk Lit. SSR, Ser. B, 2, No. 25 (1961), 67.
14.2. Rashba, E.I. – FTT 1 (1959), 407.
14.3. Sheka, V.I. – FTT 2 (1960), 1211.
14.4. Elliott, R.J. and R. Loudon. – Phys. Chem. Sol. 15 (1960), 146.
14.5. Lax, M. and J.J. Hopfield. – Phys. Rev. 124 (1961), 115.
14.6. Birman, J.L. – Phys. Rev. 127 (1962), 1093; 131 (1963), 1489; 150 (1966), 771; J. Phys. Chem. Sol. Suppl. 1 (1965), 669.
14.7. Zak, J. – J. Math. Phys. 3 (1962), 1278.
14.8. Karavaev, G.F. – FTT 6 (1964), 3676.
14.9. Lax, M. – Phys. Rev. 138A (1965), 793.
14.10. Birman, J.L., M. Lax, and R. Loudon. – Phys. Rev. 145 (1966), 620.
14.11. Bradley, C.J. – J. Math. Phys. 7 (1966), 1145.

15. APPLICATION OF GROUP THEORY TO DETERMINATION OF LINEARLY INDEPENDENT COMPONENTS OF TENSORS

15.1. Jahn, H.A. – Z. Kristallogr. 98 (1937). 191; Acta Cryst. 2 (1949), 30.

15.2. Fumi, F.G. — Nuovo Cimento 9 (1952), 739.
15.3. Fieschi, R. and F.G. Fumi. — Nuovo Cimento 10 (1953), 865.
15.4. Nye, J.F. Physical Properties of Crystals. — Oxford, Clarendon Press. 1960.

16. *kp*-THEORY

16.1. Bouckaert, L.P., R. Smoluchowski, and E.P. Wigner. — Phys. Rev. 50 (1936), 58.
16.2. Von der Lage, F.C. and H.A. Bethe. — Phys. Rev. 71 (1947), 612.
16.3. Shockley, W. — Phys. Rev. 78 (1950), 173.
16.4. Elliott, R.J. — Phys. Rev. 96 (1954), 266; 96 (1954), 280.
16.5. Dresselhaus, G.F. and M.S. Dresselhaus. — In: Opticheskie svoistva poluprovodnikov (Optical Properties of Semiconductors), 315–325. Moscow, 1970. [Russian; original not traced.]
For the inclusion of time reversal in *kp*-theory, see /14.2/, /14.3/.

17. EFFECTIVE MASS THEORY

17.1 Wannier, G.H. — Phys. Rev. 52 (1937), 191.
17.2. Kittel, C. and A.H. Mitchell. — Phys. Rev. 96 (1954), 1488.
17.3. Luttinger, J.M. and W. Kohn. — Phys. Rev. 97 (1955), 869.

18. REPRESENTATIONS OF SPACE GROUPS IN CUBIC AND HEXAGONAL CRYSTALS

18.1. Opechowski, W. — Physica 7 (1940), 552.
18.2. Herring, C. — J. Franklin Inst. 233 (1942), 525.
18.3. Döring, W. and A. Lehrer. — Ann. Phys. 6 (1953), 215.
18.4. Elliott, R.J. — Phys. Rev. 96 (1954), 280.
18.5. Koster, G.F. — Sol. St. Phys. 5 (1957), 173.
18.6. Parmenter, R.H. — Phys. Rev. 100 (1955), 573.
18.7. Casella, R.C. — Phys. Rev. 114 (1959), 1514. See also /16.1/, /14.2/, /14.3/ and /I.15/,
See also /16.1/, /14.2/, /14.3/ and /I.15/, /I.16/, /I.17/.

19. ELECTRON SPECTRUM IN CUBIC CRYSTALS

19.1. Dresselhaus, G.F., A.F. Kip, and C. Kittel. — Phys. Rev. 98 (1955), 368.
19.2. Dresselhaus, G.F. — Phys. Rev. 100 (1955), 580.
19.3. Kane, E.O. — Phys. Chem. Sol. 1 (1957), 82, 249.
19.4. Brounstein, R. and E.O. Kane. — J. Phys. Chem. Sol. 23 (1962), 1423.
19.5. Tovstyuk, K.D. and M.V. Tarnavskaya. — FTT 5 (1963), 819.
See also /16.3/, /16.4/, /17.2/, /17.3/.

20. THEORY OF INVARIANTS

20.1. Luttinger, J.M. — Phys. Rev. 102 (1956), 1030.
20.2. Pikus, G.E. — ZhETF 41 (1961), 1258, 1507.
20.3. Koster, G.F. and H. Statz. — Phys. Rev. 113 (1959), 445; 115 (1959), 1568.

21. SHALLOW IMPURITY CENTERS

21.1. Koster, G.F. and J.C. Slater. — Phys. Rev. 94 (1954), 1392.
21.2. Kohn, W. and J.M. Luttinger. — Phys. Rev. 98 (1955), 915.
21.3. Kohn, W. and D. Schechter. — Phys. Rev. 99 (1955), 1903.
21.4. Schechter, D. — J. Phys. Chem. Sol. 23 (1962), 237.
21.5. Mendelson, K.S. and H.M. James. — J. Phys. Chem. Sol. 25 (1964), 729.
21.6. Kohn, W. — Sol. St. Phys. 5 (1957), 257.
21.7. Kohn, W. and J.M. Luttinger. — Phys. Rev. 97 (1955), 883.
21.8. Appel, J. — Phys. Rev. 133A (1964), 280.
21.9. Keldysh, L.V. — ZhETF 45 (1963), 365.

21.10. Keyes, R.M. — IBM J. Res. Develop. 5 (1961), 65.
21.11. Morgan, T.N. — In: Proc. Tenth Int. Conf. Phys. Semiconductors, Cambridge, Mass., 1970, p. 266.
21.12. Suzuki, K., M. Okazaki, and H. Hasegawa. — J. Phys. Soc. Japan 19 (1964), 930.
21.13. Phillips, J.C. — Phys. Rev. B2 (1970), 4044.
21.14. Gel'mont, B.L. and M.I. D'yakonov. — ZhETF 62 (1972), 713.
21.15. Sheka, V.I. — FTT 7 (1965), 1783.
21.16. Sheka, V.I. and D.I. Sheka. — ZhETF 51 (1966), 1445.
21.17. Mendelson, K.S. and D.R. Shultz. — Phys. St. Sol. 31 (1969), 59.
21.18. Baldereschi, A. — Phys. Rev. B1 (1970), 4673.
21.19. Ning, T.H. and C.T. Sah. — Sol. St. Comm. 8 (1970), 1893.
21.20. Bir, G.L. — FTT 13 (1971), 460.

22. WANNIER-MOTT EXCITONS IN SEMICONDUCTORS WITH COMPOUND BAND STRUCTURE

22.1. Dresselhaus, G.F. — Phys. Chem. Sol. 1 (1955), 14; Phys. Rev. 105 (1957), 135.
22.2. Elliott, R.J. — Phys. Rev. 108 (1957), 1384.
22.3. Elliott, R.J. and R. Loudon. — Phys. Chem. Sol. 8 (1959), 382.
22.4. McLean, T.P. and R. Loudon. — Phys. Chem. Sol. 13 (1960), 1.
22.5. Elliott, R.J. Polarons and Excitons. — Edinburgh—London, 1963; Phys. Rev. 124 (1961), 340.
22.6. Rashba, E.I. — ZhETF 36 (1959), 1701.
22.7. Knox, R.S. Theory of Excitons (Solid State Physics, Supplement 5). — N.Y., Acad. Press, 1963.
22.8. Agranovich, V.M. Theory of Excitons. — Moscow, Nauka. 1968. (Russian)
22.9. Wheeler, R.G. and J.O. Dimmock. — Phys. Rev. 125 (1962), 1805.
22.10. Hopfield, J.J. and D.G. Thomas. — Phys. Rev. 122 (1961), 35.
22.11. Dimmock, J.O. — In: Semiconductors and Semimetals, Vol. 3, p. 259. — New York, 1967.
22.12. Baldereschi, A. and N.O. Lipari. — Phys. Rev. Lett. 25 (1970), 373, 1660.
22.13. Pikus, G.E. and G.L. Bir. — ZhETF 60 (1971), 195.
22.14. Pikus, G.E. and G.L. Bir. — ZhETF 62 (1972), 324.
A more extensive bibliography may be found in /22.7/, /22.8/ and in the review /22.11/.

23. EFFECT OF STRAIN ON SPECTRUM IN CUBIC CRYSTALS

23.1. Herring, C. — Bell System Tech. J. 34 (1955), 237.
23.2. Adams, E.N. — Phys. Rev. 96 (1954), 803.
23.3. Brooks, H. — Advances Electr. 7 (1955), 85.
23.4. Pikus, G.E. and G.L. Bir. — FTT 1 (1959), 154, 1642.
23.5. Bir, G.L. and G.E. Pikus. — FTT 3 (1961), 3050.
23.6. Pikus, G.E. and G.L. Bir. — FTT 4 (1962), 2090.
23.7. Cardona, M. — Sol. St. Comm. 5 (1967), 233.
23.8. Goroff, I. and L. Kleinman. — Phys. Rev. 132 (1963), 1080.
23.9. Brust, D. and L. Liu. — Sol. St. Comm. 4 (1966), 193.
23.10. Pollak, F.H. and M. Cardona. — Phys. Rev. 172 (1968), 816.
23.11. Kołodziejczak, F. and S. Żukotyński. — Phys. St. Sol. 14 (1966), 471; 16 (1966), K5.
23.12. Kleiner, W. and L. Roth. — Phys. Rev. Lett. 2 (1959), 334.

24. CALCULATION OF DEFORMATION POTENTIAL CONSTANTS

24.1. Goroff, I. and L. Kleinman. — Phys. Rev. 132 (1963), 1080.
24.2. Bassani, F. and D. Brust. — Phys. Rev. 131 (1963), 1524.
24.3. Ferreira, L.G. — Phys. Rev. 137A (1965), 1601.
24.4. Saravia, L.R. and D. Brust. — Phys. Rev. 178 (1969), 1240.
24.5. Van Vechten, J.A. — Phys. Rev. 187 (1969), 1007.

25. ELECTRON SPECTRUM IN CRYSTALS WITH WURTZITE LATTICE

25.1. Casella, R.C. — Phys. Rev. Lett. 5 (1960), 371.
25.2. Glasser, M.L. — Phys. Chem. Sol. 10 (1959), 229.

25.3. Rashba, E.I. — FTT 1 (1959), 407; Rashba, E.I. and V.I. Sheka. — FTT, Coll. No.2 (1959), 162.
25.4. Birman, J.L. — Phys. Rev. 115 (1959), 1493.
25.5. Balkanski, L. and des Cloiseaux, J. — J. Phys. Radium 21 (1960), 825.
25.6. Cardona, M. — J. Phys. Chem. Sol. 24 (1963), 1543.
25.7. Hopfield, J.J. — Phys. Chem. Sol. 15 (1960), 97.
25.8. Adler, S. — Phys. Rev. 126 (1962), 118.
25.9. Mahan, G.D. and J.J. Hopfield. — Phys. Rev. 135A (1964), 428.
25.10. Gutsche, E. and E. Jahne. — In: Proc. Int. Conf. II–VI Semiconductor Compounds, Providence, 1967, p. 825.
25.11. Collins, T.C., R.N. Euwema, and J.S. Dewitt. — Ibid., p. 598.
25.12. Hopfield, J.J. and D.G. Thomas. — Phys. Rev. 132 (1963), 563.
See also /14.2/, /14.3/, /18.7/.

26. EFFECT OF STRAIN ON SPECTRUM OF CRYSTALS WITH WURTZITE LATTICE

26.1. Pikus, G.E. — FTT 6 (1964), 324.
26.2. Bir, G.L., G.E. Pikus, L.G. Suslina, D.L. Fedorov, and E.B. Shadrin. — FTT 13(1971), 3551.
See also /20.2/.

27. COLLECTED DATA ON BAND STRUCTURE OF VARIOUS SEMICONDUCTORS

27.1. Phillips, J.C. — Phys. Rev. 125 (1962), 1931 (Ge, Si); Phys. Chem. Sol. 8 (1959), 369, 379 (Ge, Si).
27.2. Cohen, M.L. and T.K. Bergstresser. — Phys. Rev. 141 (1966), 789 (Ge, Si, A_3B_5).
27.3. Ghosh, A.K. — Phys. Rev. 165 (1968), 888.
27.4. Dimmock, J.O. — In: Proc. Int. Conf. II–VI Semiconductor Compounds, Providence, 1967, p. 277 (A_2B_6).
27.5. Rowe, J.E., M. Cardona, and F.H. Pollak. — Ibid., p. 112 (A_2B_6).
27.6. Lin, P.J. and L. Kleinman. — Phys. Rev. 142 (1966), 478 (A_2B_6).
27.7. Cardona, M. — J. Phys. Chem. Sol. 24 (1963), 1543 (A_3B_5).
27.8. Pollak, F.H. and M. Cardona. — Phys. Rev. 142 (1966), 530 (Ge, Si).
27.9. Pollak, F.H. — J. Phys. Chem. Sol. 27 (1966), 423 (Ge, A_3B_5).
27.10. Rodot, M. — In: Proc. Ninth Int. Conf. Phys. Semiconductors, Moscow, 1968, p. 639 (HgTe, gray tin)
27.11. Sosnowsky, L.N. — Ibid., p. 700 (HgTe, gray tin).
27.12. Groves, S.H., A.W. Ewald, and R.J. Wagner. — Ibid., p. 43 (HgTe, gray tin).
27.13. Grynberg, M. — In: Proc. Seventh Int. Conf. Phys. Semiconductors, Paris, 1964, p. 135 (A_2B_6).
27.14. Hilsum, C. — Ibid., p. 1172; Semiconductors and Semimetals, Vol. 1, p. 3. New York, 1966 (A_3B_5).
27.15. Stickler, J.J., H.J. Zeiger, and G.S. Heller. — Phys. Rev. 127 (1962), 1077 (Ge).
27.16. Pollak, F.H., G.W. Higginbotham, and M. Cardona. — In: Proc. Eighth Int. Conf. Phys. Semiconductors, Kyoto, 1966, p. 20 (A_3B_5).
27.17. Pollak, F.H., G.W. Higginbotham, and M. Cardona. — In: Proc. Ninth Int. Conf. Phys. Semiconductors, Moscow, 1968, p. 57 (A_3B_5).
27.18. Cardona, M. — In: Semiconductors and Semimetals, Vol. 3, p. 125. New York, 1967 (A_3B_5).
27.19. Lax, B. and J.G. Mavroides. — Ibid., p. 321 (A_3B_5).
27.20. Ravich, Yu.I., B.A. Efimova, and I.A. Smirnov. Methods of Semiconductor Research, Applied to Lead Chalcogenides. — Moscow, Nauka. 1968. (Russian).
27.21. Levinger, B.W. and D.R. Frankl. — Phys. Chem. Sol. 20 (1961), 281.
27.22. Reynolds, D.C., C.W. Litton, and T.C. Collins. — Phys. St. Sol. 6 (1965), 645; 12 (1965), 3 (A_2B_6).
27.23. Rowe, J.E., M. Cardona, and F.H. Pollak. — Sol. St. Comm. 6 (1968), 239 (ZnO).
27.24. Rössler, U. — Phys. Rev. 184 (1969), 733 (A_2B_6).

28. SCATTERING THEORY

Deformation potential method

28.1. Shockley, W. and J. Bardeen. — Phys. Rev. 77 (1950), 407; Shockley, W. Electrons and Holes in Semiconductors. — Princeton, N.J., Van Nostrand. 1950.

28.2. Pekar, S.I. and M.F. Deigen. — ZhETF 21 (1952), 803.
28.3. Dumke, W. — Phys. Rev. 101 (1956), 531.
28.4. Herring, C. and E. Vogt. — Phys. Rev. 101 (1956), 944.
28.5. Ehrenreich, H. and A.W. Overhauser. — Phys. Rev. 104 (1956), 331, 649.
28.6. Harrison, W. — Phys. Rev. 104 (1956), 1281.
28.7. Pikus, G.E. — Zh. Tekh. Fiz. 28 (1958), 2390.
28.8. Bir, G.L. and G.E. Pikus. — FTT 2 (1960), 2287.
28.9. Whitfield, G.D. — Phys. Rev. Lett. 2 (1959), 204; Phys. Rev. 121 (1961), 720.
28.10. Lawaetz, P. — Phys. Rev. 166 (1968), 763; 174 (1968), 864.
28.11. Wiley, J.D. — Sol. St. Comm. 8 (1970), 1865.

Effect of long-range forces on lattice vibrations (see /9.1/)

28.12. Lang, I.G. and U.S. Pashabekova. — FTT 6 (1964), 3640.
28.13. Bryksin, V.V. and Yu.A. Firsov. — ZhETF 56 (1969), 841.
28.14. Pikus, G.E. and M.G. Bresler. — FTT 13 (1971), 1734.

Scattering by optical modes in polar crystals

28.15. Fröhlich, H. — Advances Phys. 3 (1954), 325 (review).

Long-range forces in nonpolar semiconductors

28.16. Tolpygo, K.B. — FTT 4 (1962), 1765.
28.17. Kogan, Sh.M. — FTT 5 (1963), 2829.
28.18. Demidenko, Z.A. and K.B. Tolpygo. — FTT 6 (1964), 3321.

29. CYCLOTRON RESONANCE IN STRAINED CRYSTALS

29.1. Hensel, J.C. and G. Feher. — Phys. Rev. Lett. 5 (1960), 307; Phys. Rev. 129 (1963), 104.
29.2. Pikus, G.E. and G.L. Bir. — Phys. Rev. Lett. 6 (1962), 103; FTT 3 (1961), 1001.
29.3. Hasegawa, H. — Phys. Rev. 129 (1963), 1029.
29.4. Hensel, J.C. — Phys. Lett. 21 (1966), 284.
29.5. Hensel, J.C., H. Hasegawa, and M. Nakayama. — Phys. Rev. 138A (1965), 225.
29.6. Balslev, I. and P. Lawaetz. — Phys. Lett. 19 (1965), 6.
29.6a. Ohyama, T. and E. Otsuka. — Phys. Lett. A24 (1967), 586.*
29.7. Hensel, J.C. and K. Suzuki. — In: Tenth Int. Conf. Phys. Semiconductors, Cambridge, 1970, p.541.
29.8. Fujiyasu, H., K. Murase, and E. Otsuka. — J. Phys. Soc. Japan 29 (1970), 685.
29.9. Blinowski, J. and M. Grynberg. — Phys. Rev. 168 (1968), 882.
29.10. [See /29.8/.]
29.11. Murase, K., K. Enjouji, and E. Otsuka. — J. Phys. Soc. Japan 29 (1970), 1248.
29.12. Klyava, Ya.G., O.G. Koshelev, T.Yu. Lisovskaya, and A.G. Kazanskii. — FTP 5 (1971), 428.
See also /23.4/, /23.5/.

30. QUANTUM CYCLOTRON RESONANCE IN STRAINED CRYSTALS

30.1. Otsuka, E., K. Murase, and H. Fujiyasu. — Phys. Lett. 21 (1966), 284.
30.2. Hensel, J.C. — Sol. St. Comm. 4 (1966), 231.

31. PARAMAGNETIC AND COMBINED RESONANCE DUE TO FREE CARRIERS IN STRAINED CRYSTALS

31.1. Rashba, E.I. — FTT 3 (1960), 1224.
31.2. Gurgenishvili, G.E. — FTT 5 (1963), 2070; 6 (1964), 479.
31.3. Hensel, J.C. — Phys. Rev. Lett. 21 (1968), 983.
31.4. Hensel, J.C. and K. Suzuki. — Phys. Rev. Lett. 22 (1969), 838.

* [It is not clear from the Russian original which of Refs. /29.6/ and /29.6a/ is meant.]

32. EFFECT OF STRAIN ON CONDUCTIVITY OF GERMANIUM AND SILICON

32.1. Smith, C.S. — Phys. Rev. 94 (1954), 42.
32.2. Morin, F.J., T.H. Geballe, and C. Herring. — Phys. Rev. 105 (1957), 525.
32.3. Pikus, G.E. and G.L. Bir. — FTT 1 (1959), 1828.
32.4. Hall, J.J. — Phys. Rev. 128 (1962), 68.
32.5. Koenig, S.H. — In: Proc. Sixth Int. Conf. Phys. Semiconductors, Exeter, 1962, p.5.
32.6. Bir, G.L., A.I. Blum, and Yu.V. Ilisavskii. — In: Proc. Seventh Int. Conf. Phys. Semiconductors Paris, 1964, p.529.
32.7. Asche, M., V.M. Bondar', and O.G. Sarbei. — FTT 8 (1966), 1188.
32.8. Tufte, O.N. and E.L. Stelzer. — Phys. Rev. 133A (1964), 1705.
32.9. Aubrey, J.E., W. Gubler, T. Henningsen, and S.H. Koenig. — Phys. Rev. 130 (1963), 1667.
32.10. Pollak, M. — Phys. Rev. 111 (1958), 798.
32.11. Cuevas, M. and H. Fritzsche. — Phys. Rev. 139A (1965), 1628; 137A (1965), 1847.
32.12. Katz, M.J. — Phys. Rev. 140A (1965), 1323.
32.13. Baranskii, P.I. and V.V. Kolomoets. — Phys. St. Sol. (b) 45 (1971), K55.
32.14. Shmartsev, Yu.V. and M. Mirzabaev. — FTP 5 (1971), 2245.
32.15. Astrov, Yu.A. and A.A. Kastal'skii. — FTP 6 (1972), 323.

33. EFFECT OF STRAIN ON CONDUCTIVITY OF A_3B_5 COMPOUNDS

33.1. Potter, R.F. — Phys. Rev. 108 (1957), 652.
33.2. Tuzzolino, A.J. — Phys. Rev. 109 (1958), 1980.
33.3. Hutson, A.R., A. Jayaraman, and A.S. Corriell. — Phys. Rev. 155 (1967), 786.
33.4. Ghanekar, K.M. and R.J. Sladek. — Phys. Rev. 146 (1966), 505.

34. EFFECT OF STRAIN ON CONDUCTIVITY OF PbTe, PbS and PbSe

34.1. Ilisavskii, Yu.V. FTT 3 (1961), 1898, 3555; 4 (1962), 918, 1975.
34.2. Burke, J.R. — Phys. Rev. 160 (1967), 636.
34.3. Finlayson, D.M. and A.D. Stewart. — Brit. J. Appl. Phys. 17 (1966), 737.
34.4. Akimenko, N.I., Z.V. Pankevich, and P.M. Starik. — Ukrain. Fiz. Zh. 12 (1967), 977
34.5. Shogenji, K. and R. Ito. — J. Phys. Soc. Jap. 20 (1965), 172.
34.6. Bir, G.L. and G.E. Pikus. — FTT 4 (1962), 2090, 2243.
See also /27.20/.

35. EFFECT OF STRAIN ON CONDUCTIVITY OF A_2B_6 COMPOUNDS

35.1. Sagar, A. and M. Rubenstein. — Phys. Rev. 143 (1966), 552.
35.2. Sagar, A. and W. Lehmann. — Phys. Rev. 140A (1965), 923.
35.3. Kulp, B.A. and K.A. Gale. — Phys. Rev. 156 (1967), 877.

36. EFFECT OF STRAIN ON GALVANO- AND THERMOMAGNETIC EFFECTS

36.1. Keyes, R.W. — Phys. Rev. 103 (1956), 1240.
36.2. Drabble, J.R. — J. Electr. Contr. 5 (1958), 362.
36.3. Drabble, J.R. and R.G. Groves. — Phys. Rev. Lett. 2 (1959), 451.
36.4. Grynberg, M. — Phys. St. Sol. 13 (1966), 277.
36.5. L'vov, V.S. and T.V. Smirnova. — FTT 8 (1966), 1365, 1617.
36.6. Lipin, A.L., V.S. L'vov, and T.V. Smirnova. — FTT 9 (1967), 3339.
36.7. L'vov, V.S. — FTT 8 (1966), 1351.
36.8. Shmartsev, Yu.V., M. Mirzabaev, and V.M. Tuchkevich. — FTT 7 (1965), 3437.
36.9. Keyes, R.W. — Sol. St. Phys. 11 (1960), 149 (review).
36.10. Vyazovskii, V.S., M. Mirzabaev, V.V. Ryzhkov, A.S. Saidov, V.M. Tuchkevich, and Yu.V. Shmartsev. — FTP 2 (1968), 447.
36.11. Baranskii, P.I. and V.V. Kolomoets. — Phys. St. Sol. 42 (1970), K113.
36.12. Samoilovich, A.G. and I.S. Buda. — FTP 3 (1969), 400.
36.13. Baranskii, P.I., I.S. Buda, I.V. Dakhovskii, and V.V. Kolomoets. — FTP 5 (1971), 1614.
36.14. Atanchuk, L.I., M.V. Nutsovich, and V.B. Moler. — FTP 5 (1971), 1845.
36.15. Asche, M., Yu.G. Zav'yalov, and O.G. Sarbei. — FTP 7 (1971), 1305.

37. STRAIN-INDUCED CHANGE IN FREE-CARRIER ABSORPTION COEFFICIENT

37.1. Walton, A.K. and G.R. Everett. — Sol. St. Comm. 5 (1967), 275.
37.2. Walton, A.K. and G.R. Everett. — Sol. St. Comm. 4 (1966), 211.

38. FREE-CARRIER BIREFRINGENCE IN STRAINED CRYSTALS

38.1. Schmidt-Tiedemann, K.J. — Phys. Rev. Lett. 7 (1961), 372; In: Proc. Sixth Int. Conf. Phys. Semiconductors, Exeter, 1962, p.191; J. Appl. Phys. 32 (1961), 2058.
38.2. Furduna, J.K. and G.P. Soardo. — In: Proc. Seventh Int. Conf. Phys. Semiconductors, Paris, 1964, p.171.
38.3. Feldman, A. — Phys. Rev. 150 (1966), 748.
38.4. Riskaer, S. — Phys. Rev. 152 (1966), 845.
38.5. Blinowski, J. — Phys. Rev. 147 (1966), 547.
38.6. Remenyuk, A.D., Yu.I. Ukhanov, V.M. Tuchkevich, and Yu.V. Shmartsev. — FTP 1 (1967), 1113.

39. CHANGE IN THE ABSORPTION AND REFLECTION COEFFICIENTS, OTHER STRAIN-INDUCED EFFECTS DUE TO INTERBAND TRANSITIONS

39.1. Konstantinov, O.V. and V.I. Perel'. — ZhETF 37 (1959), 786.
39.2. Grynberg, M. — In: Proc. Seventh Int. Conf. Phys. Semiconductors, Paris, 1964, p.135.
39.3. Hobson, G.S. and E.G.S. Paige. — Ibid., p.143.
39.4. Riskaer, S. and I. Balslev. — Phys. Lett. 21 (1966), 16.
39.5. Erlbach, E, — Phys. Rev. 150 (1966), 767.
39.6. Engeler, W.E., M. Garfinkel, and J.J. Tiemann. — Phys. Rev. 155 (1967), 693.
39.7. Gerhardt, V. — Phys. Rev. Lett. 15 (1965), 401.
39.8. Pollak, F.H., M. Cardona, and K.L. Shaklee. — Phys. Rev. Lett. 16 (1966), 942.
39.9. Aronov, A.G., G.E. Pikus, and D.Sh. Shekhter. — FTT 10 (1968), 823.
39.10. Kane, E.O. — Phys. Rev. 178 (1969), 1368.
39.11. Pollak, F.H. — In: Proc. Tenth Int. Conf. Phys. Semiconductors, Cambridge, Mass., 1970, p.407
39.12. Bhargava, R.N. and M.I. Nathan. — Phys. Rev. 161 (1967), 695.
39.13. Laude, L.D., M. Cardona, and F.H. Pollak. — Phys. Rev. B1 (1970), 1436.
39.14. Sell, D.D. and E.O. Kane. — Phys. Rev. 185 (1969), 1103.
39.15. Tell, B., J.M. Worlock, and R.J. Martin. — Appl. Phys. Lett. 6 (1965), 123.
39.16. Pollak, F.H. and M. Cardona. — Phys. Rev. 172 (1968), 816.
39.17. Akimchenko, I.P. and V.A. Vdovenkov. — FTT 11 (1969), 658.
39.18. Nikitenko, V.I. and G.P. Martynenko.— FTT 7 (1965), 622.
39.19. Dubenskii, K.K., A.A. Kaplyanskii, and I.G. Lozovskaya. — FTT 8 (1966), 2068.
39.20. Higginbotham, G.W., M. Cardona, and F.H. Pollak. — Phys. Rev. 184 (1969), 821.
39.21. Shileika, A.Yu., M. Cardona, and F.H. Pollak. — Sol. St. Comm. 7 (1969), 1113.
39.22. [See /39.12/.]
39.23. Kravchenko, A.F., E.A. Makarov, and A.S. Mardeisov. — FTP 2 (1967), 1783.
39.24. Kagan, Yu. and V. Sabakin. — FTT 11 (1969), 1018.
39.25. Pollak, F.H. and M. Cardona. — Phys. Rev. 177 (1969), 1351.
39.26. Gavini, A. and M. Cardona. — Phys. Rev. B1 (1970), 672.
39.27. Kastal'skii, A.A. — FTP 1 (1967), 97.
39.28. Kastal'skii, A.A. and N.I. Sablina. — FTP 2 (1968), 1467, 1475.
39.29. Bailey, P.T. — Phys. Rev. B1 (1970), 588.
39.30. Benoit à la Guillaume, C. and P. Lavallard. — J. Phys. Chem. Sol. 31 (1970), 411.
39.31. Krauze, A.S. and Yu.G. Shreter. — FTP 5 (1971), 1912.
39.32. Kastal'skii, A.A., S.B. Mal'tsev, and Yu.G. Shreter. — FTP 5 (1971), 1588.

40. EFFECT OF STRAIN ON SPECTRUM OF SHALLOW IMPURITY CENTERS

40.1. Price, P.J. — Phys. Rev. 104 (1956), 1223.
40.2. Fritsche, H. — Phys. Rev. 125 (1962), 1552, 1560.
40.3. Kleiner, W.H. and L. Roth. — Phys. Rev. Lett. 2 (1959), 234.

40.4. Bir, G.L. E.I. Butikov, and G.E. Pikus. — J. Phys. Chem. Sol. 24 (1963), 1467, 1475.
40.5. Hale, E.B. and T.G. Castner. — Phys. Rev. B1 (1970), 4763.

41. PIEZO-OPTICS OF SHALLOW IMPURITY CENTERS

41.1. Weinreich, G. — In: Proc. Fifth Int. Conf. Phys. Semiconductors, Prague, 1960, p.360 (*n*-Ge).
41.2. Aggarwal, R.L. and A.K. Ramdas. — In: Proc. Seventh Int. Conf. Phys. Semiconductors, Paris, 1964, p.797; Phys. Rev. 137 (1965), 602 (*n*-Si).
41.3. Reuszer, J.H. and P. Fisher. — Phys. Rev. 135 (1964), 1125; 140 A (1965), 245; 165 (1968), 909 (*n*-Ge).
41.4. Aggarwal, R.L., P. Fisher, V. Mourzine, and A.K. Ramdas. — Phys. Rev. 138 (1965), 882 (*n*-Si).
41.5. Jones, R.L. and P. Fisher. — Sol. St. Comm. 2 (1964), 369 (*p*-Ge).
41.6. Dickey, D.H. and J.O. Dimmock. — J. Phys. Chem. Sol. 28 (1967), 529.
41.7. Fisher, P. and A.K. Ramdas. — Phys. Lett. 16 (1965), 26 (*p*-Si).
41.8. Onton, A., P. Fisher, and A.K. Ramdas. — Phys. Rev. 163 (1967), 686 (*p*-Si).
41.9. Feofilov, P.P. and A.A. Kaplyanskii. — UFN 76 (1962), 201 (review).
41.10. Krag, W.E., W.H. Kleiner, and H.J. Zeiger. — In: Proc. Tenth Int. Conf. Phys. Semiconductors, Cambridge, Mass., 1970, p.271.
41.11. Kleiner, W.H. and W.E. Krag. — Phys. Rev. Lett. 25 (1970), 1490.
41.12. Jones, R.L. and P. Fisher. — Phys. Rev. B2 (1970), 2016.
41.13. Kucherenko, I.V. — FTP 2 (1968), 1069.
41.14. Paul, W. — In: Proc. Ninth Int. Conf. Phys. Semiconductors, Moscow, 1968, p.16.
41.15. Bul', A.Ya., G.L. Bir, and Yu.V. Shmartsev. — FTP 4 (1970), 2331.
41.16. Ahlburn, V.T. and A.K. Ramdas. — Phys. Lett. 29 A (1969), 135.
41.17. Alferov, Zh.S., D.Z. Garbuzov, O.A. Ninya, and V.G. Trofim. — FTP 5 (1971), 1400.

42. EFFECT OF STRAIN ON EPR OF SHALLOW IMPURITY CENTERS

42.1. Feher, G., J.C. Hensel, and E.A. Gere. — Phys. Rev. Lett. 5 (1960), 309.
42.2. Wilson, D.K. and G. Feher. — Phys. Rev. 124 (1961), 1068.
42.3. Wilson, D.K. — Phys. Rev. 134 A (1964), 264.
42.4. Morigaki, K. and T. Mitsuma. — J. Phys. Soc. Jap. 18 (1963), 462; 20 (1965), 491.
42.5. Nakayama, M. and H. Hasegawa. — J. Phys. Soc. Jap. 18 (1963), 229.
42.6. Watkins, G.D. — In: Fourth Annual Solid State Conf., Manchester, 1967, p.79.
42.7. Ludwig, G.W. and H.H. Woodbury. Electron Spin Resonance in Semiconductors. — In: Solid State Physics. 13, 223–306. N.Y., Academic Press, 1962.
42.8. Bir, G.L. and G.E. Pikus. — In: Proc. Seventh Int. Conf. Phys. Semiconductors, Paris, 1966, p.789.
42.9. Suzuki, K., M. Okazaki, and H. Hasegawa. — J. Phys. Soc. Jap. 19 (1964), 930.
42.10. Butikov, E.I. — FTT 10 (1968), 3364.
42.11. Zhurkin, B.G., N.A. Penin, and N.N. Sibel'din. — FTP 2 (1968), 827.
42.12. Lin-Chung, P.I. and R.F. Wallis. — In: Proc. Ninth Int. Conf. Phys. Semiconductors, Moscow, 1968, p.341.
42.13. Shimizu, T. and M. Nakayama. — J. Phys. Soc. Jap. 19 (1964), 1829.
42.14. Till, R.S. — IBM J. Res. Develop. 7 (1963), 68.

43. PIEZO-OPTICS OF EXCITONS

43.1. Gross, E.F., A.A. Kaplyanskii, and V.T. Arekyan. — FTT 4 (1963), 1009, 2170.
43.2. Gross, E.F. and A.A. Kaplyanskii. — FTT 2 (1960), 1676, 2968.
43.3. Kaplyanskii, A.A. and L.G. Suslina. — FTT 7 (1965), 2327.
43.4. Bobrysheva, A.I. and S.A. Moskalenko. — FTT 4 (1962), 1994; FTP 2 (1968), 438.
43.5. Thomas, D.G. — J. Appl. Phys. Suppl. 32 (1961), 2298 (CdTe).
43.6. Kaplyanskii, A.A. — Optika i Spektroskopiya, 16 (1964), 1031.
43.7. Balslev, I. — In: Proc. Eighth Int. Conf. Phys. Semiconductors, Kyoto, 1966, p.101 (GaP).
43.8. Glass, A.M. — Can. J. Phys. 43 (1963), 12 (Ge).
43.9. Osipov, V.Yu. — FTT 8 (1966), 2280 (Ge).

43.10. Balslev, I. – Phys. Rev. 143 (1966), 636; Phys. Lett. A24 (1967), 113; Sol. St. Comm. 5 (1967), 315.
43.11. Adler, E. and E. Erlbach. – Phys. Rev. Lett. 16 (1966), 87, 927 (Ge).
43.12. Koda, T. and D.W. Langer. – Phys. Rev. Lett. 20 (1968), 50; In: Proc. Ninth Int. Conf. Phys. Semiconductors, Moscow, 1968, p. 242 (ZnO, PbS, PbSe).
43.13. Akimoto, O. and H. Hasegawa. – Phys. Rev. Lett. 20 (1968), 916.
43.14. Bir, G.L., G.E. Pikus, L.G. Suslina, and D.L. Fedorov. – FTT 12 (1970), 1187 (ZnS).
43.15. Bir, G.L., G.E. Pikus, L.G. Suslina, and D.L. Fedorov. – FTT 12 (1970), 3218 (ZnS).
43.16. Gavini, A. and M. Cardona. – Phys. Rev. B1 (1970), 672.
43.17. Langer, D.W., R.N. Euwema, K. Era, and T. Koda. – Phys. Rev. B2 (1970), 4005.
43.18. Onodera, Y. and Y. Toyozawa. – J. Phys. Soc. Jap. 22 (1967), 833.
43.19. Skettrup, T. and I. Balslev. – Phys. St. Sol. 40 (1970), 93.
43.20. Gilleo, M.A., P.T. Bailey, and D.E. Hill. – J. Luminesc. 1/2 (1970), 562.
43.21. Morgan, J.W. and T.N. Morgan. – Phys. Rev. B1 (1970), 739.
43.22. Laude, L.D., F.H. Pollak, and M. Cardona. – Phys. Rev. B3 (1971), 2623.
43.23. Pollak, F.H. and R.L. Aggarwal. – Phys. Rev. B4 (1971), 432.
43.24. Bir, G.L., G.E. Pikus, L.G. Suslina, and D.L. Fedorov. – FTT 14 (1972), 858.
See also /26.2/.

NOTE (Abbreviations Used in Bibliography for Russian Journals):

FTP: Fizika i Tekhnika Poluprovodnikov
FTT: Fizika Tverdogo Tela
UFN: Uspekhi Fizicheskikh Nauk
ZhETF: Zhurnal Eksperimental'noi i Tekhnicheskoi Fiziki

SUBJECT INDEX

HALSTED PRESS
A Division of JOHN WILEY & SONS, Inc.,
605 Third Avenue, New York, N.Y. 10016

ISRAEL PROGRAM FOR SCIENTIFIC TRANSLATIONS
P.O.B. 7145, Jerusalem, Israel

Cover designed by Avraham Pladot

IPST Cat. No. 22084